

**When two are better than one: bright phosphorescence from
non-stereogenic dinuclear iridium(III) complexes**

R. E. Daniels, S. Culham, M. Hunter, M. C. Durrant, M. R. Probert, W. Clegg,
J. A. G. Williams* and V. N. Kozhevnikov*

Supporting Information

Table of Contents

1. Synthetic procedures and characterisation of new compounds.....	2
(a) Synthesis of the tridentate proligands.....	2
(b) Synthesis of chloro-bridged iridium(III) dimers.....	4
(c) Synthesis of the dinuclear iridium complexes.....	5
(d) Metathesis of the monodentate ligand.....	9
2. TD-DFT results and correlation with experimental data.....	11
(a) Tables of excitation energies, their oscillator strengths and main orbital components.....	11
(b) Simulated absorption spectra	19
(c) Additional plots showing experimental versus calculated data	21
(d) Frontier orbital plots of the dinuclear complexes.....	22
3. X-ray crystallography of complex A3.....	30

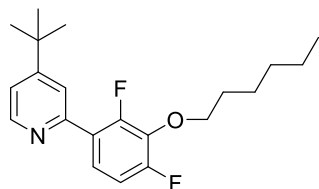
Appendix: NMR spectra of new ligands and complexes

* E-mail: valery.kozhevnikov@northumbria.ac.uk j.a.g.williams@durham.ac.uk

1. Synthetic procedures and characterisation of new compounds

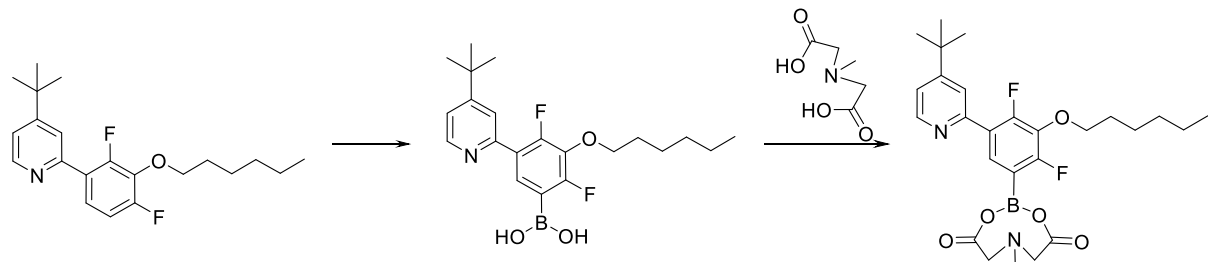
(a) Synthesis of the tridentate proligands

4-t-butyl-2-(2,4-difluoro-3-hexyloxyphenyl)pyridine, 2



Potassium phosphate (12.7 g, 60.0 mmol) was dissolved in water (20 mL) and the solution was deaerated by bubbling nitrogen through the mixture for 30 min. A mixture of [2,4-difluoro-3-(hexyloxy)phenyl]boronic acid (5.00 g, 19.4 mmol), 2-chloro-4-tertbutylpyridine (2.78 g, 16.4 mmol), dioxane (60 mL) was deoxygenated by bubbling nitrogen through the mixture for 15 min. Palladium acetate (184 mg, 0.820 mmol), S-Phos (660 mg, 1.64 mmol) and the above solution of K₃PO₄ were added and the mixture was stirred at 100°C (bath) for 14 h. Toluene 10 (mL) was added and the layers were separated. The organic layer was evaporated to dryness by rotary evaporation under reduced pressure. The product was then purified by column chromatography (silica gel) using a 3/1 petroleum ether/ethyl acetate eluent. Yield: 5.50 g, 96 %. ¹H-NMR (400 MHz, CDCl₃): δ 8.66 (br s, 1H), 7.99 (t, 1H, *J* = 15.1, 7.8), 7.68 (br s, 1H), 7.64 (br s, 1H), 7.27 (br s, 1H), 4.09 (t, 2H, *J* = 12.8, 6.4), 1.81-1.71 (m, 2H), 1.51-1.40 (m, 2H), 1.36-1.23 (m, 13H), 0.92-0.80 (m, 3H).

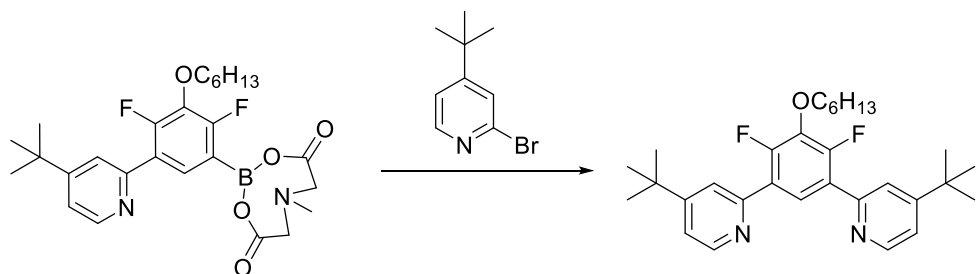
5-(4-t-butylpyridine-2-yl)-2,4-difluoro-3-n-hexyloxyphenyl boronic acid MIDA ester



Compound **2** (5.00 g, 14.4 mmol) and N,N,N',N'',N'''-pentamethyldiethylenetriamine (2.55 g, 16.0 mmol) were dissolved in dry THF (40 mL), and the solution was cooled to -78°C. To this solution, 1.6 M solution of *n*-butyllithium in hexane (10 mL, 16.0 mmol) was added dropwise. Solution was stirred at -78°C for 45 min. Tri-isopropylborate (5 mL, 21.6 mmol) was added dropwise. The mixture was stirred at -78°C for 3 h and at room temperature for a further 14 h. 1M aqueous

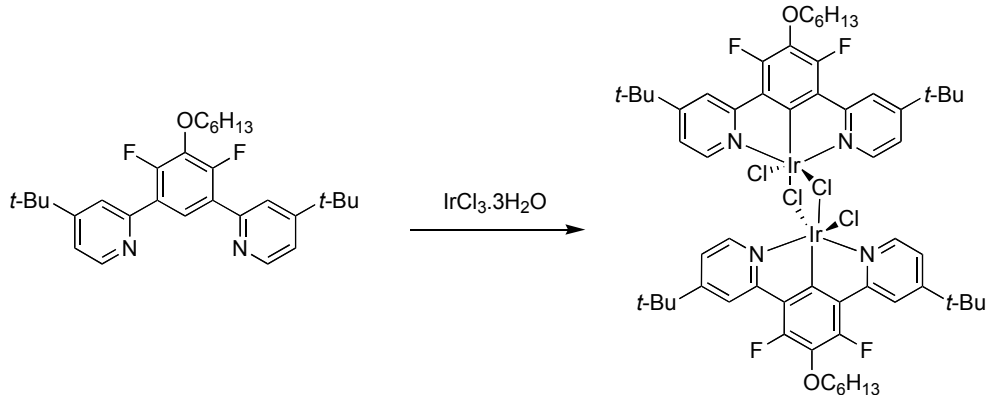
hydrochloric acid was added to neutralise the reaction mixture. The mixture was separated, the organic layer was washed with brine and all volatiles removed under reduced pressure. The residue was dissolved in DMSO (10 mL) at 40-50°C. MIDA (2.10 g, 14.4 mmol) and toluene (160 mL) were added and the mixture was heated with Dean-Stark adapter for 3 h. All volatiles were removed under reduced pressure. The residue was triturated with petrol ether. The petrol ether phase was decanted and the product was left overnight. During this time, a semi-solid formed which was suspended in water and filtered. Yield: 3.96g, 55%. The product was used directly in the subsequent reaction.

1,5-bis(3-*tert*-butylphenyl)-2,4-difluoro-3-(hexyloxy)benzene, L⁴H

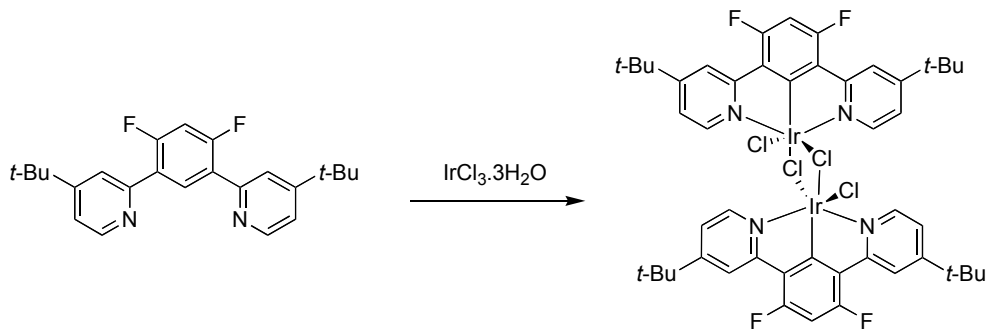


A mixture of the boronic acid derivative (1.0 g, 2.6 mmol), 2-chloro-4-*tert*-butylpyridine (0.44 g, 2.4 mmol) and toluene (30 mL) was deoxygenated by bubbling nitrogen through the mixture for 15 min. Pd(PPh₃)₄ (0.12 g, 0.12 mmol) was added and the mixture additionally deoxygenated by bubbling nitrogen for 5 min. An aqueous solution of sodium carbonate (2 M, 3.6 mL, 7.2 mmol) was added and the mixture was additionally degassed for 5 min. The mixture was heated under reflux under nitrogen for 24 h. Brine (30 mL) was added and layers were separated. The organic layer was separated, washed with brine, dried over anhydrous MgSO₄ and filtered. The solvent was removed under reduced pressure. The product was purified by column chromatography (silica gel) using a mixture petroleum ether/ethyl acetate, 3/1 as eluent. A colourless solid was obtained. Yield: 43 %. ¹H NMR (400 MHz, CDCl₃): δ 8.60 (d, 2H, *J* = 5.4), 8.09 (t, 1H, *J* = 8.5), 7.69 (br s, 2H), 7.20 (dd, 2H, *J* = 5.4, 2.1), 4.21 (t, 2H, *J* = 7.0), 1.57 (q, 2H, *J* = 7.2), 1.34 (m, 6H), 0.90 (t, 3H, *J* = 7.2); ¹⁹F NMR (400 MHz): δ -131.30 (d, *J* = 21.5)

(b) Synthesis of chloro-bridged iridium(III) dimers

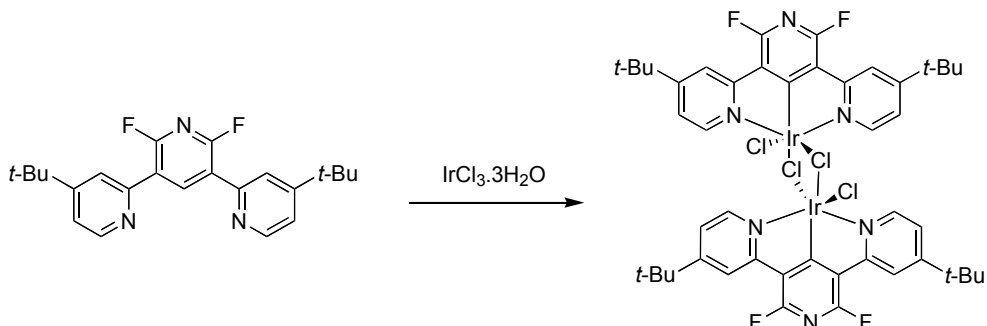


A mixture of the proligand **L^AH** (2.10 g, 4.38 mmol), iridium chloride hydrate (1.59 g, 4.38 mmol), 2-ethoxyethanol (90 mL) and water (30 mL) was heated under reflux for 14 h. The solid was filtered off and washed with water and ethanol to give, after drying, the dichloro-bridged compound. Yield: 2.60 g, 80%. ¹H NMR (400 MHz, CDCl₃): δ 8.43 (d, 2H, *J* = 5.9), 8.25 (br s, 2H), 6.96 (dd, 2H, *J* = 5.9, 1.9), 4.18 (t, 2H, *J* = 6.5), 1.89 (m, 2H), 1.58 (m, 2H), 1.49 (s, 18H), 1.42 (m, 4H), 0.95 (t, 3H, *J* = 6.9); ¹⁹F NMR (400 MHz, CDCl₃): δ -125.1.



A mixture of **L^BH** (0.221 g, 0.581 mmol) and iridium chloride hydrate (0.211 g, 0.581 mmol) were added to a 3:1 mixture of 2-ethoxyethanol and water (25 mL). The reaction mixture was heated to reflux (130°C) for 24 h under argon. The solvent was removed *in vacuo* and the resulting orange solid was filtered and washed with ethanol and water to give the desired product. Yield: 308 mg, 0.486 mmol, 84%. ¹H NMR (400 MHz, *d*⁶-DMSO) δ 8.94 (d, 2H, *J* = 6.0), 8.05 (br s, 2H), 7.73 (br d, 2H, *J* = 6.4), 7.27 (t, 1H, *J* = 11.6,), 1.40 (s, 18H); ¹⁹F NMR (400 MHz, *d*⁶-DMSO): δ -107.38 (d, *J* = 12.8).

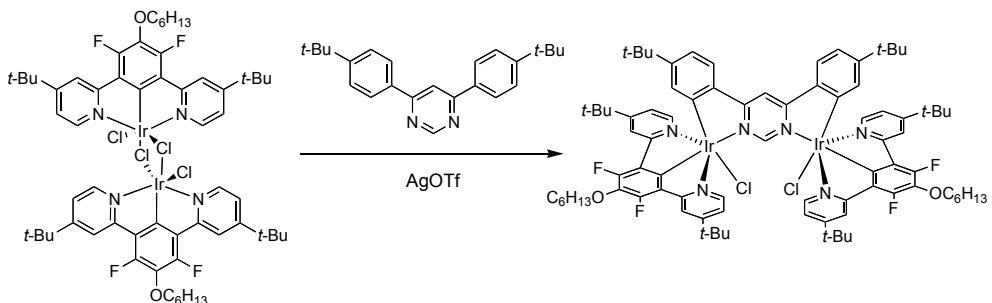
[IrL^CCl(μ-Cl)]₂



A mixture of 3,5-bis(4-tert-butylpyridin-2-yl)-2,6-difluoropyridine[†] (0.151 g, 0.396 mmol) and iridium chloride hydrate (0.144 g, 0.396 mmol) were added to a 3:1 mixture of 2-ethoxyethanol and water (60 mL). The reaction mixture was heated to reflux (130 °C) for 24 h under argon. The solvent was removed *in vacuo* and the resulting orange solid was filtered and washed with ethanol and water. Yield: 162 mg, 0.267 mmol, 67%. A satisfactory NMR spectrum could not be obtained in this instance, apparently due to low solubility, so the compound was used directly in the subsequent reactions to form the dinuclear complexes.

(c) Synthesis of the dinuclear iridium complexes

{IrL^ACl}₂L¹ (A1)

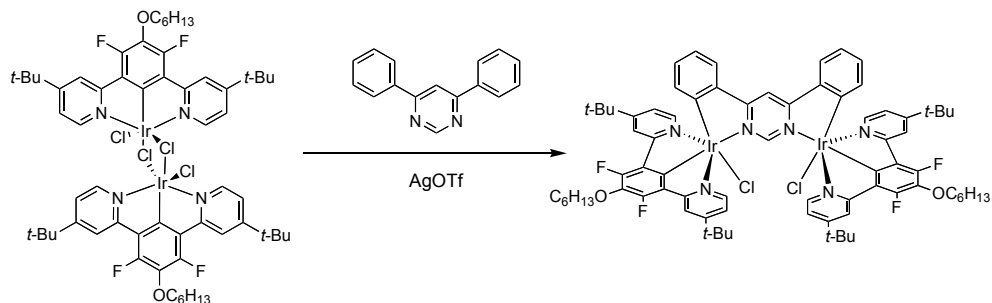


A mixture of [IrL^ACl(μ-Cl)]₂ (370 mg, 0.50 mmol), the bis-N^AC proligand L¹H₂ (90 mg, 0.26 mmol), silver triflate (191 mg, 0.74 mmol) and toluene (60 mL) was heated under reflux for 8 h. The heating was removed and 10 mL of 3M HCl was added to a still warm mixture. After stirring for 5 min, the organic phase was separated, the solvent evaporated off under reduced pressure and the residue treated with methanol (40 mL). The solid was filtered off, washed with methanol, then dissolved in dichloromethane (20 mL) and the solution filtered. To the filtrate, methanol (40 mL) was added and the volume of the mixture was reduced to approximately 10 mL under reduced pressure. The orange product that formed was filtered off, washed with a small amount of

[†] Prepared as described in patent WO/2014/009716

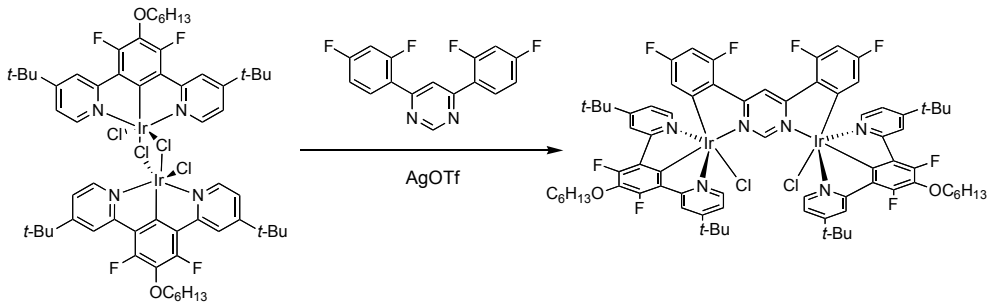
methanol, and dried. Yield: 210 mg, 48%. ^1H NMR (400 MHz, CDCl_3) δ 11.77 (s, 1H), 8.40 (s, 1H), 8.12 (s, 4H), 7.81 (d, 2H, J = 8.0 Hz), 7.79 (d, 4H, J = 5.9), 6.95 (dd, 2H, J = 8.0, 1.6), 6.92 (dd, 4H, J = 5.9, 1.6), 6.28 (d, 2H, J = 1.6), 4.20 (t, 4H, J = 6.5), 1.92 (m, 4H), 1.62 (m, 4H), 1.44 (m, 8H), 1.32 (s, 36H), 1.01 (s, 18H), 0.97 (t, 6H, J = 6.9); ^{19}F NMR (400 MHz): δ -126.9; (FTMS $^+$): for $[\text{M}-\text{Cl}]^+$ calc'd 1721.6791, found 1721.6795; for $[\text{M}+\text{Na}]^+$ calc'd 1779.6362, found 1779.6771; for $[\text{M}+\text{NH}_4]^+$ calc'd 1770.6761, found 1770.6771.

$\{\text{IrL}^\text{A}\text{Cl}\}_2\text{L}^2$ (A2)



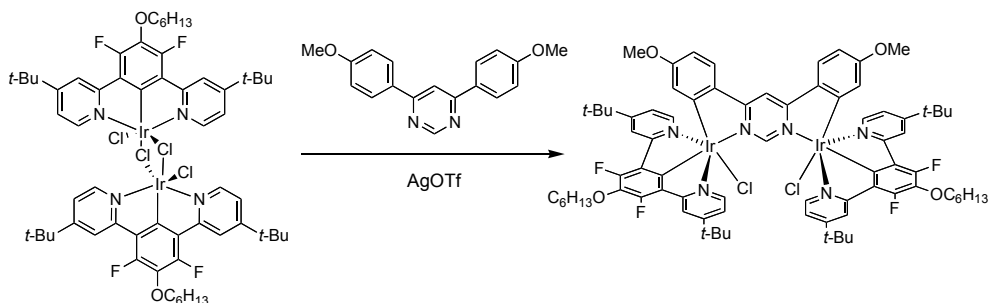
A mixture of $[\text{IrL}^\text{A}\text{Cl}(\mu\text{-Cl})]_2$ (148 mg, 0.2 mmol, 2 equiv.), the bis-N $^{\text{C}}$ proligand L^2H_2 (24 mg, 0.1 mmol), silver triflate (77 mg, 0.3 mmol, 3 equiv.) and toluene (30 mL) was heated under reflux for 15 h. To the still warm solution, 5 mL of 2M HCl was added and the mixture was stirred for 15 min. The volume of the mixture was reduced to approximately 3 mL. The aqueous layer was decanted, and the solid residue was triturated with methanol (25 mL), filtered and the solid washed with methanol. The solid was then dissolved in dichloromethane and the solution filtered through celite. To the filtrate, methanol (5 mL) was added and the mixture was reduced to a volume of 2 mL, causing formation of solid, which was filtered off and washed with methanol to give the desired product as an orange solid. Yield: 143 mg, 87%. ^1H NMR (400 MHz, CDCl_3): δ 11.86 (s, 1H), 8.53 (s, 1H), 8.12 (br s, 4H), 7.91 (br d, 2H, J = 7.8), 7.74 (d, 4H, J = 6.0), 6.92 (m, 6H), 6.78 (br t, 2H, J = 7.8), 5.78 (d, 2H, J = 7.7), 4.21 (t, 4H, J = 6.4), 1.91 (m, 4H), 1.61 (m, 4H), 1.43 (m, 8H), 1.32 (s, 36H), 0.97 (t, 6H, J = 6.9); ^{19}F NMR (400 MHz): δ -126.4(s); HRMS (FTMS $^+$): for $[\text{M}-\text{Cl}]^+$ calc'd 1609.5539, found 1609.5524; for $[\text{M}+\text{Na}]^+$ calc'd 1667.5108, found 1667.5055.

$\{\text{IrL}^{\text{A}}\text{Cl}\}_2\text{L}^3$ (A3)



A mixture of $[\text{IrL}^{\text{A}}\text{Cl}(\mu\text{-Cl})]_2$ (148 mg, 0.2 mmol, 2 equiv.), the bis-N^{HC} proligand L^3H_2 (30 mg, 0.1 mmol), silver triflate (77 mg, 0.3 mmol, 3 equiv.) and toluene (30 mL) was heated under reflux for 15 h. To a still warm solution, 5 mL of 2M HCl was added and the mixture was stirred for 15 min. The volume of the mixture was reduced to approximately 5 mL. The residue was triturated with methanol (40 mL), filtered and the solid residue was washed with methanol. The solid was dissolved in dichloromethane and filtered through celite. To the filtrate, methanol (5 ml) was added and the mixture evaporated to a volume of 2 mL causing formation of solid. This orange product was filtered off and washed with methanol. Yield: 116 mg, 68%. ¹H NMR (400 MHz, CDCl₃): δ 11.93 (s, 1H), 9.30 (br t, 1H, *J* = 3.7), 8.15 (d, 4H, *J* = 1.8), 7.79 (d, 4H, *J* = 6.0), 6.97 (dd, 4H, *J* = 6.0, 1.8), 6.38 (ddd, 2H, *J* = 11.2, 8.8, 2.4), 5.78 (dd, 2H, *J* = 8.8, 2.4), 4.21 (t, 4H, *J* = 6.4), 1.92 (m, 4H), 1.61 (m, 4H), 1.43 (m, 8H), 1.34 (s, 36H), 0.97 (t, 6H, *J* = 6.9); ¹⁹F NMR (400 MHz): δ –103.3 (m), –105.6 (m), –126.9; HRMS (FTMS⁺): for [M+Na]⁺ calc'd 1739.4731, found 1739.4670.

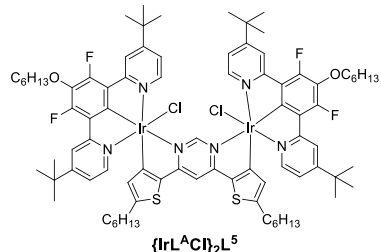
$\{\text{IrL}^{\text{A}}\text{Cl}\}_2\text{L}^4$ (A4)



A mixture of $[\text{IrL}^{\text{A}}\text{Cl}(\mu\text{-Cl})]_2$ (150 mg, 0.2 mmol), the bis-N^{HC} proligand L^4H_2 (66 mg, 0.22 mmol), silver triflate (67 mg, 0.26 mmol, 1.3 eq.) and toluene (7 mL) was heated to reflux for 8 h before the solution was allowed to cool to room temperature and the toluene removed under reduced pressure. The crude mixture was purified by column chromatography (silica gel), gradient elution DCM / EtOAc (0–20%), R_f in DCM / EtOAc (9:1) = 0.69. The product obtained after evaporation of the eluent was treated with methanol and filtered. The solid was recrystallised from DMSO, washed with methanol and dried in vacuum (5 mm Hg) at 140°C for 24 h. Yield: 57 mg,

17%. ^1H NMR (400 MHz, CDCl_3): δ 11.65 (s, 1H), 8.23 (s, 1H), 8.12 (s, 4H), 7.81 (d, 2H, $J = 8.7$), 7.78 (d, 4H, $J = 6.0$), 6.93 (dd, 2H, $J = 6.0, 1.8$), 5.75 (d, $J = 2.8$), 4.19 (t, 4H, $J = 6.4$), 3.55 (s, 6H) 1.91 (m, 4H), 1.61 (m, 9H), 1.49 (s, 2H), 1.42 (m, 8H), 1.33 (s, 36H), 1.25 (s, 6H), 0.96 (t, $J = 6.9$, 6H); ^{19}F NMR (400 MHz, CDCl_3): δ -126.49.

$\{\text{IrL}^{\text{A}}\text{Cl}\}_2\text{L}^{\text{5}}$ (**A5**)



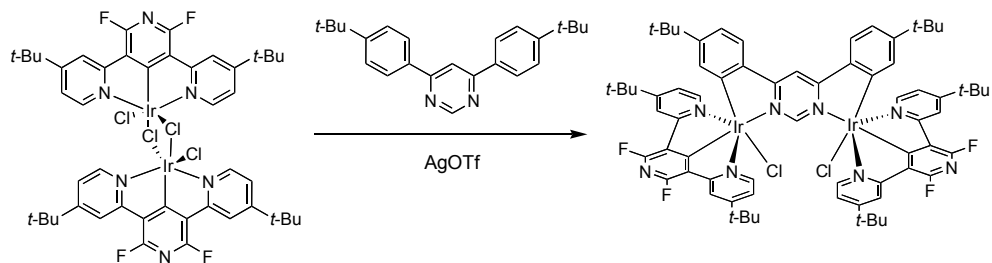
A mixture of $[\text{IrL}^{\text{A}}\text{Cl}(\mu\text{-Cl})]_2$ (148 mg, 0.2 mmol, 2 equiv.), the bis-N^{HC} proligand L^{5H_2} (41 mg, 0.1 mmol), silver triflate (77 mg, 0.3 mmol, 3 equiv.) and toluene was heated under reflux for 15 hours. To the still warm solution, 5 mL of 2M HCl was added and the mixture was stirred for 15 minutes. The mixture was evaporated to a volume of around 3 mL. The aqueous layer was decanted and the solid residue was triturated with methanol (25 mL), filtered and the solid washed with methanol. The solid was then dissolved in DCM and filtered through celite. To the filtrate, methanol (5 mL) was added and the mixture was evaporated to a volume of 2 mL leading to a solid being formed. The orange solid product was filtered off, washed with methanol and dried. Yield 139 mg, 76%. ^1H NMR (400 MHz, CDCl_3): δ 11.15 (s, 1H), 8.10 (s, 4H), 7.88 (d, 4H, $J = 6.4$), 7.39 (s, 1H), 7.00 (dd, 4H, $J = 6.0, 1.6$), 5.60 (s, 2H), 4.19 (t, 4H, $J = 6.8$), 2.62 (t, 4H, $J = 7.8$), 1.95-1.88 (m, 4H), 1.65-1.57 (m, 4H), 1.51-1.41 (m, 12H), 1.35 (s, 36H), 1.20-1.16 (m, 12H), 0.97 (t, $J = 7.2$, 6H), 0.81 (t, 6H, $J = 6.8$); ^{19}F NMR (400 MHz, CDCl_3): δ -126.76; (FTMS⁺): for $[\text{M-Cl}]^+$ calc'd 1789.6545, found 1789.6530; for $[\text{M+Na}]^+$ calc'd 1847.6114, found 1847.6053; for $[\text{M+NH}_4]^+$ calc'd 1838.6525, found 1838.6506.

$\{\text{IrL}^{\text{B}}\text{Cl}\}_2\text{L}^{\text{1}}$ (**B1**)

A mixture of $[\text{IrL}^{\text{A}}\text{Cl}(\mu\text{-Cl})]_2$ (150 mg, 0.23 mmol), the bis-N^{HC} proligand L^{1H_2} (40 mg, 0.12 mmol), silver trifluoromethanesulfonate (90 mg, 0.35 mmol) and xylene (30 mL) was heated to 160°C for 8 h. To the cooled reaction mixture, dichloromethane (10 mL) was added and the mixture filtered *in vacuo*. The filtered solid was washed with dichloromethane. Concentrated hydrochloric acid (3 mL) was added to the filtrate and the resulting mixture stirred for 5 min, then filtered through celite and the celite washed with further dichloromethane. The filtrate was

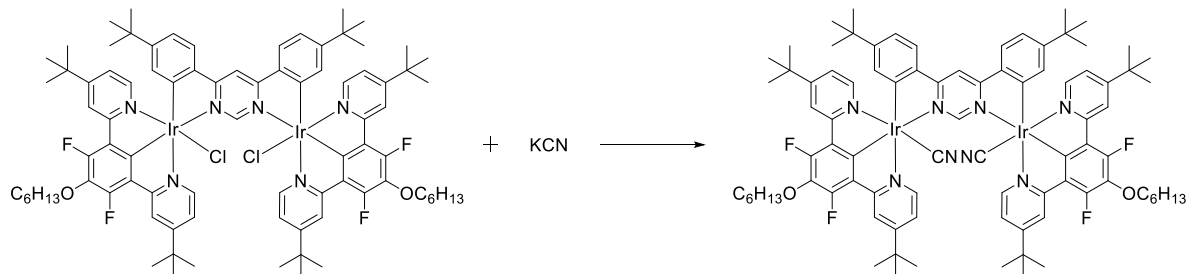
evaporated to dryness under reduced pressure and the residue treated with methanol (20 mL). The orange product was filtered off and washed with methanol. Yield: 125 mg, 0.08 mmol, 69%. ^1H NMR (CDCl_3 , 400 MHz): δ 11.75 (s, 1H), 8.41 (s, 1H), 8.11 (s, 4H), 7.81 (d, 6H, J = 6.8), 6.94 (d, 6H, J = 6.4), 6.82 (t, 2H, J = 11.8), 6.27 (s, 2H), 1.32 (s, 36H), 1.02 (s, 18H); ^{19}F NMR (CDCl_3 , 400 MHz): δ -109.49 (d, J = 12); HRMS (FTMS $^+$): for $[\text{M}-\text{Cl}]^+$ calc'd 1521.5015, found 1521.5026; for $[\text{M}-(\text{Ir}(\text{NCN})\text{Cl})-\text{Cl}]^+$ calc'd 915.3789, found 915.3784; for $[\text{M}-2\text{Cl}]^{2+}$ calc'd 743.2663, found 743.2655.

$\{\text{IrL}^{\text{C}}\text{Cl}\}_2\text{L}^1$ (C1)



A mixture of $[\text{IrL}^{\text{C}}\text{Cl}(\mu\text{-Cl})]_2$ (150 mg, 0.25 mmol), the bis-N^{HC} prolidyl ligand L^1H_2 (43 mg, 0.12 mmol), silver trifluoromethanesulfonate (101 mg, 0.37 mmol) and xylene (30 mL) was heated at 160°C for 8 h. To the cooled reaction mixture, dichloromethane (15 mL) and concentrated hydrochloric acid (3 mL) were added the mixture stirred for 5 min. The resulting mixture was filtered through celite and the celite washed with further dichloromethane. The filtrate was evaporated to dryness under reduced pressure and the residue treated with methanol (20 mL). The resulting orange-yellow product was filtered off and washed with methanol. Yield: 114 mg, 0.07 mmol, 59%. ^1H NMR (CDCl_3 , 400 MHz): δ 11.76 (s, 1H), 8.46 (s, 1H), 8.12 (d, 4H, J = 2.0), 7.85 (d, 2H, J = 8.4), 7.82 (d, 4H, J = 6.0), 7.02 (dd, 4H, J = 6.4, 2.4), 6.99 (dd, 2H, J = 8.4, 1.6), 6.24 (s, 2H), 1.35 (s, 36H), 1.02 (s, 18H); ^{19}F NMR (CDCl_3 , 400 MHz): δ -69.43 (s); HRMS (FTMS $^+$) for $[\text{M}-\text{Cl}]^+$ calc'd 1523.4920, found 1523.4917; for $[\text{M}-(\text{Ir}(\text{NCN})\text{Cl})-\text{Cl}]^+$ calc'd 916.3742, found 916.3735; for $[\text{M}+\text{NH}_4]^+$ calc'd 1572.4900, found 1572.4914.

(d) Metathesis of the monodentate ligand to form $\{\text{IrL}^{\text{A}}(\text{CN})\}_2\text{L}^1$ (A1')



To a solution of $\{\text{IrL}^{\text{A}}\text{Cl}\}_2\text{L}^1$ (88 mg, 0.05 mmol) in dichloromethane (15 mL), a solution of KCN (65 mg, 1 mmol) in methanol (15 mL) was added and the mixture was stirred at RT for 4 h. The mixture was then reduced to a volume of 2 mL. Methanol (10 mL) was added, and the resulting yellow solid product was filtered off, washed with methanol and dried. Yield: 65 mg, 75%. ^1H NMR (400 MHz, CDCl_3): δ 11.47 (s, 1H), 8.47 (s, 1H), 8.15 (br s, 4H), 7.87 (d, 2H, J = 8.0), 7.83 (d, 4H, J = 5.9), 7.00 (dd, 2H, J = 8.0, 1.6), 6.93 (dd, 4H, J = 5.9, 1.6), 6.30 (d, 2H, J = 1.6), 4.22 (t, 4H, J = 6.5), 1.94 (m, 4H), 1.64 (m, 4H), 1.44 (m, 8H), 1.34 (s, 36H), 1.02 (s, 18H), 0.97 (t, 6H, J = 6.9); ^{19}F NMR (400 MHz, CDCl_3): δ -126.5; HRMS (FTMS $^+$) for $[\text{M}+\text{H}]^+$ calc'd 1739.7252, found 1739.7240.

2. TD-DFT results and correlation with experimental data

(a) Tables of excitation energies, their oscillator strengths and main orbital components

Table S1 Selected calculated excitation energies (ΔE), oscillator strengths (f), and main orbital components for complex A1.^a

vacuum			dichloromethane		
ΔE , nm	f	transition (coefficient)	ΔE , nm	f	transition (coefficient)
526	(triplet)	HOMO-1 → LUMO (0.59) HOMO → LUMO (0.32)	499	(triplet)	HOMO-1 → LUMO (0.50) HOMO → LUMO (-0.43)
516	(triplet)	HOMO-3 → LUMO (0.55) HOMO-2 → LUMO (0.37)	484	(triplet)	HOMO-5 → LUMO (0.16) HOMO-3 → LUMO (0.60)
499	(triplet)	HOMO-1 → LUMO (-0.32) HOMO → LUMO (0.60)	462	(triplet)	HOMO-2 → LUMO+1 (0.31) HOMO-1 → LUMO+2 (-0.32)
494	0.033	HOMO → LUMO (0.70)	461	(triplet)	HOMO-2 → LUMO+2 (-0.28) HOMO-1 → LUMO+1 (0.35)
490	0.118	HOMO-1 → LUMO (0.70)	459	(triplet)	HOMO-3 → LUMO+1 (0.26) HOMO → LUMO+2 (0.36)
441	0.060	HOMO-2 → LUMO+1 (0.42) HOMO → LUMO+2 (0.39)	459	(triplet)	HOMO-2 → LUMO+2 (-0.30) HOMO → LUMO+1 (0.41)
433	0.018	HOMO-3 → LUMO+1 (0.42) HOMO-1 → LUMO+2 (-0.38)	456	0.308	HOMO-1 → LUMO (-0.47) HOMO → LUMO (0.52)
418	0.115	HOMO-3 → LUMO+4 (-0.33) HOMO-1 → LUMO+3 (0.38)	408	0.157	HOMO-2 → LUMO+1 (0.44) HOMO → LUMO+2 (-0.37)
412	0.053	HOMO-2 → LUMO+4 (0.40) HOMO → LUMO+3 (0.40)	398	0.020	HOMO-3 → LUMO+1 (0.42) HOMO-1 → LUMO+2 (-0.37)
379	0.371	HOMO-5 → LUMO (-0.17) HOMO-4 → LUMO (0.60)	387	0.219	HOMO-3 → LUMO+5 (-0.34) HOMO-1 → LUMO+3 (0.37)
369	0.040	HOMO-6 → LUMO (0.49) HOMO → LUMO+4 (-0.28)	381	0.114	HOMO-2 → LUMO+5 (0.36) HOMO → LUMO+3 (-0.36)
369	0.030	HOMO-6 → LUMO (0.43) HOMO-2 → LUMO+3 (-0.35)	380	0.030	HOMO-2 → LUMO+3 (0.41) HOMO-1 → LUMO+5 (-0.31)
			374	0.092	HOMO-4 → LUMO (0.48) HOMO-3 → LUMO+4 (-0.36)
			373	0.018	HOMO → LUMO+4 (0.41) HOMO → LUMO+5 (0.40)
			364	0.160	HOMO-3 → LUMO+1 (0.39) HOMO-1 → LUMO+2 (0.36)
			362	0.054	HOMO-5 → LUMO (0.54) HOMO-3 → LUMO+2 (0.33)
			362	0.024	HOMO-5 → LUMO (-0.32) HOMO-3 → LUMO+2 (0.38)
			359	0.109	HOMO-2 → LUMO+1 (0.32) HOMO-2 → LUMO+4 (0.28)
			359	0.075	HOMO-3 → LUMO+4 (0.32) HOMO → LUMO+2 (-0.30)

^aFor brevity, only transitions with f > 0.01 and/or ΔE > 350 nm are included, and only the two largest components of each transition are listed.

Table S2 Selected calculated excitation energies (ΔE), oscillator strengths (f), and main orbital components for complex **B1**.^a

vacuum			dichloromethane		
ΔE , nm	f	transition (coefficient)	ΔE , nm	f	transition (coefficient)
527	(triplet)	HOMO-1 → LUMO (-0.20) HOMO → LUMO (0.64)	498	(triplet)	HOMO-4 → LUMO (0.18) HOMO → LUMO (0.66)
516	(triplet)	HOMO-3 → LUMO (-0.16) HOMO-2 → LUMO (0.65)	483	(triplet)	HOMO-3 → LUMO (-0.19) HOMO-2 → LUMO (0.59)
492	0.130	HOMO → LUMO (0.70)	453	0.305	HOMO → LUMO (0.70)
486	0.012	HOMO-1 → LUMO (0.70)	399	0.107	HOMO-3 → LUMO+1 (-0.35) HOMO-1 → LUMO+2 (0.44)
433	0.026	HOMO-2 → LUMO+1 (0.32) HOMO-1 → LUMO+2 (0.44)	393	0.011	HOMO-2 → LUMO+2 (0.36) HOMO → LUMO+1 (0.52)
428	0.026	HOMO-2 → LUMO+1 (-0.34) HOMO → LUMO+2 (0.49)	393	0.029	HOMO-2 → LUMO+1 (0.37) HOMO → LUMO+2 (0.50)
415	0.127	HOMO-2 → LUMO+5 (-0.34) HOMO → LUMO+3 (0.43)	383	0.268	HOMO-2 → LUMO+4 (-0.32) HOMO → LUMO+3 (0.45)
406	0.048	HOMO-2 → LUMO+4 (-0.37) HOMO-1 → LUMO+3 (0.42)	374	0.240	HOMO-4 → LUMO (0.37) HOMO-1 → LUMO+3 (0.41)
398	0.019	HOMO-2 → LUMO+4 (0.43) HOMO-2 → LUMO+5 (0.28)	373	0.034	HOMO-3 → LUMO+3 (0.32) HOMO-1 → LUMO+4 (0.33)
380	0.015	HOMO-3 → LUMO+1 (0.44) HOMO-1 → LUMO+2 (-0.39)	371	0.048	HOMO-4 → LUMO (0.43) HOMO-2 → LUMO+5 (0.42)
379	0.341	HOMO-4 → LUMO (0.61) HOMO-2 → LUMO+4 (-0.19)	369	0.045	HOMO-5 → LUMO (-0.36) HOMO → LUMO+5 (0.49)
369	0.067	HOMO-5 → LUMO (0.68)	360	0.128	HOMO-2 → LUMO+1 (-0.33) HOMO → LUMO+2 (0.43)
			360	0.046	HOMO-5 → LUMO (0.54) HOMO-1 → LUMO+4 (-0.25)
			356	0.111	HOMO-3 → LUMO+5 (-0.30) HOMO-2 → LUMO+5 (0.34)

^aFor brevity, only transitions with f > 0.01 and/or ΔE > 350 nm are included, and only the two largest components of each transition are listed.

Table S3 Selected calculated excitation energies (ΔE), oscillator strengths (f), and main orbital components for complex **C1**.^a

vacuum			dichloromethane		
ΔE , nm	f	transition (coefficient)	ΔE , nm	f	transition (coefficient)
520	(triplet)	HOMO-4 → LUMO (-0.17) HOMO → LUMO (0.67)	492	(triplet)	HOMO-4 → LUMO (0.19) HOMO → LUMO (0.65)
509	(triplet)	HOMO-7 → LUMO (-0.13) HOMO-1 → LUMO (0.66)	476	(triplet)	HOMO-1 → LUMO (0.61) HOMO → LUMO+5 (-0.18)
484	0.144	HOMO → LUMO (0.70)	449	(triplet)	HOMO-1 → LUMO+1 (-0.36) HOMO → LUMO+2 (0.38)
409	0.127	HOMO-3 → LUMO+1 (-0.35) HOMO-2 → LUMO+2 (0.42)	449	(triplet)	HOMO-1 → LUMO+2 (-0.36) HOMO → LUMO+1 (0.38)
396	0.014	HOMO-1 → LUMO+4 (-0.30) HOMO-1 → LUMO+5 (0.47)	448	0.324	HOMO → LUMO (0.70)
390	0.071	HOMO-3 → LUMO+4 (-0.31) HOMO-2 → LUMO+3 (0.44)	397	0.013	HOMO-1 → LUMO+2 (-0.43) HOMO → LUMO+1 (0.54)
376	0.142	HOMO-4 → LUMO (0.40) HOMO-3 → LUMO+5 (0.37)	397	0.016	HOMO-1 → LUMO+1 (-0.44) HOMO → LUMO+2 (0.52)
375	0.204	HOMO-4 → LUMO (0.45) HOMO-3 → LUMO+5 (-0.37)	374	0.277	HOMO-3 → LUMO+1 (-0.42) HOMO-2 → LUMO+2 (0.47)
365	0.070	HOMO-5 → LUMO (0.68)	368	0.093	HOMO-4 → LUMO (0.46) HOMO-1 → LUMO+5 (0.42)
			363	0.189	HOMO-1 → LUMO+1 (0.43) HOMO → LUMO+2 (0.38)
			360	0.246	HOMO-2 → LUMO+3 (-0.29) HOMO-1 → LUMO+5 (0.46)
			360	0.120	HOMO-5 → LUMO (0.63) HOMO-2 → LUMO+4 (0.20)

^aFor brevity, only transitions with f > 0.01 and/or ΔE > 350 nm are included, and only the two largest components of each transition are listed.

Table S4 Selected calculated excitation energies (ΔE), oscillator strengths (f), and main orbital components for complex A1'.^a

vacuum			dichloromethane		
ΔE , nm	f	transition (coefficient)	ΔE , nm	f	transition (coefficient)
496	(triplet)	HOMO-5 → LUMO (0.21) HOMO-2 → LUMO (0.65)	482	(triplet)	HOMO-5 → LUMO (0.24) HOMO-2 → LUMO (0.63)
483	(triplet)	HOMO-3 → LUMO (0.47) HOMO-1 → LUMO (0.36)	466	(triplet)	HOMO-4 → LUMO (0.36) HOMO-3 → LUMO (0.42)
472	(triplet)	HOMO-1 → LUMO+1 (-0.34) HOMO → LUMO (0.50)	451	(triplet)	HOMO-1 → LUMO+1 (0.37) HOMO → LUMO+2 (0.33)
470	(triplet)	HOMO-1 → LUMO+2 (0.40) HOMO → LUMO+1 (0.42)	451	(triplet)	HOMO-1 → LUMO+2 (0.37) HOMO → LUMO+1 (0.36)
463	(triplet)	HOMO → LUMO (0.47) HOMO → LUMO+2 (0.37)	445	(triplet)	HOMO-1 → LUMO+1 (0.26) HOMO → LUMO+2 (0.31)
450	0.237	HOMO-2 → LUMO (0.69)	445	(triplet)	HOMO-3 → LUMO+2 (0.26) HOMO → LUMO+1 (-0.30)
413	0.023	HOMO-1 → LUMO+2 (0.48) HOMO → LUMO+1 (0.48)	438	(triplet)	HOMO → LUMO (0.64) HOMO → LUMO+2 (0.18)
412	0.151	HOMO-1 → LUMO+1 (0.48) HOMO → LUMO+2 (0.48)	431	0.418	HOMO-2 → LUMO (0.69)
390	0.046	HOMO-3 → LUMO+1 (-0.40) HOMO-2 → LUMO+2 (0.50)	393	0.041	HOMO-1 → LUMO+2 (0.48) HOMO → LUMO+1 (0.49)
379	0.010	HOMO-1 → LUMO+1 (-0.20) HOMO-1 → LUMO+3 (0.60)	392	0.286	HOMO-1 → LUMO+1 (0.48) HOMO → LUMO+2 (0.49)
375	0.177	HOMO-5 → LUMO (0.43) HOMO → LUMO+4 (-0.35)	371	0.017	HOMO-3 → LUMO+2 (0.36) HOMO-2 → LUMO+1 (0.54)
374	0.048	HOMO-1 → LUMO+4 (0.36) HOMO → LUMO+5 (0.40)	371	0.041	HOMO-3 → LUMO+1 (0.37) HOMO-2 → LUMO+2 (0.54)
370	0.032	HOMO-5 → LUMO (0.33) HOMO-3 → LUMO+3 (0.38)	364	0.133	HOMO-4 → LUMO (0.61) HOMO-1 → LUMO+4 (0.21)
368	0.109	HOMO-3 → LUMO+5 (-0.40) HOMO-2 → LUMO+4 (0.51)	363	0.351	HOMO-8 → LUMO (-0.17) HOMO-5 → LUMO (0.62)
367	0.057	HOMO-3 → LUMO+4 (-0.38) HOMO-2 → LUMO+5 (0.47)	358	0.035	HOMO-1 → LUMO+3 (0.51) HOMO → LUMO+4 (-0.29)
360	0.123	HOMO-3 → LUMO+1 (0.37) HOMO-2 → LUMO+2 (0.37)	354	0.014	HOMO-1 → LUMO+3 (0.33) HOMO-1 → LUMO+5 (-0.32)
356	0.050	HOMO-3 → LUMO+1 (0.33) HOMO-3 → LUMO+3 (0.47)	351	0.096	HOMO-3 → LUMO+5 (-0.40) HOMO-2 → LUMO+4 (0.53)
			351	0.015	HOMO-2 → LUMO+3 (0.29) HOMO-2 → LUMO+5 (0.31)
			351	0.011	HOMO-2 → LUMO+3 (-0.32) HOMO-2 → LUMO+5 (0.41)

^aFor brevity, only transitions with f > 0.01 and/or ΔE > 350 nm are included, and only the two largest components of each transition are listed.

Table S5 Selected calculated excitation energies (ΔE), oscillator strengths (f), and main orbital components for complex **A2**.^a

vacuum			dichloromethane		
ΔE , nm	f	transition (coefficient)	ΔE , nm	f	transition (coefficient)
535	(triplet)	HOMO-1 → LUMO (0.64) HOMO → LUMO (-0.21)	504	(triplet)	HOMO-1 → LUMO (0.64) HOMO → LUMO (-0.21)
525	(triplet)	HOMO-3 → LUMO (0.62) HOMO-2 → LUMO (-0.26)	490	(triplet)	HOMO-3 → LUMO (0.64) HOMO-1 → LUMO+3 (-0.14)
510	(triplet)	HOMO-1 → LUMO (0.22) HOMO → LUMO (0.66)	466	(triplet)	HOMO-1 → LUMO (0.20) HOMO → LUMO (0.62)
497	0.123	HOMO-1 → LUMO (0.70)	461	0.202	HOMO-1 → LUMO (-0.48) HOMO → LUMO (0.51)
438	0.070	HOMO-2 → LUMO+1 (-0.42) HOMO → LUMO+2 (0.45)	459	0.059	HOMO-1 → LUMO (0.51) HOMO → LUMO (0.48)
430	0.017	HOMO-3 → LUMO+1 (0.45) HOMO-1 → LUMO+2 (0.43)	405	0.177	HOMO-2 → LUMO+1 (-0.45) HOMO → LUMO+2 (0.46)
415	0.116	HOMO-3 → LUMO+5 (0.42) HOMO-1 → LUMO+4 (-0.42)	394	0.011	HOMO-3 → LUMO+2 (-0.40) HOMO-1 → LUMO+1 (0.48)
412	0.057	HOMO-2 → LUMO+5 (0.35) HOMO → LUMO+4 (0.41)	394	0.024	HOMO-3 → LUMO+1 (-0.42) HOMO-1 → LUMO+2 (0.45)
382	0.171	HOMO-5 → LUMO (-0.29) HOMO-4 → LUMO (0.58)	384	0.215	HOMO-3 → LUMO+5 (0.42) HOMO-1 → LUMO+4 (0.46)
380	0.110	HOMO-5 → LUMO (0.56) HOMO-4 → LUMO (0.36)	380	0.143	HOMO-2 → LUMO+5 (0.37) HOMO → LUMO+4 (0.41)
370	0.021	HOMO-7 → LUMO (0.33) HOMO-6 → LUMO (0.61)	379	0.018	HOMO-2 → LUMO+4 (0.36) HOMO → LUMO+5 (0.34)
368	0.013	HOMO-2 → LUMO+4 (0.38) HOMO → LUMO+5 (-0.37)	376	0.058	HOMO-4 → LUMO (0.48) HOMO-3 → LUMO+3 (-0.45)
368	0.025	HOMO-7 → LUMO (0.48) HOMO-2 → LUMO+4 (0.31)	373	0.023	HOMO-5 → LUMO (0.27) HOMO-1 → LUMO+3 (0.56)
			362	0.180	HOMO-4 → LUMO (0.39) HOMO-1 → LUMO+2 (0.33)
			362	0.061	HOMO-5 → LUMO (0.61) HOMO-1 → LUMO+3 (-0.19)
			358	0.026	HOMO-3 → LUMO+1 (0.38) HOMO-3 → LUMO+3 (-0.36)

^aFor brevity, only transitions with f > 0.01 and/or ΔE > 350 nm are included, and only the two largest components of each transition are listed.

Table S6 Selected calculated excitation energies (ΔE), oscillator strengths (f), and main orbital components for complex **A3**.^a

vacuum			dichloromethane		
ΔE , nm	f	transition (coefficient)	ΔE , nm	f	transition (coefficient)
518	(triplet)	HOMO-2 → LUMO (0.59) HOMO → LUMO (0.33)	492	(triplet)	HOMO-2 → LUMO (0.63) HOMO → LUMO (0.21)
509	(triplet)	HOMO-3 → LUMO (0.57) HOMO-1 → LUMO (-0.37)	481	(triplet)	HOMO-3 → LUMO (0.58) HOMO-1 → LUMO (-0.28)
506	(triplet)	HOMO-2 → LUMO (-0.33) HOMO → LUMO (0.61)	473	(triplet)	HOMO-2 → LUMO (-0.21) HOMO → LUMO (0.66)
501	(triplet)	HOMO → LUMO (0.70)	470	(triplet)	HOMO-3 → LUMO+2 (0.31) HOMO → LUMO+4 (-0.40)
487	0.092	HOMO-2 → LUMO (0.70)	468	0.016	HOMO → LUMO (0.70)
426	0.082	HOMO-1 → LUMO+1 (0.45) HOMO → LUMO+2 (0.46)	456	0.195	HOMO-2 → LUMO (0.70)
413	0.029	HOMO-3 → LUMO+1 (0.42) HOMO-2 → LUMO+2 (0.41)	397	0.016	HOMO-1 → LUMO+2 (-0.46) HOMO → LUMO+1 (0.50)
402	0.072	HOMO-3 → LUMO+4 (0.39) HOMO → LUMO+3 (-0.36)	396	0.214	HOMO-1 → LUMO+1 (-0.46) HOMO → LUMO+2 (0.49)
399	0.119	HOMO-2 → LUMO+3 (0.31) HOMO-1 → LUMO+4 (0.38)	379	0.011	HOMO-1 → LUMO+4 (-0.34) HOMO → LUMO+3 (0.37)
397	0.021	HOMO-1 → LUMO+3 (0.41) HOMO → LUMO+4 (-0.38)	378	0.402	HOMO-5 → LUMO (0.59) HOMO-2 → LUMO+2 (-0.23)
385	0.121	HOMO-5 → LUMO (-0.30) HOMO-4 → LUMO (0.48)	373	0.095	HOMO-4 → LUMO (0.55) HOMO → LUMO+4 (-0.24)
380	0.022	HOMO-1 → LUMO+1 (0.40) HOMO → LUMO+2 (-0.35)	371	0.036	HOMO-3 → LUMO+3 (-0.44) HOMO-2 → LUMO+4 (0.47)
374	0.015	HOMO-1 → LUMO+1 (0.27) HOMO-1 → LUMO+5 (0.56)	371	0.145	HOMO-3 → LUMO+4 (-0.45) HOMO-2 → LUMO+3 (0.48)
373	0.044	HOMO-3 → LUMO+1 (-0.43) HOMO-2 → LUMO+2 (0.46)			
373	0.018	HOMO-6 → LUMO (0.47) HOMO-3 → LUMO+2 (-0.34)			
368	0.084	HOMO-5 → LUMO (-0.22) HOMO-3 → LUMO+5 (0.60)			
368	0.043	HOMO-7 → LUMO (0.55) HOMO-2 → LUMO+5 (0.35)			

^aFor brevity, only transitions with f > 0.01 and/or ΔE > 350 nm are included, and only the two largest components of each transition are listed.

Table S7 Selected calculated excitation energies (ΔE), oscillator strengths (f), and main orbital components for complex A4.^a

vacuum			dichloromethane		
ΔE , nm	f	transition (coefficient)	ΔE , nm	f	transition (coefficient)
510	(triplet)	HOMO-4 → LUMO (0.21) HOMO → LUMO (0.60)	497	(triplet)	HOMO-4 → LUMO (0.17) HOMO → LUMO (0.65)
490	(triplet)	HOMO-3 → LUMO (-0.39) HOMO-2 → LUMO (0.43)	475	(triplet)	HOMO-5 → LUMO (-0.26) HOMO-3 → LUMO (0.52)
485	(triplet)	HOMO-2 → LUMO+1 (0.37) HOMO-1 → LUMO+2 (0.41)	459	(triplet)	HOMO-3 → LUMO+1 (-0.22) HOMO → LUMO+2 (0.24)
485	(triplet)	HOMO-2 → LUMO+2 (0.34) HOMO-1 → LUMO+1 (0.46)	459	(triplet)	HOMO-3 → LUMO+2 (-0.23) HOMO → LUMO+1 (0.24)
476	(triplet)	HOMO-3 → LUMO+1 (0.31) HOMO → LUMO+2 (0.39)	456	(triplet)	HOMO-2 → LUMO+1 (0.40) HOMO-1 → LUMO+2 (0.41)
476	(triplet)	HOMO-3 → LUMO+2 (0.31) HOMO → LUMO+1 (0.40)	456	(triplet)	HOMO-2 → LUMO+2 (0.38) HOMO-1 → LUMO+1 (0.44)
461	0.238	HOMO → LUMO (0.69)	438	0.529	HOMO → LUMO (0.69)
457	0.024	HOMO-2 → LUMO+1 (0.10) HOMO-1 → LUMO (0.69)	406	0.148	HOMO-2 → LUMO+1 (0.43) HOMO-1 → LUMO+2 (0.47)
441	0.054	HOMO-2 → LUMO+1 (0.36) HOMO-1 → LUMO+2 (0.47)	387	0.224	HOMO-3 → LUMO+4 (-0.37) HOMO → LUMO+3 (0.50)
419	0.121	HOMO-3 → LUMO+4 (0.32) HOMO → LUMO+3 (0.46)	379	0.030	HOMO-2 → LUMO+4 (0.40) HOMO-1 → LUMO+3 (0.47)
410	0.021	HOMO-2 → LUMO+4 (0.33) HOMO-1 → LUMO+3 (0.48)	378	0.016	HOMO-2 → LUMO+3 (0.43) HOMO-1 → LUMO+4 (0.44)
384	0.062	HOMO-4 → LUMO (0.41) HOMO-2 → LUMO+5 (0.42)	367	0.232	HOMO-4 → LUMO (0.51) HOMO-3 → LUMO+1 (0.28)
370	0.366	HOMO-4 → LUMO (0.48) HOMO-3 → LUMO+5 (0.28)	352	0.091	HOMO-4 → LUMO (0.15) HOMO-2 → LUMO+5 (0.65)
368	0.073	HOMO-3 → LUMO+4 (0.36) HOMO-2 → LUMO+4 (0.37)	352	0.137	HOMO-7 → LUMO (-0.13) HOMO-5 → LUMO (0.67)
358	0.056	HOMO-8 → LUMO+1 (0.17) HOMO-4 → LUMO+2 (0.63)	350	0.292	HOMO-4 → LUMO (0.27) HOMO-3 → LUMO+5 (0.61)
354	0.103	HOMO-8 → LUMO (-0.16) HOMO-5 → LUMO (0.64)			
353	0.023	HOMO-7 → LUMO+1 (-0.14) HOMO-6 → LUMO (0.68)			

^aFor brevity, only transitions with f > 0.01 and/or ΔE > 350 nm are included, and only the two largest components of each transition are listed.

Table S8 Selected calculated excitation energies (ΔE), oscillator strengths (f), and main orbital components for complex **A5**.^a

vacuum			dichloromethane		
ΔE , nm	f	transition (coefficient)	ΔE , nm	f	transition (coefficient)
581	(triplet)	HOMO-4 → LUMO (-0.18) HOMO → LUMO (0.63)	572	(triplet)	HOMO-2 → LUMO+5 (-0.13) HOMO → LUMO (0.65)
546	(triplet)	HOMO-2 → LUMO (0.51) HOMO → LUMO+5 (-0.30)	536	(triplet)	HOMO-2 → LUMO (0.51) HOMO → LUMO+5 (-0.35)
485	(triplet)	HOMO-3 → LUMO+1 (0.43) HOMO-1 → LUMO+2 (0.38)	461	(triplet)	HOMO-2 → LUMO+2 (0.28) HOMO → LUMO+1 (0.34)
484	(triplet)	HOMO-3 → LUMO+2 (0.39) HOMO-1 → LUMO+1 (0.48)	461	(triplet)	HOMO-2 → LUMO+1 (0.28) HOMO → LUMO+2 (0.33)
479	(triplet)	HOMO-2 → LUMO+2 (0.35) HOMO → LUMO+1 (0.45)	461	0.620	HOMO → LUMO (0.69)
478	(triplet)	HOMO-2 → LUMO+1 (0.36) HOMO → LUMO+2 (0.43)	408	0.049	HOMO-1 → LUMO+2 (0.37) HOMO → LUMO+3 (0.41)
477	0.362	HOMO-2 → LUMO+1 (0.10) HOMO → LUMO (0.69)	394	0.322	HOMO-1 → LUMO+2 (-0.35) HOMO → LUMO+3 (0.45)
455	0.012	HOMO-2 → LUMO (0.64) HOMO → LUMO+1 (0.21)	378	0.019	HOMO-2 → LUMO+1 (0.52) HOMO-1 → LUMO+3 (-0.22)
440	0.034	HOMO-3 → LUMO+1 (0.37) HOMO-1 → LUMO+2 (0.43)	373	0.013	HOMO-2 → LUMO+2 (0.54) HOMO-1 → LUMO+4 (-0.24)
422	0.157	HOMO-2 → LUMO+4 (-0.31) HOMO → LUMO+3 (0.47)	368	0.106	HOMO-4 → LUMO (0.56) HOMO-2 → LUMO+5 (-0.29)
385	0.098	HOMO-4 → LUMO (0.55) HOMO-2 → LUMO+5 (0.38)	362	0.012	HOMO-2 → LUMO+4 (0.55) HOMO → LUMO+3 (-0.33)
368	0.088	HOMO-3 → LUMO+4 (0.43) HOMO-1 → LUMO+3 (-0.41)			
366	0.203	HOMO-3 → LUMO+4 (-0.34) HOMO-2 → LUMO+5 (0.45)			
355	0.066	HOMO-4 → LUMO+2 (0.61) HOMO-2 → LUMO+5 (-0.19)			
354	0.017	HOMO-7 → LUMO+1 (0.12) HOMO-5 → LUMO (0.68)			
350	0.148	HOMO-8 → LUMO (-0.26) HOMO-6 → LUMO (0.61)			

^aFor brevity, only transitions with f > 0.01 and/or ΔE > 350 nm are included, and only the two largest components of each transition are listed.

(b) Simulated absorption spectra

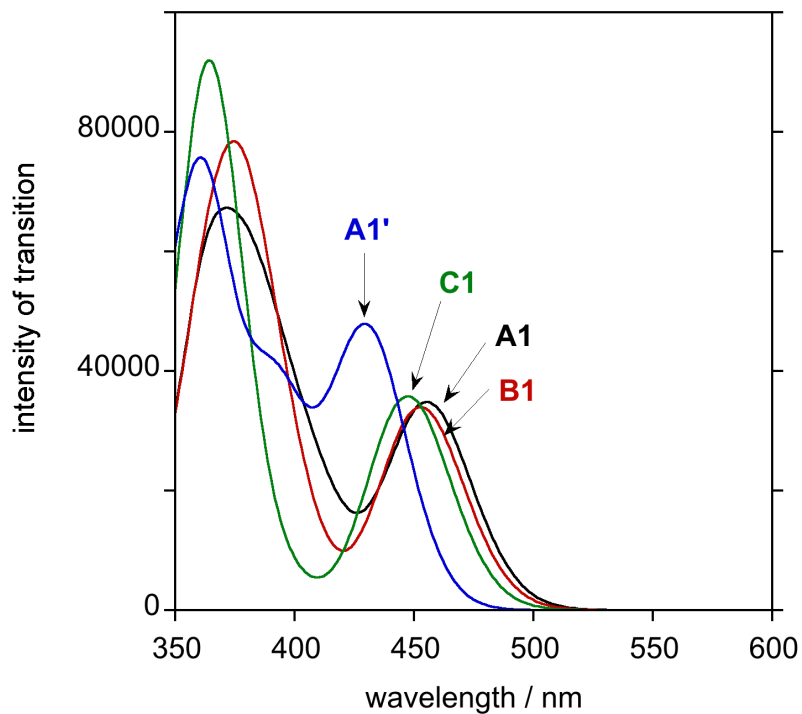
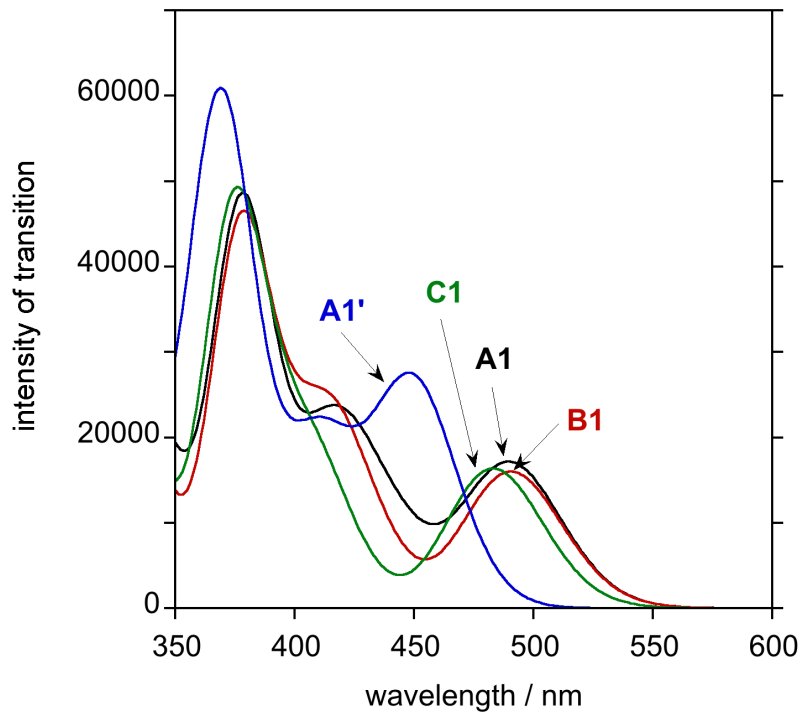


Figure S1 Simulated absorption spectra of the A1–C1 series of complexes, also including A1', using the spin-allowed transitions obtained from TD-DFT calculations; **top:** in vacuum; **bottom:** in DCM using the polarised continuum model.

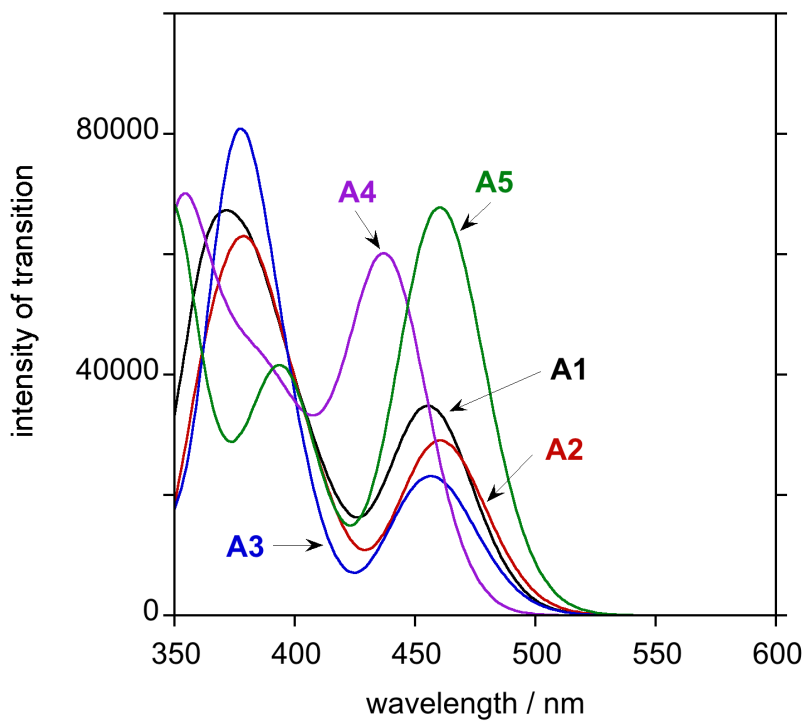
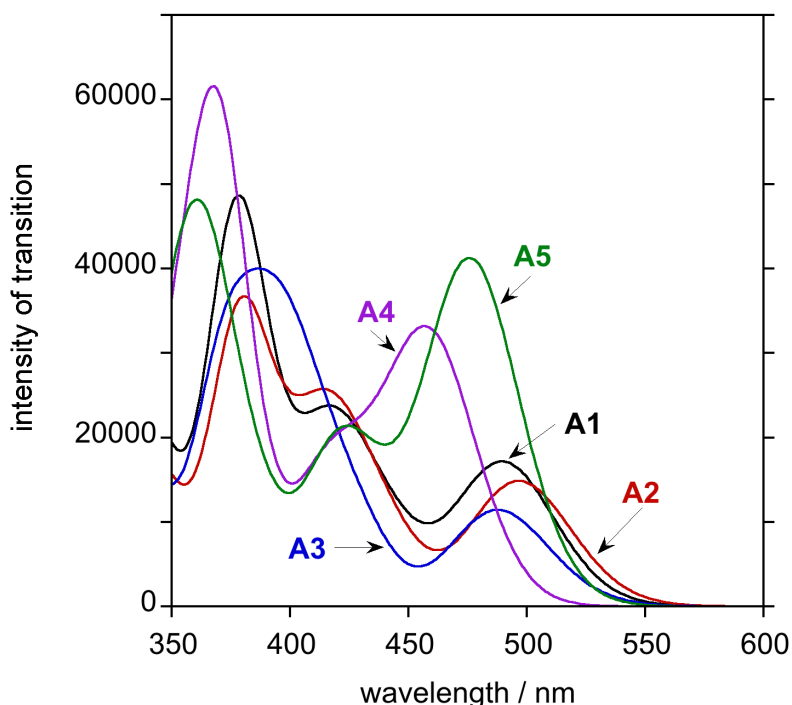


Figure S2 Simulated absorption spectra of the A1–A5 series of complexes generated using the spin-allowed transitions obtained from TD-DFT calculations; **top:** in vacuum; **bottom:** in DCM using the polarised continuum model.

(c) Additional plots showing experimental versus calculated data

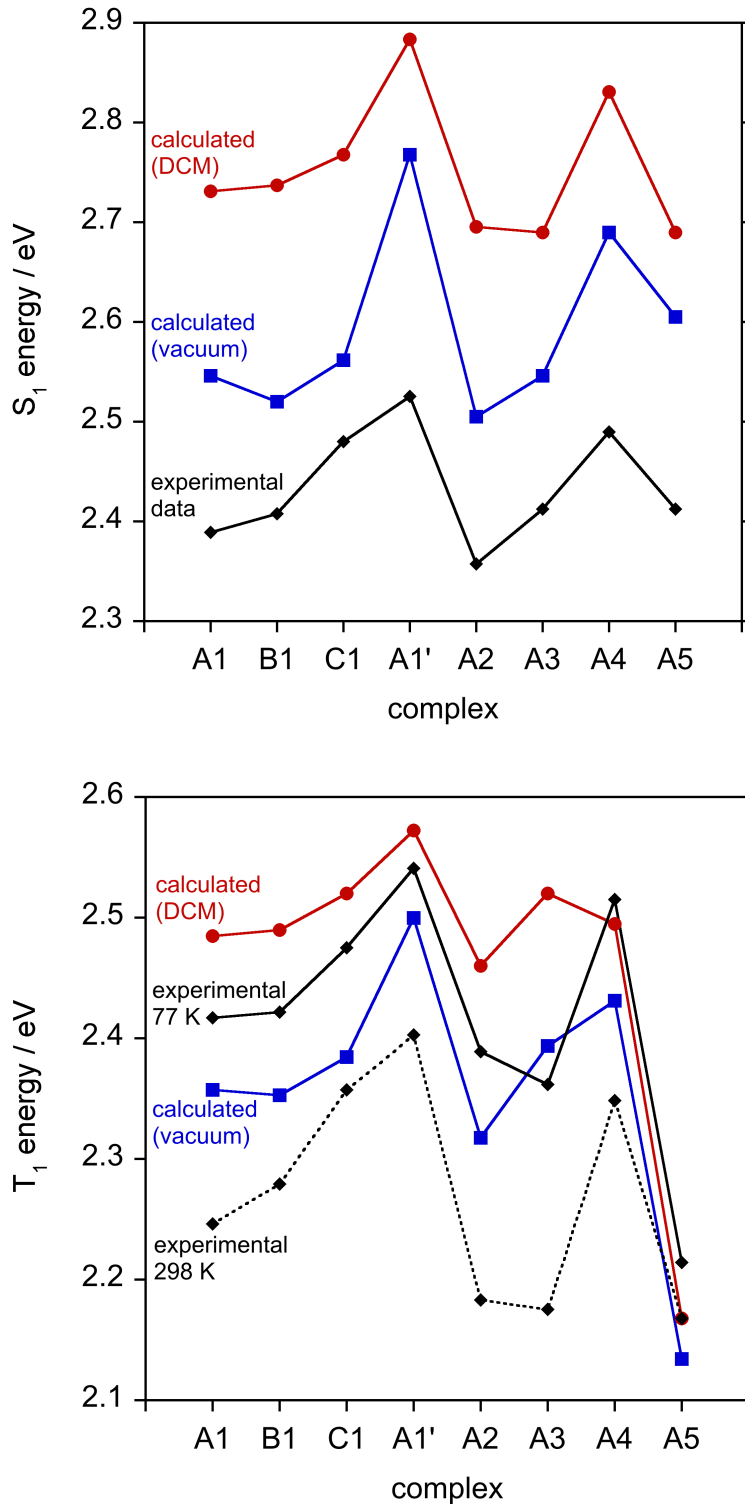


Figure S3 Top: Calculated energy of the first-excited singlet state S_1 of the dinuclear complexes in vacuum (blue) and in DCM (red), with the experimental value shown in black, estimated based on λ_{\max} of the lowest-energy absorption band (excluding the weak band at 554 nm for **A5**, which is concluded to be a triplet transition, $S_0 \rightarrow T_1$ – see text). **Bottom:** Corresponding plots for the lowest-lying triplet state T_1 , using experimental $\lambda_{\max}(0,0)$ values from emission spectra at 298 K and at 77 K. The lines between points are provided solely as a guide to aid the eye.

(d) Frontier orbital plots of the dinuclear complexes, with their energies in Hartree (energies in eV in parenthesis)

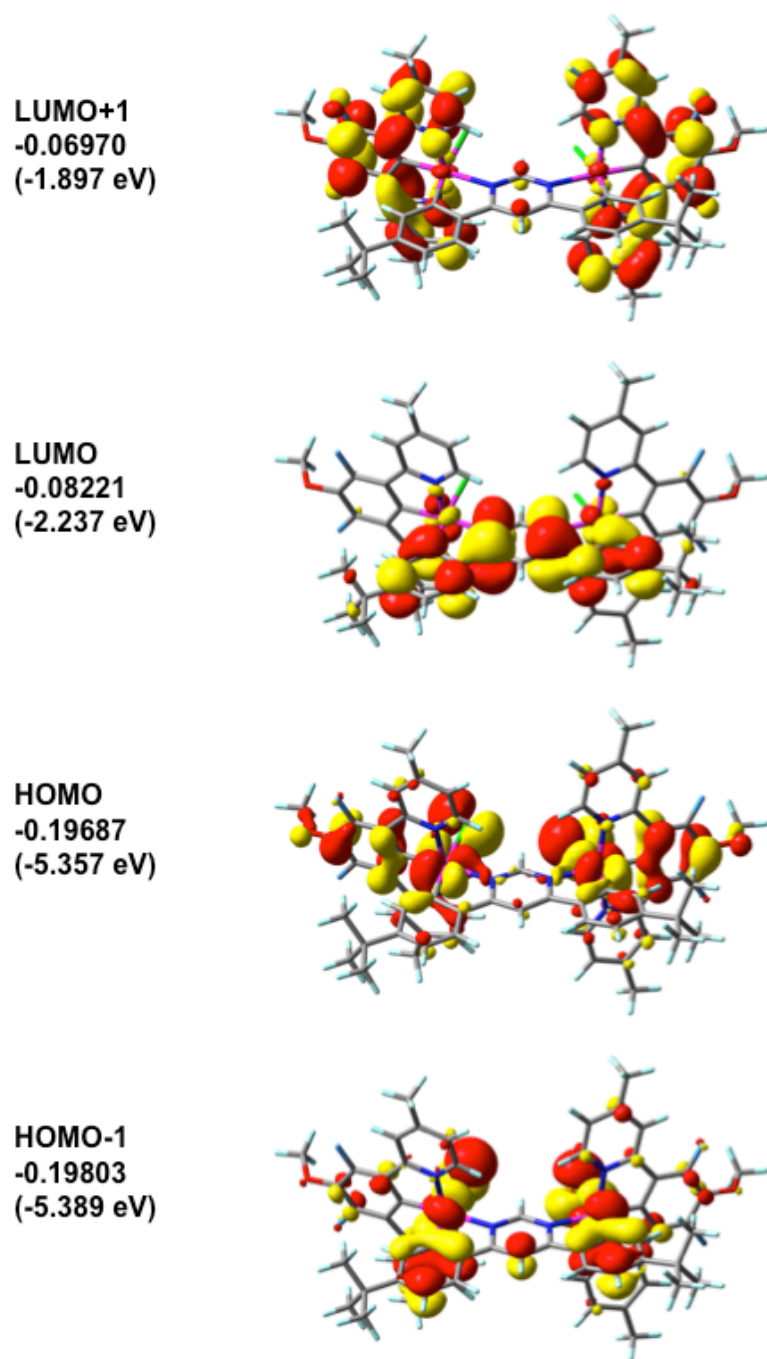


Figure S4 Frontier orbitals and their energies in Hartree (eV) for complex A1

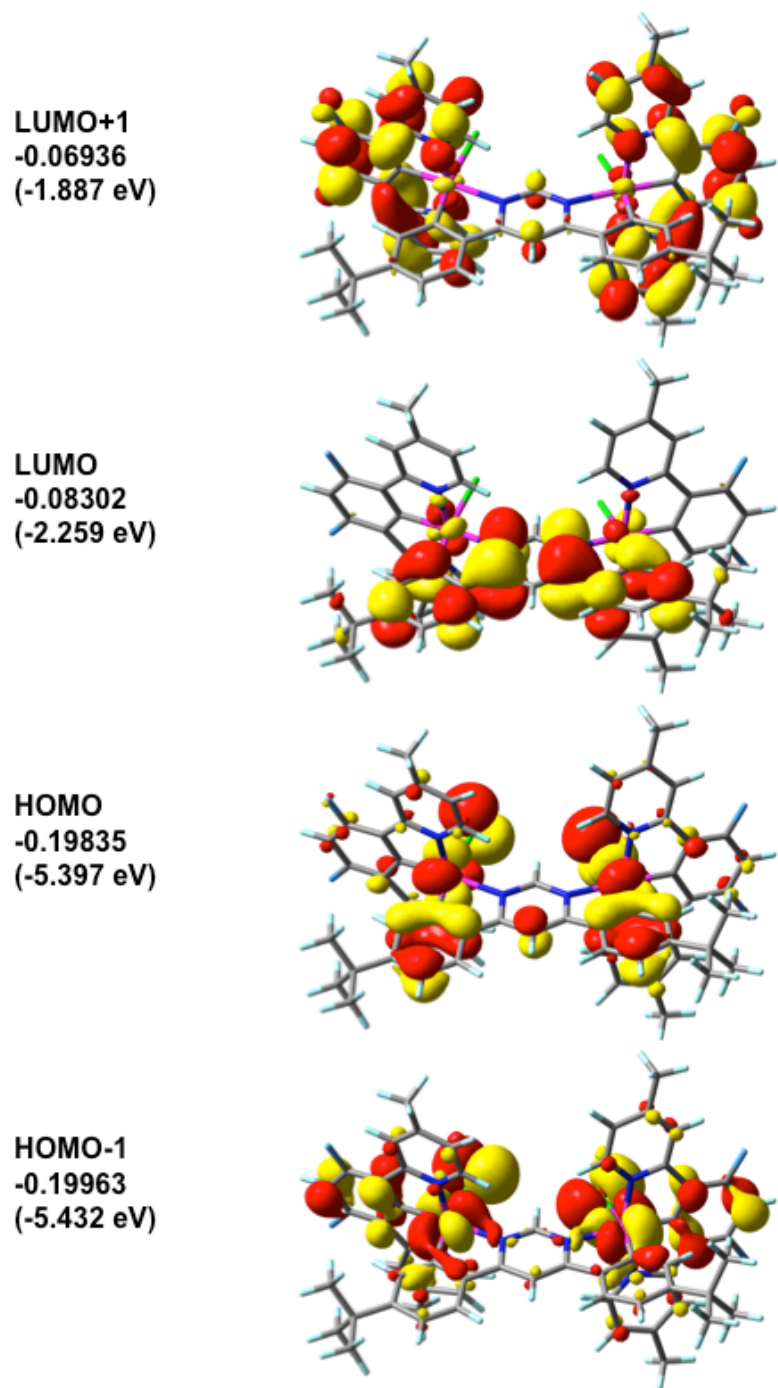


Figure S5 Frontier orbitals and their energies in Hartree (eV) of complex **B1**

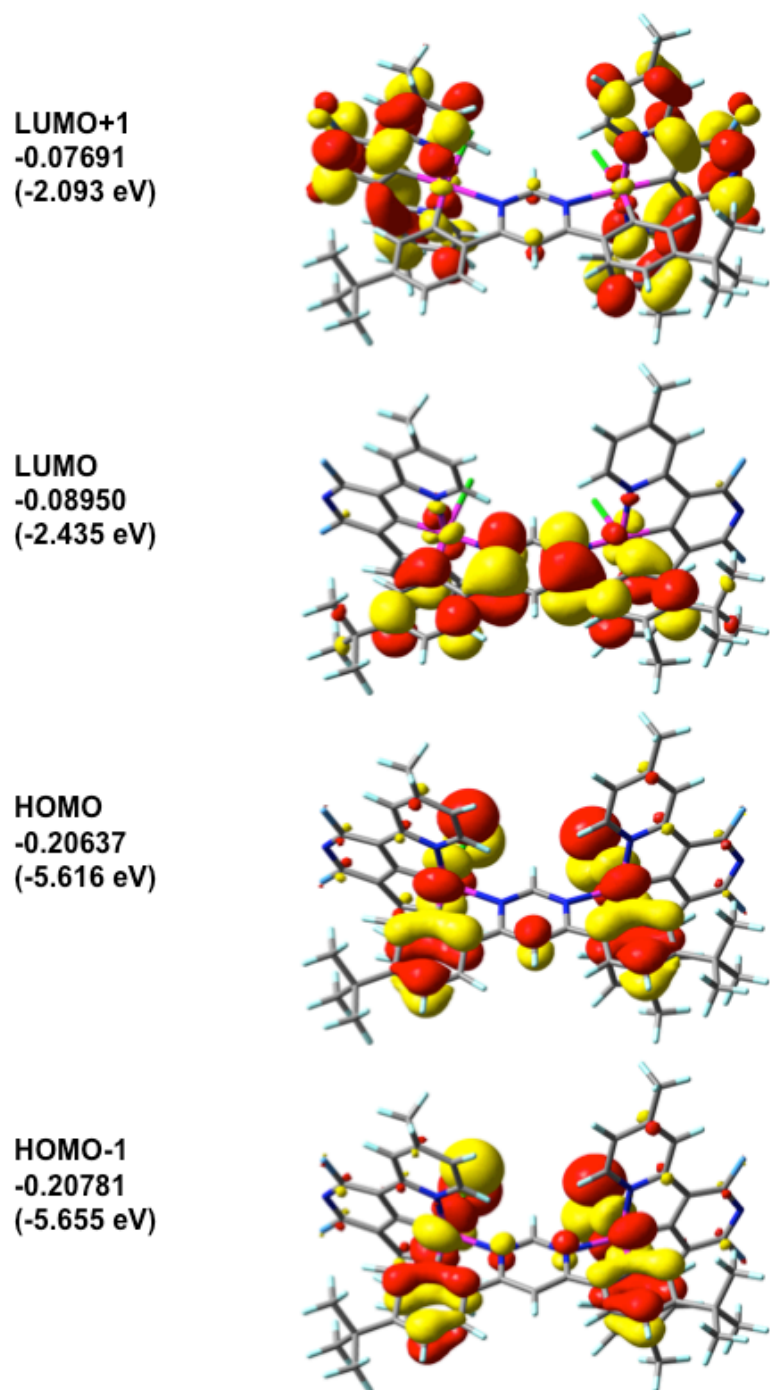


Figure S6 Frontier orbitals and their energies in Hartree (eV) of complex **C1**

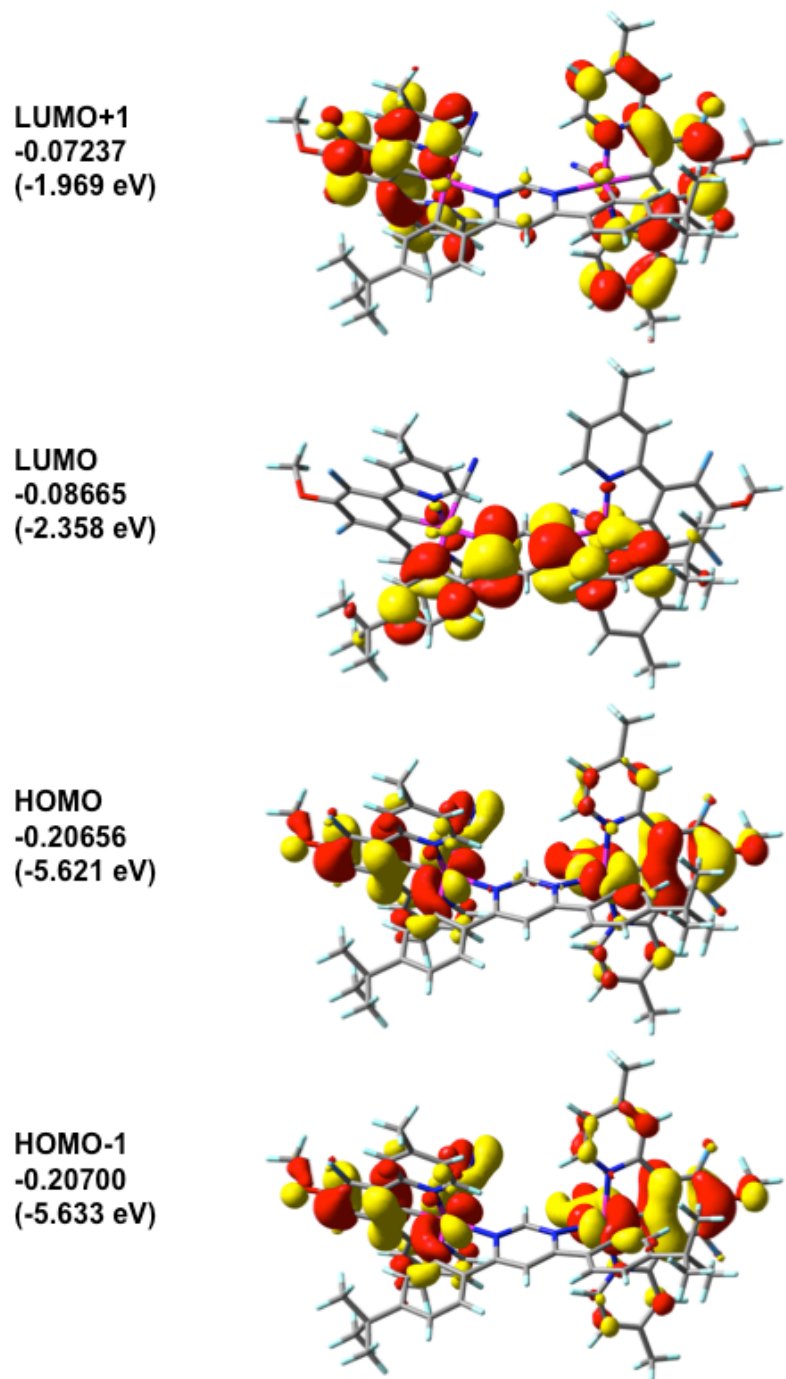


Figure S7 Frontier orbitals and their energies in Hartree (eV) of complex **A1'**

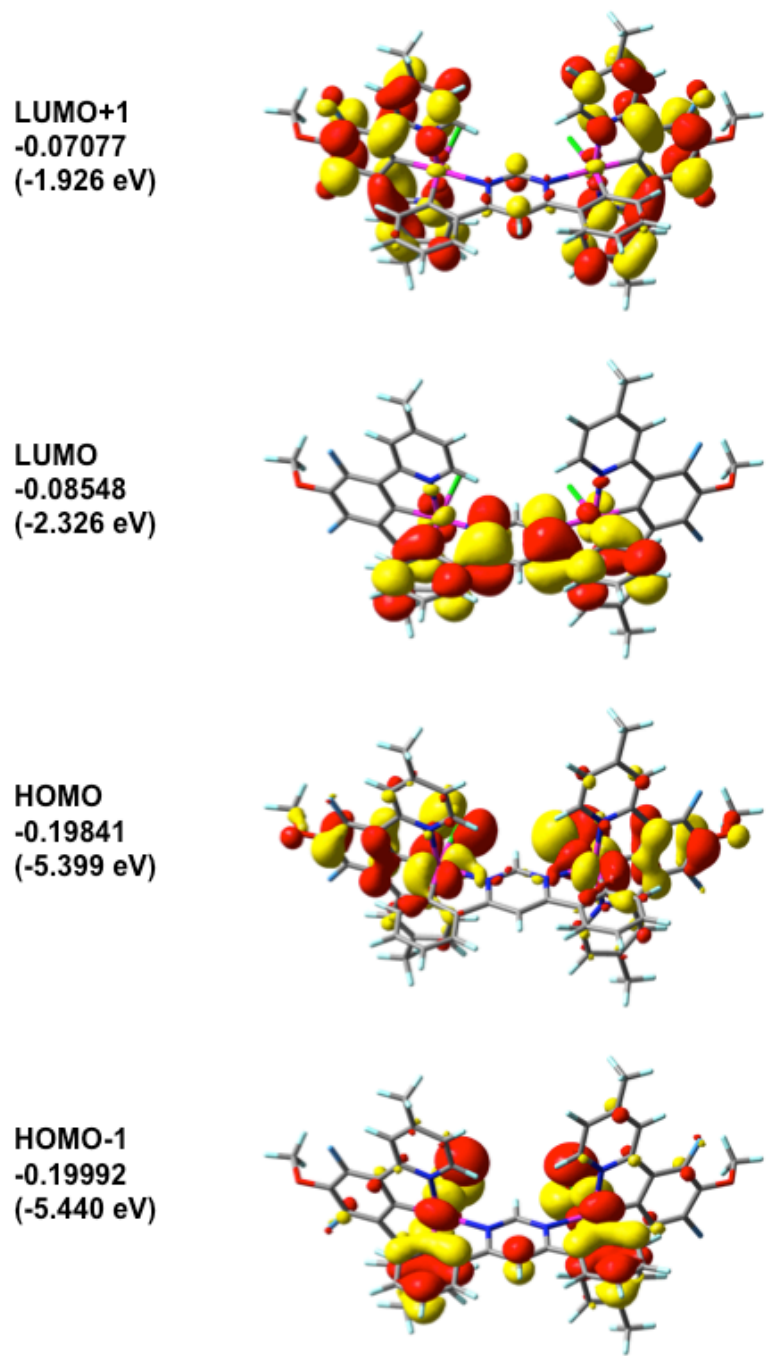


Figure S8 Frontier orbitals and their energies in Hartree (eV) of complex **A2**

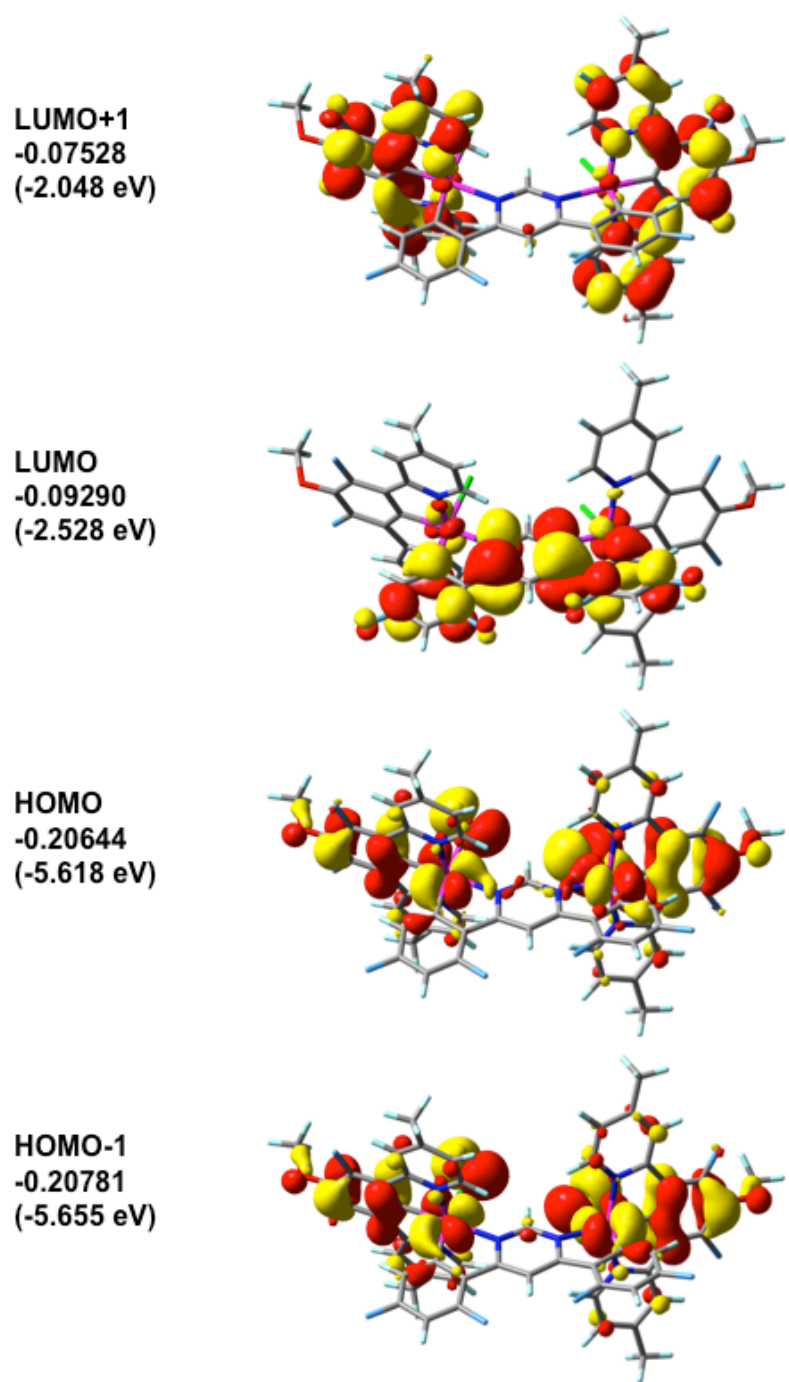


Figure S9 Frontier orbitals and their energies in Hartree (eV) of complex **A3**

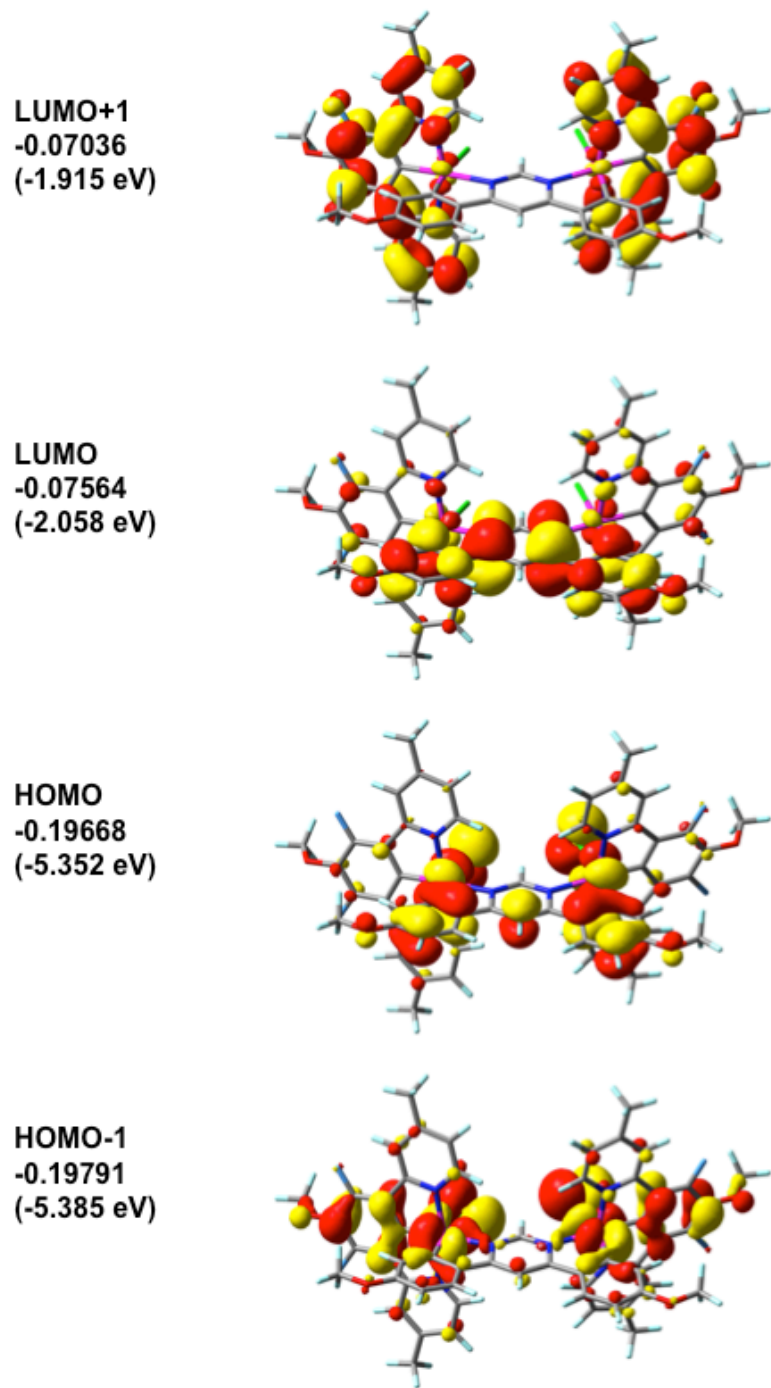


Figure S10 Frontier orbitals and their energies in Hartree (eV) of complex **A4**

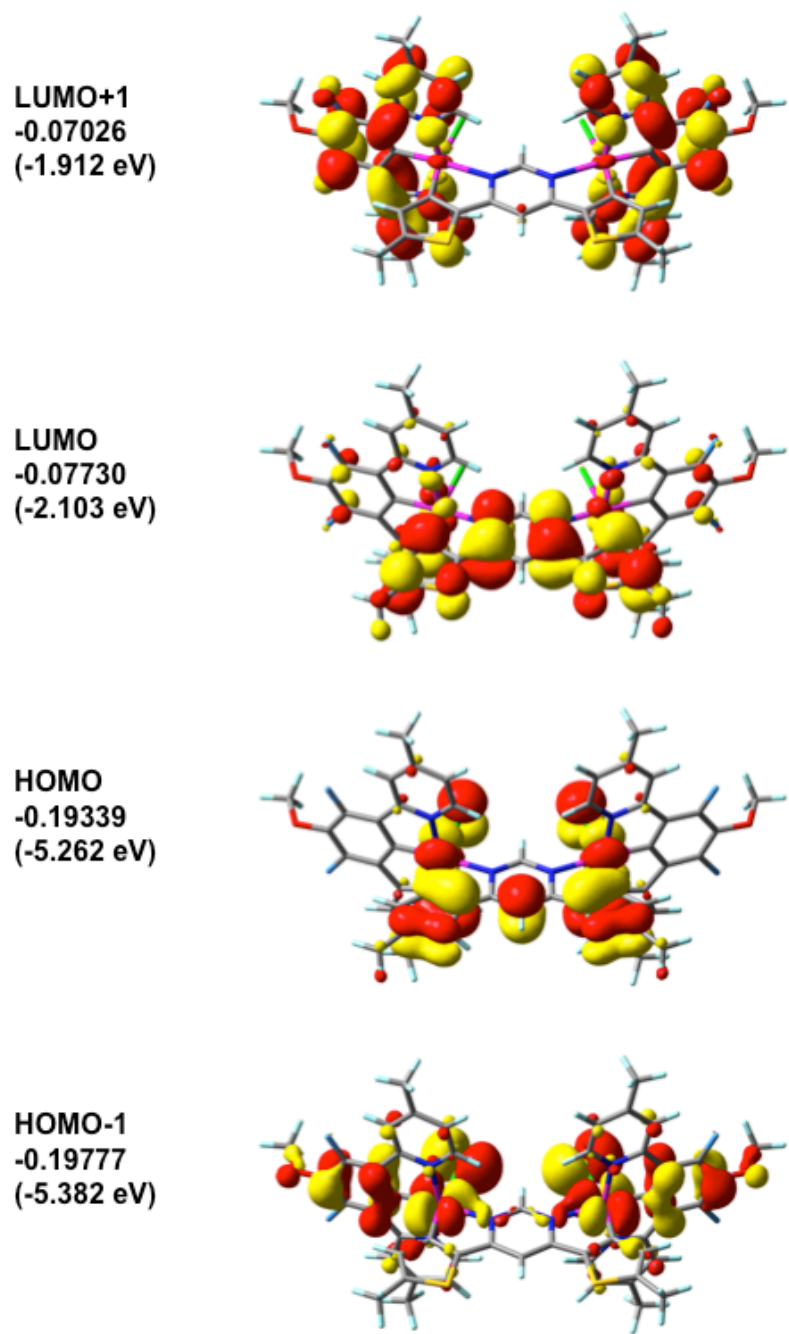
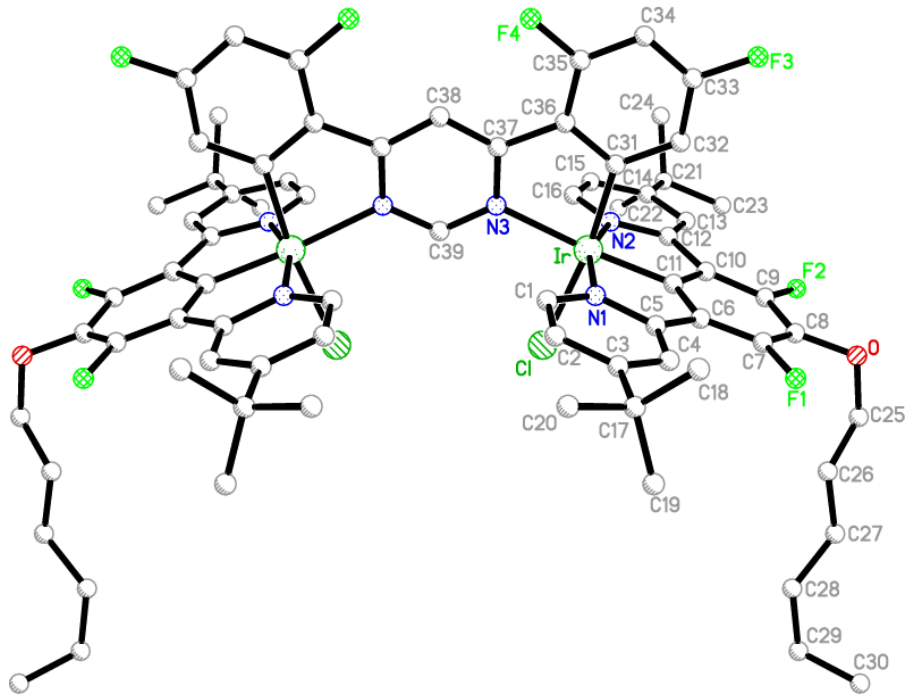


Figure S11 Frontier orbitals and their energies in Hartree (eV) of complex **A5**

3. X-ray crystallography of complex A3

Data collected at Diamond Light Source, April 2014
Bill Clegg and Mike Probert



The molecular structure with H atoms omitted. The molecule has a crystallographic mirror plane, passing through atoms C38 and C39. Twofold disorder was modelled for atoms C28–C30 (and their H atoms) of the hexyl chain (minor disorder component not shown). Displacement parameters and residual electron density peaks suggest further disorder of this chain and of the t-butyl groups, but this was not modelled.

The structure contains highly disordered and unidentified solvent in large void volumes (shown in yellow in the *a*-axis projection below) between the molecules of the dinuclear Ir complex. This was dealt with by the SQUEEZE procedure of the program PLATON. Calculations based on unit cell contents do not include this solvent.

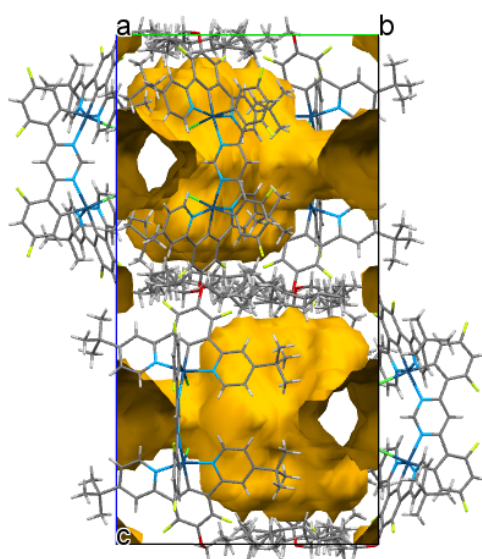


Table S9 Crystal data and structure refinement for complex **A3**

Identification code	vnk93 (manuscript code = A3)
Chemical formula (moiety)	C ₇₆ H ₈₀ Cl ₂ F ₈ Ir ₂ N ₆ O ₂
Chemical formula (total)	C ₇₆ H ₈₀ Cl ₂ F ₈ Ir ₂ N ₆ O ₂
Formula weight	1716.76
Temperature	100(2) K
Radiation, wavelength	synchrotron, 0.6889 Å
Crystal system, space group	hexagonal, P6 ₃ /m
Unit cell parameters	a = 20.589(3) Å α = 90° b = 20.589(3) Å β = 90° c = 34.721(5) Å γ = 120°
Cell volume	12747(4) Å ³
Z	6
Calculated density	1.342 g/cm ³
Absorption coefficient μ	2.965 mm ⁻¹
F(000)	5124
Crystal colour and size	orange, 0.30 × 0.18 × 0.05 mm ³
Reflections for cell refinement	9883 (θ range 2.2 to 29.6°)
Data collection method	Rigaku Saturn 724+ on kappa diffractometer wide-frame ω scans
θ range for data collection	1.1 to 29.7°
Index ranges	h -29 to 26, k -19 to 28, l -49 to 48
Completeness to θ = 24.4°	99.8 %
Reflections collected	149879
Independent reflections	13393 ($R_{\text{int}} = 0.0498$)
Reflections with $F^2 > 2\sigma$	9776
Absorption correction	multi-scan (SADABS)
Min. and max. transmission	0.624 and 0.862
Structure solution	direct methods
Refinement method	Full-matrix least-squares on F^2
Weighting parameters a, b	0, 86.0783
Data / restraints / parameters	13393 / 141 / 473
Final R indices [$F^2 > 2\sigma$]	R1 = 0.0566, wR2 = 0.1098
R indices (all data)	R1 = 0.0839, wR2 = 0.1266
Goodness-of-fit on F^2	1.169
Extinction coefficient	0.00015(3)
Largest and mean shift/su	0.004 and 0.000
Largest diff. peak and hole	3.54 and -3.83 e Å ⁻³

Table S10 Atomic coordinates and equivalent isotropic displacement parameters (\AA^2) for **A3**. U_{eq} is defined as one third of the trace of the orthogonalised U^{ij} tensor.

	x	y	z	U_{eq}
Ir	0.74455(2)	0.63133(2)	0.66018(2)	0.03736(8)
Cl	0.72751(9)	0.73180(8)	0.68640(5)	0.0478(3)
N1	0.6306(3)	0.5613(3)	0.65937(16)	0.0434(11)
N2	0.8502(3)	0.7101(2)	0.64296(16)	0.0430(12)
C1	0.5877(4)	0.5197(3)	0.6885(2)	0.0519(16)
C2	0.5109(4)	0.4745(4)	0.6857(3)	0.064(2)
C3	0.4749(3)	0.4686(4)	0.6514(3)	0.063(2)
C4	0.5187(4)	0.5121(4)	0.6210(3)	0.0609(19)
C5	0.5960(4)	0.5587(4)	0.6251(2)	0.0517(16)
C6	0.6487(4)	0.6093(3)	0.5960(2)	0.0510(15)
C7	0.6344(4)	0.6225(4)	0.5588(2)	0.0605(18)
C8	0.6905(5)	0.6745(5)	0.5350(2)	0.066(2)
C9	0.7637(5)	0.7115(4)	0.5488(2)	0.0590(19)
C10	0.7830(4)	0.6998(3)	0.58551(19)	0.0471(14)
C11	0.7233(3)	0.6496(3)	0.60859(19)	0.0432(13)
C12	0.8553(4)	0.7339(3)	0.6058(2)	0.0492(16)
C13	0.9241(4)	0.7882(3)	0.5909(2)	0.0539(17)
C14	0.9885(4)	0.8214(3)	0.6134(2)	0.0569(19)
C15	0.9810(4)	0.7973(3)	0.6513(3)	0.0590(19)
C16	0.9123(3)	0.7422(3)	0.6647(2)	0.0500(15)
C17	0.3901(4)	0.4173(5)	0.6456(3)	0.082(3)
C18	0.3778(4)	0.3605(5)	0.6139(3)	0.084(3)
C19	0.3554(5)	0.4649(6)	0.6347(5)	0.128(5)
C20	0.3542(5)	0.3743(5)	0.6826(4)	0.108(4)
C21	1.0642(4)	0.8835(4)	0.5987(3)	0.079(3)
C22	1.0925(5)	0.9501(4)	0.6270(4)	0.102(4)
C23	1.0580(6)	0.9100(5)	0.5586(3)	0.108(4)
C24	1.1211(6)	0.8558(6)	0.6007(5)	0.161(7)
F1	0.5642(3)	0.5861(3)	0.54402(14)	0.0794(14)
F2	0.8184(3)	0.7606(2)	0.52486(13)	0.0724(13)
O	0.6750(4)	0.6857(4)	0.49756(17)	0.092(2)
C25	0.6569(6)	0.7433(6)	0.4935(3)	0.095(3)
C26	0.5965(7)	0.7427(6)	0.5149(3)	0.097(3)
C27	0.5757(6)	0.8003(6)	0.5078(3)	0.091(3)
C28	0.5230(11)	0.8083(11)	0.5355(5)	0.087(4)
C29	0.5016(9)	0.8679(10)	0.5291(5)	0.081(4)
C30	0.4647(10)	0.8646(11)	0.4931(5)	0.087(5)
C28'	0.4975(12)	0.7776(15)	0.5192(9)	0.108(7)
C29'	0.4791(14)	0.8370(16)	0.5071(8)	0.107(6)
C30'	0.4092(14)	0.8207(18)	0.5247(10)	0.137(10)
N3	0.7635(2)	0.5976(2)	0.71594(15)	0.0382(10)
C31	0.7610(3)	0.5468(3)	0.6458(2)	0.0414(13)
C32	0.7643(4)	0.5236(3)	0.6083(2)	0.0510(16)
C33	0.7744(4)	0.4620(4)	0.6029(2)	0.062(2)
C34	0.7810(4)	0.4215(4)	0.6321(3)	0.063(2)
C35	0.7776(3)	0.4447(3)	0.6686(2)	0.0531(17)
C36	0.7692(3)	0.5064(3)	0.6763(2)	0.0464(15)

C37	0.7683(3)	0.5340(3)	0.71550(19)	0.0399(13)
C38	0.7716(4)	0.5022(4)	0.7500	0.046(2)
C39	0.7615(5)	0.6265(4)	0.7500	0.0423(18)
F3	0.7782(3)	0.4416(3)	0.56609(15)	0.0846(15)
F4	0.7815(2)	0.4031(2)	0.69783(14)	0.0640(12)

Table S11 Bond lengths [Å] and angles [°] for A3.

Ir–Cl	2.4406(15)	Ir–N1	2.049(5)
Ir–N2	2.048(5)	Ir–C11	1.926(7)
Ir–N3	2.157(5)	Ir–C31	1.996(5)
N1–C1	1.334(8)	N1–C5	1.376(9)
N2–C12	1.366(9)	N2–C16	1.341(8)
C1–H1	0.950	C1–C2	1.380(9)
C2–H2	0.950	C2–C3	1.375(12)
C3–C4	1.388(11)	C3–C17	1.536(9)
C4–H4	0.950	C4–C5	1.395(9)
C5–C6	1.467(10)	C6–C7	1.382(10)
C6–C11	1.401(9)	C7–C8	1.388(12)
C7–F1	1.353(8)	C8–C9	1.392(11)
C8–O	1.384(10)	C9–C10	1.390(10)
C9–F2	1.358(8)	C10–C11	1.397(8)
C10–C12	1.470(10)	C12–C13	1.392(8)
C13–H13	0.950	C13–C14	1.388(11)
C14–C15	1.390(11)	C14–C21	1.525(9)
C15–H15	0.950	C15–C16	1.378(8)
C16–H16	0.950	C17–C18	1.531(13)
C17–C19	1.521(12)	C17–C20	1.526(15)
C18–H18A	0.980	C18–H18B	0.980
C18–H18C	0.980	C19–H19A	0.980
C19–H19B	0.980	C19–H19C	0.980
C20–H20A	0.980	C20–H20B	0.980
C20–H20C	0.980	C21–C22	1.545(13)
C21–C23	1.526(15)	C21–C24	1.539(12)
C22–H22A	0.980	C22–H22B	0.980
C22–H22C	0.980	C23–H23A	0.980
C23–H23B	0.980	C23–H23C	0.980
C24–H24A	0.980	C24–H24B	0.980
C24–H24C	0.980	O–C25	1.417(11)
C25–H25A	0.990	C25–H25B	0.990
C25–C26	1.442(13)	C26–H26A	0.990
C26–H26B	0.990	C26–C27	1.470(13)
C27–H27A	0.990	C27–H27B	0.990
C27–H27C	0.990	C27–H27D	0.990
C27–C28	1.521(16)	C27–C28'	1.488(18)
C28–H28A	0.990	C28–H28B	0.990
C28–C29	1.512(17)	C29–H29A	0.990
C29–H29B	0.990	C29–C30	1.447(19)
C30–H30A	0.980	C30–H30B	0.980
C30–H30C	0.980	C28'–H28C	0.990

C28'-H28D	0.990	C28'-C29'	1.51(2)
C29'-H29C	0.990	C29'-H29D	0.990
C29'-C30'	1.44(2)	C30'-H30D	0.980
C30'-H30E	0.980	C30'-H30F	0.980
N3-C37	1.361(6)	N3-C39	1.334(6)
C31-C32	1.399(9)	C31-C36	1.408(9)
C32-H32	0.950	C32-C33	1.397(9)
C33-C34	1.361(11)	C33-F3	1.361(8)
C34-H34	0.950	C34-C35	1.367(10)
C35-C36	1.392(7)	C35-F4	1.357(8)
C36-C37	1.478(9)	C37-C38	1.384(7)
C38-C37a	1.384(7)	C38-H38	0.950
C39-N3a	1.334(6)	C39-H39	0.950
Cl-Ir-N1	90.12(14)	Cl-Ir-N2	89.05(13)
Cl-Ir-C11	92.16(17)	Cl-Ir-N3	93.66(12)
Cl-Ir-C31	172.6(2)	N1-Ir-N2	160.4(2)
N1-Ir-C11	80.3(2)	N1-Ir-N3	96.5(2)
N1-Ir-C31	91.0(2)	N2-Ir-C11	80.1(2)
N2-Ir-N3	103.0(2)	N2-Ir-C31	92.4(2)
C11-Ir-N3	173.4(2)	C11-Ir-C31	95.3(3)
N3-Ir-C31	78.9(2)	Ir-N1-C1	126.8(5)
Ir-N1-C5	115.3(4)	C1-N1-C5	117.8(5)
Ir-N2-C12	114.9(4)	Ir-N2-C16	126.8(5)
C12-N2-C16	118.2(5)	N1-C1-H1	118.4
N1-C1-C2	123.2(7)	H1-C1-C2	118.4
C1-C2-H2	119.8	C1-C2-C3	120.4(7)
H2-C2-C3	119.8	C2-C3-C4	117.0(6)
C2-C3-C17	123.6(8)	C4-C3-C17	119.5(8)
C3-C4-H4	119.5	C3-C4-C5	121.1(8)
H4-C4-C5	119.5	N1-C5-C4	120.4(7)
N1-C5-C6	112.5(5)	C4-C5-C6	127.1(7)
C5-C6-C7	128.9(7)	C5-C6-C11	114.1(6)
C7-C6-C11	117.0(7)	C6-C7-C8	122.1(7)
C6-C7-F1	121.3(7)	C8-C7-F1	116.6(7)
C7-C8-C9	118.1(7)	C7-C8-O	121.0(8)
C9-C8-O	120.7(8)	C8-C9-C10	123.2(7)
C8-C9-F2	117.5(7)	C10-C9-F2	119.3(7)
C9-C10-C11	115.6(6)	C9-C10-C12	131.6(6)
C11-C10-C12	112.7(6)	Ir-C11-C6	117.7(5)
Ir-C11-C10	118.4(5)	C6-C11-C10	123.9(6)
N2-C12-C10	113.7(5)	N2-C12-C13	120.2(7)
C10-C12-C13	126.0(7)	C12-C13-H13	119.2
C12-C13-C14	121.6(7)	H13-C13-C14	119.2
C13-C14-C15	116.6(6)	C13-C14-C21	123.4(8)
C15-C14-C21	120.0(8)	C14-C15-H15	120.0
C14-C15-C16	120.0(7)	H15-C15-C16	120.0
N2-C16-C15	123.2(7)	N2-C16-H16	118.4
C15-C16-H16	118.4	C3-C17-C18	108.5(7)
C3-C17-C19	109.2(7)	C3-C17-C20	110.0(8)
C18-C17-C19	111.2(9)	C18-C17-C20	108.3(8)
C19-C17-C20	109.6(9)	C17-C18-H18A	109.5

C17–C18–H18B	109.5	C17–C18–H18C	109.5
H18A–C18–H18B	109.5	H18A–C18–H18C	109.5
H18B–C18–H18C	109.5	C17–C19–H19A	109.5
C17–C19–H19B	109.5	C17–C19–H19C	109.5
H19A–C19–H19B	109.5	H19A–C19–H19C	109.5
H19B–C19–H19C	109.5	C17–C20–H20A	109.5
C17–C20–H20B	109.5	C17–C20–H20C	109.5
H20A–C20–H20B	109.5	H20A–C20–H20C	109.5
H20B–C20–H20C	109.5	C14–C21–C22	107.8(7)
C14–C21–C23	111.8(8)	C14–C21–C24	108.9(6)
C22–C21–C23	109.0(7)	C22–C21–C24	106.3(10)
C23–C21–C24	112.8(9)	C21–C22–H22A	109.5
C21–C22–H22B	109.5	C21–C22–H22C	109.5
H22A–C22–H22B	109.5	H22A–C22–H22C	109.5
H22B–C22–H22C	109.5	C21–C23–H23A	109.5
C21–C23–H23B	109.5	C21–C23–H23C	109.5
H23A–C23–H23B	109.5	H23A–C23–H23C	109.5
H23B–C23–H23C	109.5	C21–C24–H24A	109.5
C21–C24–H24B	109.5	C21–C24–H24C	109.5
H24A–C24–H24B	109.5	H24A–C24–H24C	109.5
H24B–C24–H24C	109.5	C8–O–C25	114.2(7)
O–C25–H25A	106.8	O–C25–H25B	106.8
O–C25–C26	121.9(9)	H25A–C25–H25B	106.7
H25A–C25–C26	106.8	H25B–C25–C26	106.8
C25–C26–H26A	107.2	C25–C26–H26B	107.2
C25–C26–C27	120.3(9)	H26A–C26–H26B	106.9
H26A–C26–C27	107.2	H26B–C26–C27	107.2
C26–C27–H27A	107.4	C26–C27–H27B	107.4
C26–C27–H27C	108.7	C26–C27–H27D	108.7
C26–C27–C28	119.6(10)	C26–C27–C28'	114.1(12)
H27A–C27–H27B	107.0	H27A–C27–C28	107.4
H27B–C27–C28	107.4	H27C–C27–H27D	107.6
H27C–C27–C28'	108.7	H27D–C27–C28'	108.7
C27–C28–H28A	107.2	C27–C28–H28B	107.2
C27–C28–C29	120.6(14)	H28A–C28–H28B	106.8
H28A–C28–C29	107.2	H28B–C28–C29	107.2
C28–C29–H29A	108.2	C28–C29–H29B	108.2
C28–C29–C30	116.6(15)	H29A–C29–H29B	107.3
H29A–C29–C30	108.2	H29B–C29–C30	108.2
C29–C30–H30A	109.5	C29–C30–H30B	109.5
C29–C30–H30C	109.5	H30A–C30–H30B	109.5
H30A–C30–H30C	109.5	H30B–C30–H30C	109.5
C27–C28'–H28C	109.7	C27–C28'–H28D	109.7
C27–C28'–C29'	110.0(16)	H28C–C28'–H28D	108.2
H28C–C28'–C29'	109.7	H28D–C28'–C29'	109.7
C28'–C29'–H29C	110.0	C28'–C29'–H29D	110.0
C28'–C29'–C30'	109(2)	H29C–C29'–H29D	108.4
H29C–C29'–C30'	110.0	H29D–C29'–C30'	110.0
C29'–C30'–H30D	109.5	C29'–C30'–H30E	109.5
C29'–C30'–H30F	109.5	H30D–C30'–H30E	109.5
H30D–C30'–H30F	109.5	H30E–C30'–H30F	109.5
Ir–N3–C37	114.3(4)	Ir–N3–C39	127.0(4)

C37–N3–C39	118.2(6)	Ir–C31–C32	126.1(5)
Ir–C31–C36	116.6(5)	C32–C31–C36	117.3(5)
C31–C32–H32	120.4	C31–C32–C33	119.2(7)
H32–C32–C33	120.4	C32–C33–C34	124.3(7)
C32–C33–F3	117.5(8)	C34–C33–F3	118.2(6)
C33–C34–H34	122.0	C33–C34–C35	115.9(6)
H34–C34–C35	122.0	C34–C35–C36	123.3(7)
C34–C35–F4	116.3(6)	C36–C35–F4	120.4(7)
C31–C36–C35	119.9(7)	C31–C36–C37	116.0(5)
C35–C36–C37	124.0(6)	N3–C37–C36	113.6(5)
N3–C37–C38	119.4(6)	C36–C37–C38	127.0(5)
C37–C38–C37a	119.9(7)	C37–C38–H38	120.0
C37a–C38–H38	120.0	N3–C39–N3a	124.9(7)
N3–C39–H39	117.5	N3a–C39–H39	117.5

Symmetry operations for equivalent atoms
a x,y,-z+3/2

Table S12 Torsion angles [°] for A3.

Ir–N1–C1–C2	179.2(5)	C5–N1–C1–C2	0.2(10)
N1–C1–C2–C3	2.1(11)	C1–C2–C3–C4	-2.6(11)
C1–C2–C3–C17	177.7(7)	C2–C3–C4–C5	1.0(10)
C17–C3–C4–C5	-179.2(7)	Ir–N1–C5–C4	179.1(5)
Ir–N1–C5–C6	-1.7(7)	C1–N1–C5–C4	-1.7(9)
C1–N1–C5–C6	177.5(5)	C3–C4–C5–N1	1.1(10)
C3–C4–C5–C6	-178.0(6)	N1–C5–C6–C7	-178.8(7)
N1–C5–C6–C11	0.3(8)	C4–C5–C6–C7	0.3(12)
C4–C5–C6–C11	179.5(6)	C5–C6–C7–C8	177.7(7)
C5–C6–C7–F1	-0.9(12)	C11–C6–C7–C8	-1.4(10)
C11–C6–C7–F1	180.0(6)	C6–C7–C8–C9	3.0(11)
C6–C7–C8–O	178.7(7)	F1–C7–C8–C9	-178.3(6)
F1–C7–C8–O	-2.6(11)	C7–C8–C9–C10	-1.2(11)
C7–C8–C9–F2	178.2(6)	O–C8–C9–C10	-176.9(6)
O–C8–C9–F2	2.4(10)	C8–C9–C10–C11	-2.0(10)
C8–C9–C10–C12	-178.2(6)	F2–C9–C10–C11	178.6(5)
F2–C9–C10–C12	2.5(11)	C9–C10–C11–Ir	-179.0(4)
C9–C10–C11–C6	3.8(9)	C12–C10–C11–Ir	-2.1(7)
C12–C10–C11–C6	-179.4(5)	C5–C6–C11–Ir	1.3(7)
C5–C6–C11–C10	178.6(6)	C7–C6–C11–Ir	-179.4(5)
C7–C6–C11–C10	-2.1(9)	Ir–N2–C12–C10	1.8(6)
Ir–N2–C12–C13	179.1(4)	C16–N2–C12–C10	-175.1(5)
C16–N2–C12–C13	2.2(8)	C9–C10–C12–N2	176.3(6)
C9–C10–C12–C13	-0.9(11)	C11–C10–C12–N2	0.1(7)
C11–C10–C12–C13	-177.1(6)	N2–C12–C13–C14	-2.2(9)
C10–C12–C13–C14	174.8(6)	C12–C13–C14–C15	0.5(9)
C12–C13–C14–C21	-177.2(6)	C13–C14–C15–C16	1.0(9)
C21–C14–C15–C16	178.8(6)	Ir–N2–C16–C15	-177.2(5)
C12–N2–C16–C15	-0.7(9)	C14–C15–C16–N2	-1.0(10)

C2–C3–C17–C18	-119.5(9)	C2–C3–C17–C19	119.1(10)
C2–C3–C17–C20	-1.2(11)	C4–C3–C17–C18	60.8(10)
C4–C3–C17–C19	-60.6(12)	C4–C3–C17–C20	179.1(7)
C13–C14–C21–C22	126.2(8)	C13–C14–C21–C23	6.4(10)
C13–C14–C21–C24	-118.8(10)	C15–C14–C21–C22	-51.4(9)
C15–C14–C21–C23	-171.2(7)	C15–C14–C21–C24	63.5(12)
C7–C8–O–C25	92.0(10)	C9–C8–O–C25	-92.4(10)
C8–O–C25–C26	-56.1(14)	O–C25–C26–C27	-175.3(10)
C25–C26–C27–C28	-168.1(13)	C25–C26–C27–C28'	157.2(18)
C26–C27–C28–C29	179.1(14)	C27–C28–C29–C30	59(2)
C26–C27–C28'–C29'	-174.2(19)	C27–C28'–C29'–C30'	-169(3)
Ir–C31–C32–C33	-178.4(5)	C36–C31–C32–C33	0.7(9)
C31–C32–C33–C34	0.5(11)	C31–C32–C33–F3	-179.2(6)
C32–C33–C34–C35	-0.4(11)	F3–C33–C34–C35	179.3(6)
C33–C34–C35–C36	-0.9(10)	C33–C34–C35–F4	177.7(6)
C34–C35–C36–C31	2.1(9)	C34–C35–C36–C37	-177.6(6)
F4–C35–C36–C31	-176.4(5)	F4–C35–C36–C37	3.8(9)
Ir–C31–C36–C35	177.3(4)	Ir–C31–C36–C37	-2.9(6)
C32–C31–C36–C35	-1.9(8)	C32–C31–C36–C37	177.8(5)
Ir–N3–C37–C36	7.3(6)	Ir–N3–C37–C38	-172.5(5)
C39–N3–C37–C36	179.3(6)	C39–N3–C37–C38	-0.6(9)
C31–C36–C37–N3	-3.2(7)	C31–C36–C37–C38	176.6(6)
C35–C36–C37–N3	176.5(5)	C35–C36–C37–C38	-3.6(10)
N3–C37–C38–C37a	1.5(11)	C36–C37–C38–C37a	-178.4(4)
Ir–N3–C39–N3a	170.4(4)	C37–N3–C39–N3a	-0.4(11)

Symmetry operations for equivalent atoms:

a x,y,-z+3/2

Table S13 Anisotropic displacement parameters (\AA^2) for **A3**. The anisotropic displacement factor exponent takes the form: $-2\pi^2[h^2a^{*2}U^{11} + \dots + 2hka^*b^*U^{12}]$

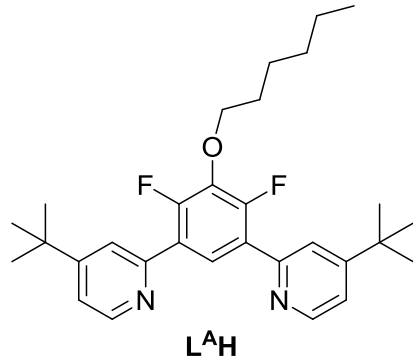
	U ¹¹	U ²²	U ³³	U ²³	U ¹³	U ¹²
Ir	0.03063(11)	0.02389(10)	0.05143(13)	-0.00175(9)	0.00398(9)	0.00903(8)
Cl	0.0537(8)	0.0362(7)	0.0589(9)	-0.0006(6)	0.0023(7)	0.0265(7)
N1	0.029(2)	0.035(2)	0.064(3)	-0.002(2)	0.002(2)	0.0136(19)
N2	0.032(2)	0.024(2)	0.065(3)	-0.004(2)	0.009(2)	0.0082(18)
C1	0.039(3)	0.041(3)	0.071(4)	0.002(3)	0.007(3)	0.016(3)
C2	0.034(3)	0.044(4)	0.096(6)	0.002(4)	0.012(4)	0.005(3)
C3	0.029(3)	0.038(3)	0.117(7)	-0.008(4)	-0.003(4)	0.013(3)
C4	0.037(3)	0.048(4)	0.096(6)	-0.013(4)	-0.011(4)	0.021(3)
C5	0.040(3)	0.039(3)	0.072(5)	-0.009(3)	-0.007(3)	0.016(3)
C6	0.053(4)	0.036(3)	0.062(4)	-0.007(3)	-0.006(3)	0.021(3)
C7	0.064(5)	0.048(4)	0.065(5)	-0.011(3)	-0.013(4)	0.025(4)
C8	0.092(6)	0.060(5)	0.057(4)	-0.018(4)	-0.014(4)	0.045(5)
C9	0.080(5)	0.040(3)	0.057(4)	0.004(3)	0.019(4)	0.030(4)
C10	0.052(4)	0.031(3)	0.055(4)	-0.003(3)	0.009(3)	0.018(3)
C11	0.048(3)	0.025(2)	0.055(4)	-0.007(2)	0.003(3)	0.017(2)

C12	0.057(4)	0.025(3)	0.065(4)	0.002(3)	0.020(3)	0.019(3)
C13	0.053(4)	0.028(3)	0.080(5)	0.006(3)	0.025(3)	0.019(3)
C14	0.041(3)	0.024(3)	0.100(6)	0.006(3)	0.028(4)	0.012(2)
C15	0.034(3)	0.029(3)	0.101(6)	-0.008(3)	0.007(3)	0.006(2)
C16	0.039(3)	0.032(3)	0.069(4)	-0.006(3)	0.004(3)	0.010(2)
C17	0.029(3)	0.063(5)	0.151(9)	-0.006(5)	-0.005(4)	0.020(3)
C18	0.037(4)	0.067(5)	0.129(8)	-0.003(5)	-0.017(4)	0.012(4)
C19	0.042(5)	0.083(7)	0.258(17)	-0.018(9)	-0.030(7)	0.032(5)
C20	0.046(5)	0.068(6)	0.177(12)	-0.011(7)	0.020(6)	0.004(4)
C21	0.049(4)	0.035(3)	0.151(9)	0.026(4)	0.044(5)	0.019(3)
C22	0.047(4)	0.036(4)	0.191(12)	0.018(6)	0.011(6)	-0.003(3)
C23	0.082(7)	0.065(6)	0.147(10)	0.030(6)	0.060(7)	0.014(5)
C24	0.090(7)	0.080(7)	0.33(2)	0.085(10)	0.124(11)	0.053(6)
F1	0.082(3)	0.071(3)	0.080(3)	-0.020(2)	-0.032(3)	0.034(3)
F2	0.100(4)	0.057(3)	0.062(3)	0.008(2)	0.024(2)	0.040(3)
O	0.145(6)	0.087(4)	0.056(3)	-0.014(3)	-0.006(4)	0.068(5)
C25	0.106(7)	0.098(7)	0.088(7)	0.036(6)	0.016(5)	0.056(6)
C26	0.118(7)	0.109(7)	0.081(6)	0.012(5)	-0.002(5)	0.070(6)
C27	0.089(6)	0.094(6)	0.087(6)	0.036(5)	0.006(5)	0.044(5)
C28	0.082(9)	0.089(10)	0.091(9)	0.002(7)	-0.012(7)	0.042(8)
C29	0.069(8)	0.092(10)	0.084(9)	0.006(7)	-0.007(7)	0.042(8)
C30	0.075(10)	0.092(12)	0.096(10)	0.002(8)	-0.010(8)	0.043(9)
C28'	0.091(9)	0.110(13)	0.117(16)	0.024(11)	0.005(9)	0.045(9)
C29'	0.086(10)	0.098(13)	0.125(16)	0.003(11)	-0.034(10)	0.037(9)
C30'	0.097(12)	0.14(2)	0.16(2)	-0.004(17)	-0.015(13)	0.054(13)
N3	0.029(2)	0.024(2)	0.060(3)	0.0005(19)	0.005(2)	0.0120(17)
C31	0.029(2)	0.021(2)	0.070(4)	0.000(2)	0.009(2)	0.0091(19)
C32	0.044(3)	0.030(3)	0.066(4)	-0.006(3)	0.011(3)	0.009(2)
C33	0.057(4)	0.036(3)	0.076(5)	-0.012(3)	0.019(4)	0.012(3)
C34	0.051(4)	0.039(3)	0.097(6)	-0.003(4)	0.022(4)	0.022(3)
C35	0.039(3)	0.026(3)	0.093(5)	-0.002(3)	0.014(3)	0.015(2)
C36	0.035(3)	0.021(2)	0.085(5)	-0.004(3)	0.009(3)	0.015(2)
C37	0.024(2)	0.022(2)	0.070(4)	0.001(2)	0.006(2)	0.0095(19)
C38	0.033(4)	0.025(3)	0.079(6)	0.000	0.000	0.014(3)
C39	0.038(4)	0.028(4)	0.062(5)	0.000	0.000	0.017(3)
F3	0.103(4)	0.058(3)	0.089(3)	-0.018(2)	0.026(3)	0.037(3)
F4	0.066(3)	0.0367(19)	0.100(3)	0.005(2)	0.022(2)	0.0334(19)

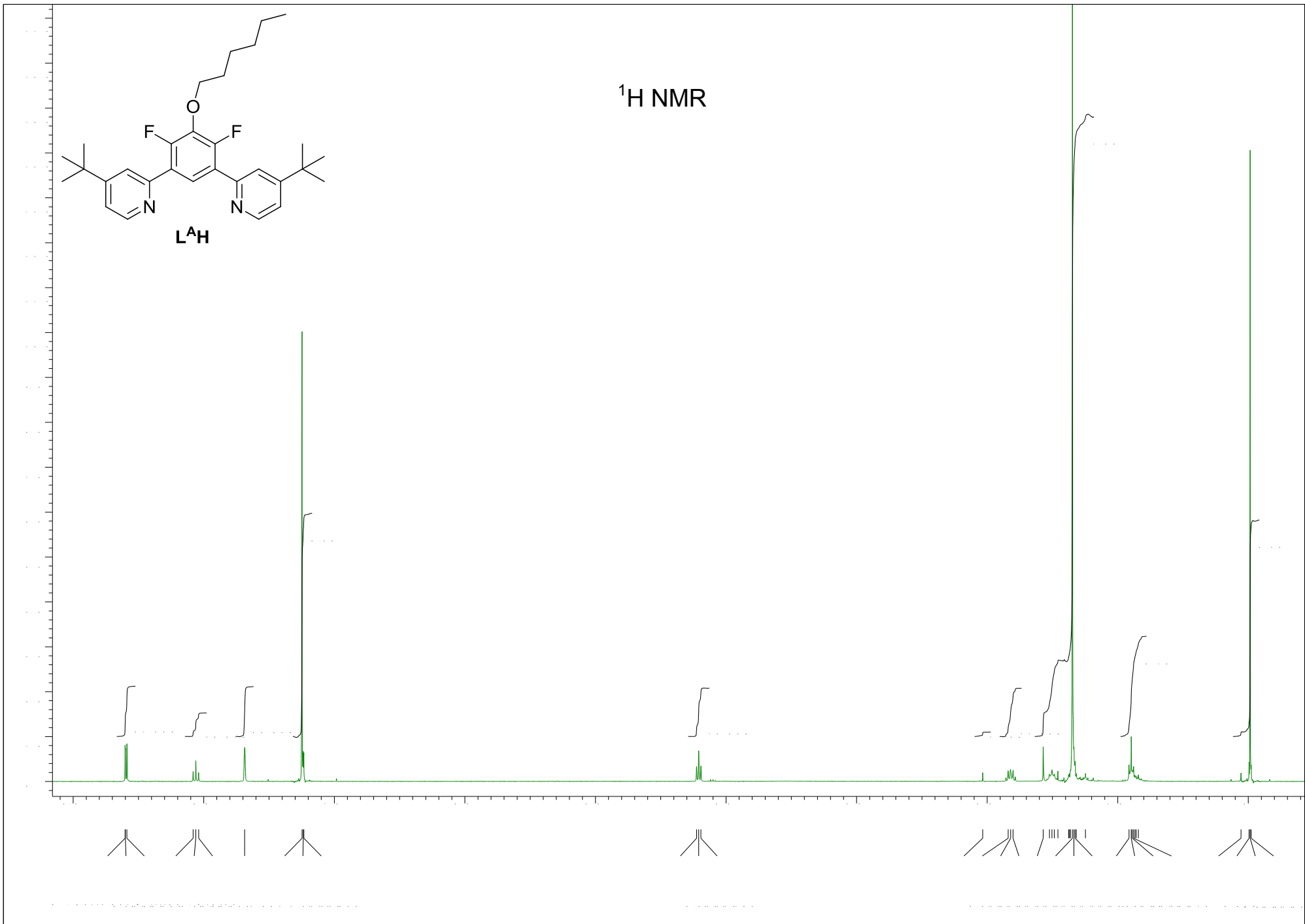
Table S14 Hydrogen coordinates and isotropic displacement parameters (\AA^2) for **A3**.

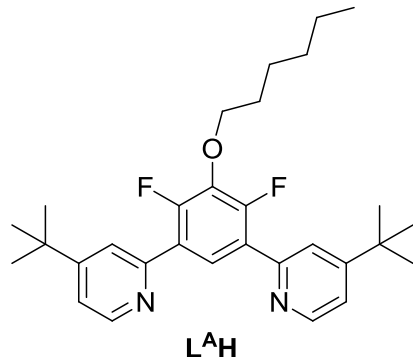
	x	y	z	U
H1	0.6111	0.5213	0.7123	0.062
H2	0.4828	0.4473	0.7076	0.077
H4	0.4957	0.5102	0.5970	0.073
H13	0.9270	0.8028	0.5647	0.065
H15	1.0231	0.8188	0.6681	0.071
H16	0.9087	0.7261	0.6907	0.060
H18A	0.4018	0.3316	0.6214	0.126

H18B	0.3997	0.3871	0.5898	0.126
H18C	0.3239	0.3264	0.6104	0.126
H19A	0.3736	0.4873	0.6092	0.191
H19B	0.3695	0.5048	0.6538	0.191
H19C	0.3007	0.4334	0.6340	0.191
H20A	0.3781	0.3453	0.6901	0.161
H20B	0.3005	0.3403	0.6783	0.161
H20C	0.3610	0.4098	0.7031	0.161
H22A	1.1431	0.9890	0.6196	0.153
H22B	1.0935	0.9328	0.6532	0.153
H22C	1.0587	0.9708	0.6262	0.153
H23A	1.1078	0.9485	0.5498	0.162
H23B	1.0246	0.9310	0.5594	0.162
H23C	1.0376	0.8674	0.5407	0.162
H24A	1.1719	0.8983	0.5970	0.241
H24B	1.1099	0.8185	0.5804	0.241
H24C	1.1178	0.8330	0.6259	0.241
H25A	0.6463	0.7455	0.4659	0.114
H25B	0.7029	0.7911	0.4997	0.114
H26A	0.6091	0.7452	0.5426	0.116
H26B	0.5512	0.6933	0.5105	0.116
H27A	0.5527	0.7908	0.4818	0.109
H27B	0.6226	0.8493	0.5066	0.109
H27C	0.5819	0.8127	0.4800	0.109
H27D	0.6106	0.8463	0.5221	0.109
H28A	0.4759	0.7594	0.5363	0.105
H28B	0.5457	0.8167	0.5614	0.105
H29A	0.4681	0.8647	0.5504	0.097
H29B	0.5477	0.9176	0.5309	0.097
H30A	0.4576	0.9081	0.4911	0.131
H30B	0.4158	0.8185	0.4922	0.131
H30C	0.4957	0.8649	0.4716	0.131
H28C	0.4921	0.7708	0.5475	0.130
H28D	0.4621	0.7293	0.5069	0.130
H29C	0.5195	0.8871	0.5153	0.128
H29D	0.4748	0.8372	0.4787	0.128
H30D	0.3995	0.8619	0.5195	0.205
H30E	0.4121	0.8151	0.5525	0.205
H30F	0.3684	0.7740	0.5139	0.205
H32	0.7596	0.5494	0.5867	0.061
H34	0.7875	0.3797	0.6274	0.075
H38	0.7762	0.4585	0.7500	0.055
H39	0.7584	0.6710	0.7500	0.051

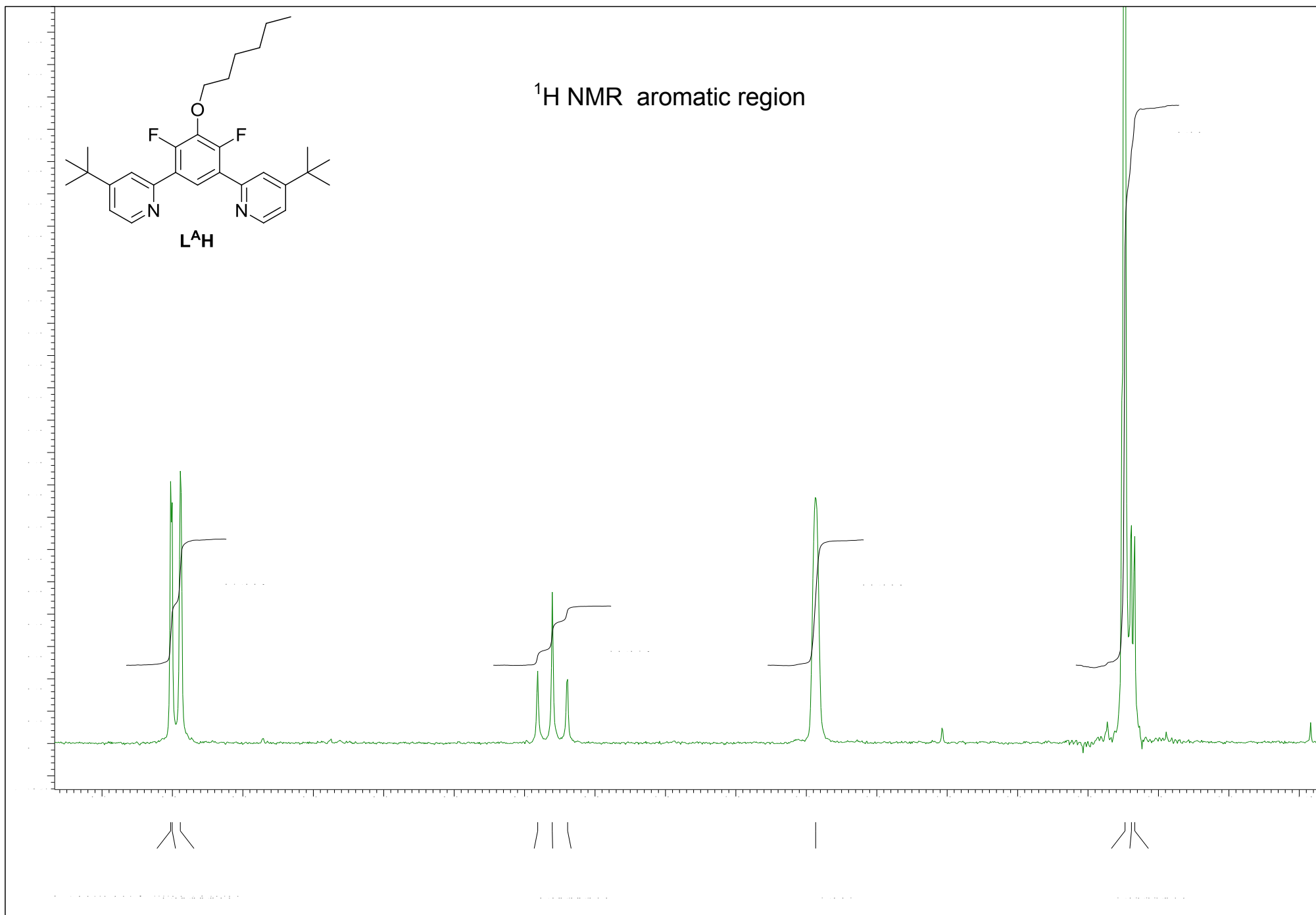


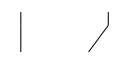
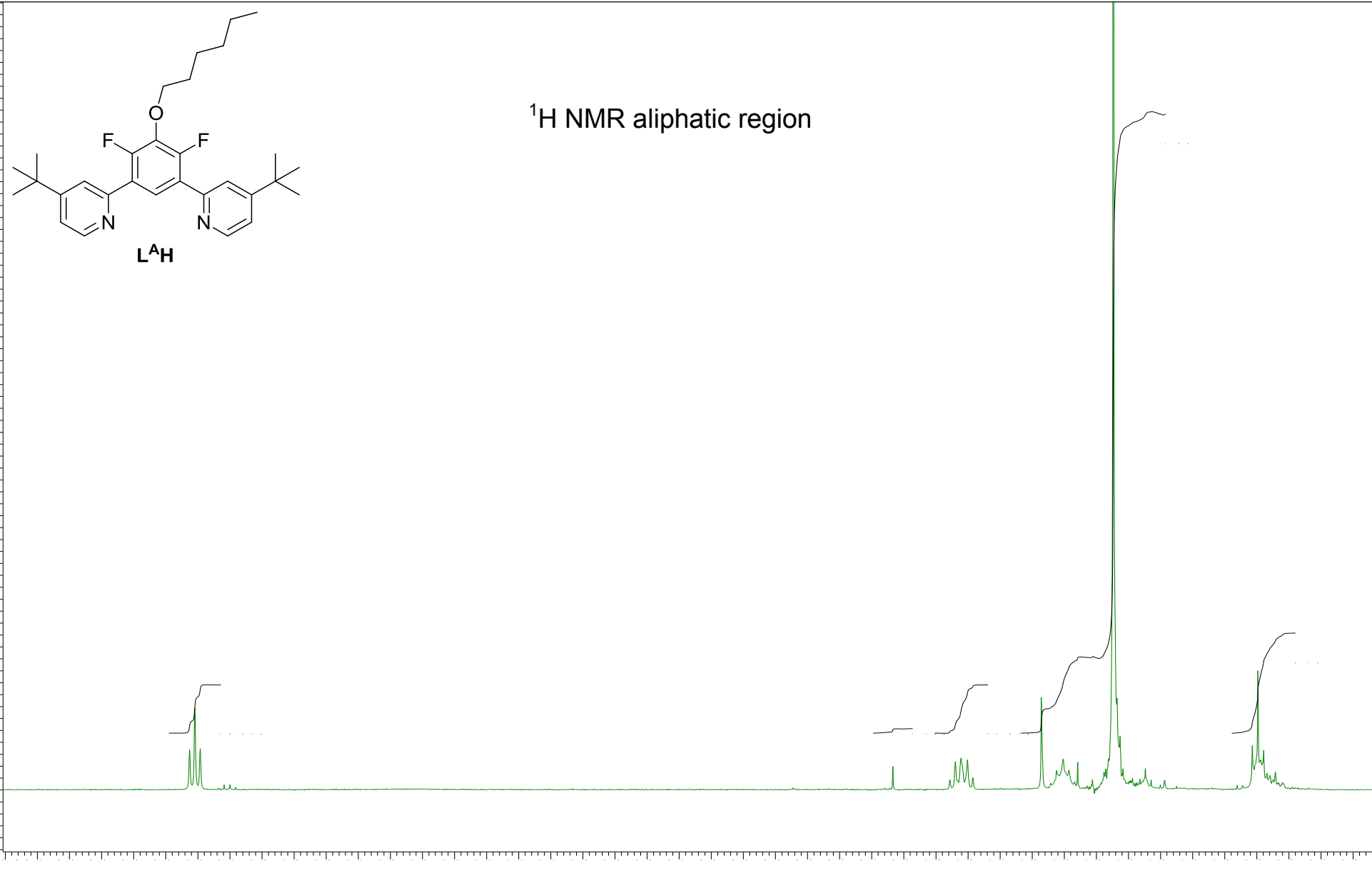
^1H NMR

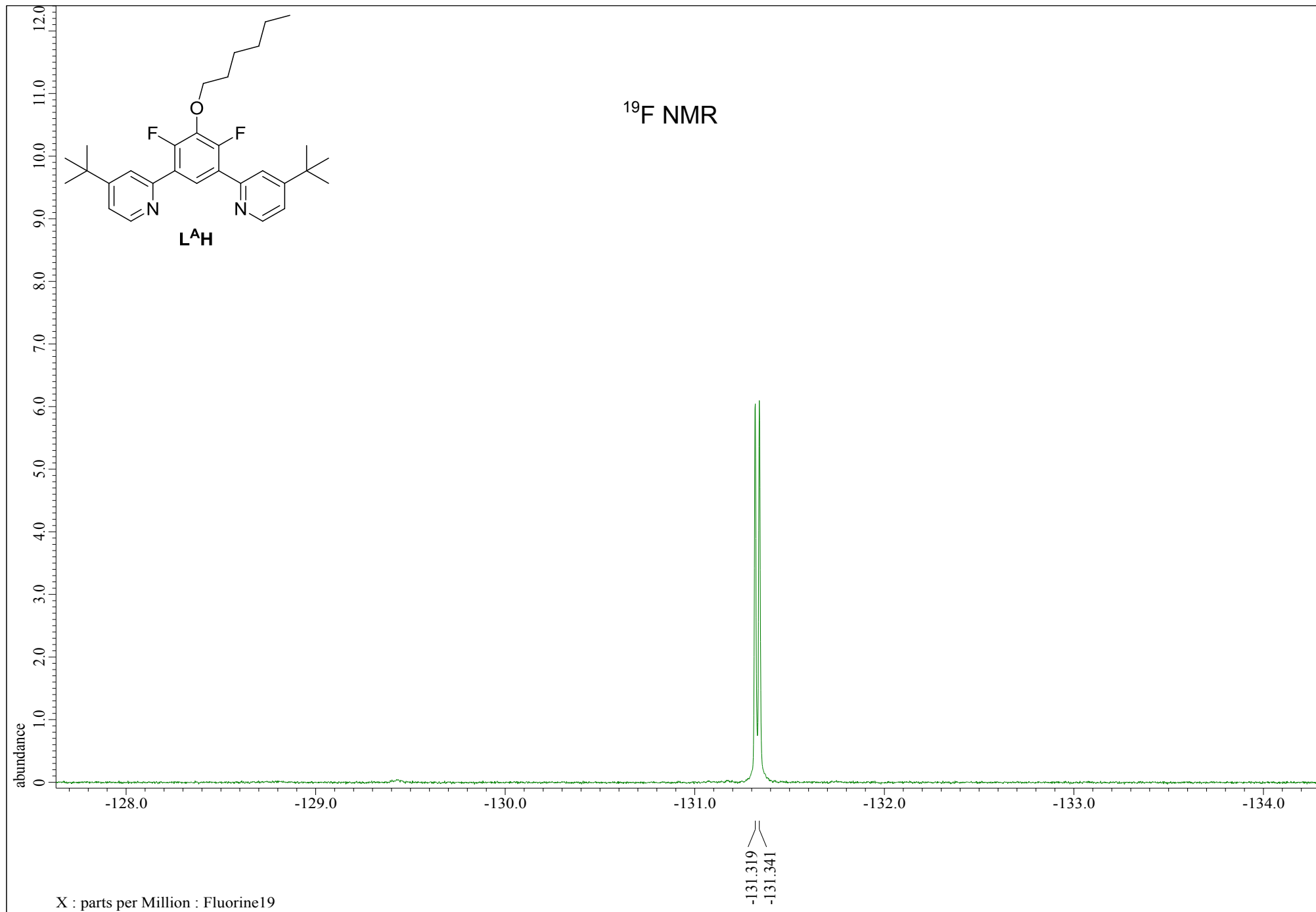


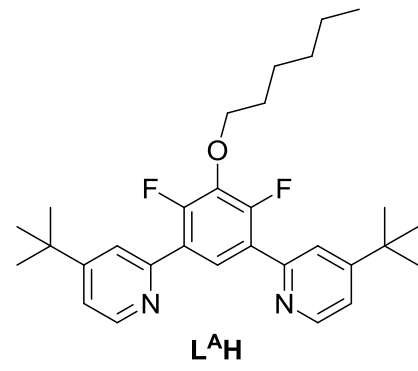


^1H NMR aromatic region

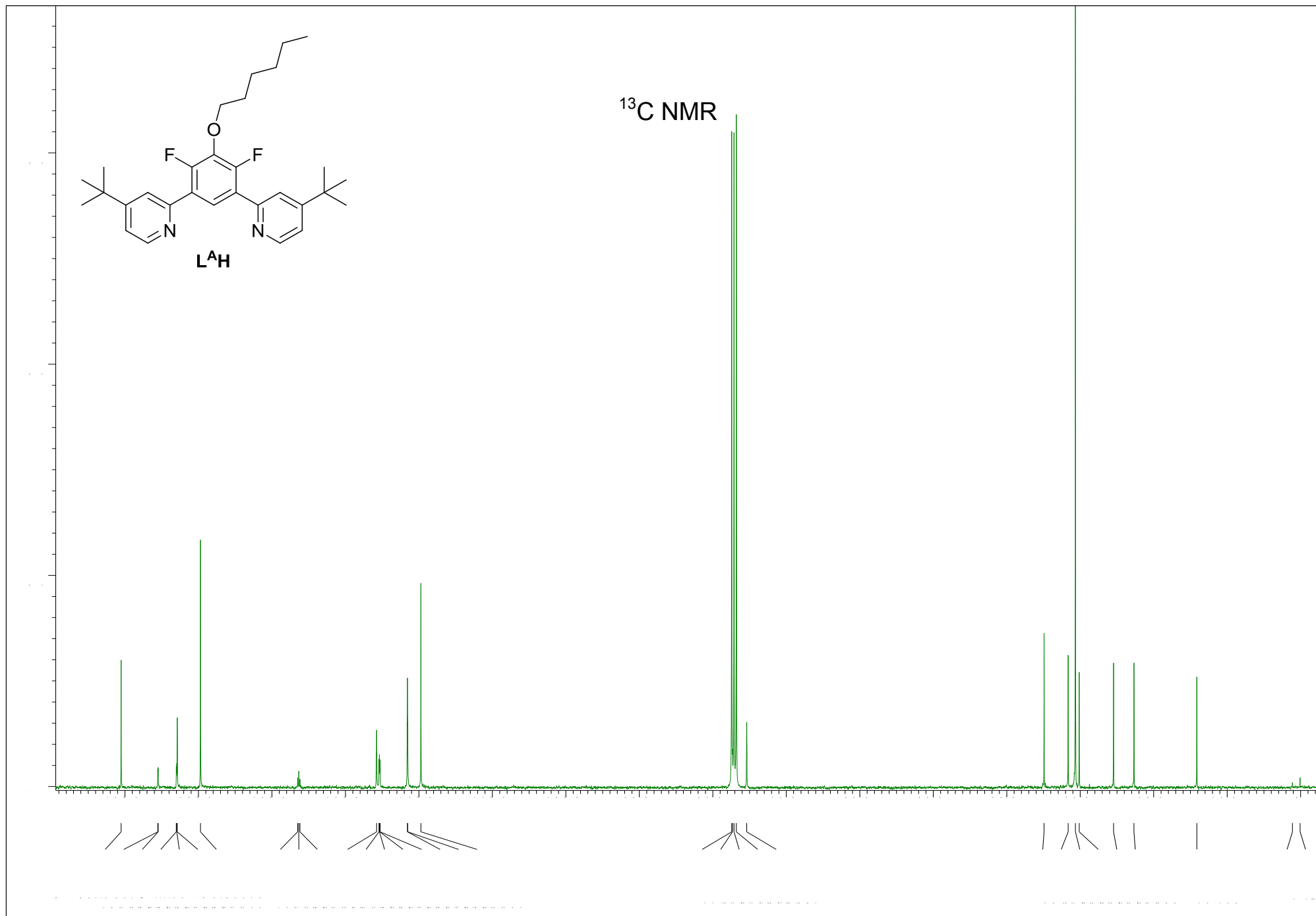


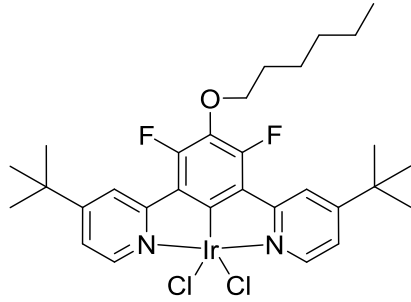






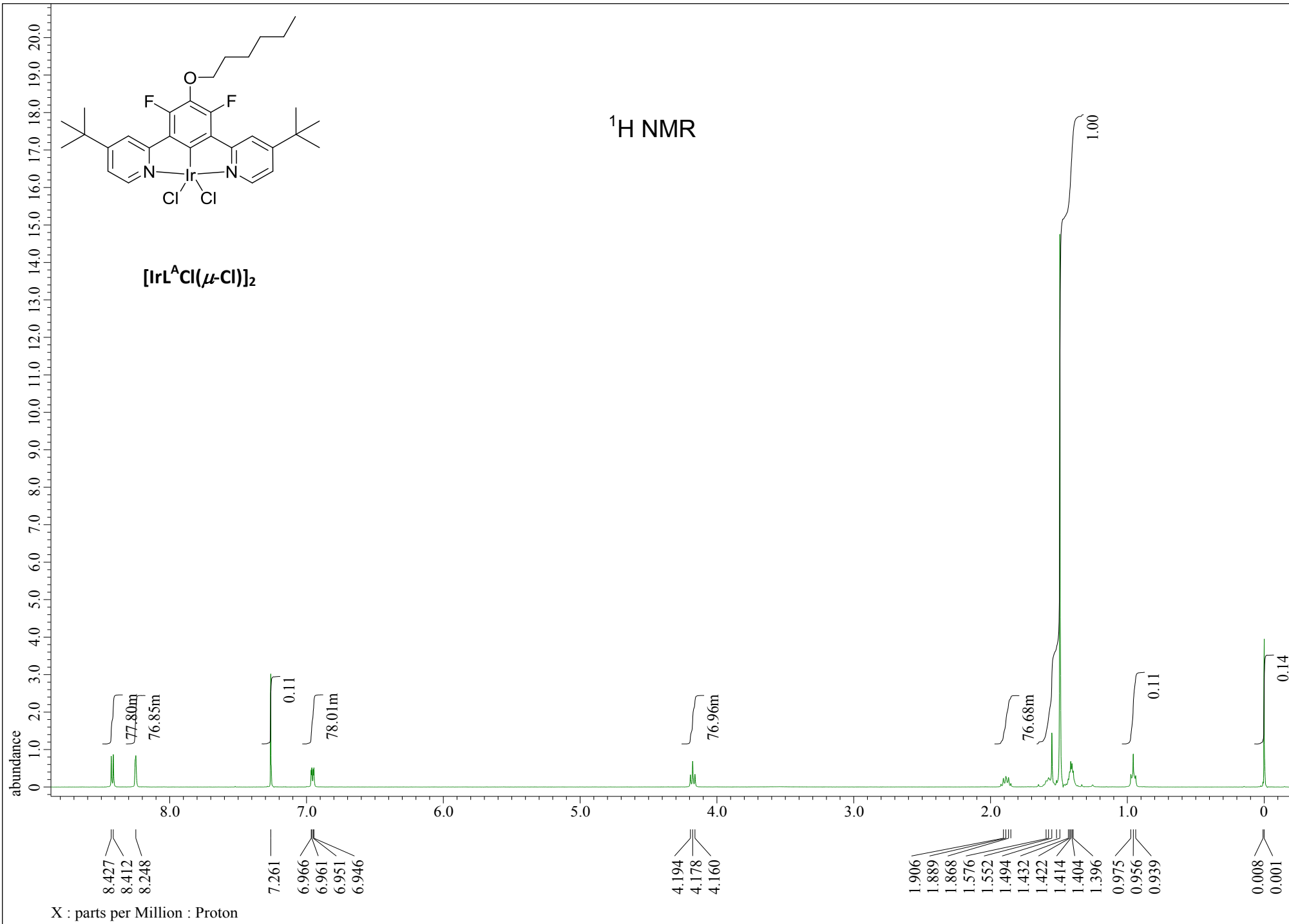
¹³C NMR

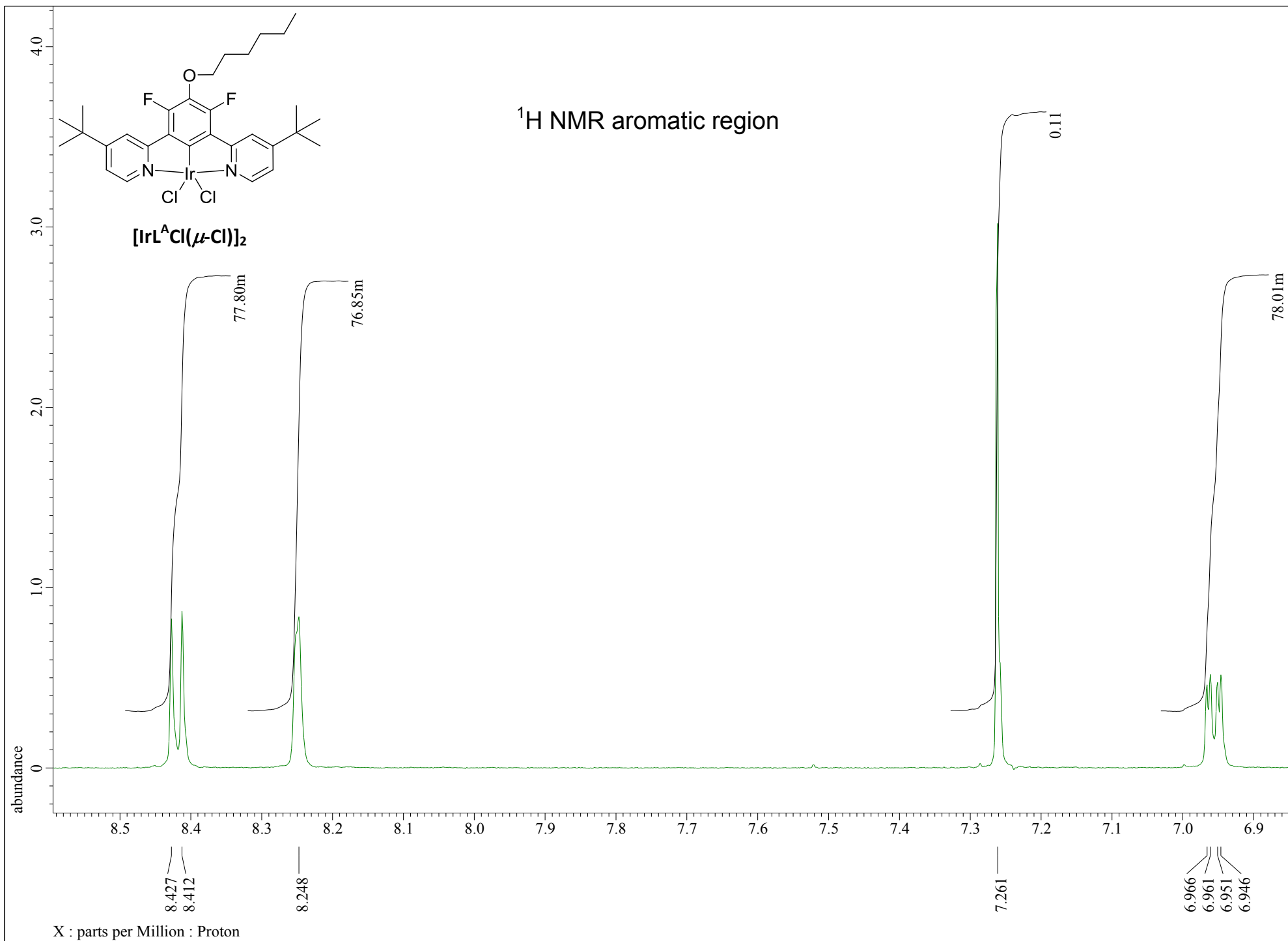


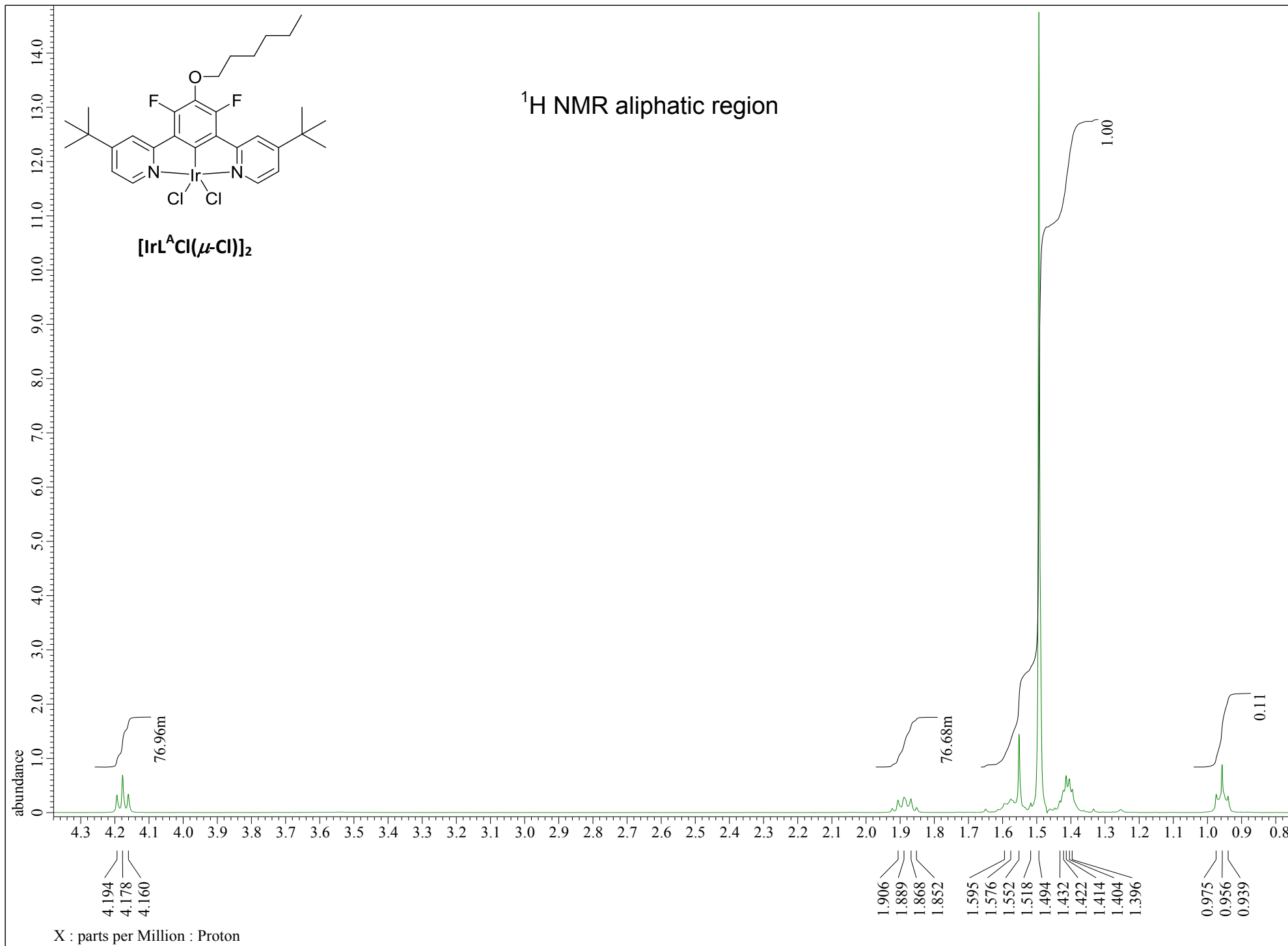


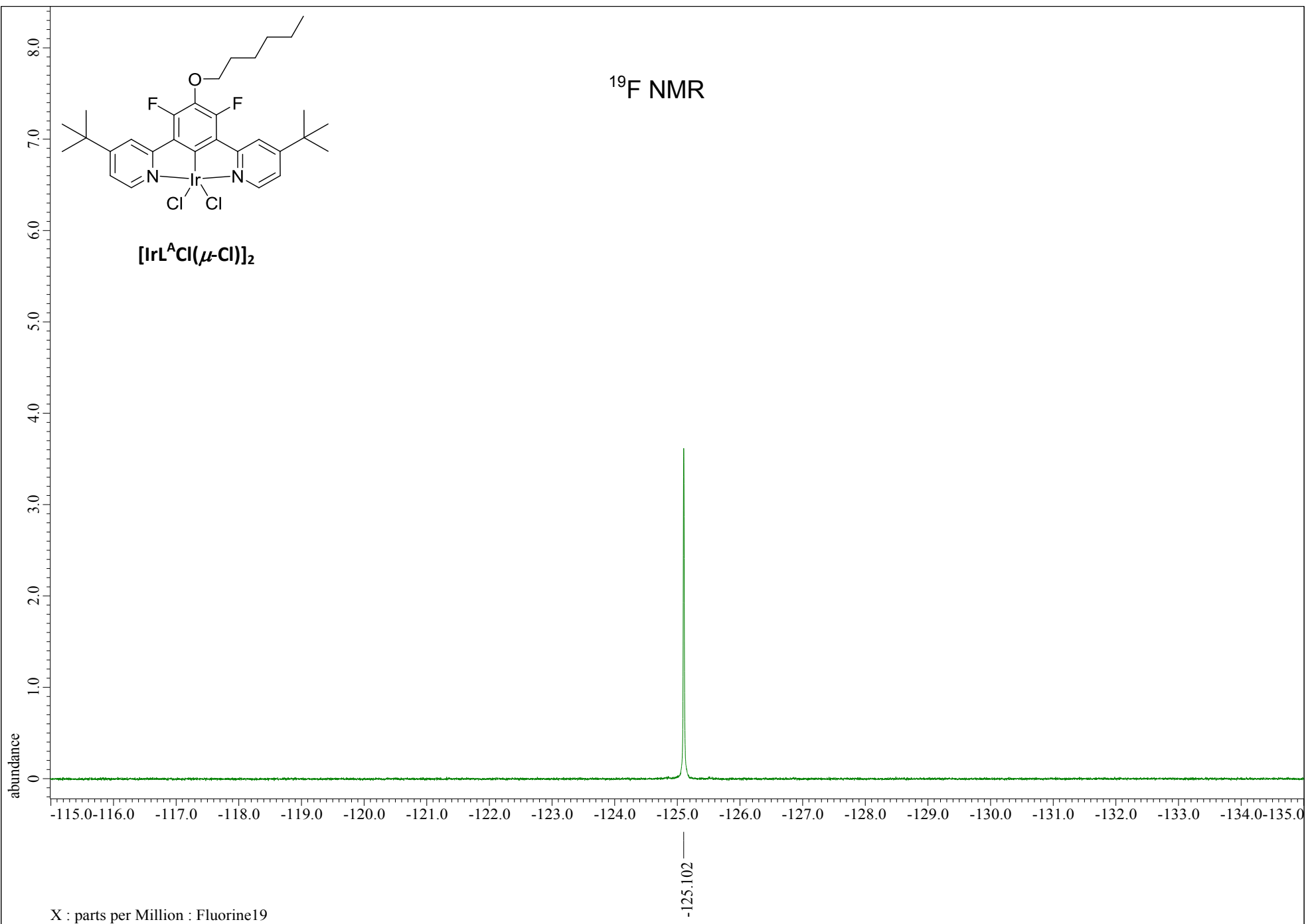
$[\text{IrL}^{\text{A}} \text{Cl}(\mu\text{-Cl})]_2$

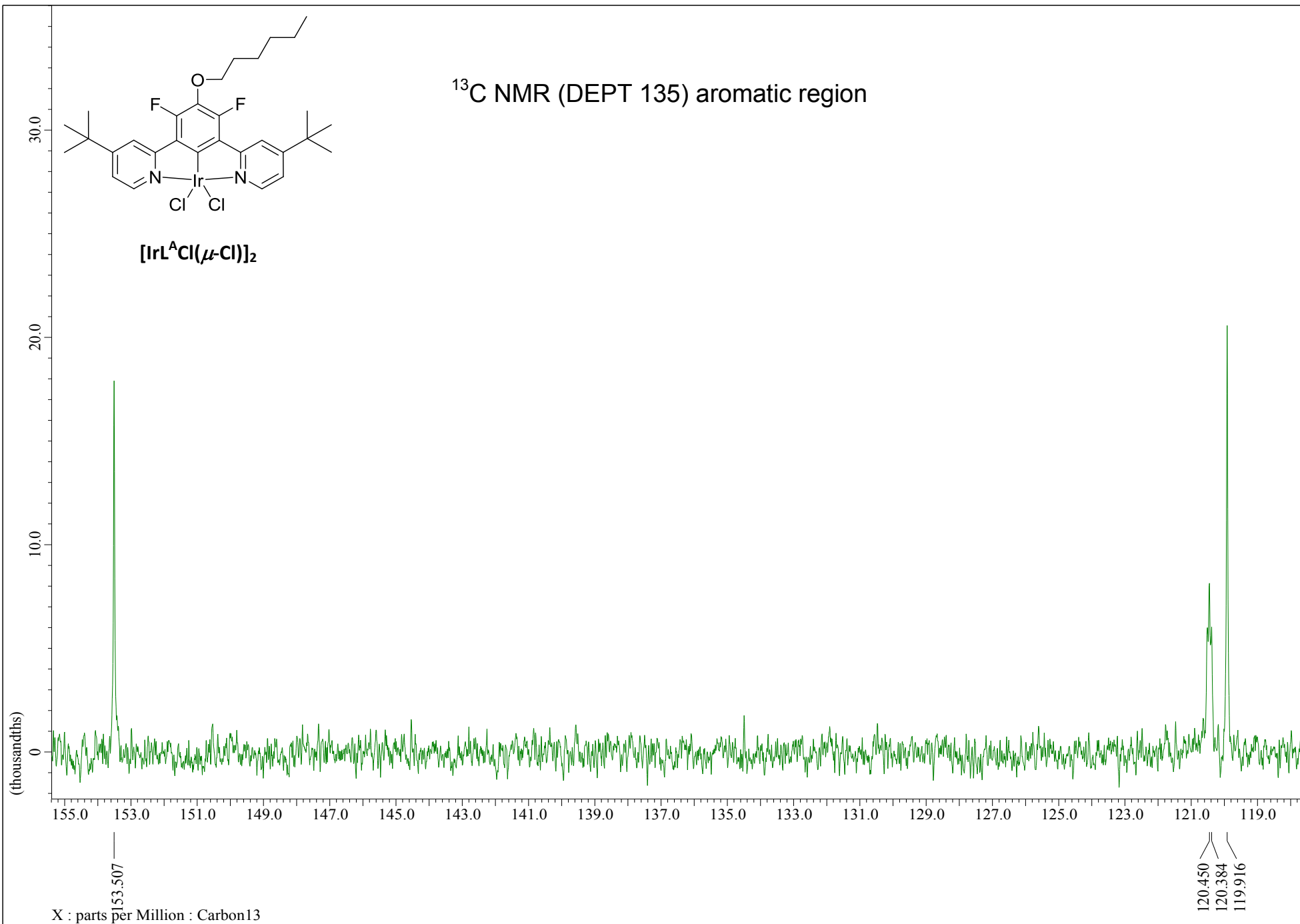
^1H NMR

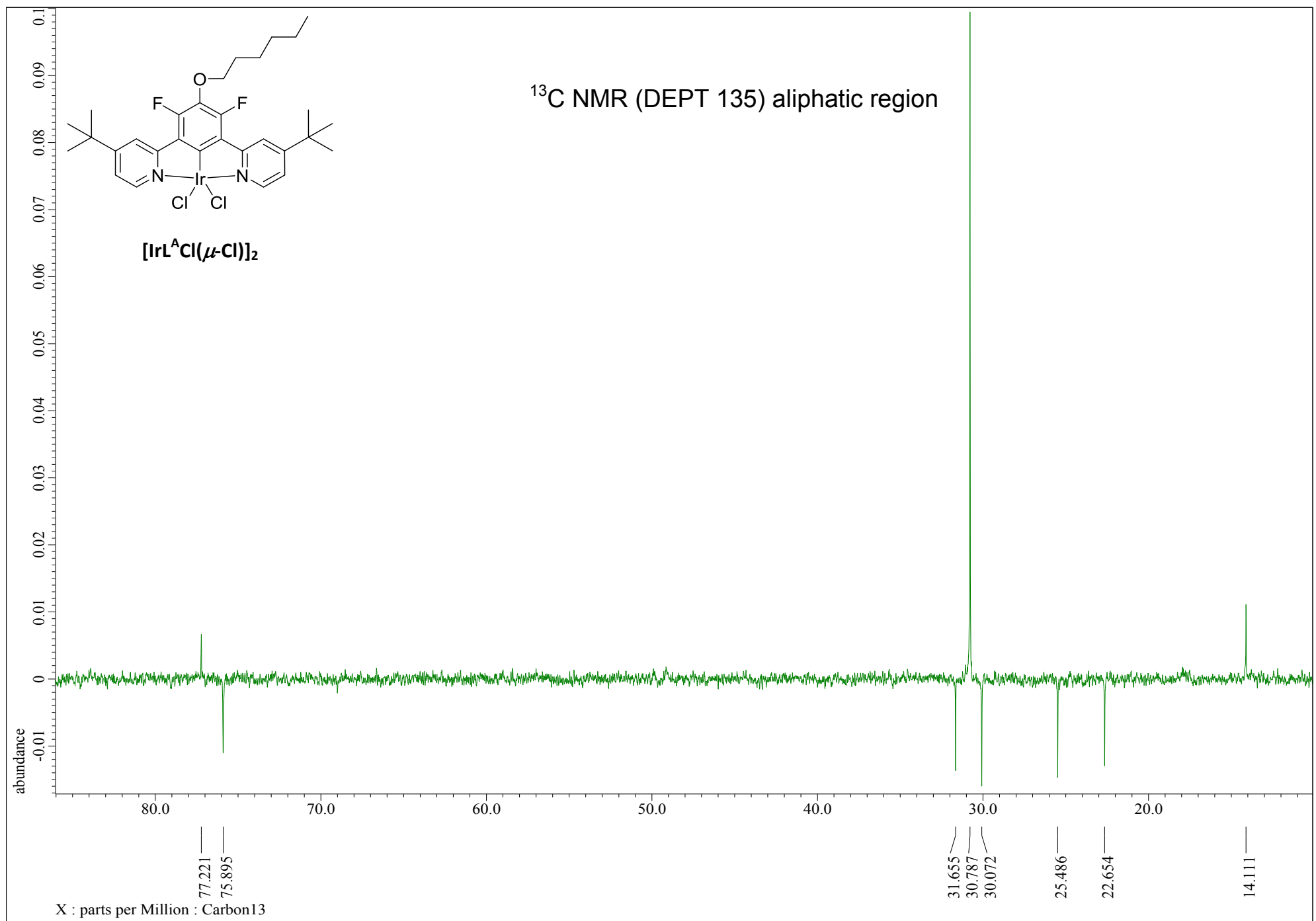


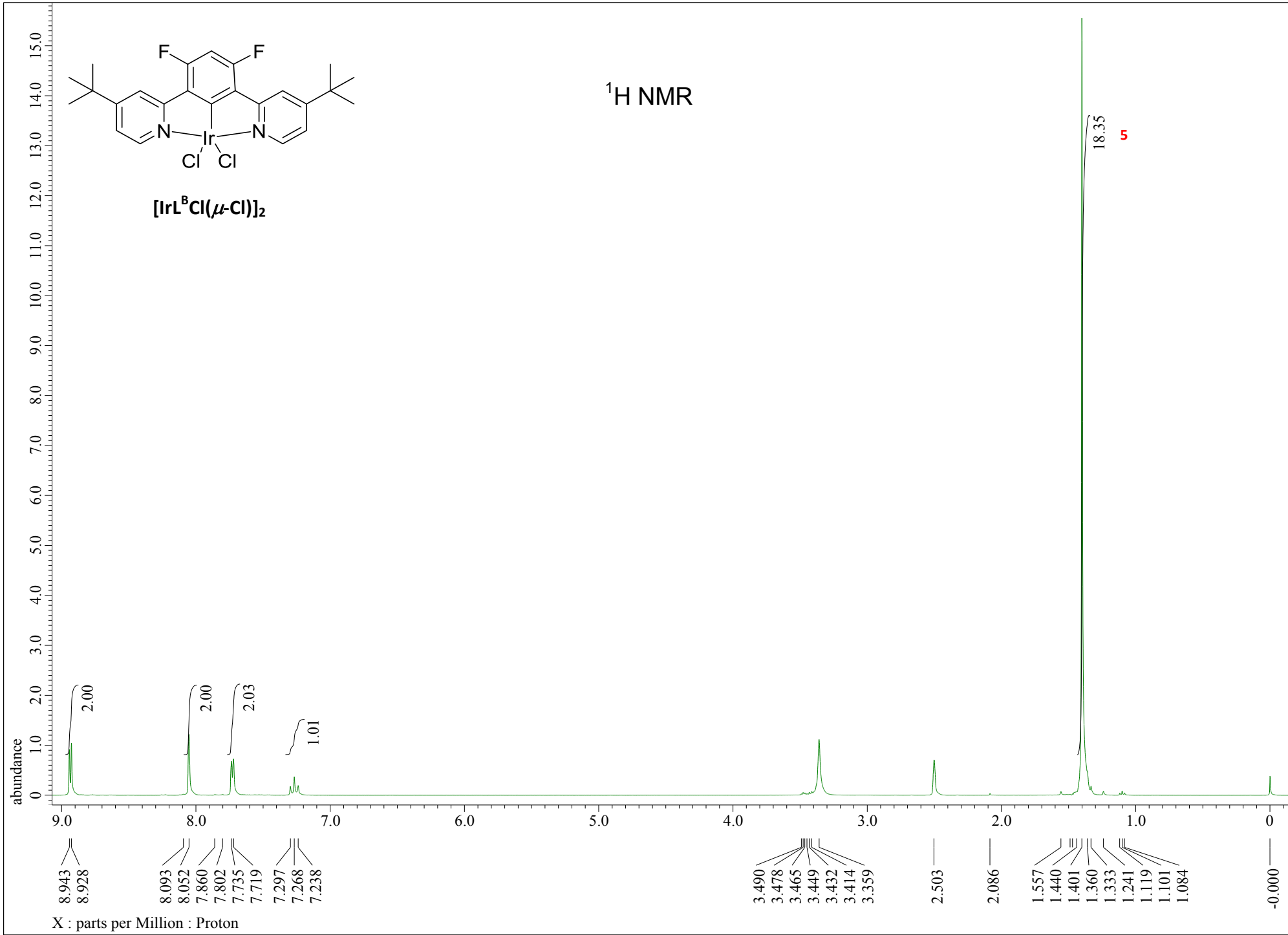


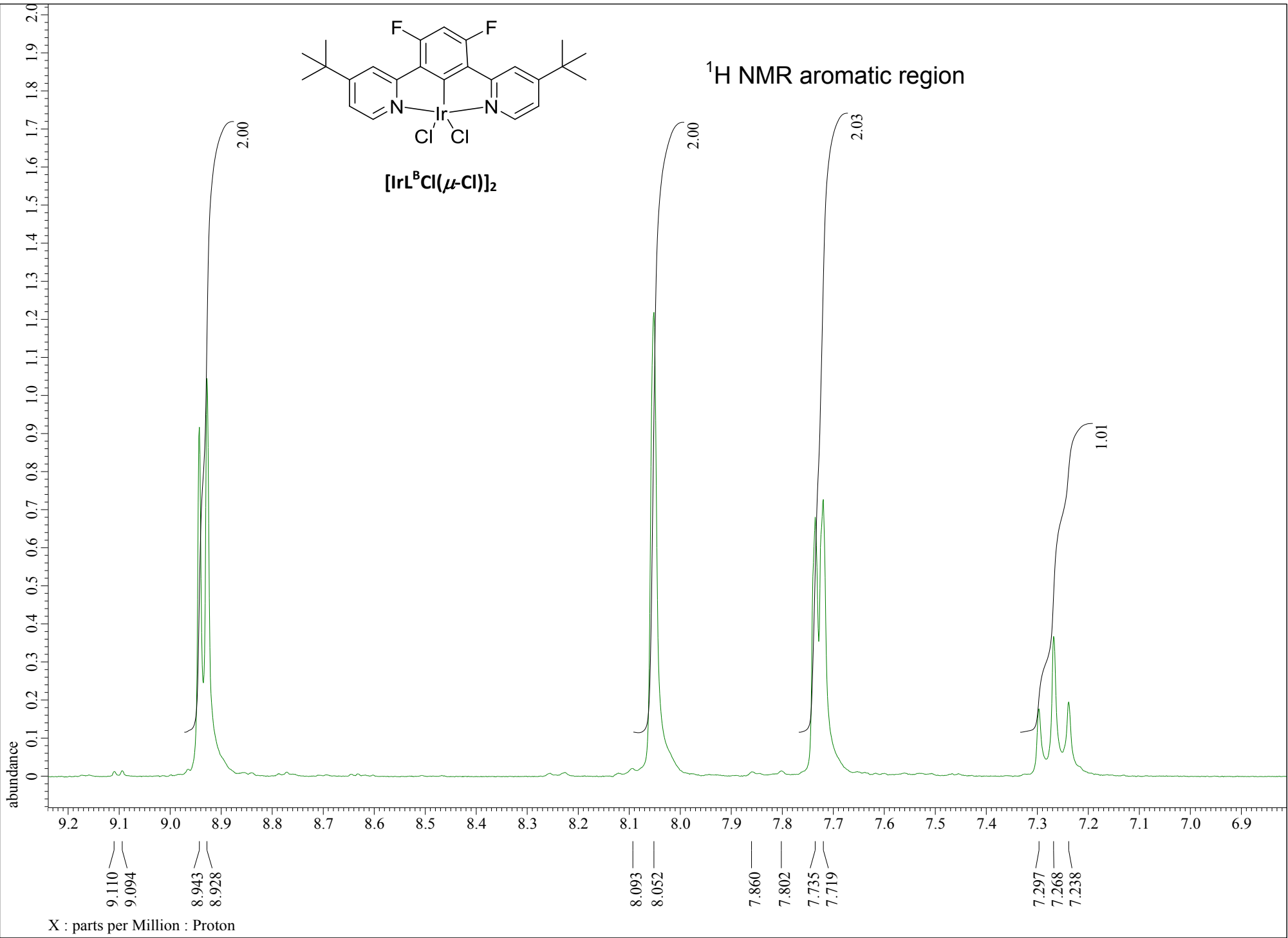


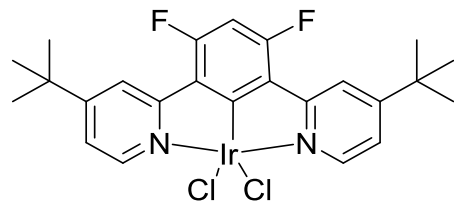






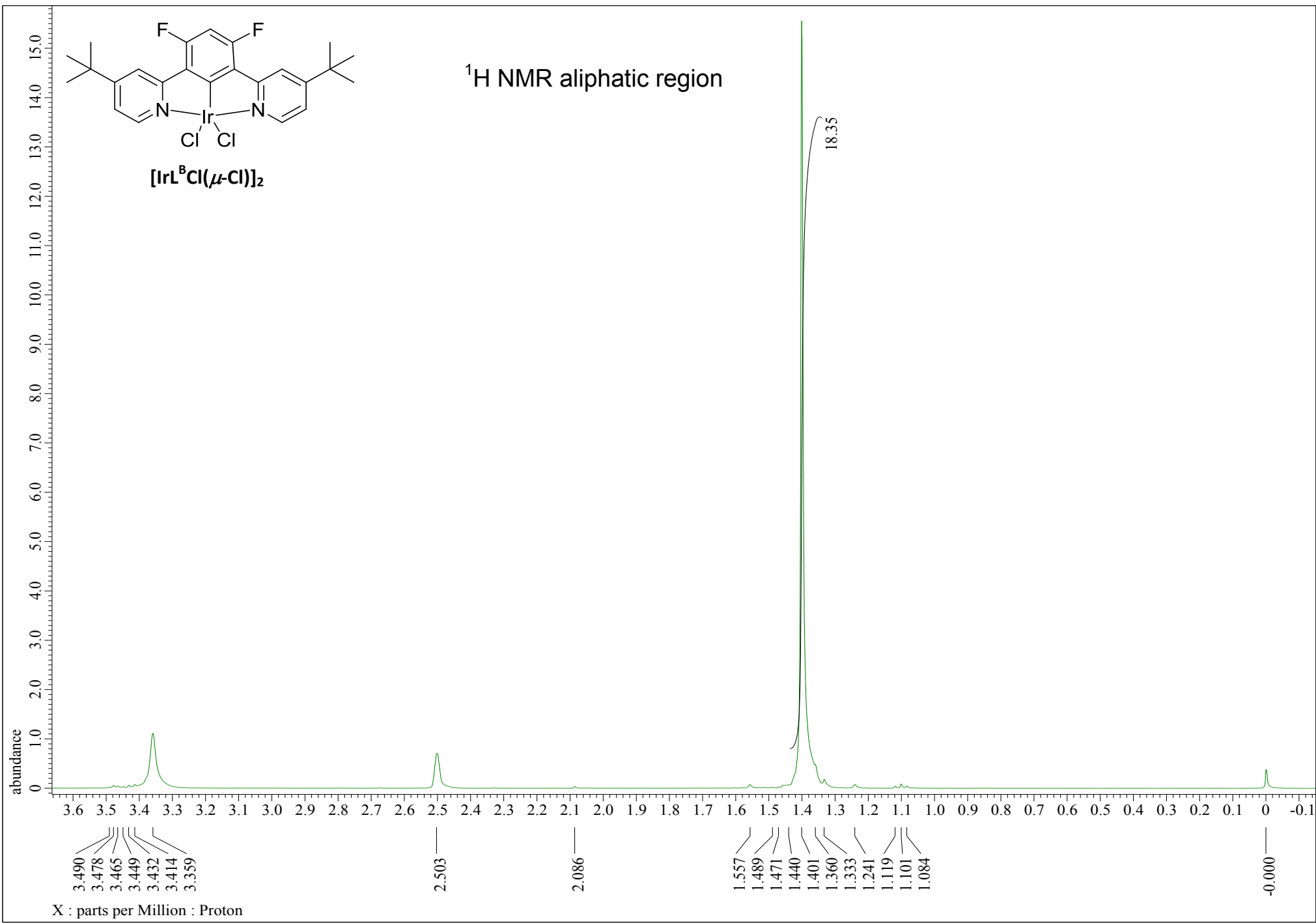


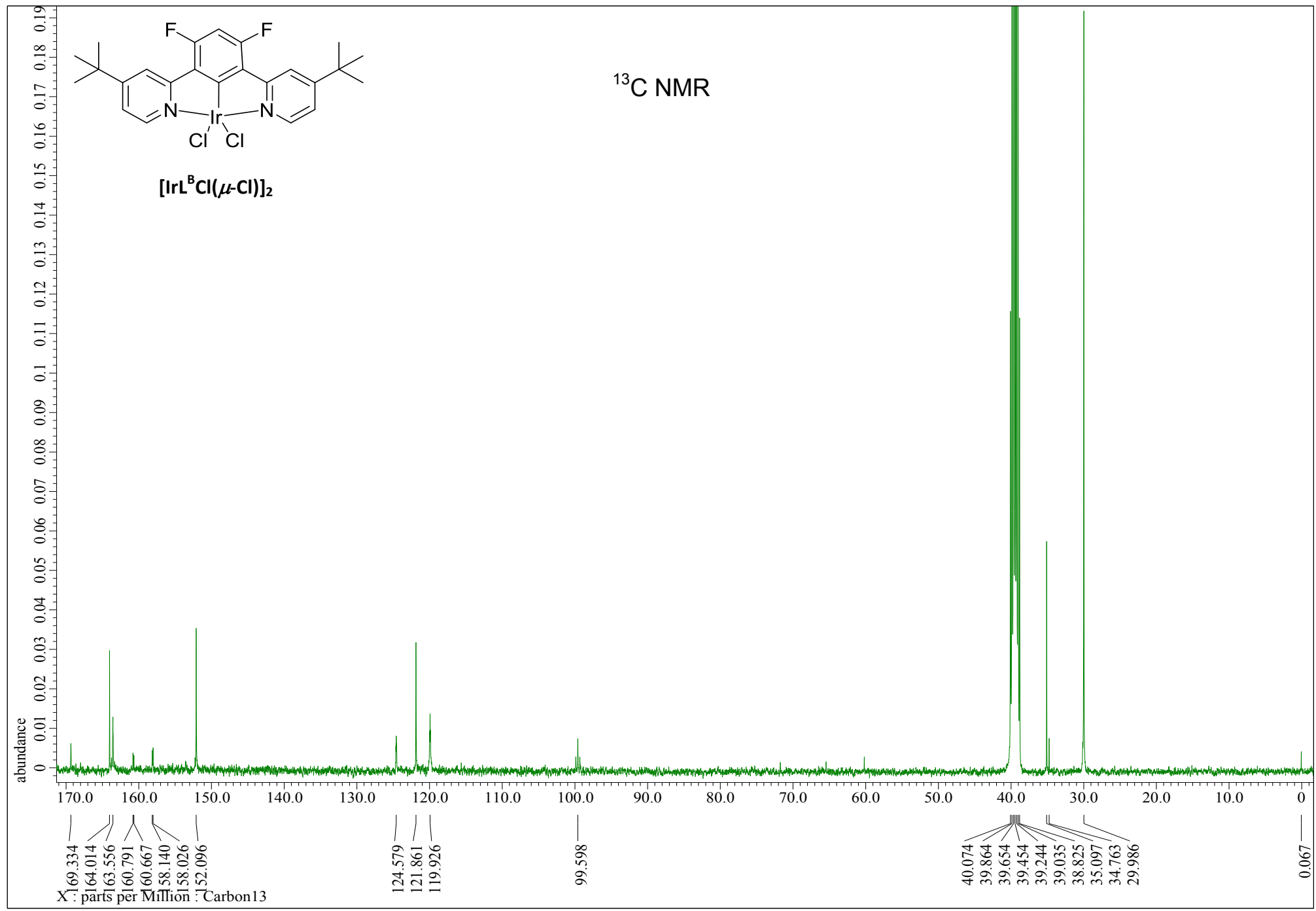


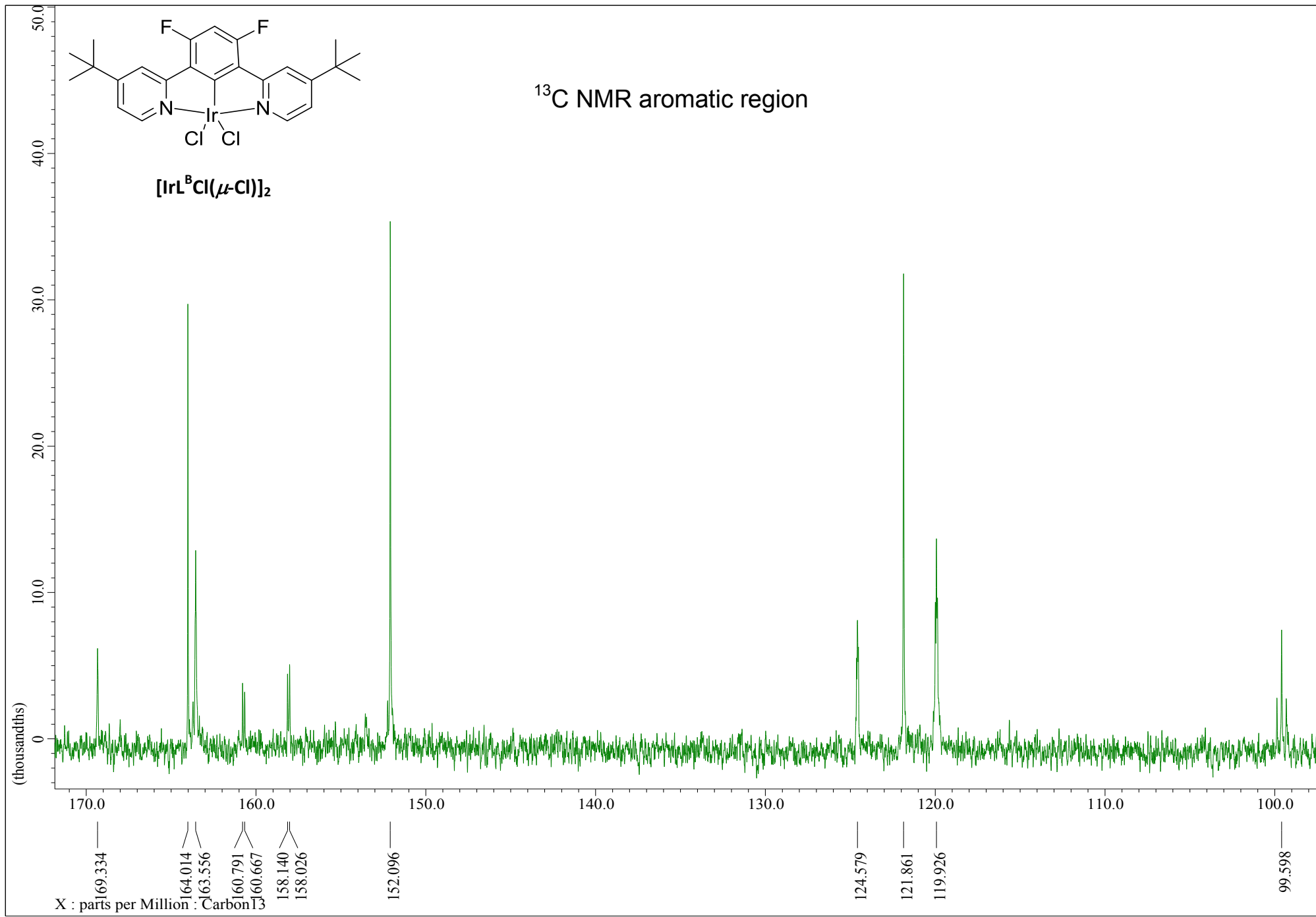


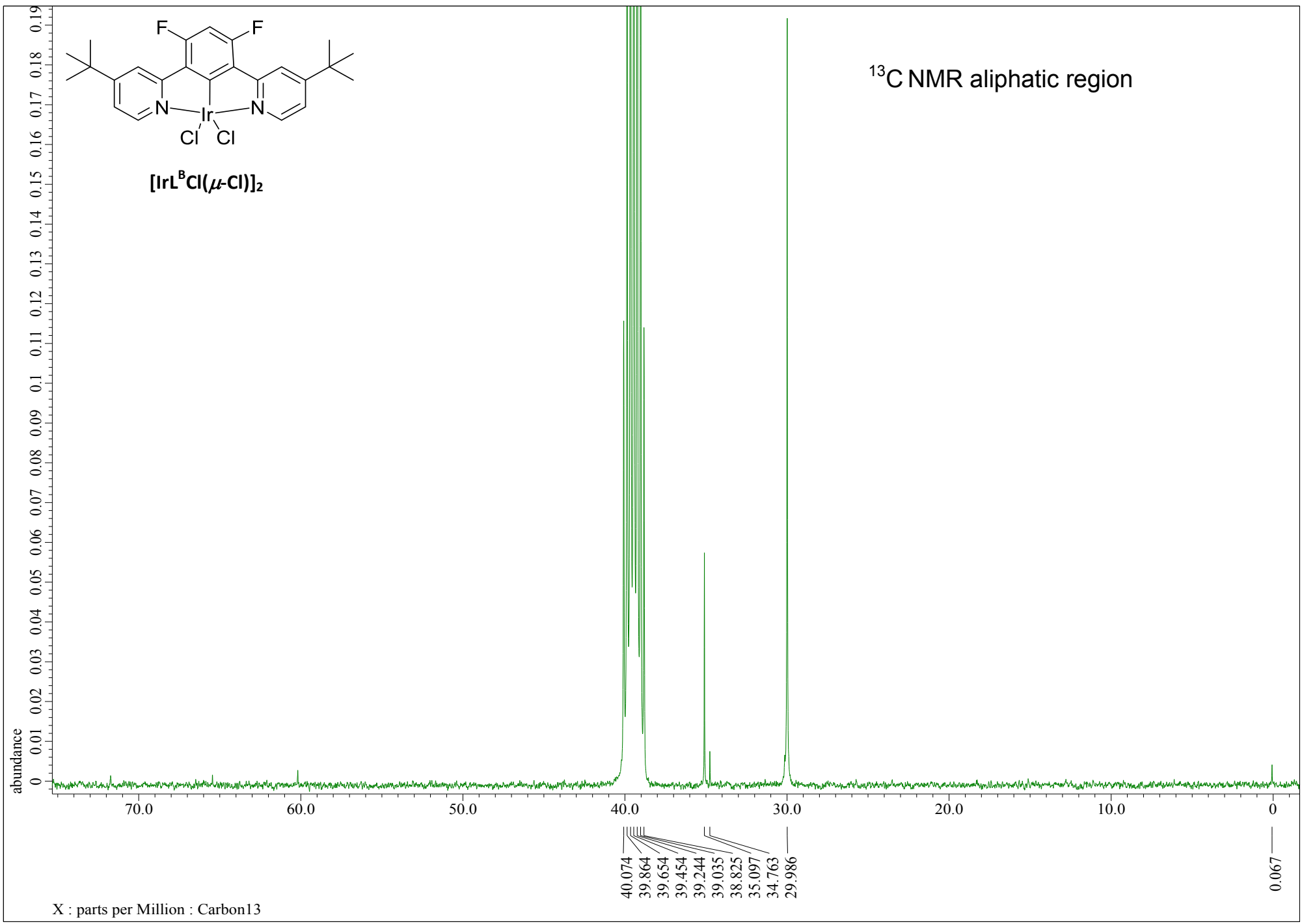
$[\text{IrL}^{\text{B}}\text{Cl}(\mu\text{-Cl})]_2$

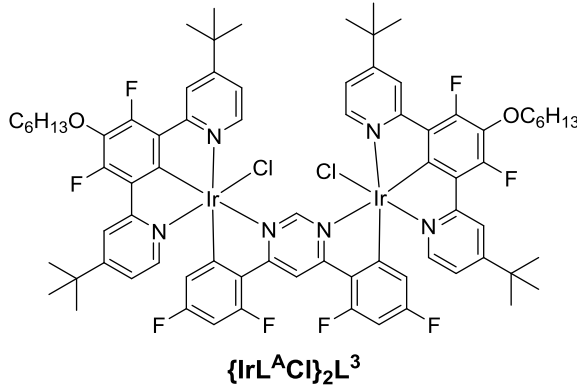
^1H NMR aliphatic region



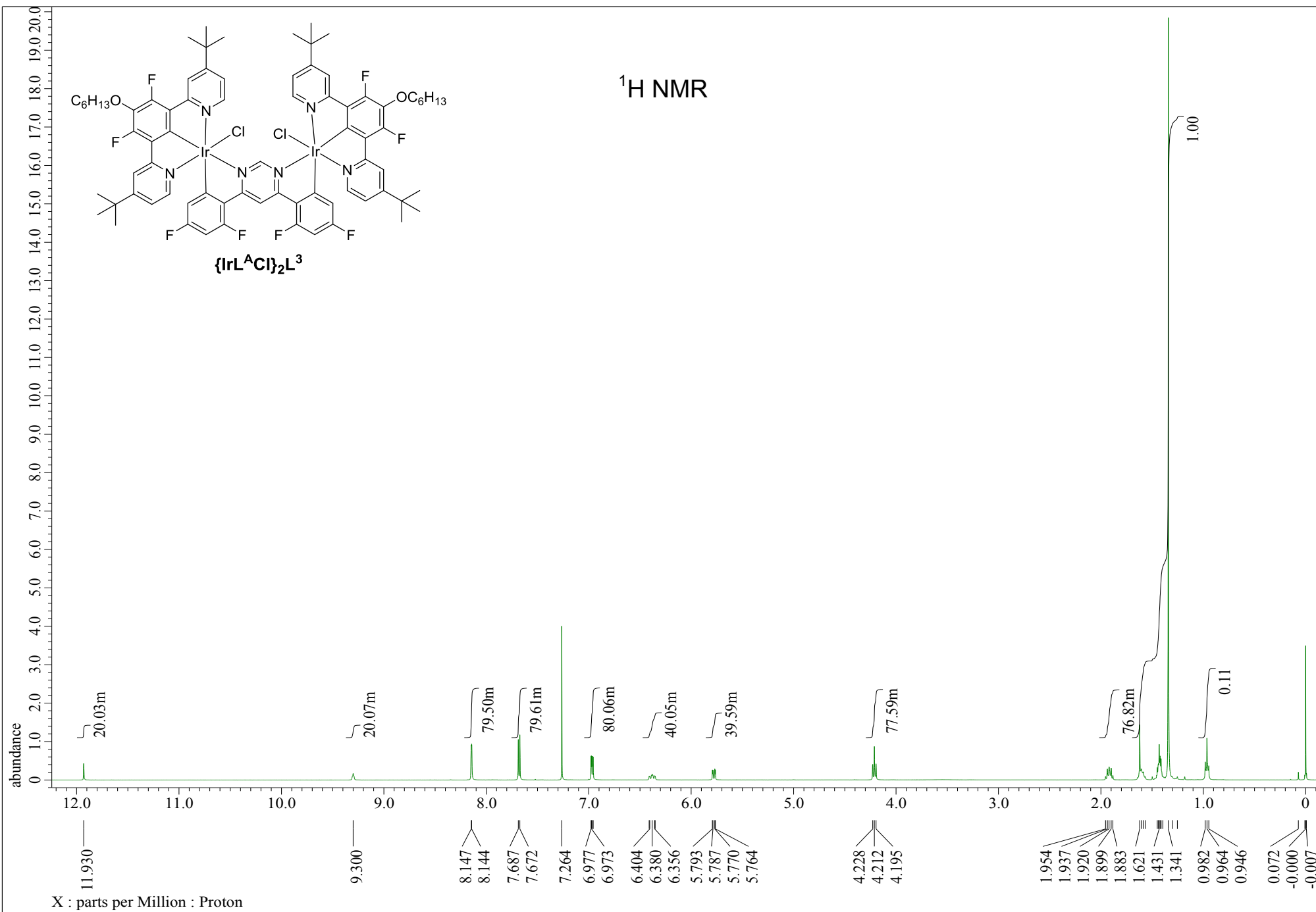


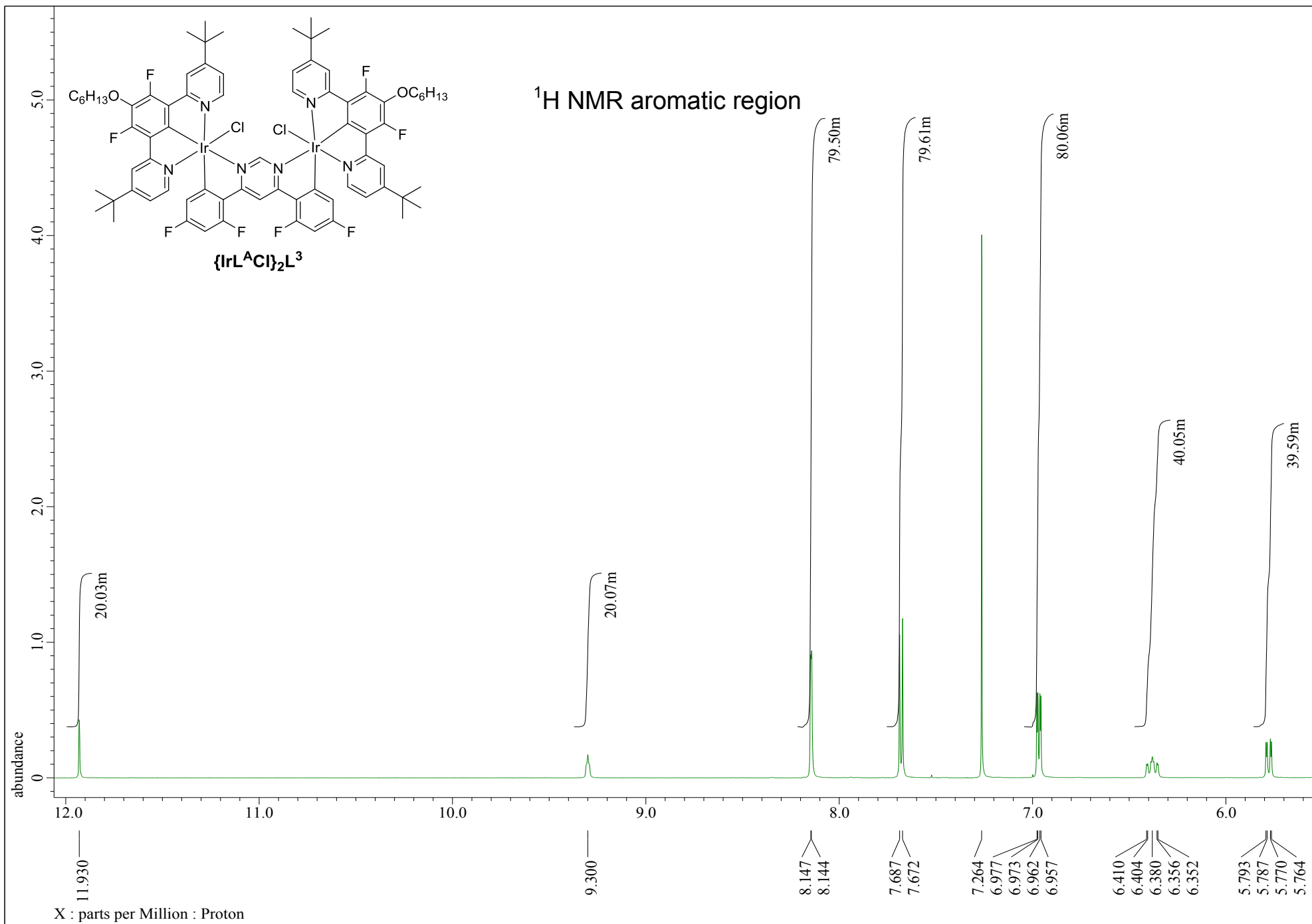


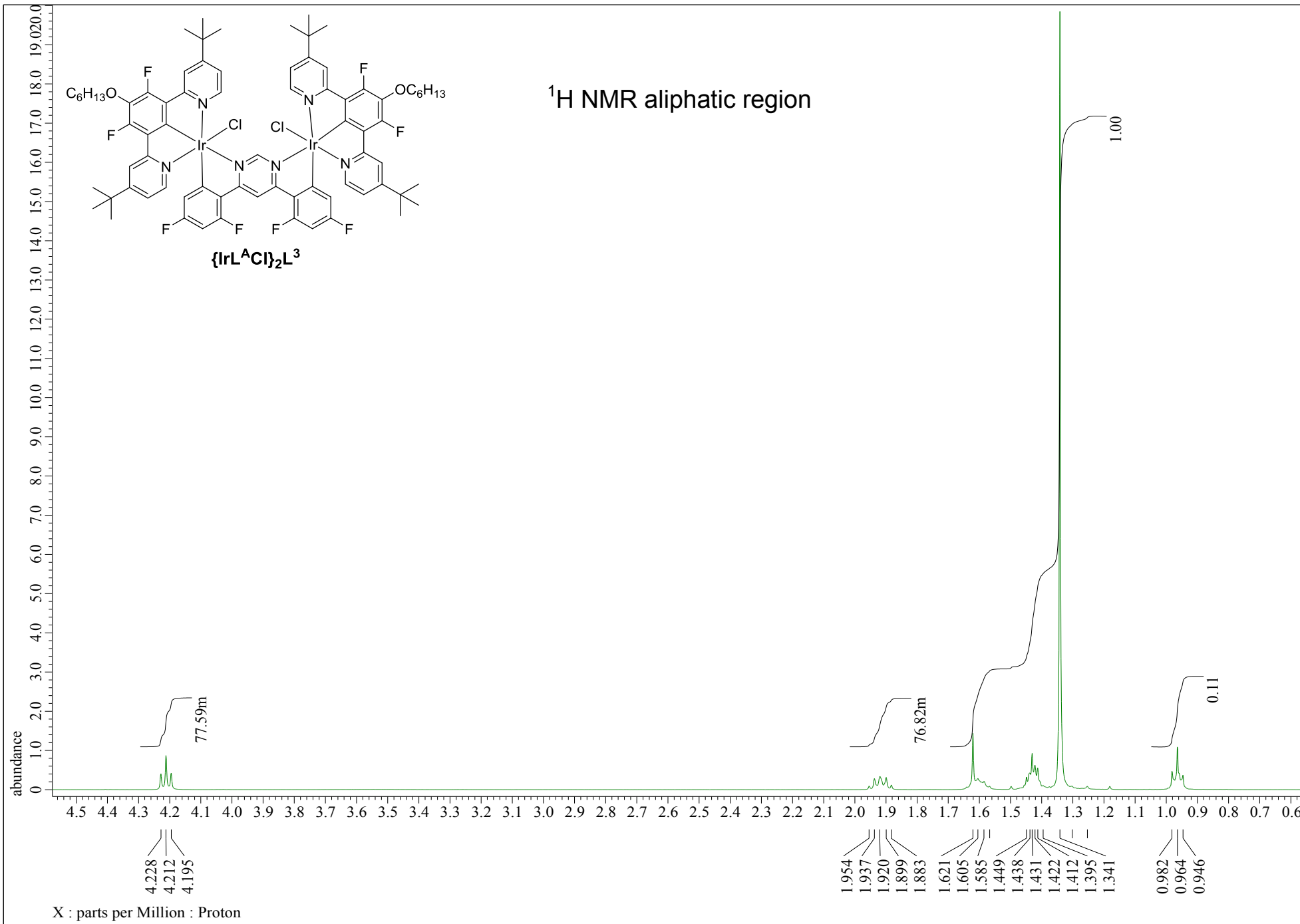


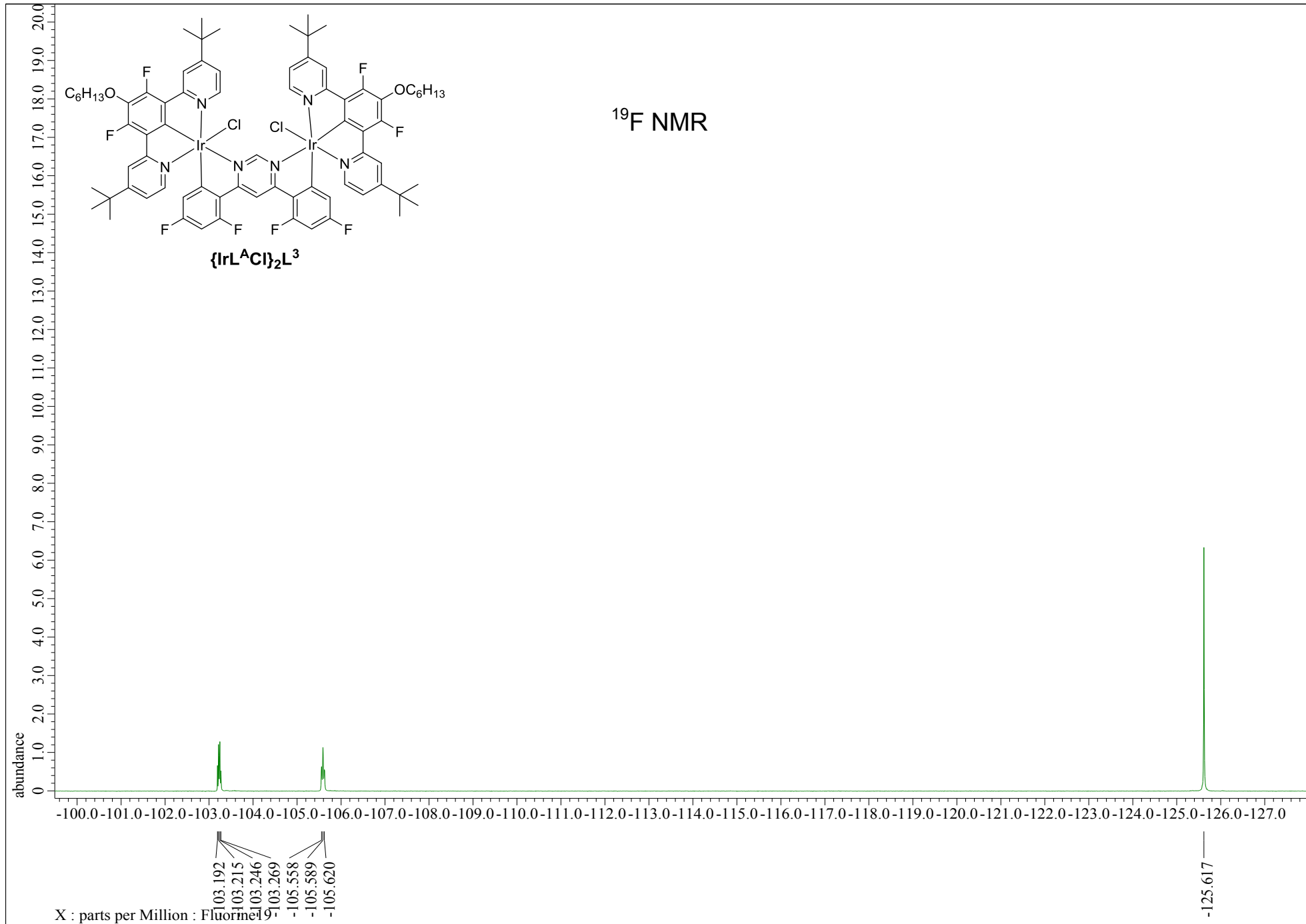


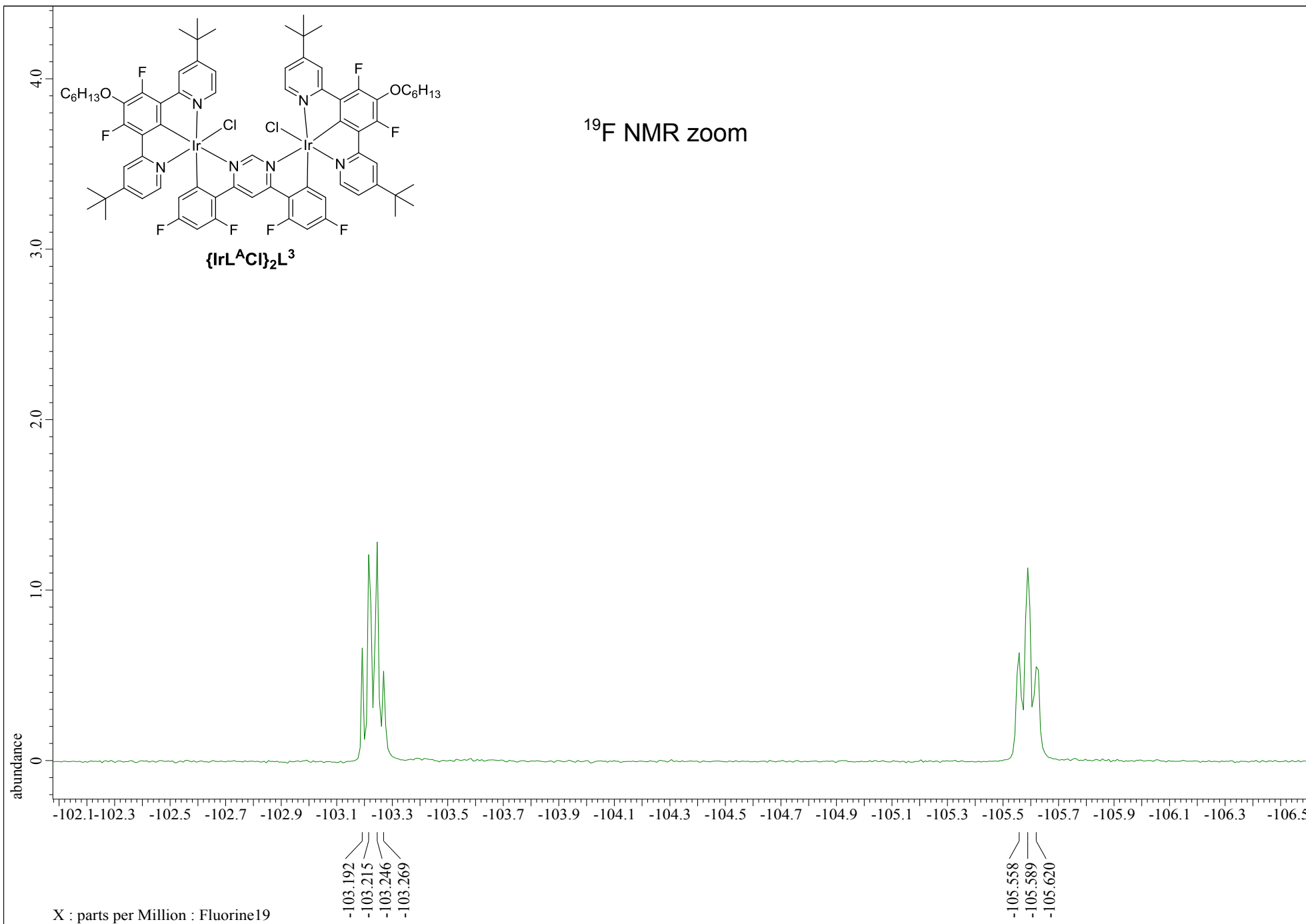
^1H NMR

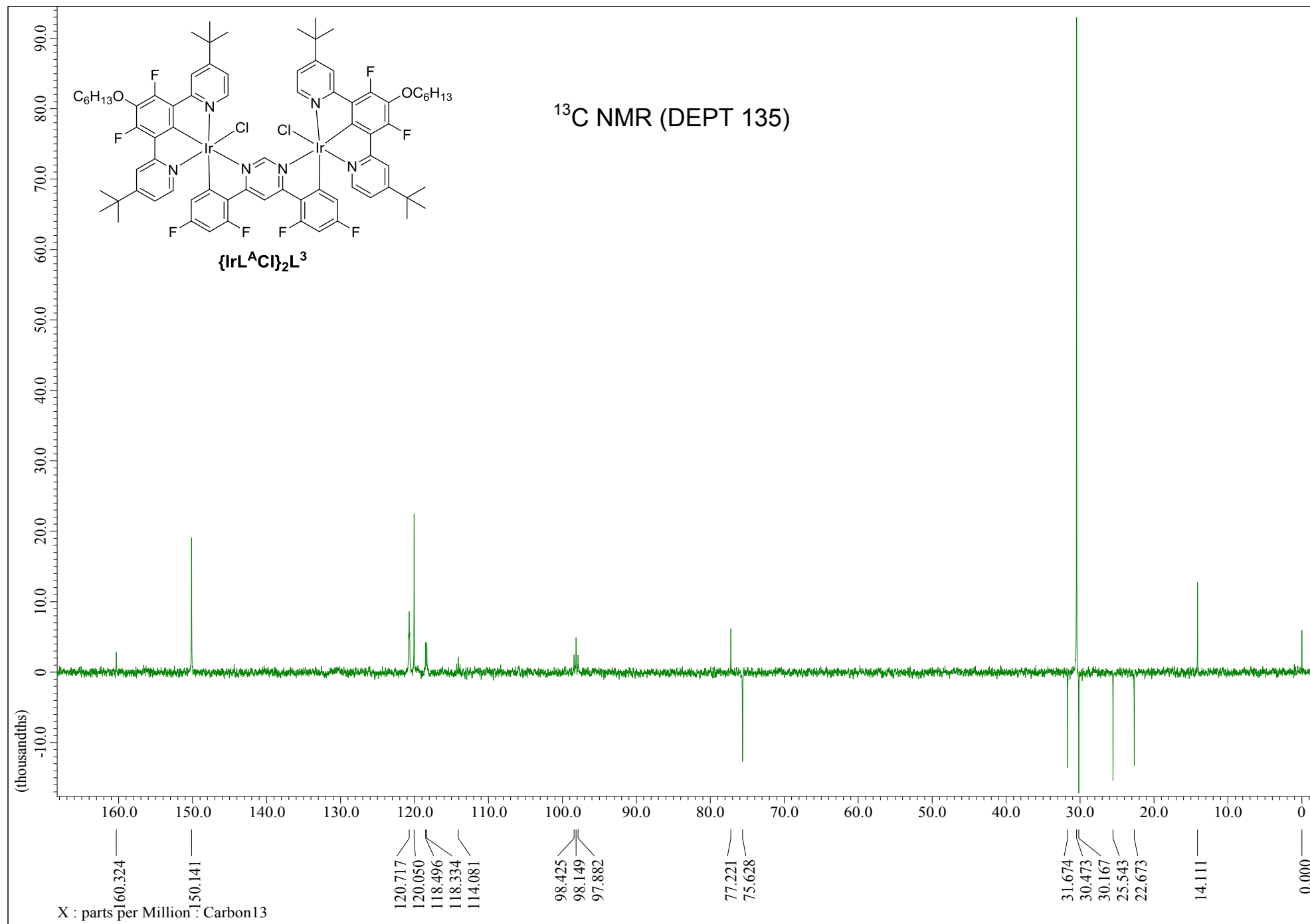


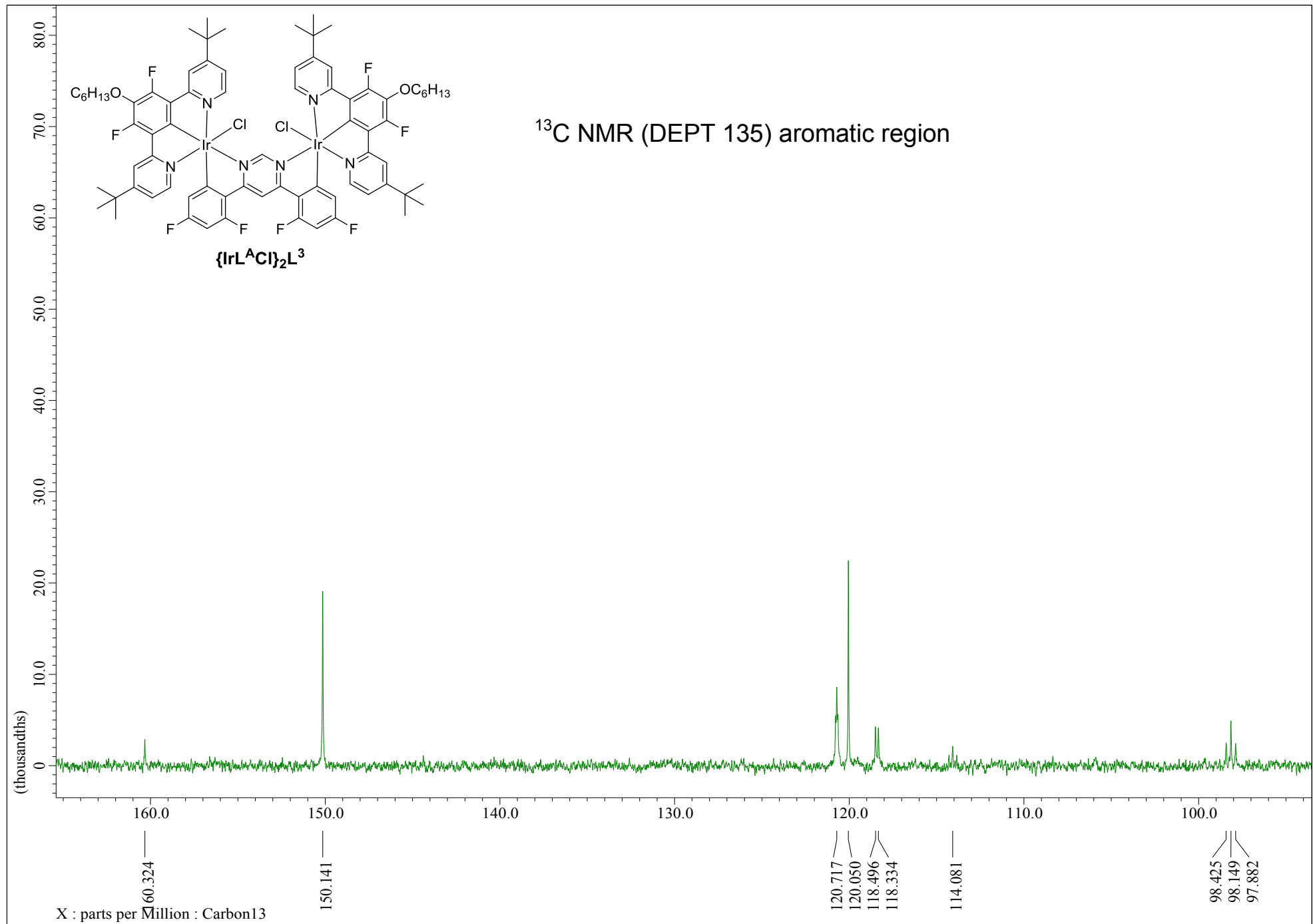


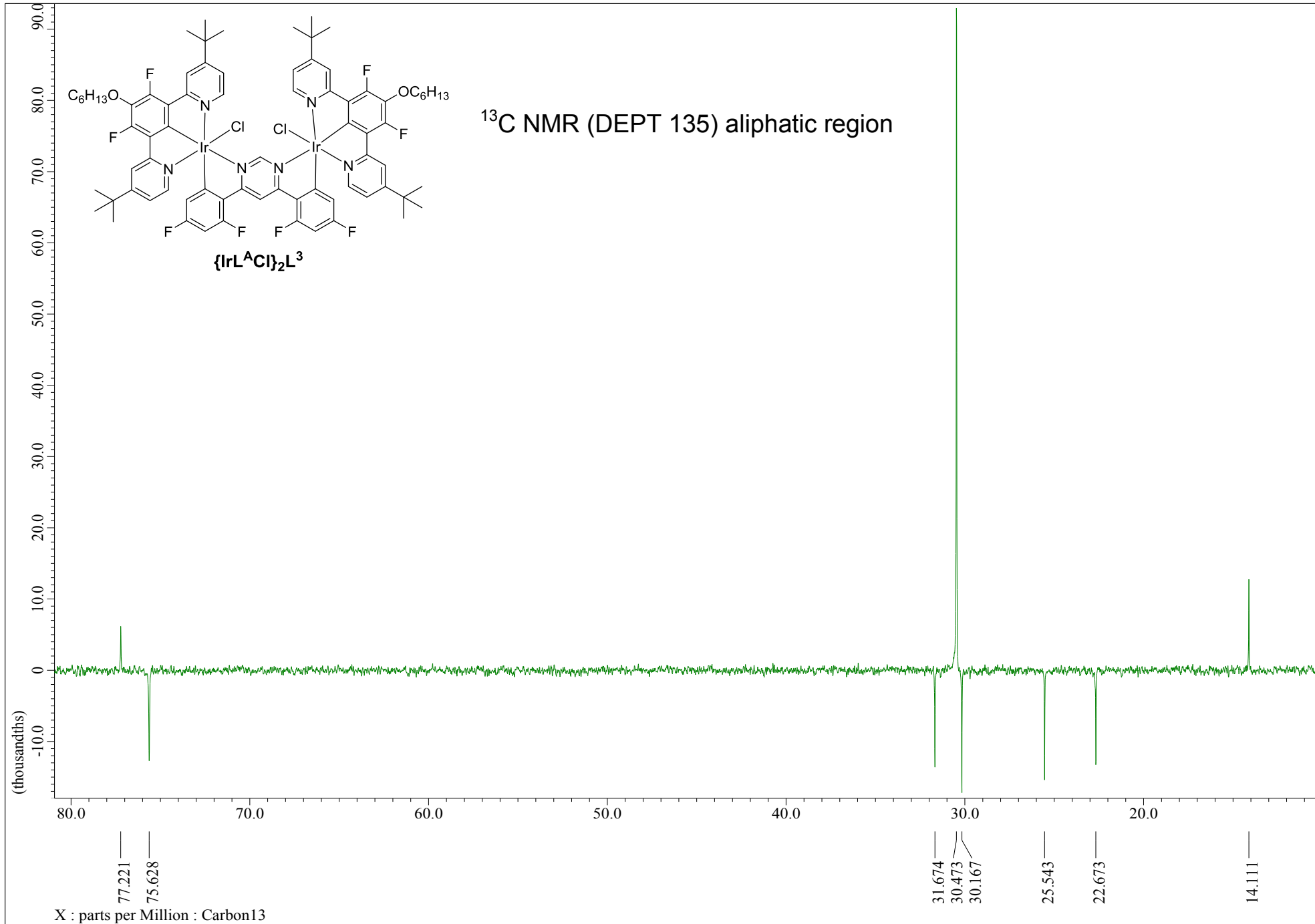






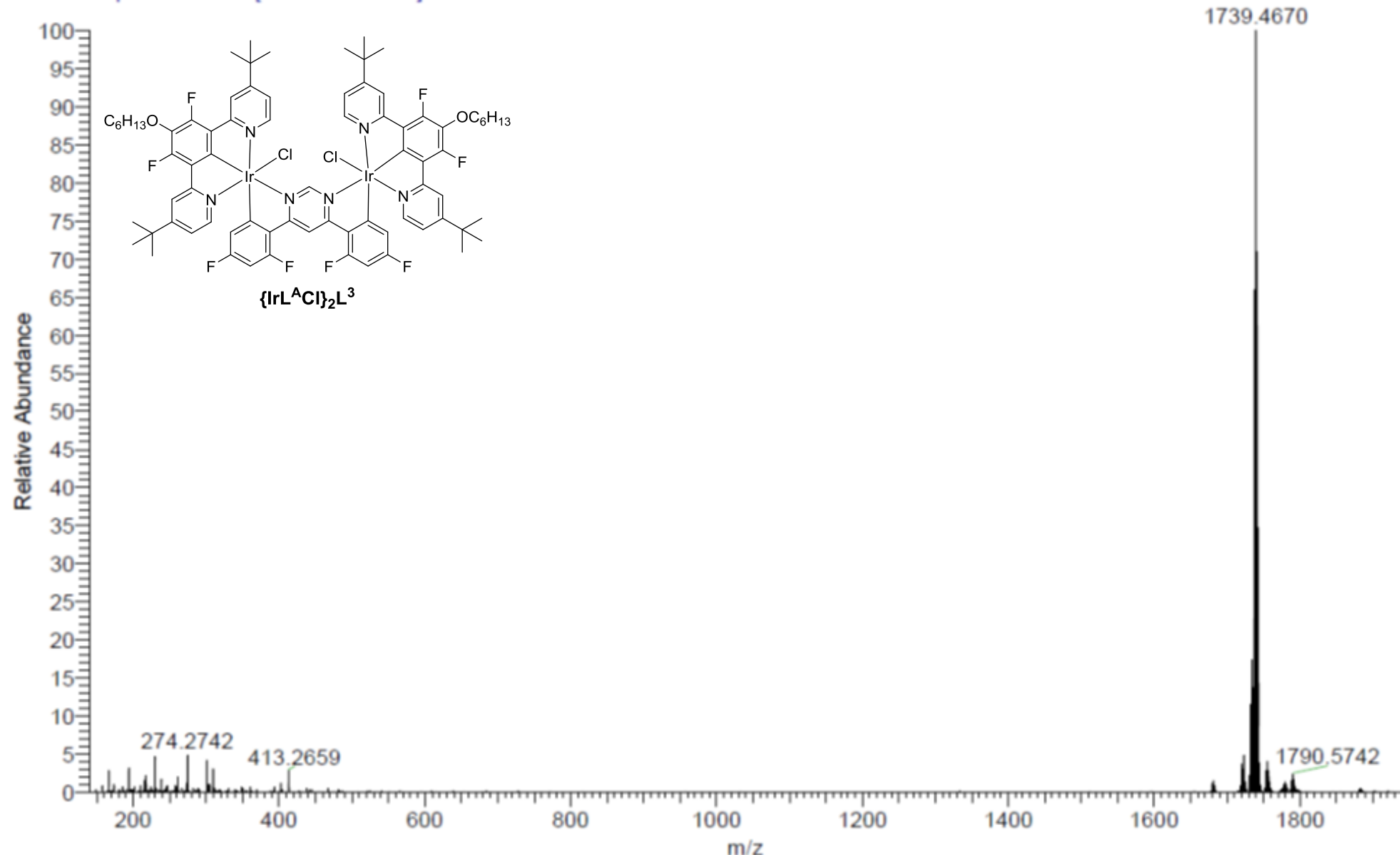






MW=1716?
(DCM)/MeCN
C76H80Cl2F8Ir2N6O2
NORKOZ048-OJ-HNESP #28-45 RT: 0.66-1.03 AV: 15 SM: 7G NL: 5.11E6
T: FTMS + p NSI Full ms [140.00-1935.00]

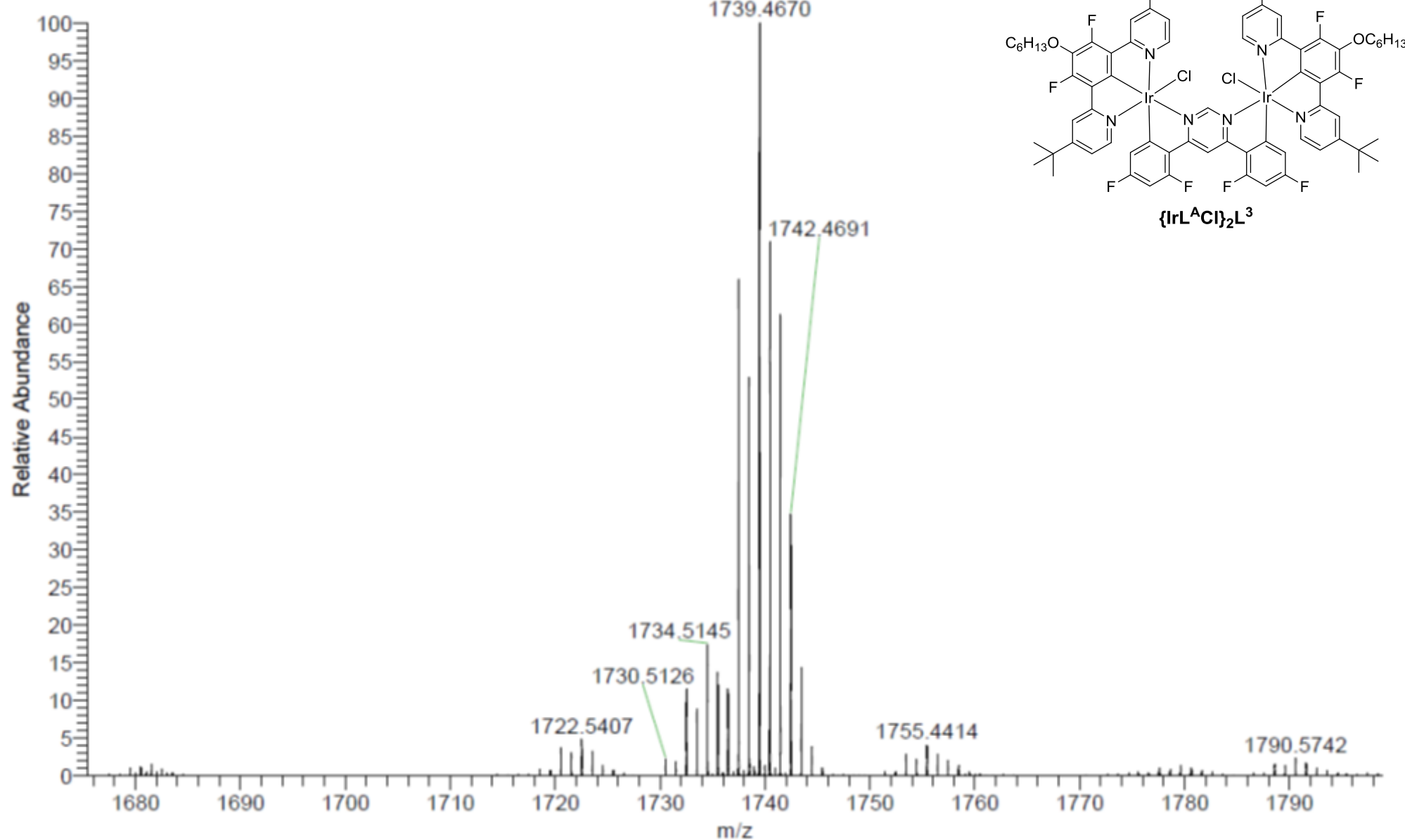
EPSRC National Facility Swansea
LTQ Orbitrap XL

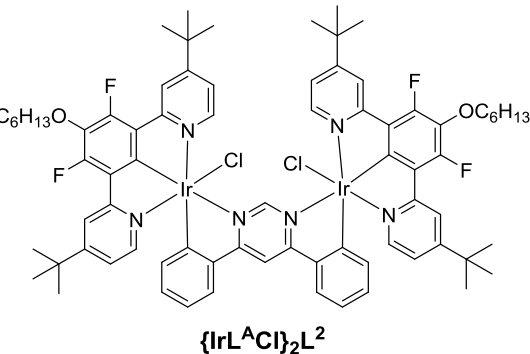
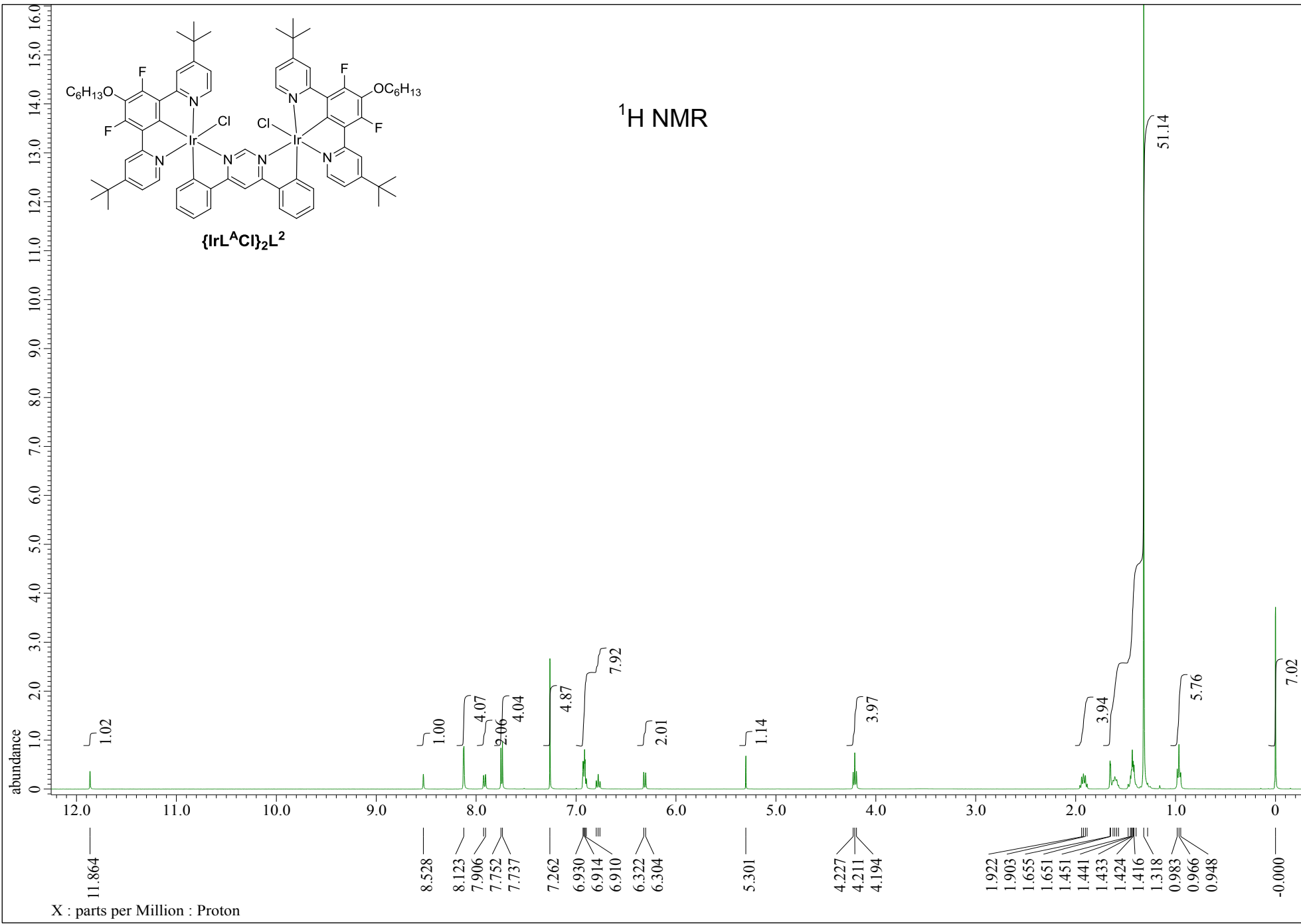


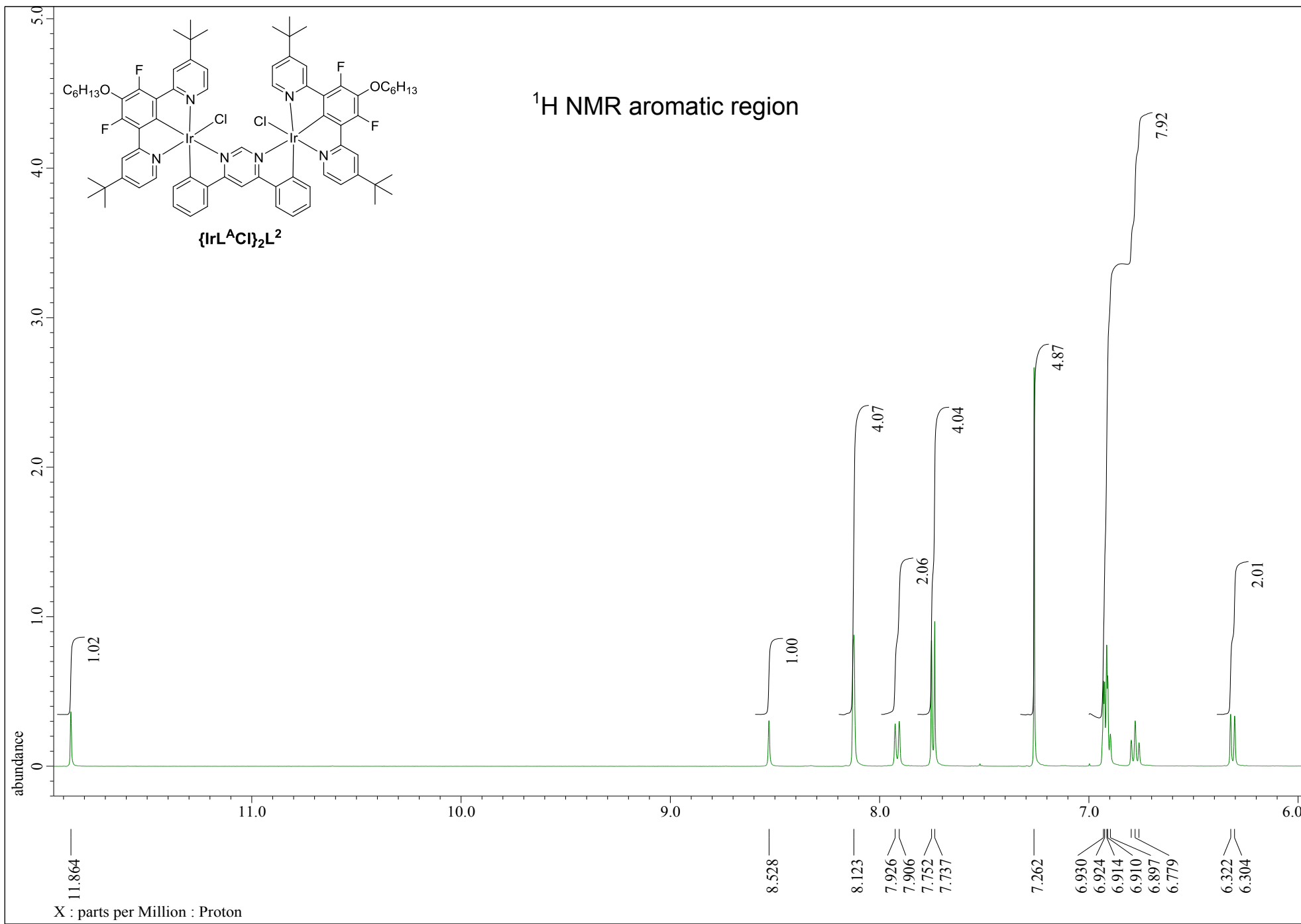
MW=1716?
(DCM)/MeCN
C76H80Cl2F8Ir2N6O2

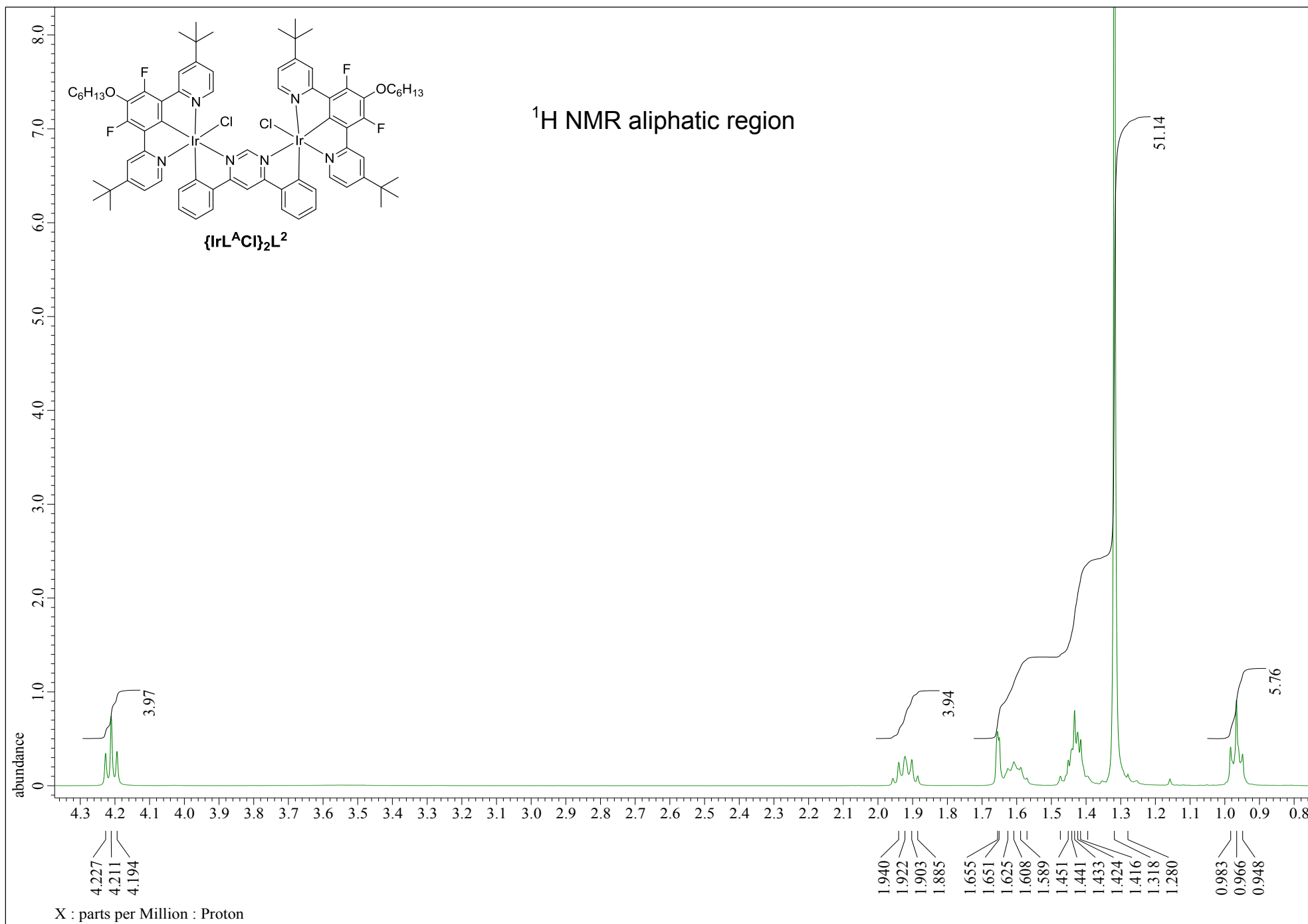
EPSRC National Facility Swansea
LTQ Orbitrap XL

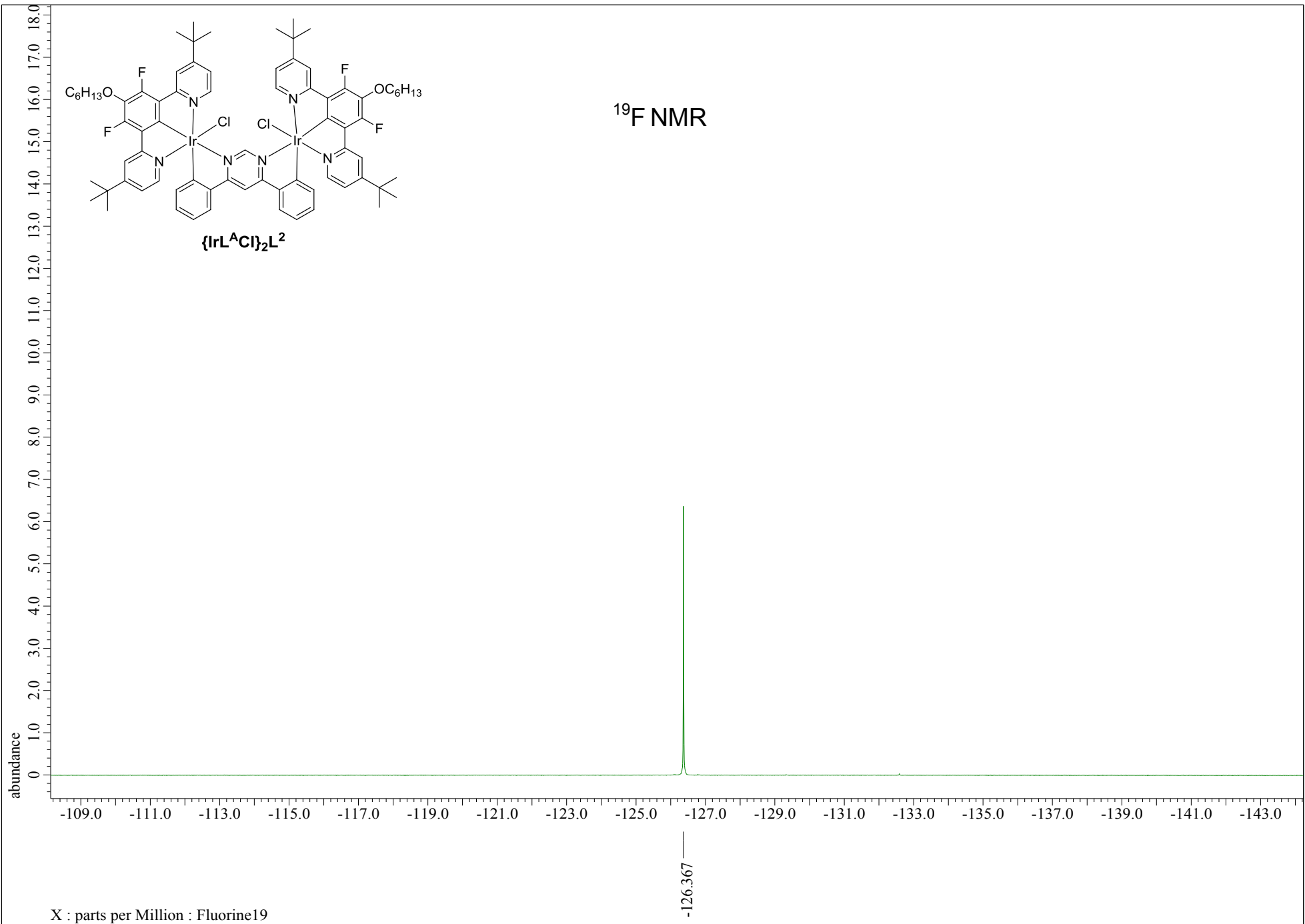
NORKOZ048-OJ-HNESP #28-45 RT: 0.66-1.03 AV: 15 SM: 7G NL: 5.11E6
T: FTMS + p NSI Full ms [140.00-1935.00]

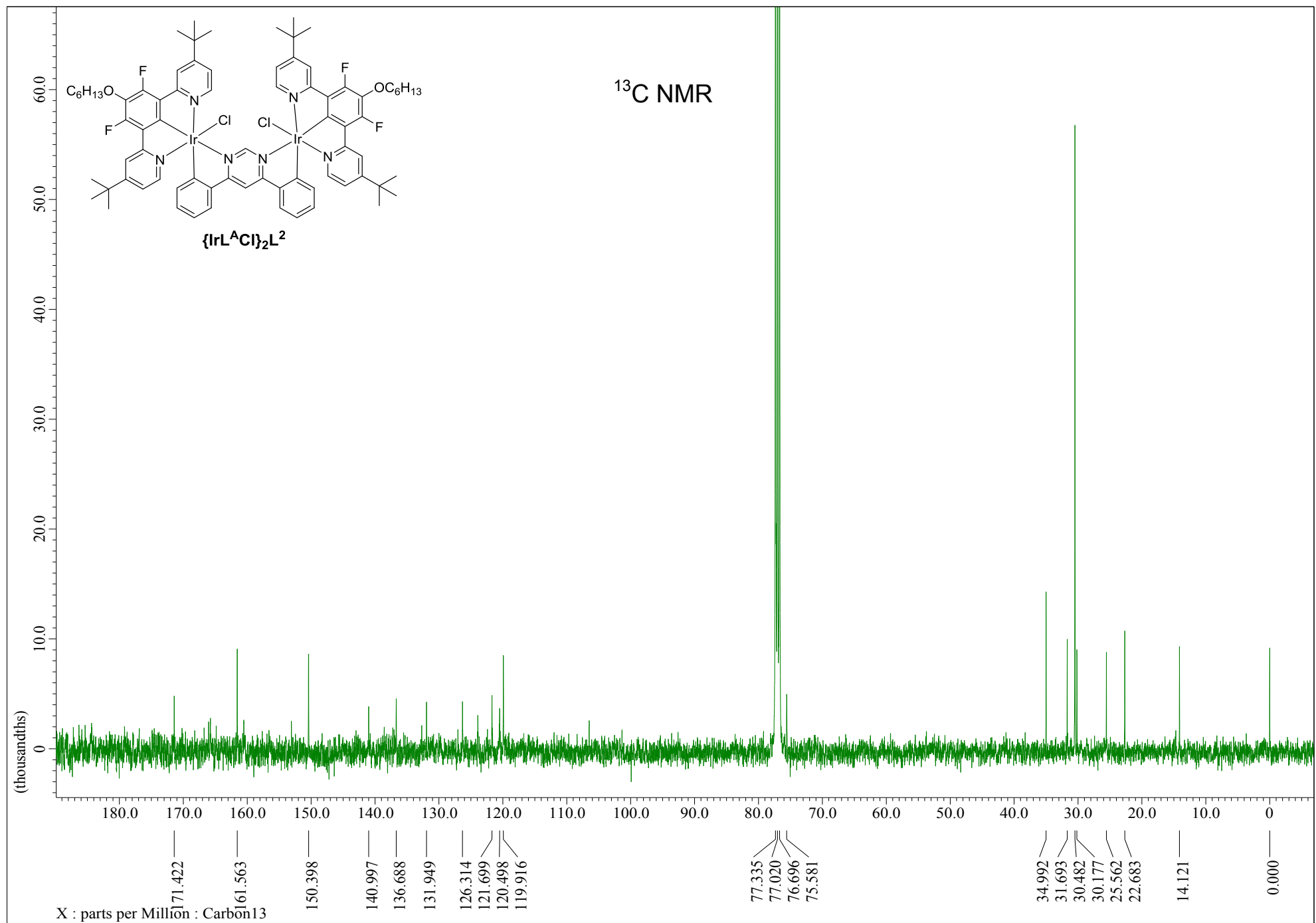


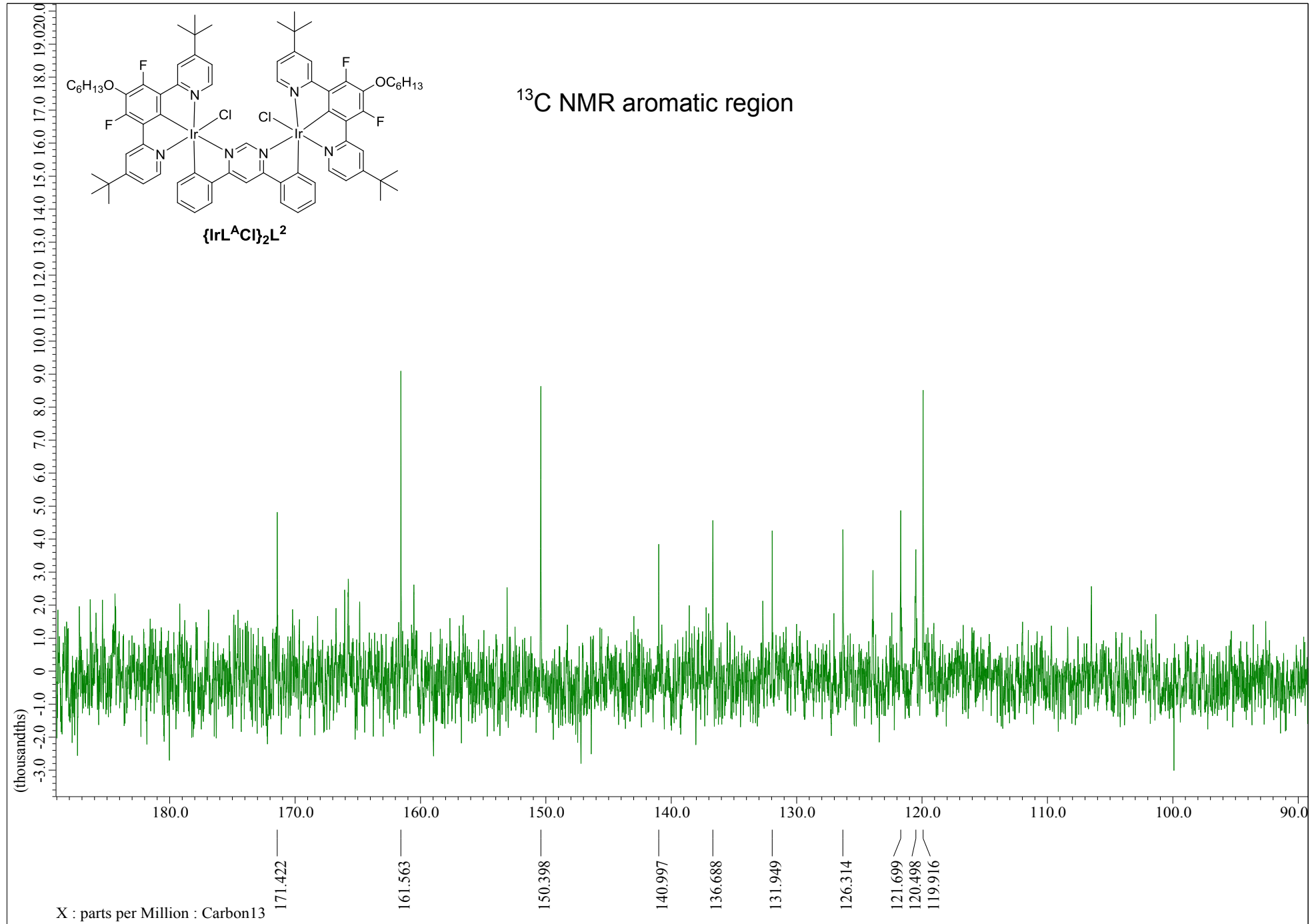


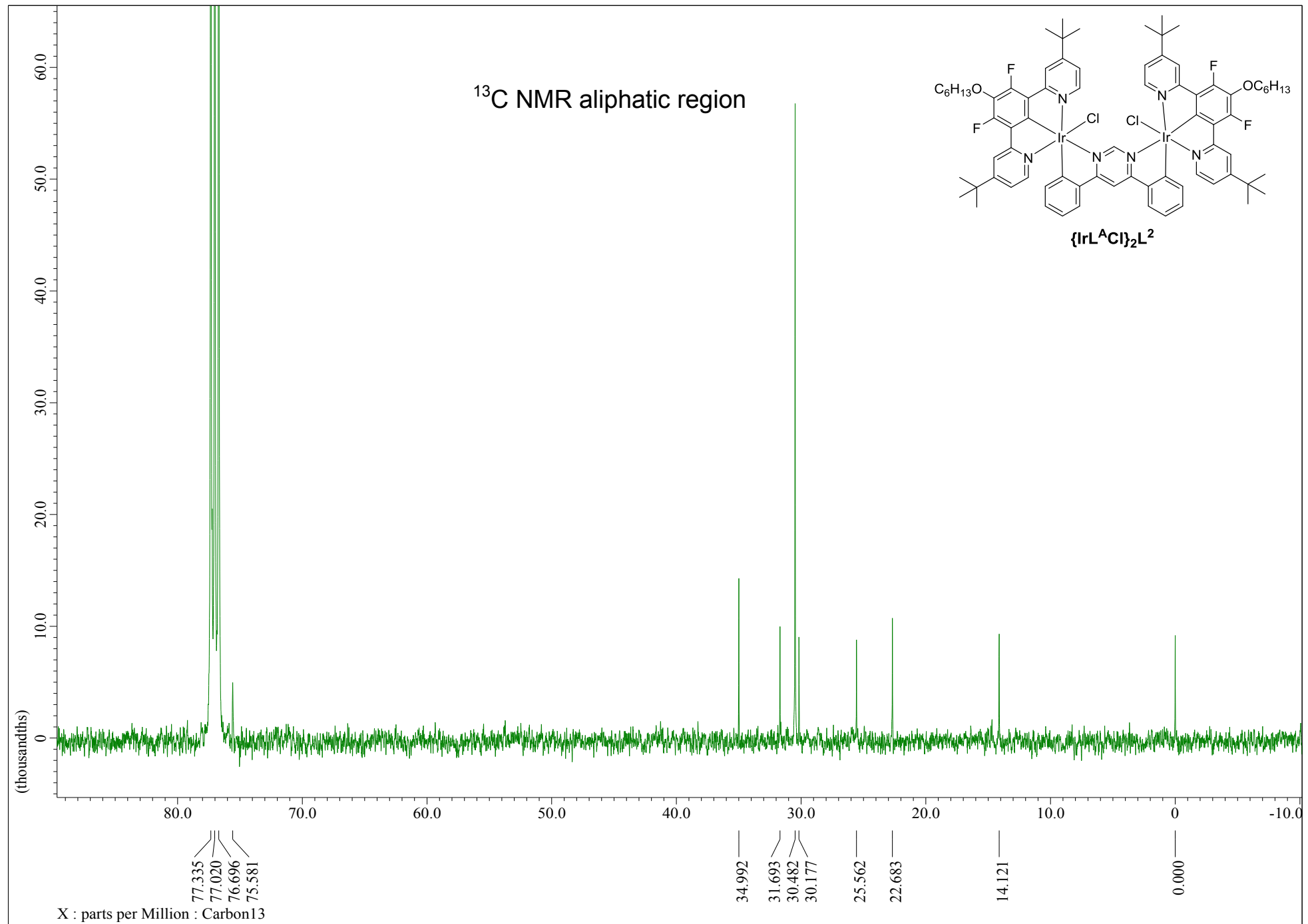


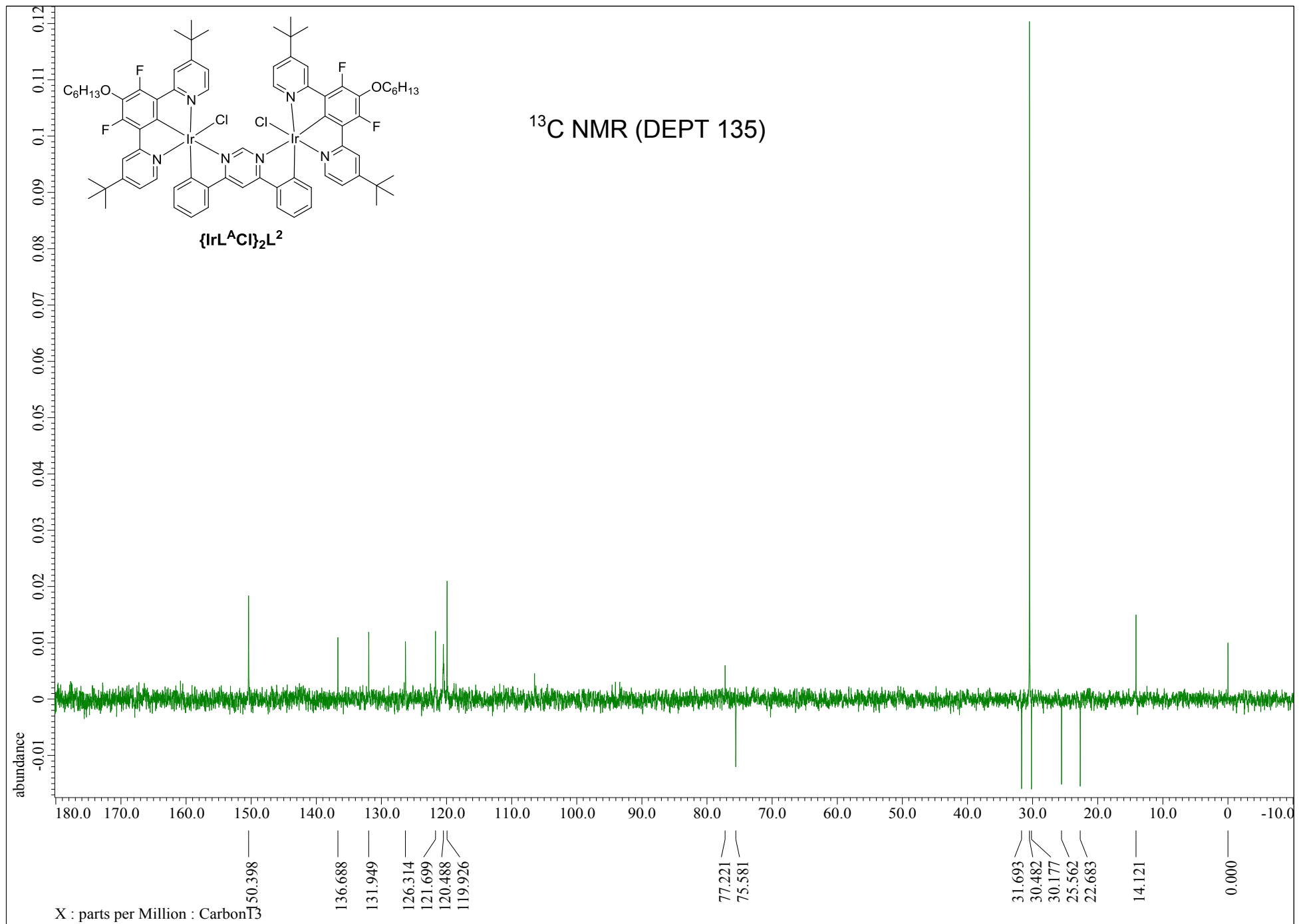








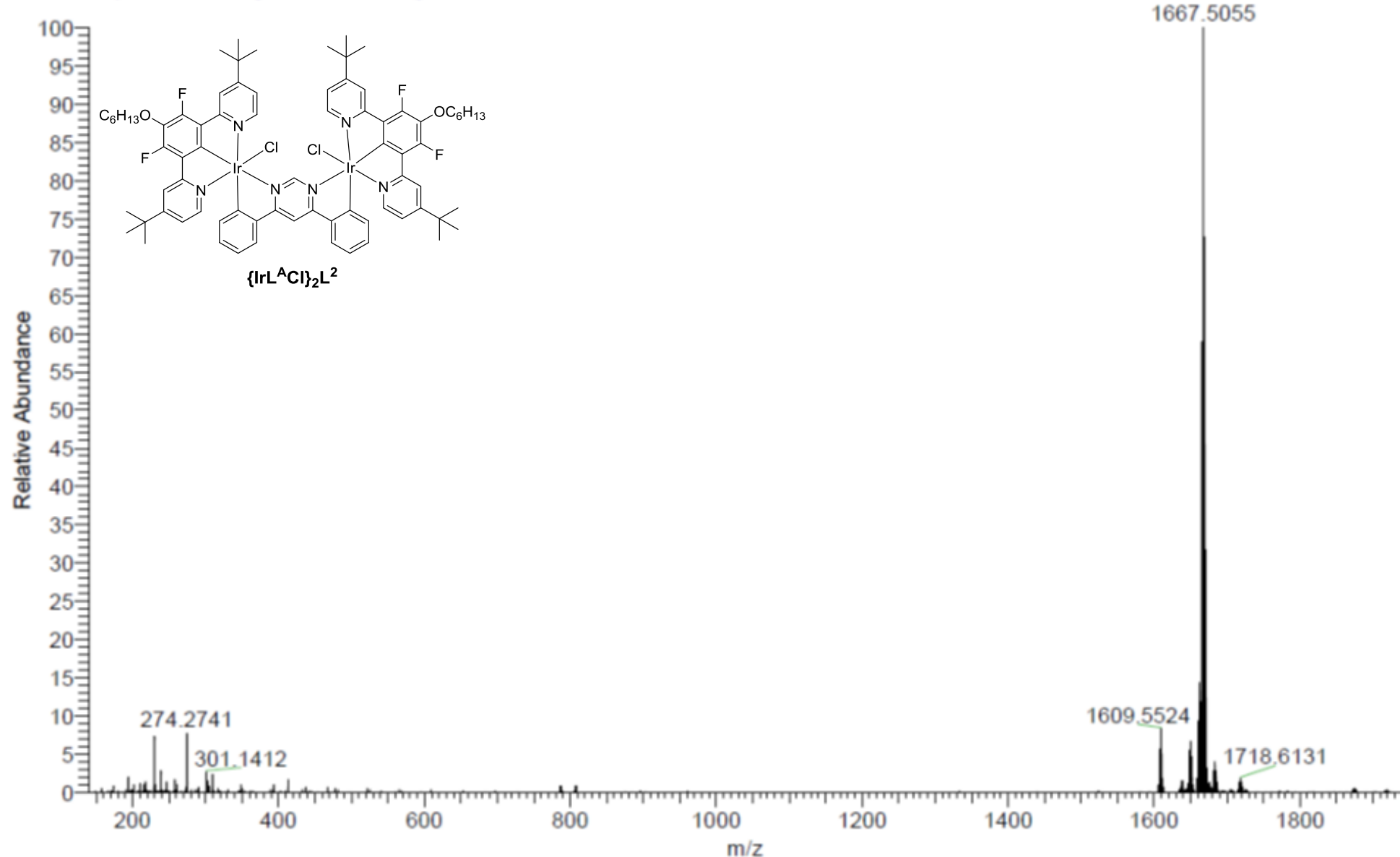




MW=1644?
(DCM)/MeCN
C76H84Cl2F4Ir2N6O2

EPSRC National Facility Swansea
LTQ Orbitrap XL

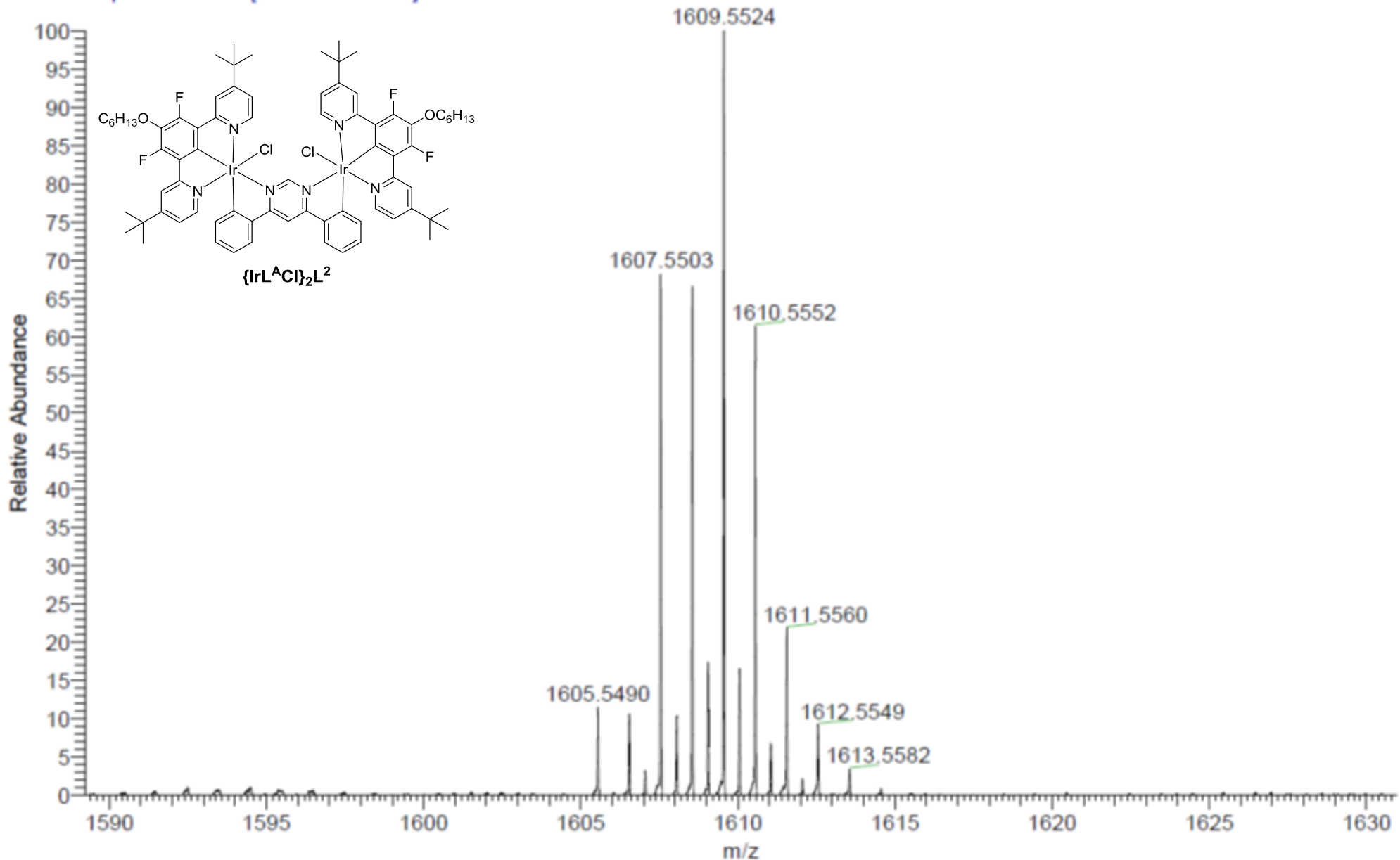
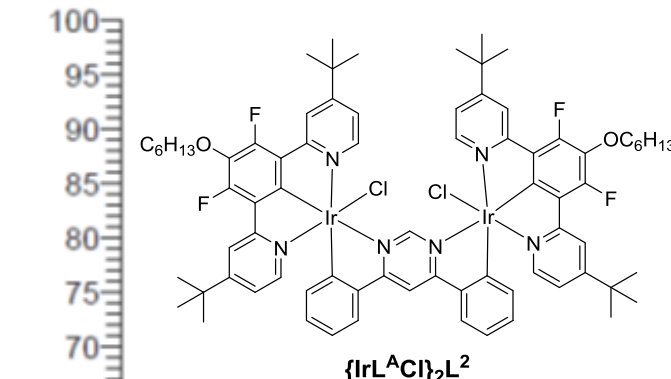
NORKOZ049-OJ-HNESP #32-45 RT: 0.72-1.03 AV: 12 SM: 7G NL: 8.96E6
T: FTMS + p NSI Full ms [140.00-1935.00]



MW=1644?
(DCM)/MeCN
C76H84Cl2F4Ir2N6O2

EPSRC National Facility Swansea
LTQ Orbitrap XL

NORKOZ049-OJ-HNESP #32-45 RT: 0.72-1.03 AV: 12 SM: 7G NL: 7.43E5
T: FTMS + p NSI Full ms [140.00-1935.00]

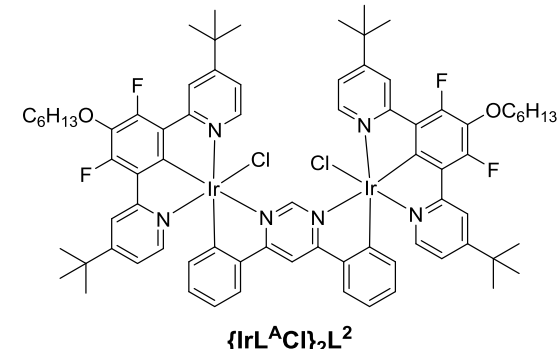
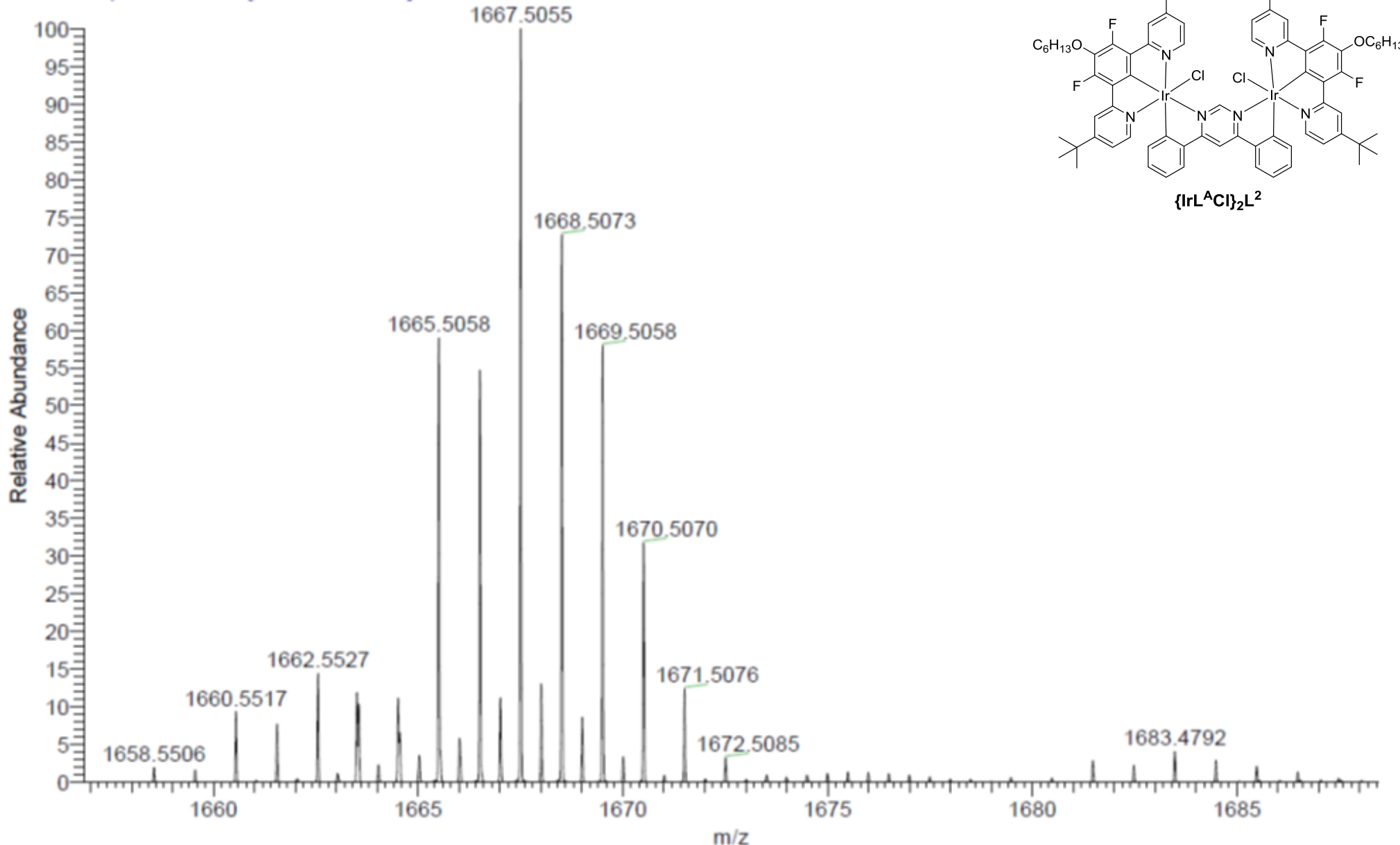


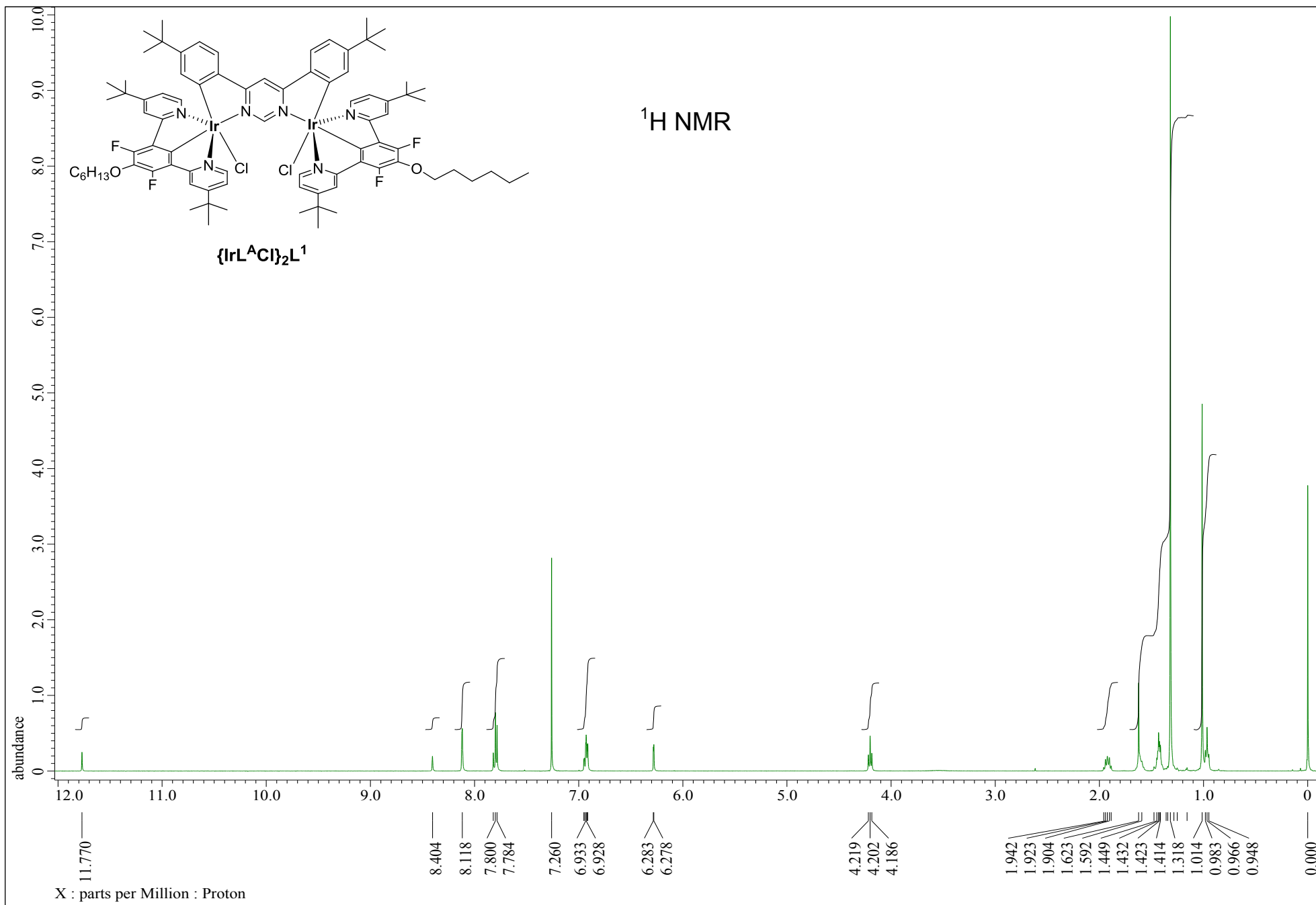
MW=1644?

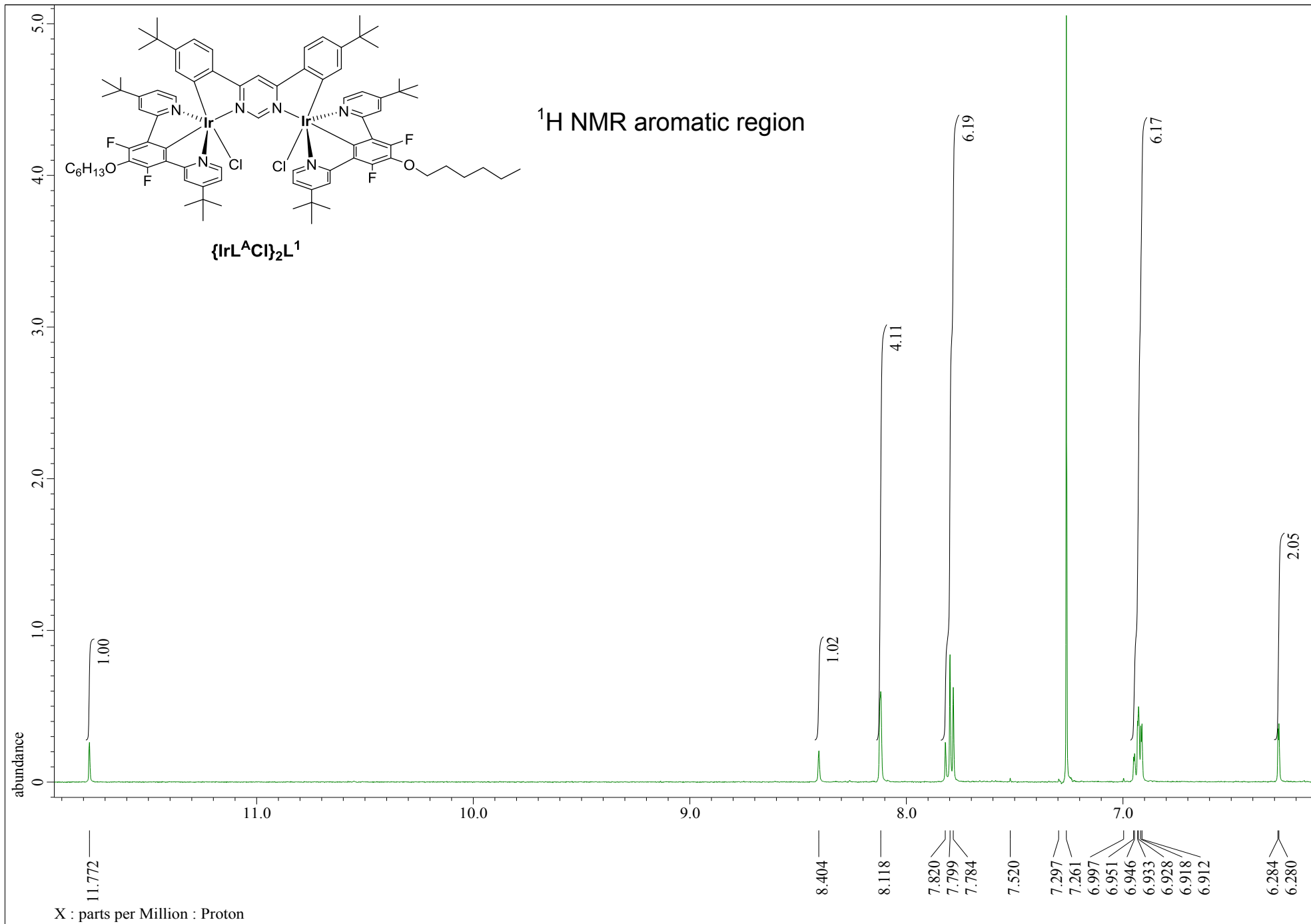
(DCM)/MeCN
C76H84Cl2F4Ir2N6O2

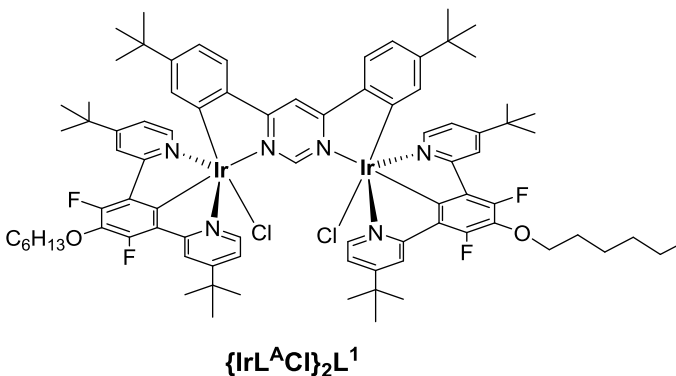
NORKOZ049-OJ-HNESP #32-45 RT: 0.72-1.03 AV: 12 SM: 7G NL: 8.96E6
T: FTMS + p NSI Full ms [140.00-1935.00]

EPSRC National Facility Swansea
LTQ Orbitrap XL

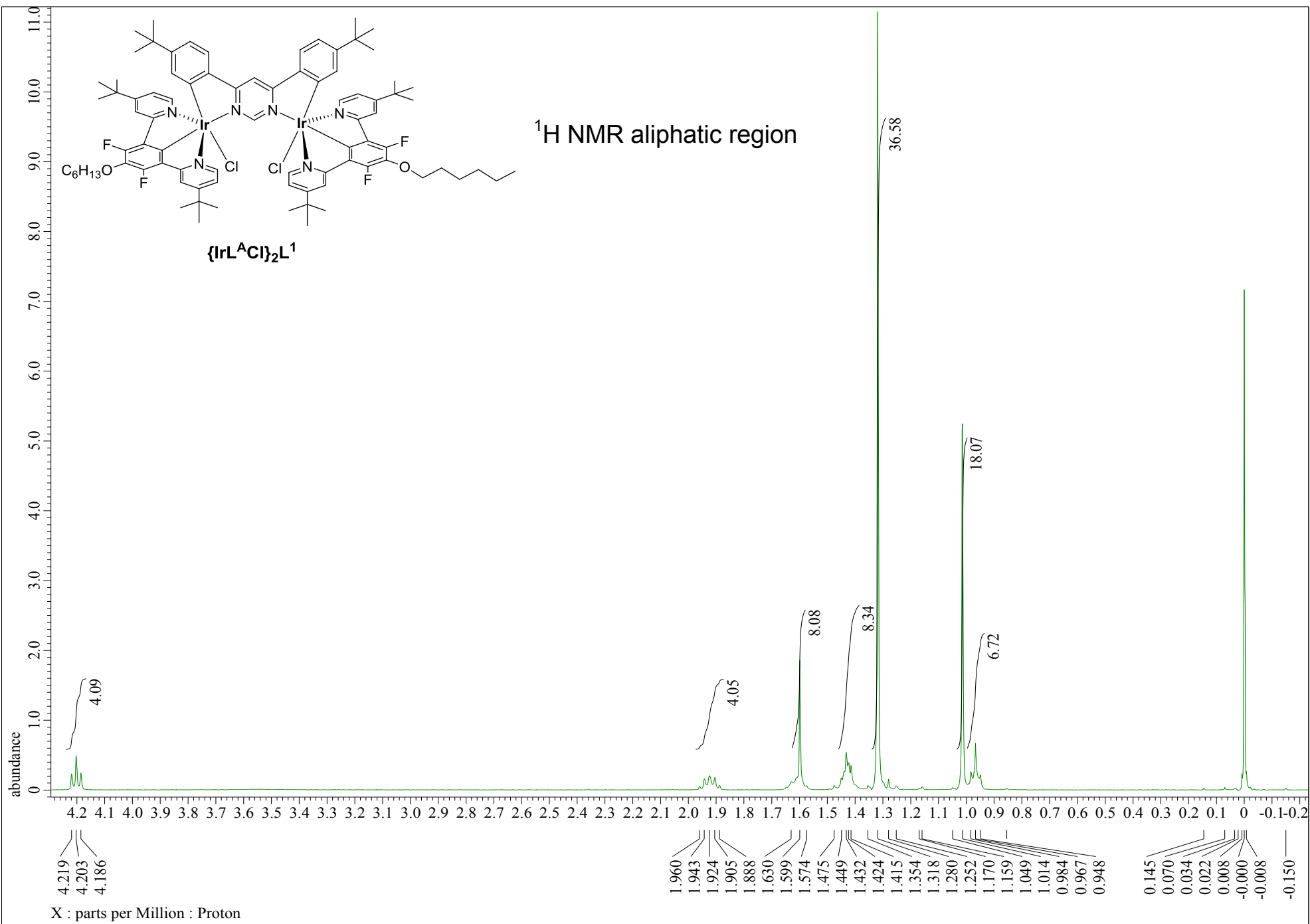


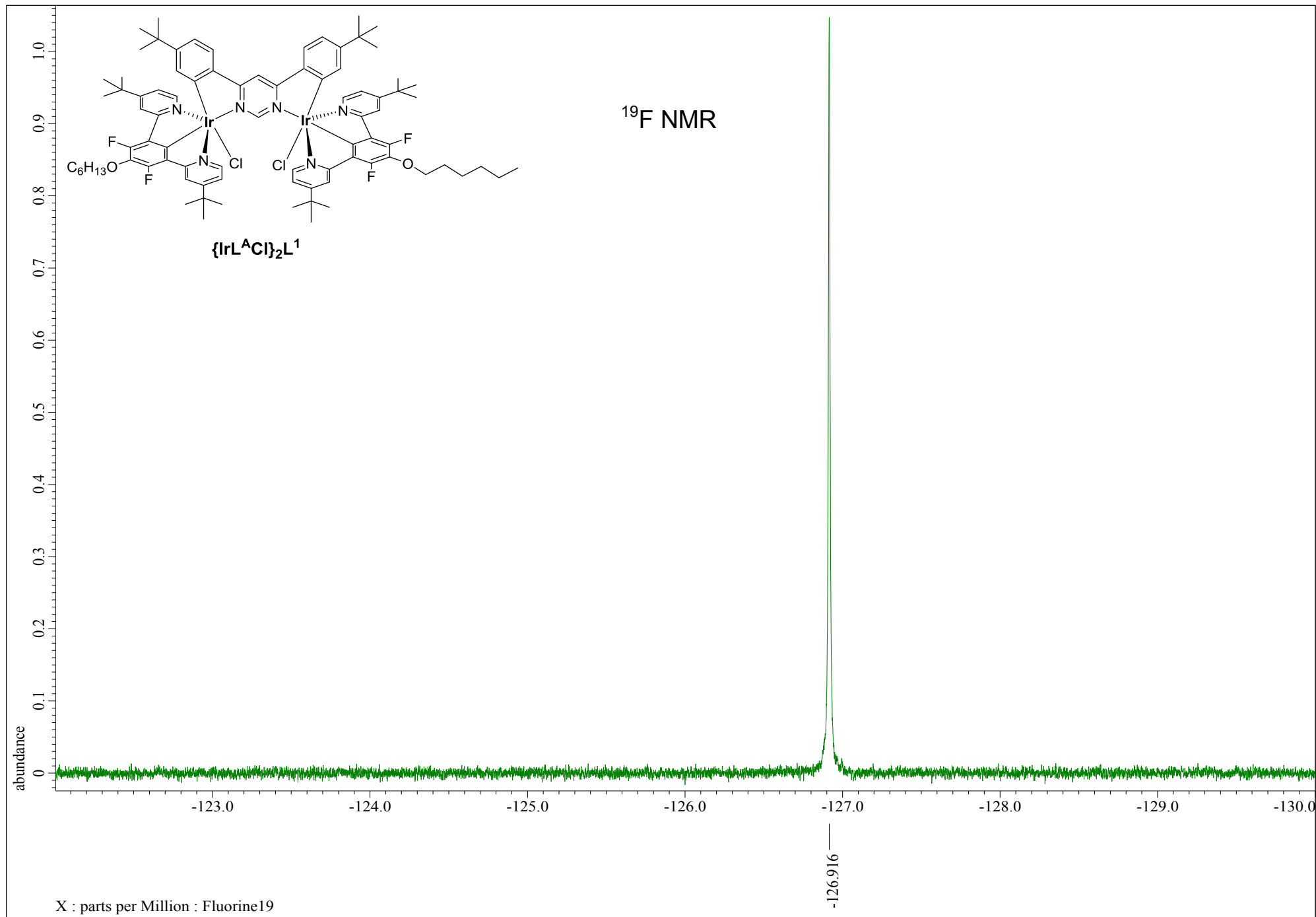


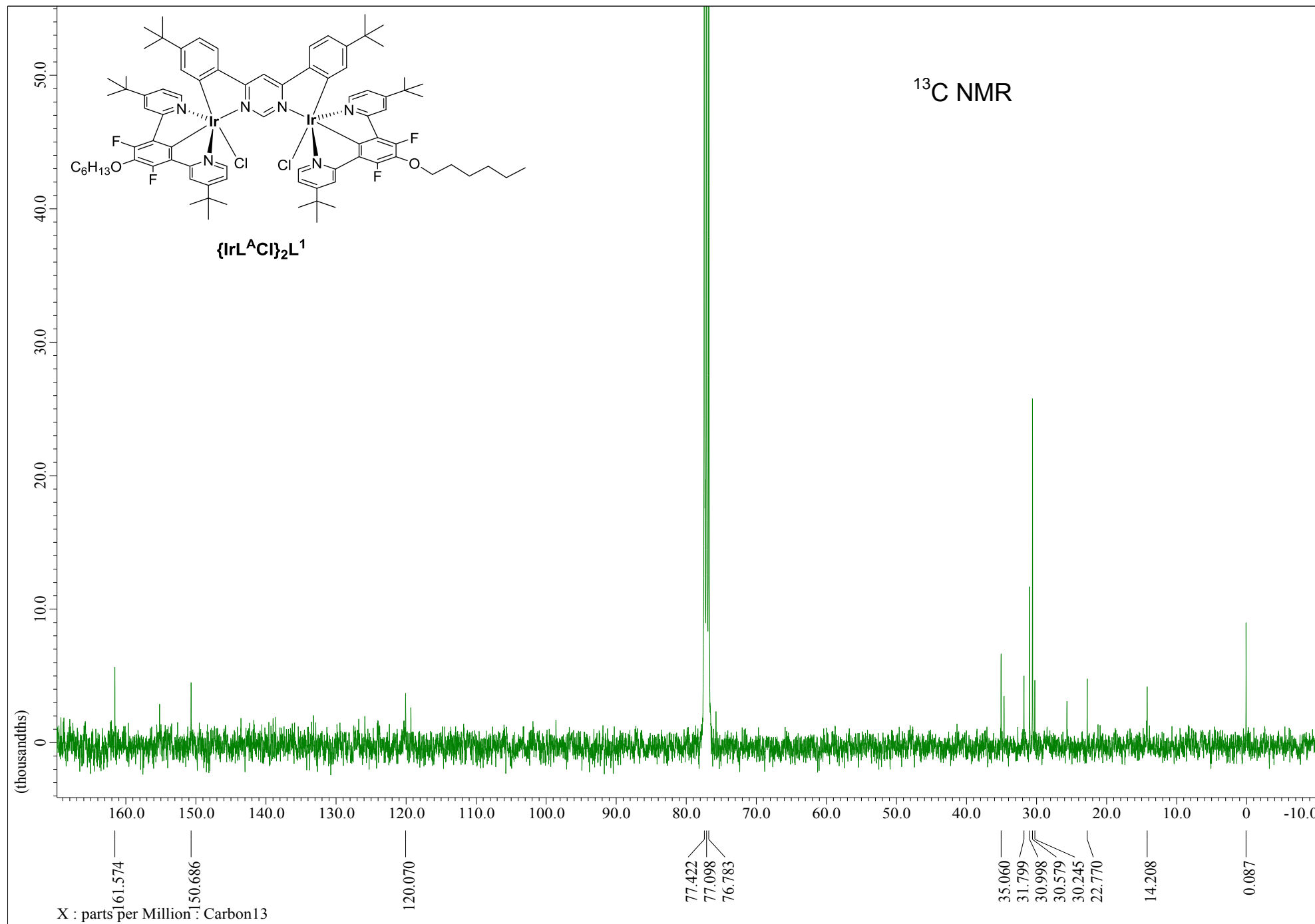


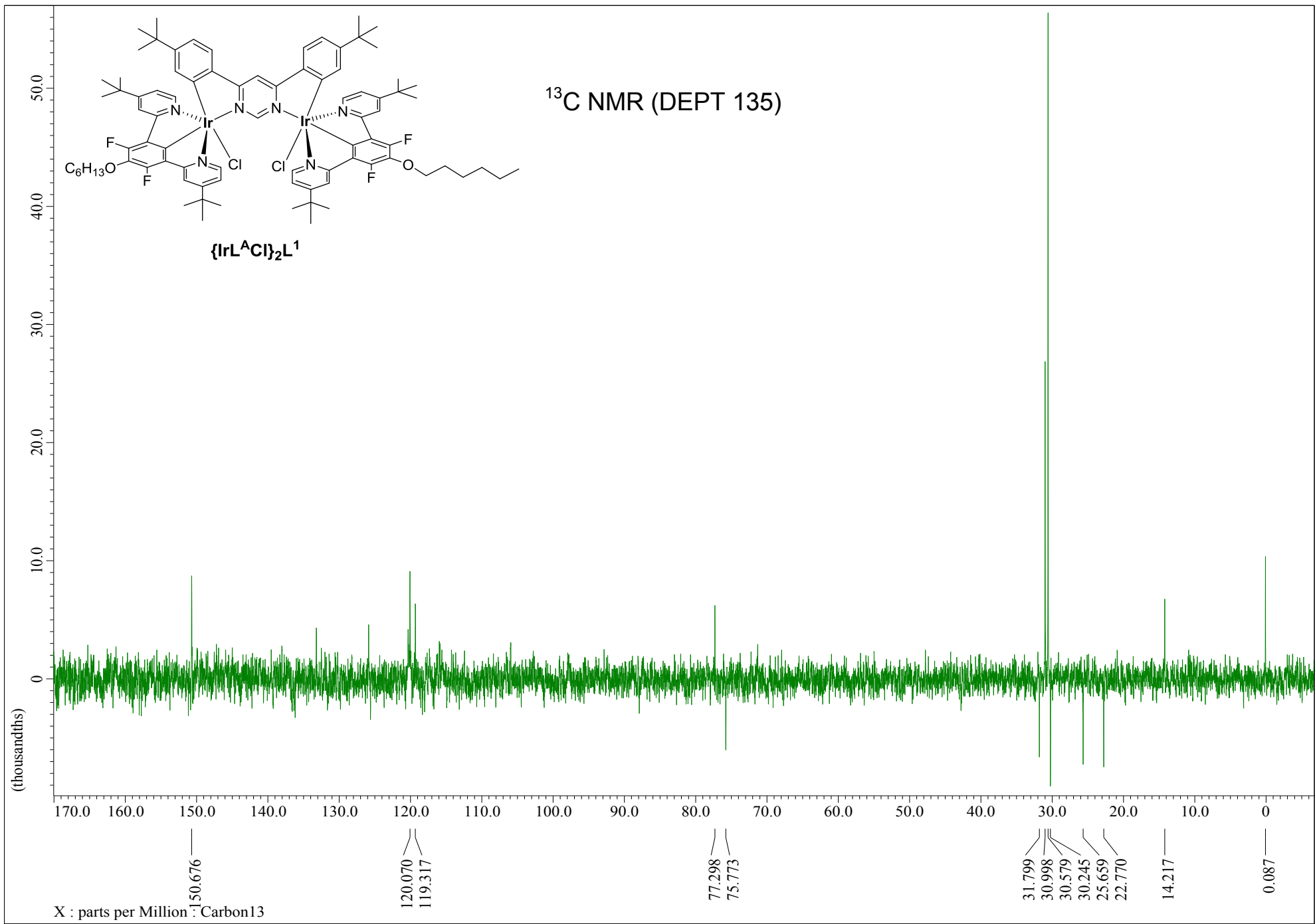


¹H NMR aliphatic region









MW=1757?

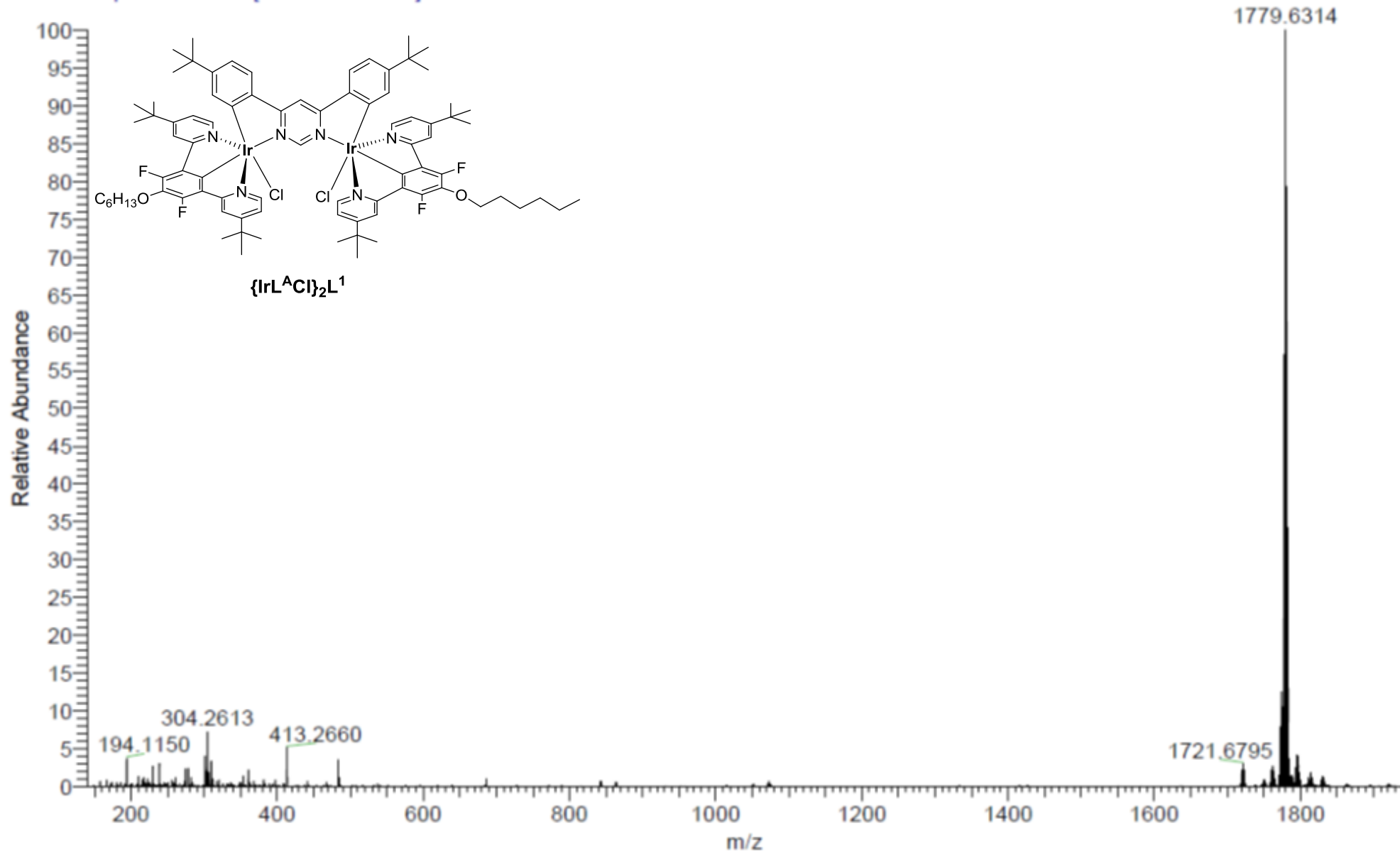
(DCM)/MeCN

C84H100Cl2F4Ir2N6O2

NORKOZ050-OJ-HNESP #27-45 RT: 0.67-1.03 AV: 15 SM: 7G NL: 1.18E7

T: FTMS + p NSI Full ms [140.00-1935.00]

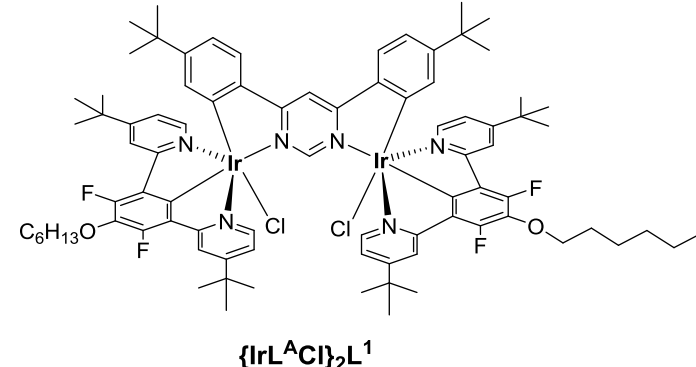
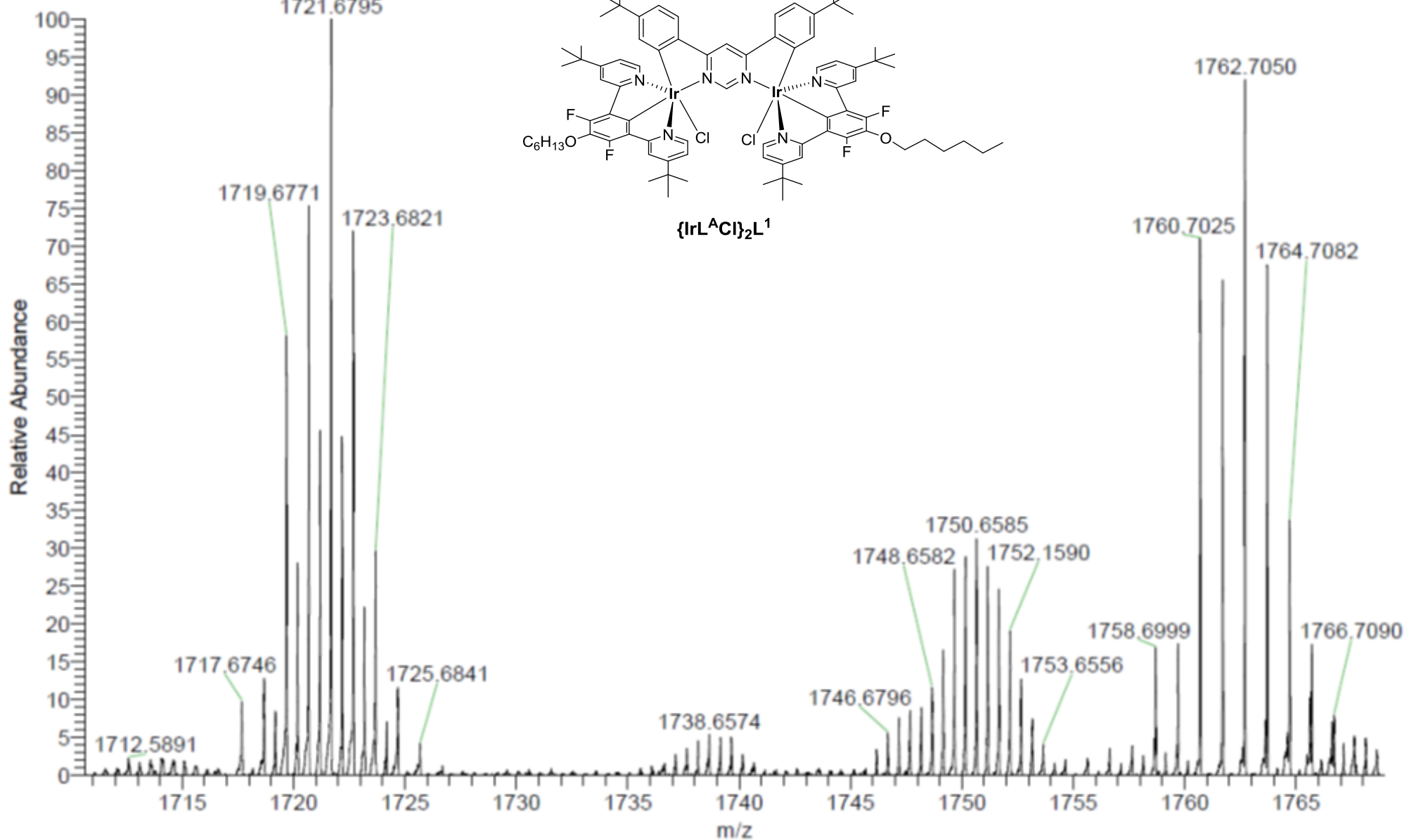
EPSRC National Facility Swansea
LTQ Orbitrap XL



MW=1757?
(DCM)/MeCN
C₈₄H₁₀₀Cl₂F₄Ir₂N₆O₂

EPSRC National Facility Swansea
LTQ Orbitrap XL

NORKOZ050-OJ-HNESP #27-45 RT: 0.67-1.03 AV: 15 SM: 7G NL: 3.52E5
T: FTMS + p NSI Full ms [140.00-1935.00]



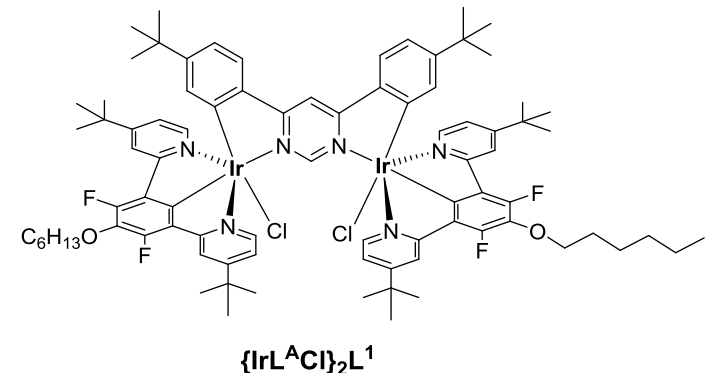
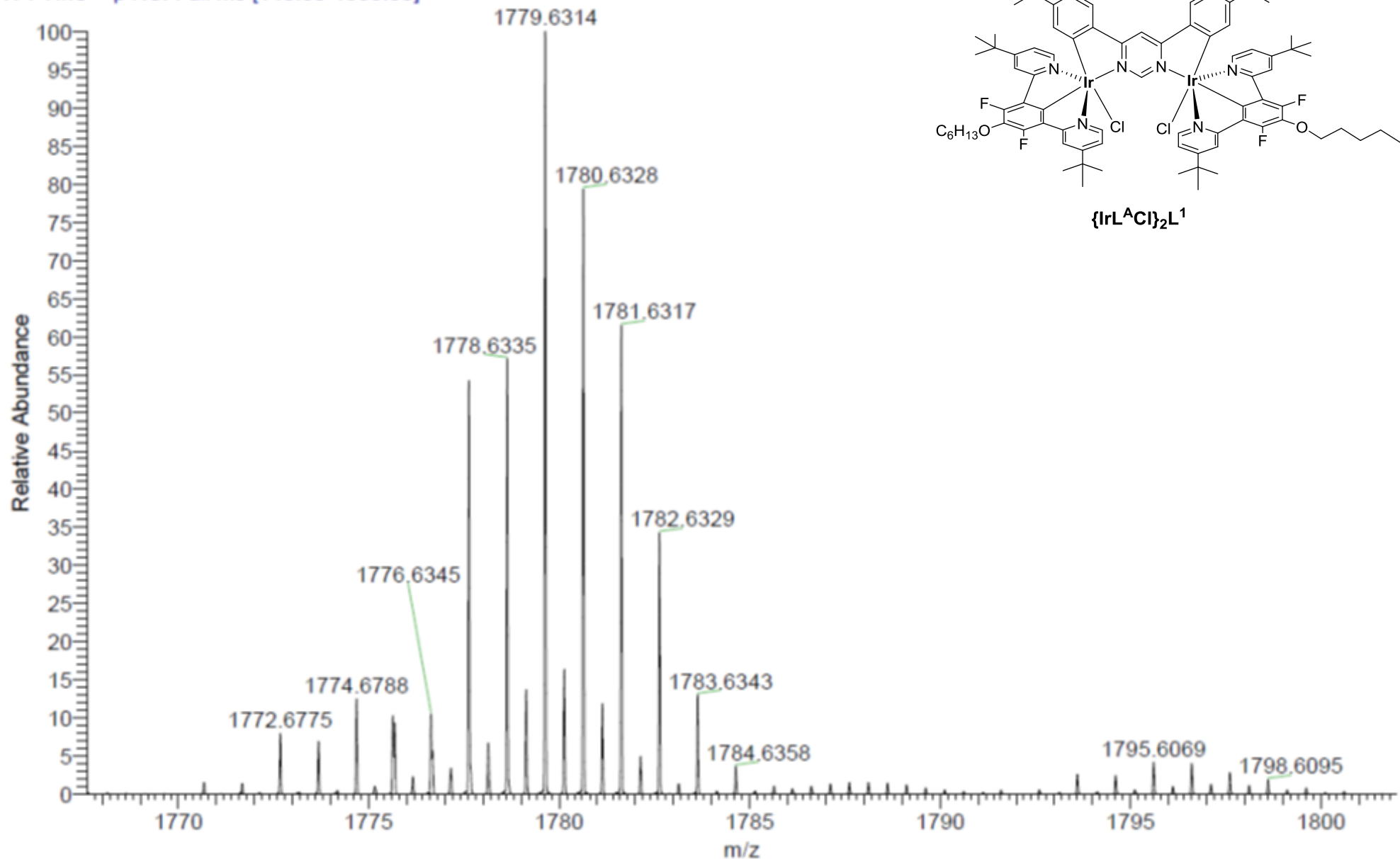
MW=1757?

(DCM)/MeCN
C84H100Cl2F4Ir2N6O2

EPSRC National Facility Swansea
LTQ Orbitrap XL

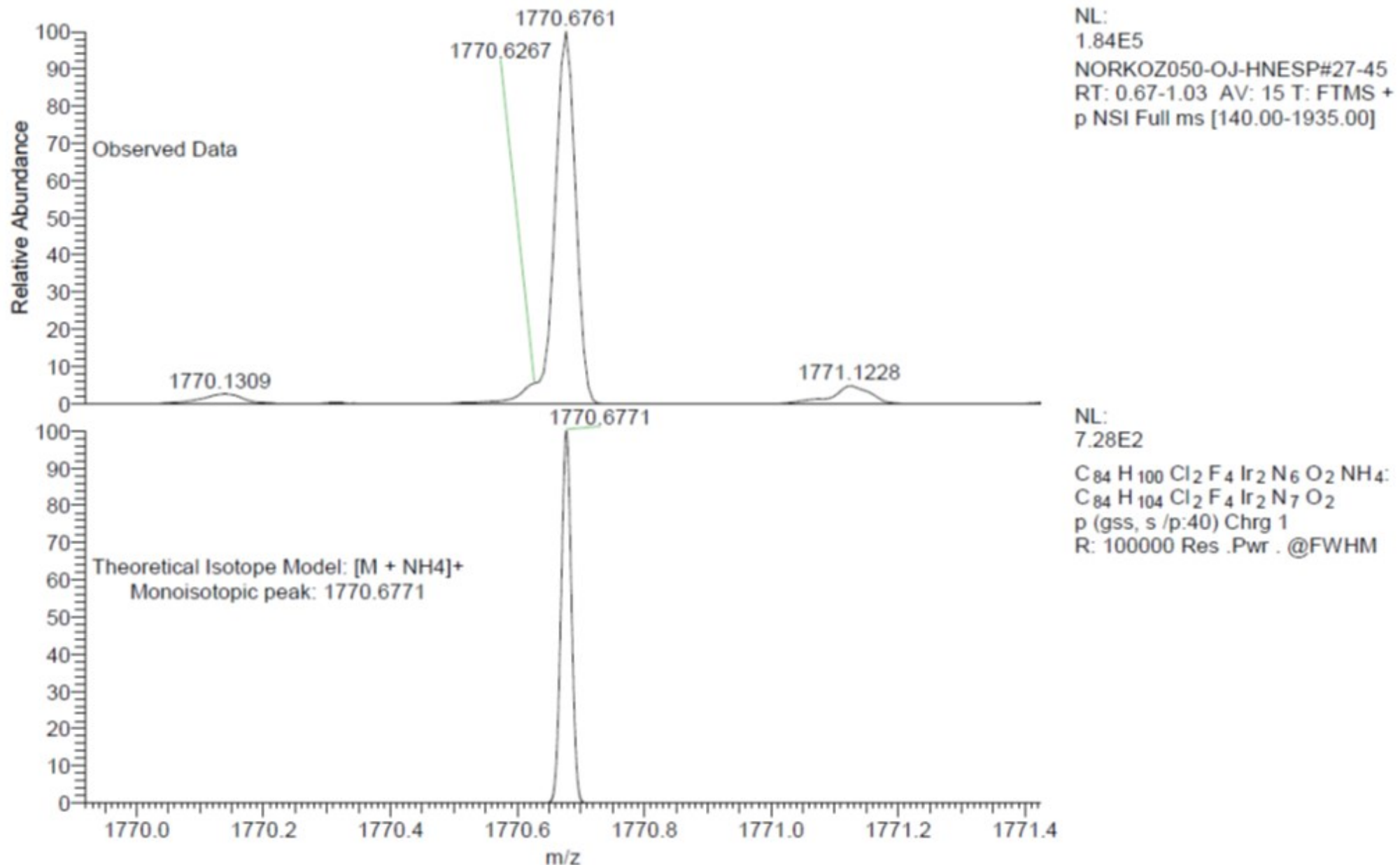
NORKOZ050-OJ-HNESP #27-45 RT: 0.67-1.03 AV: 15 SM: 7G NL: 1.18E7

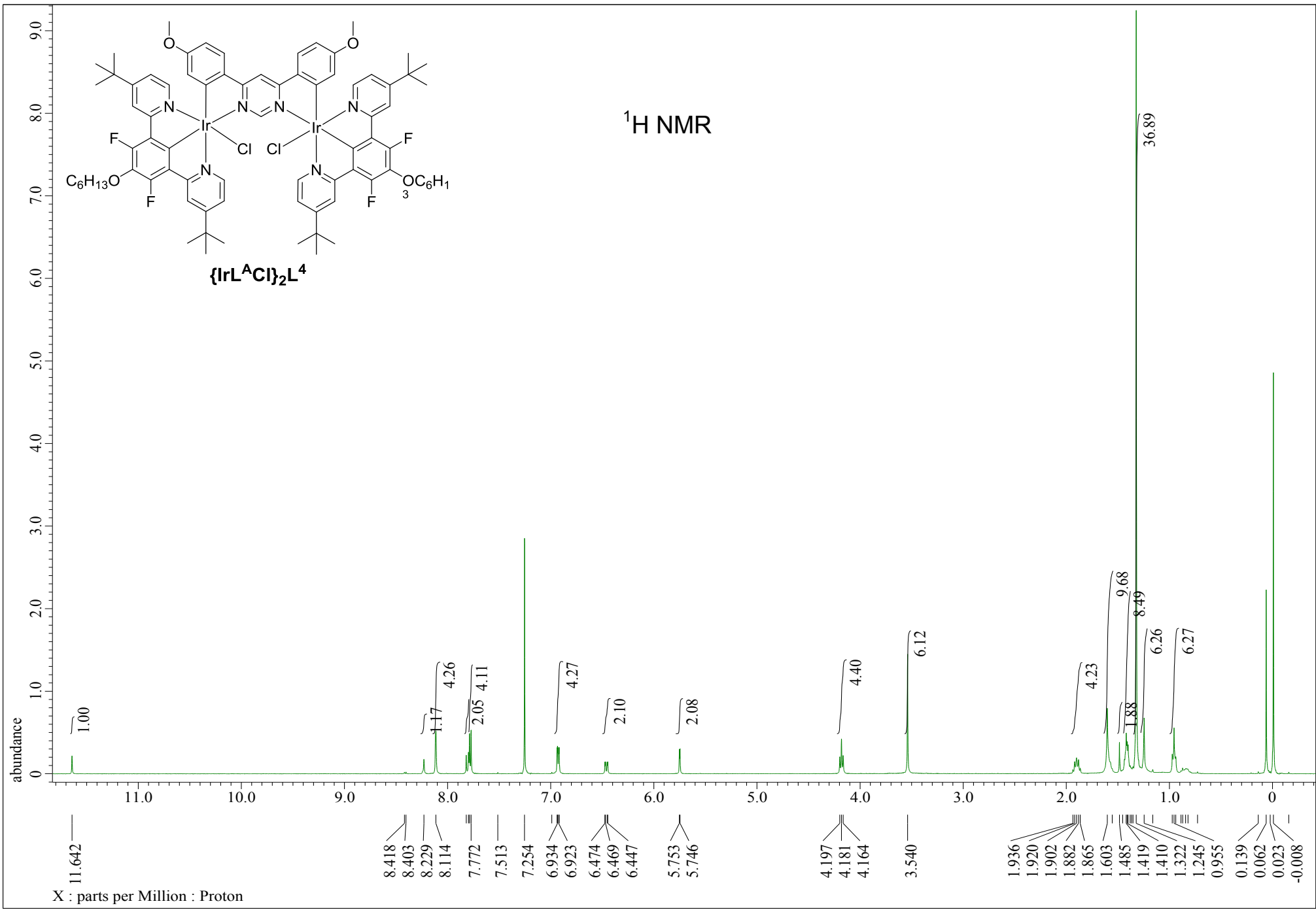
T: FTMS + p NSI Full ms [140.00-1935.00]

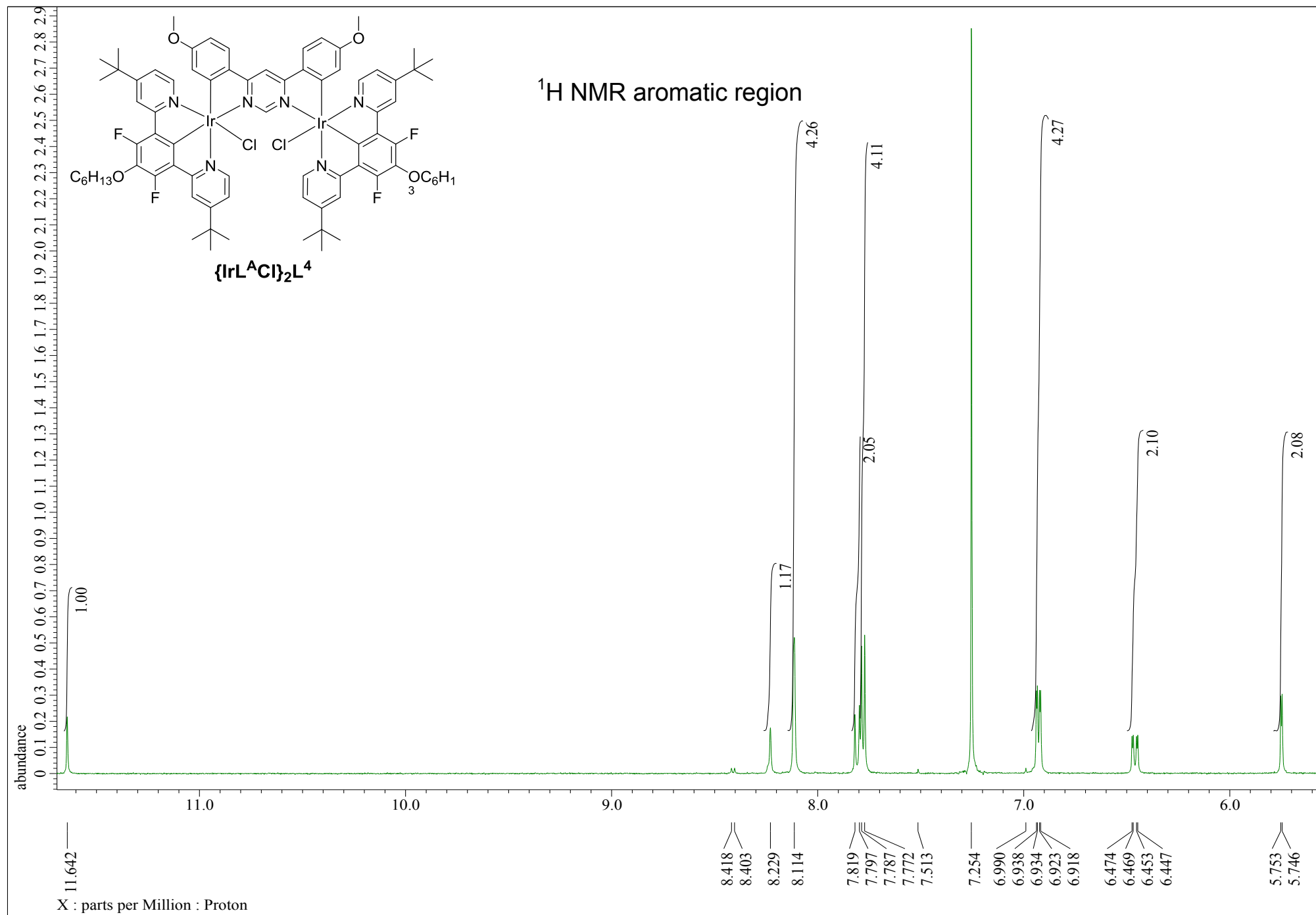


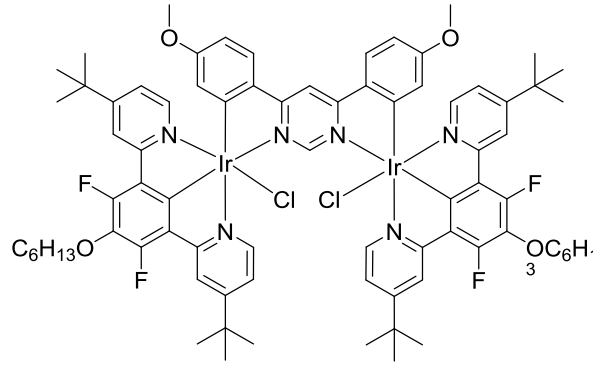
MW=1757?
(DCM)/MeCN
C84H100Cl2F4Ir2N6O2

EPSRC National Facility Swansea
LTQ Orbitrap XL



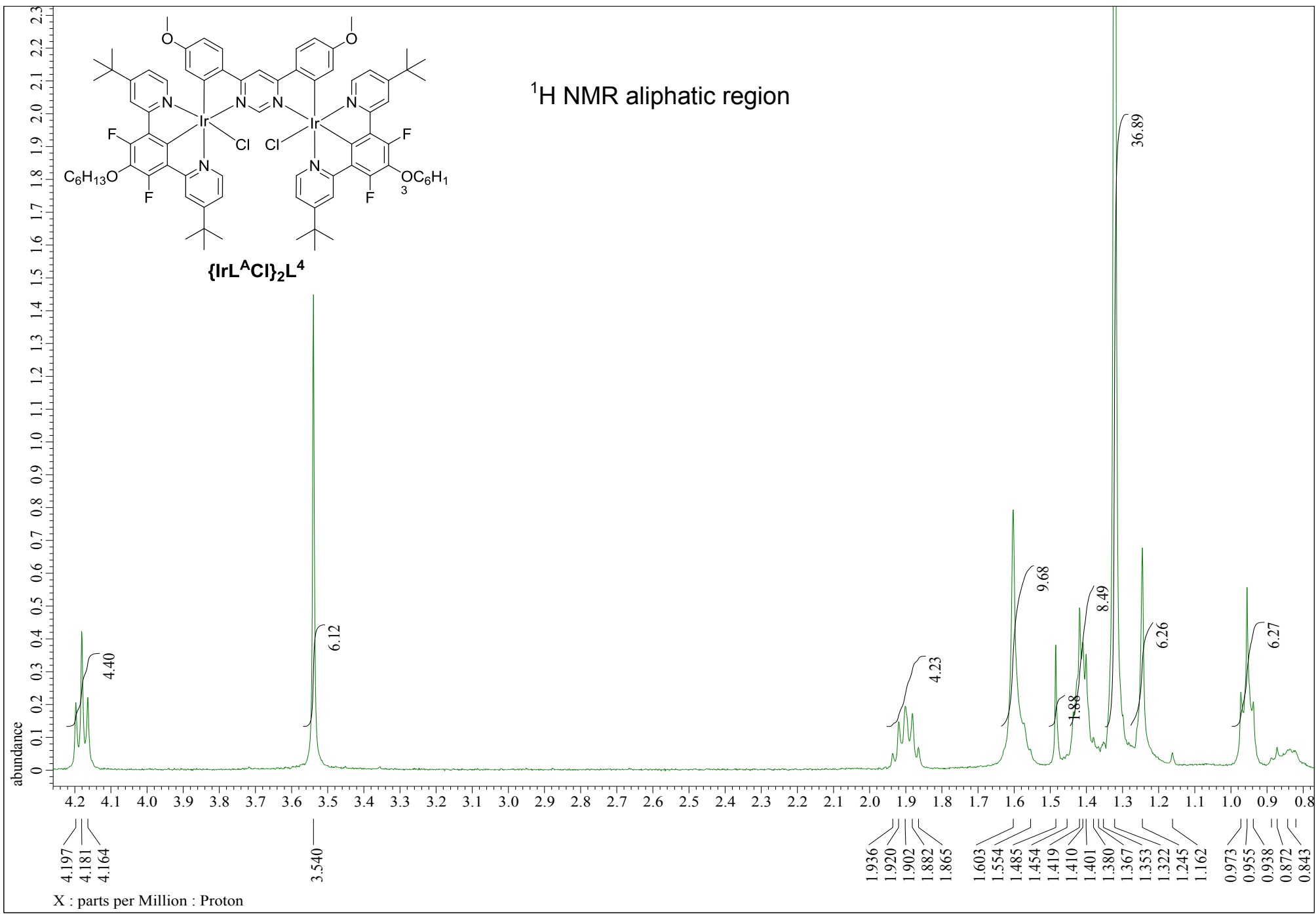


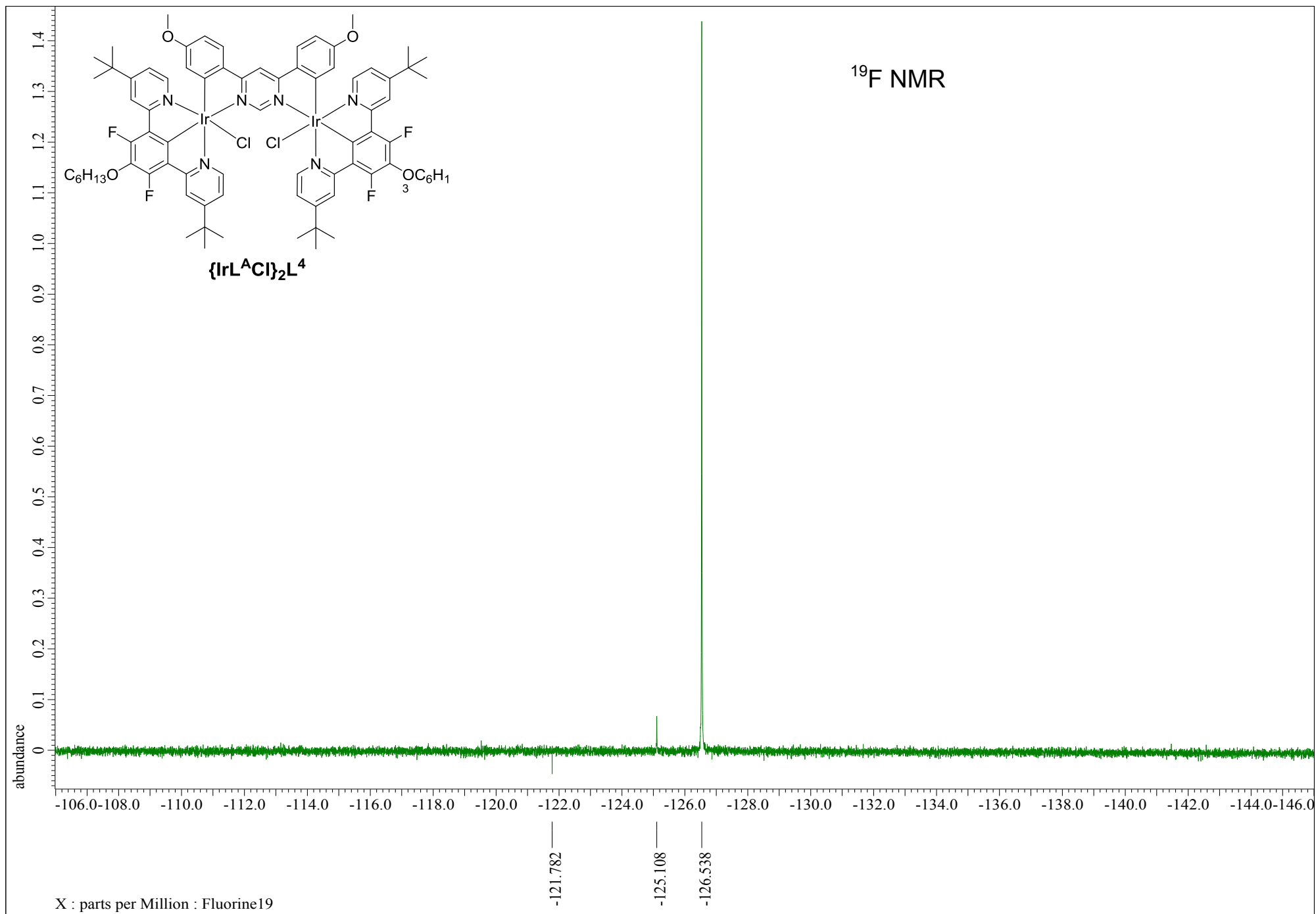


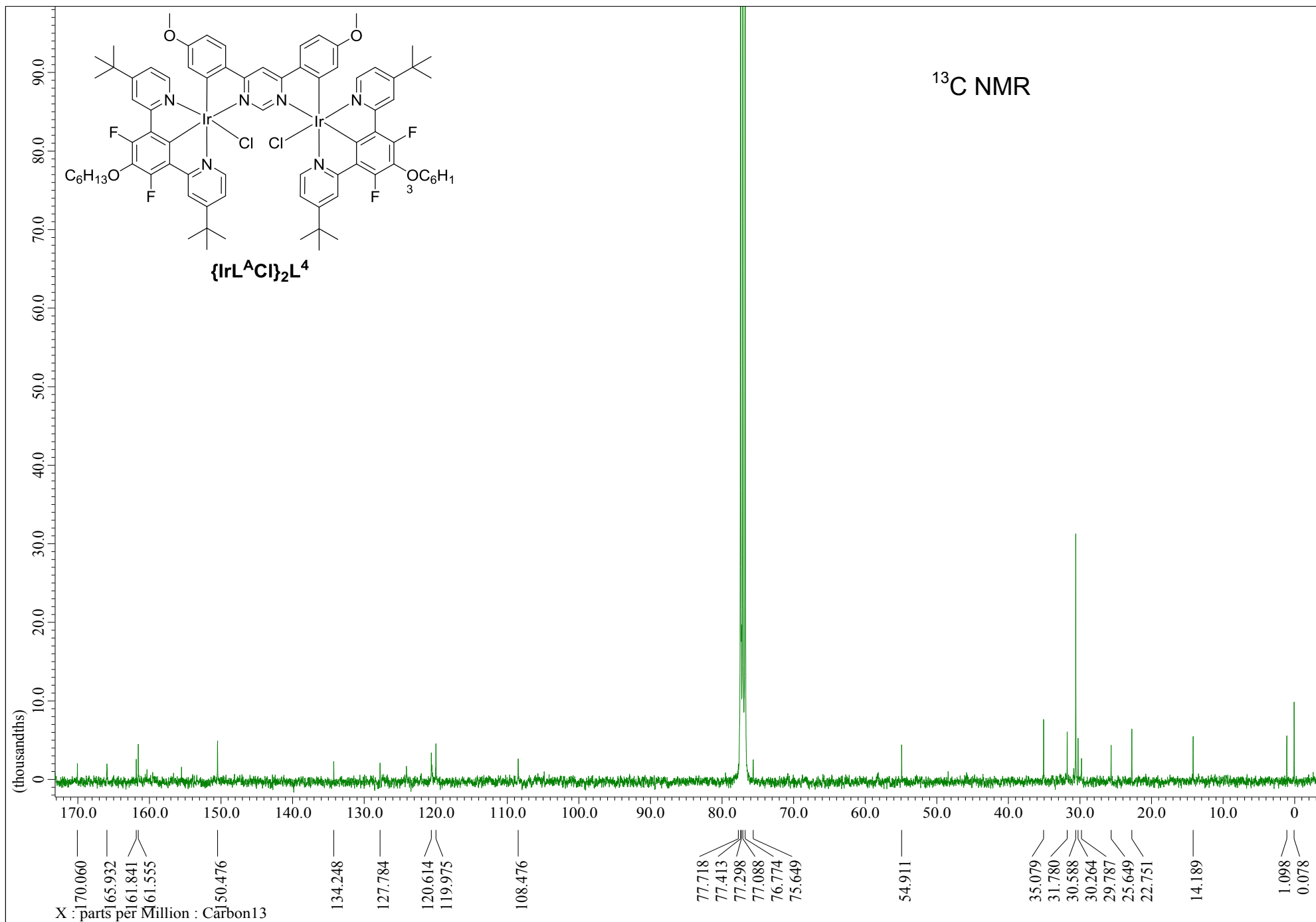


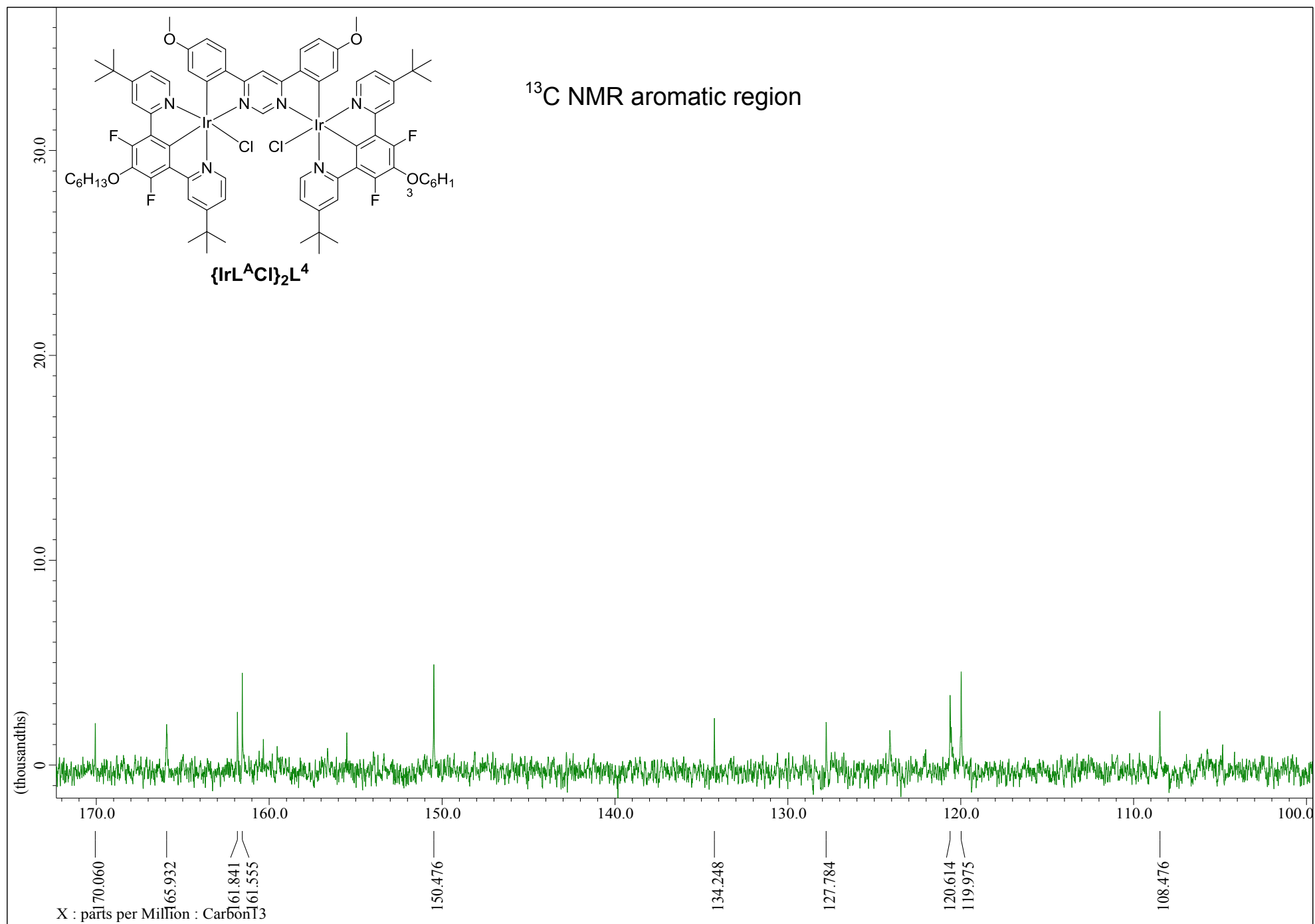
$\{IrL^A Cl\}_2 L^4$

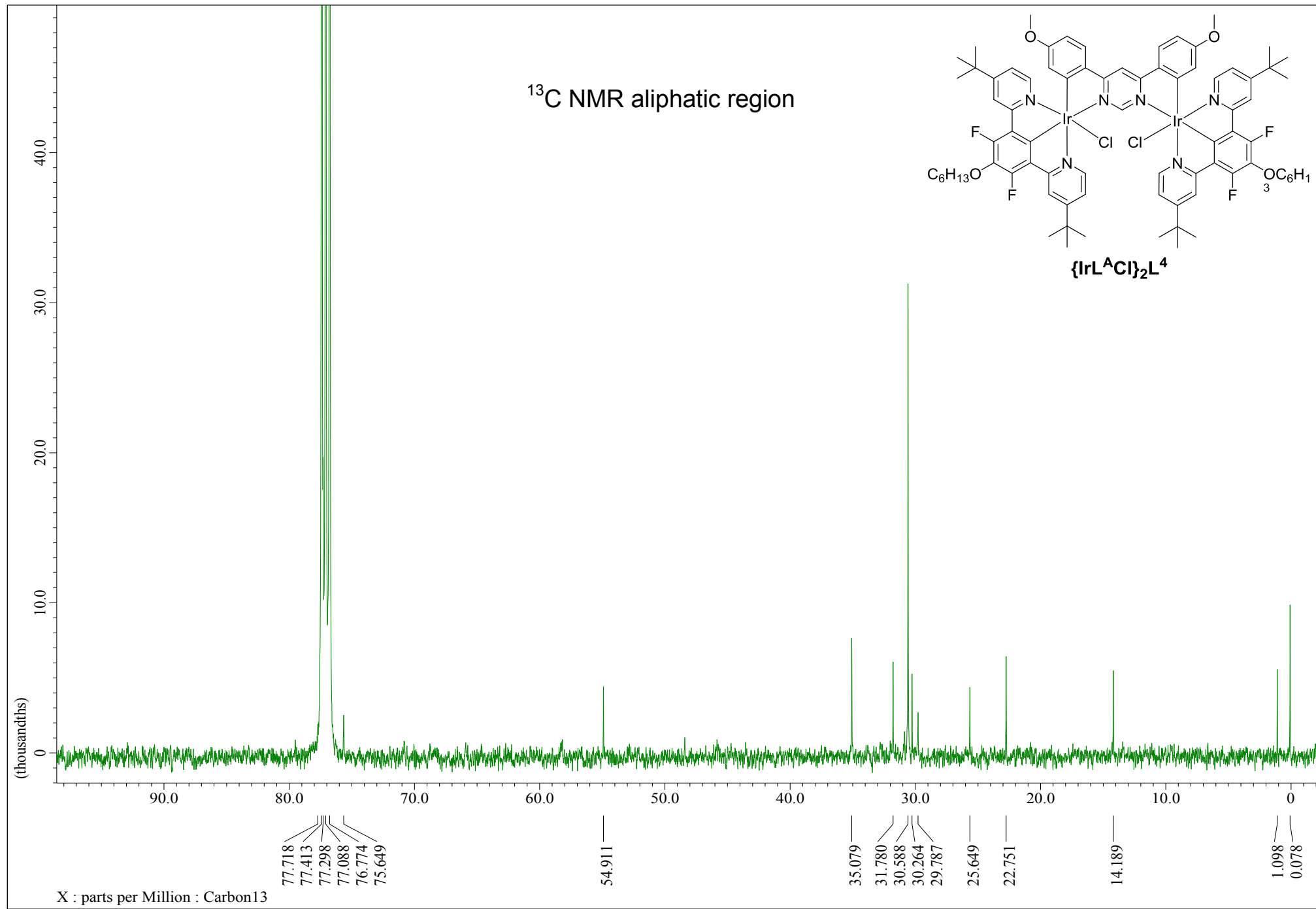
1H NMR aliphatic region

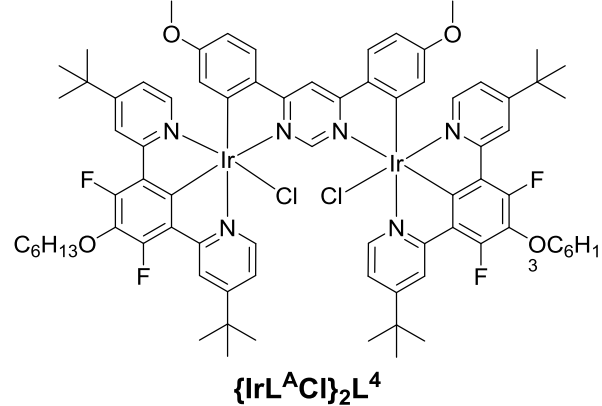




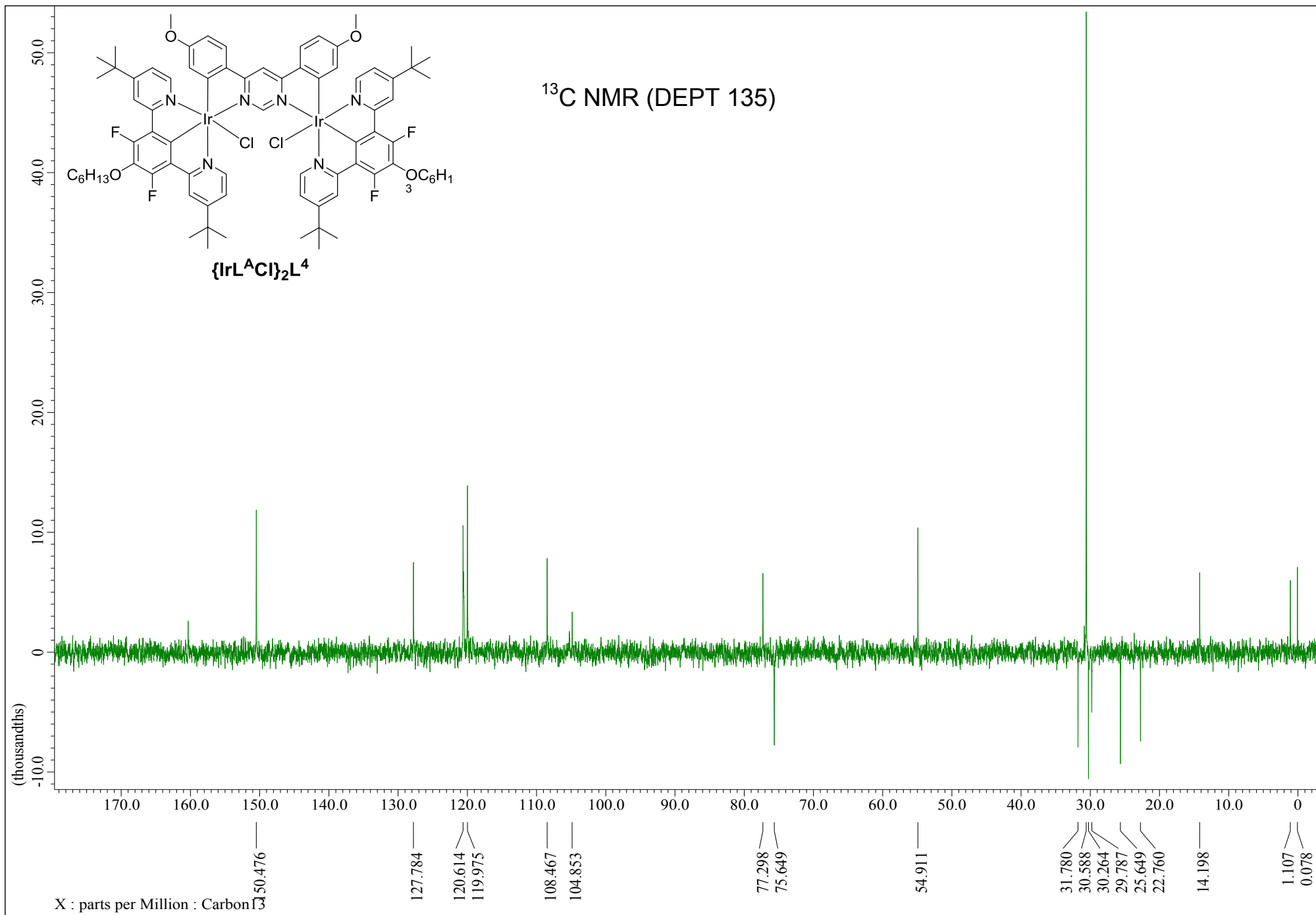


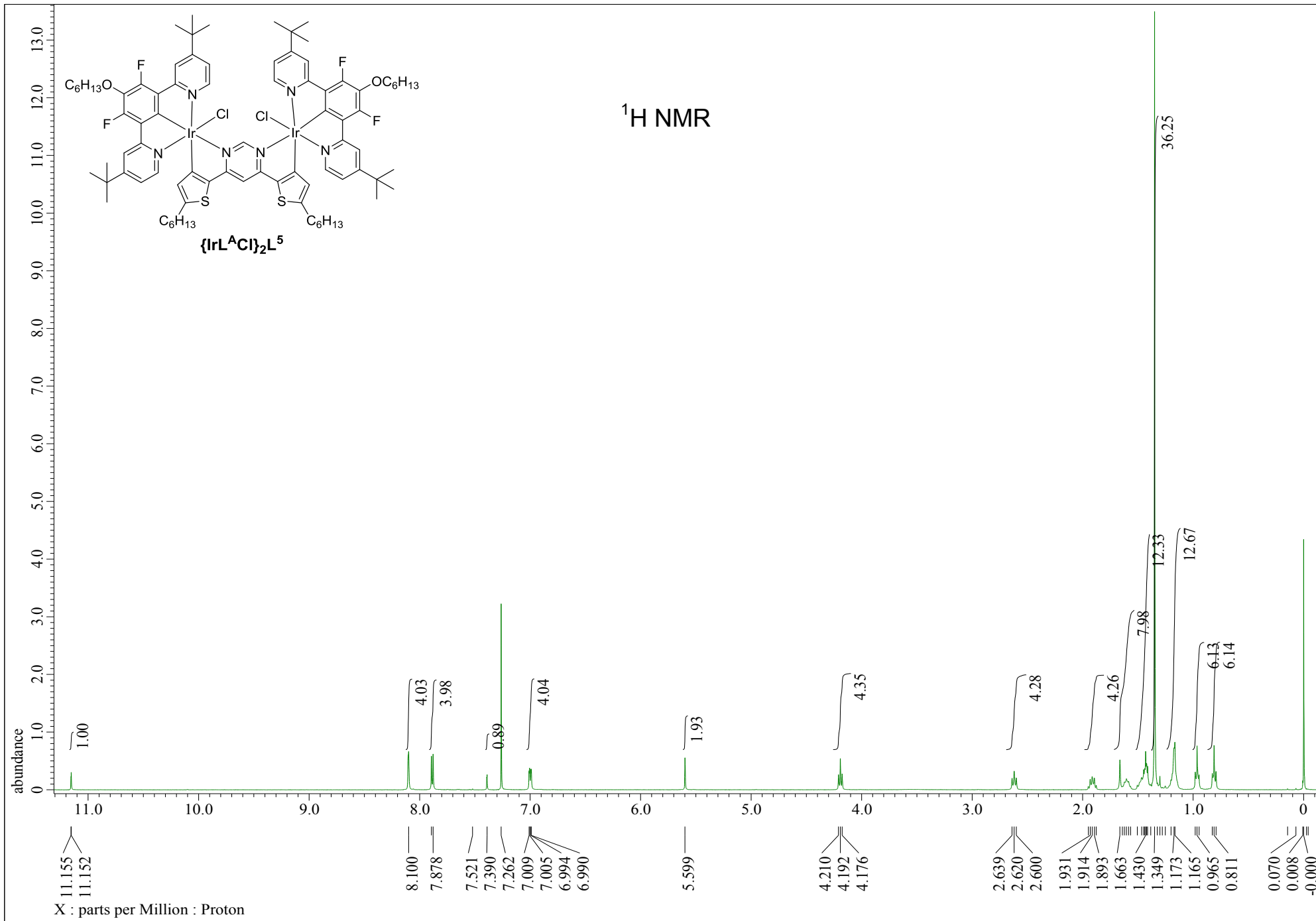


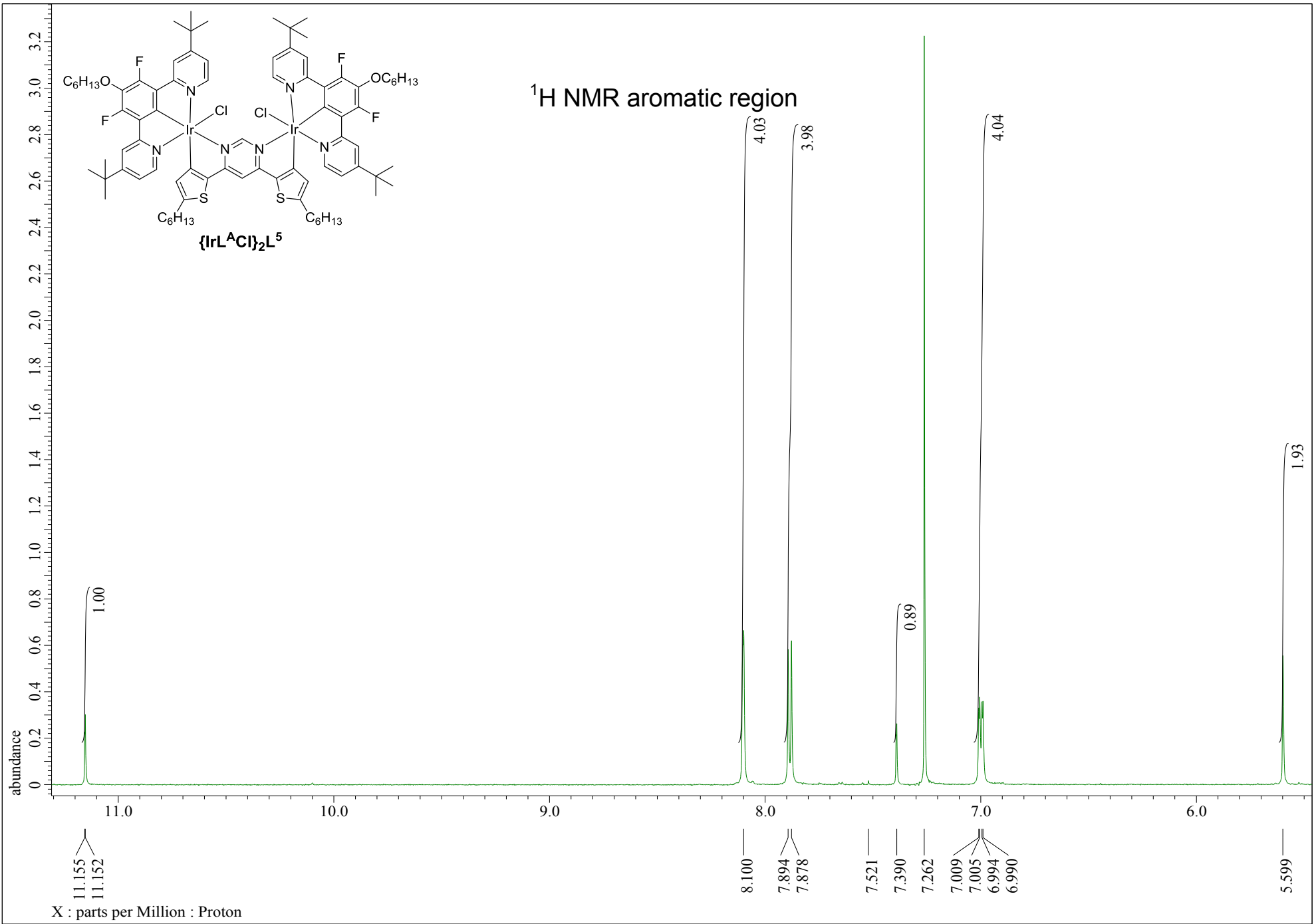


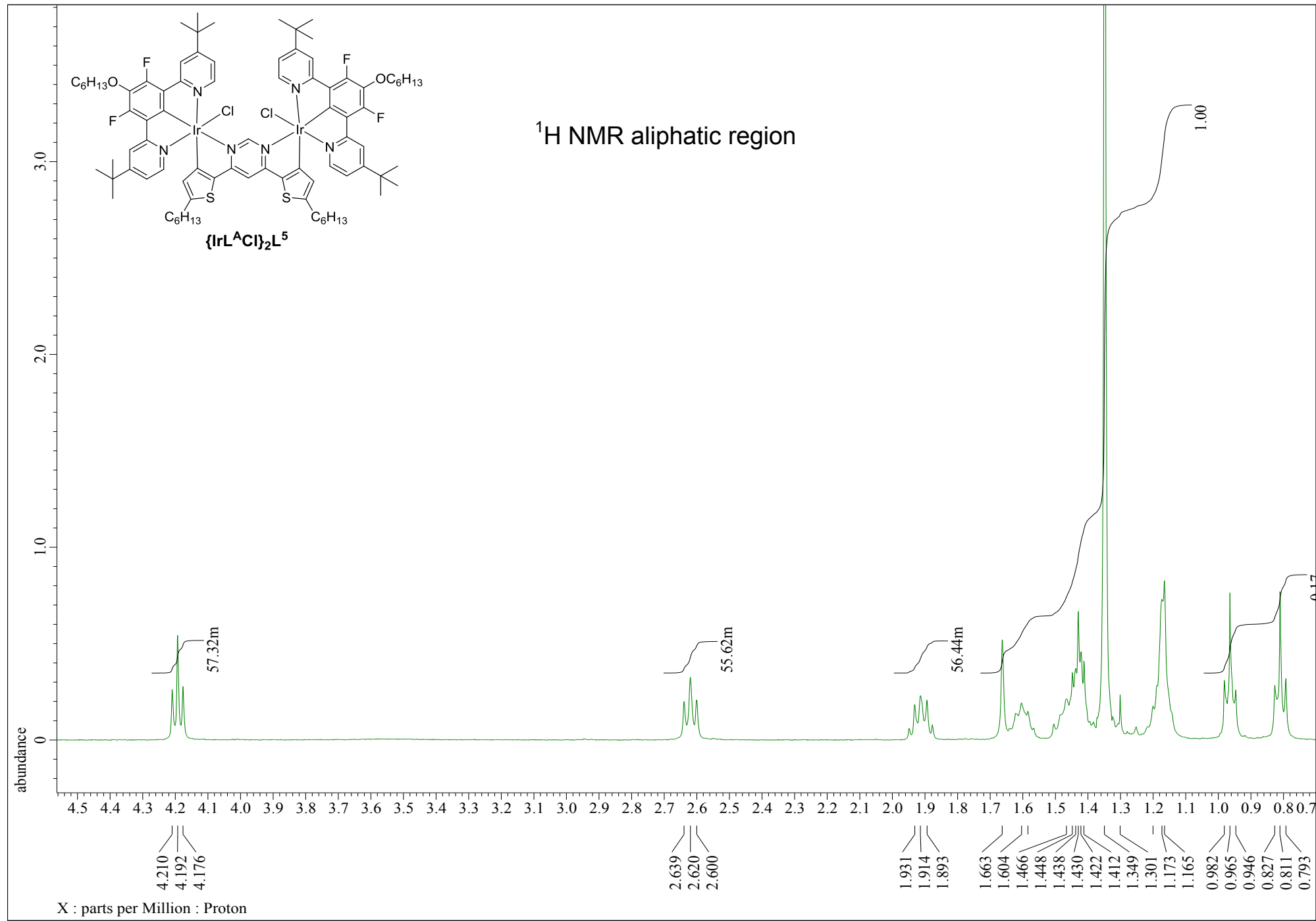


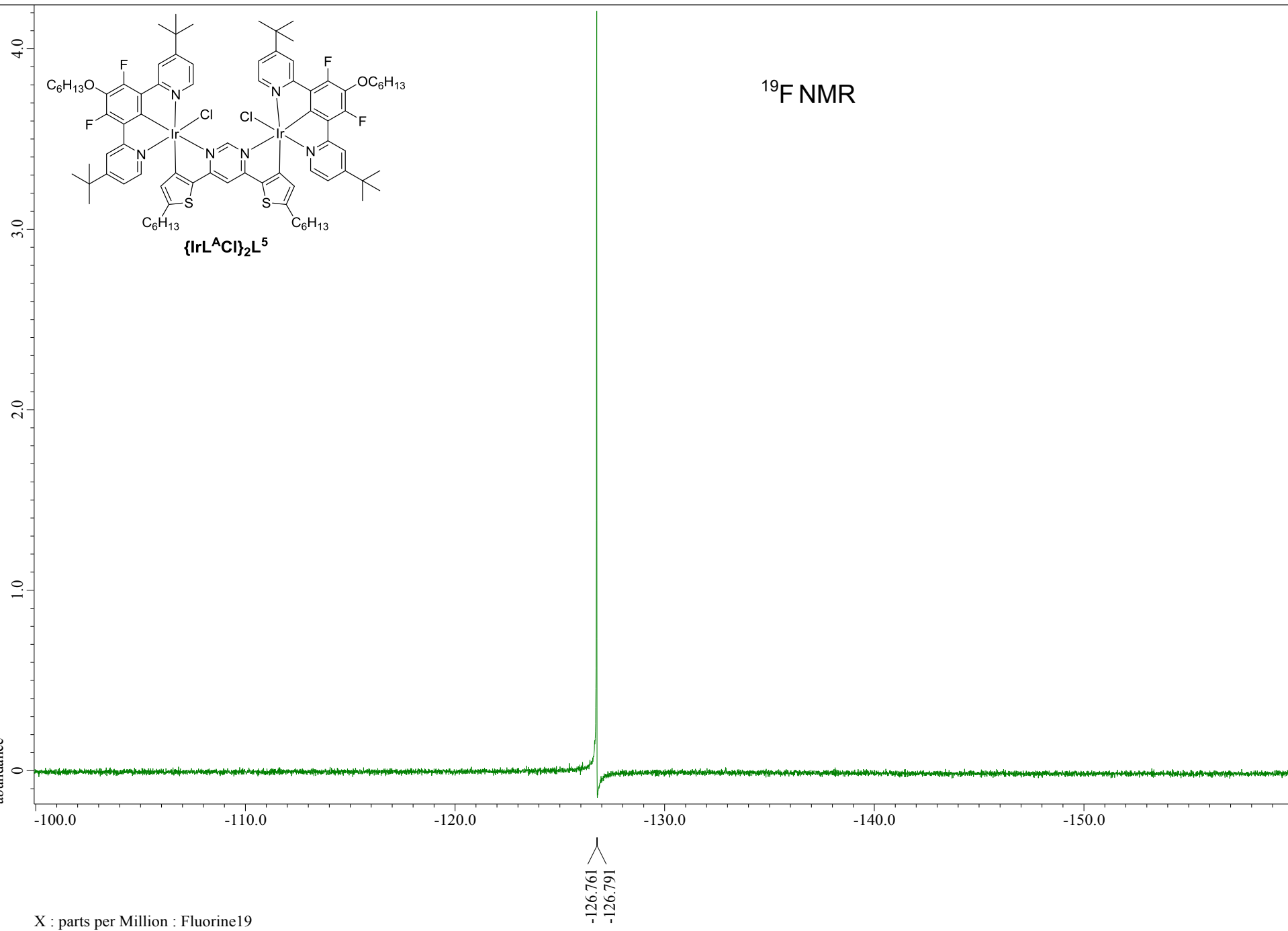
¹³C NMR (DEPT 135)

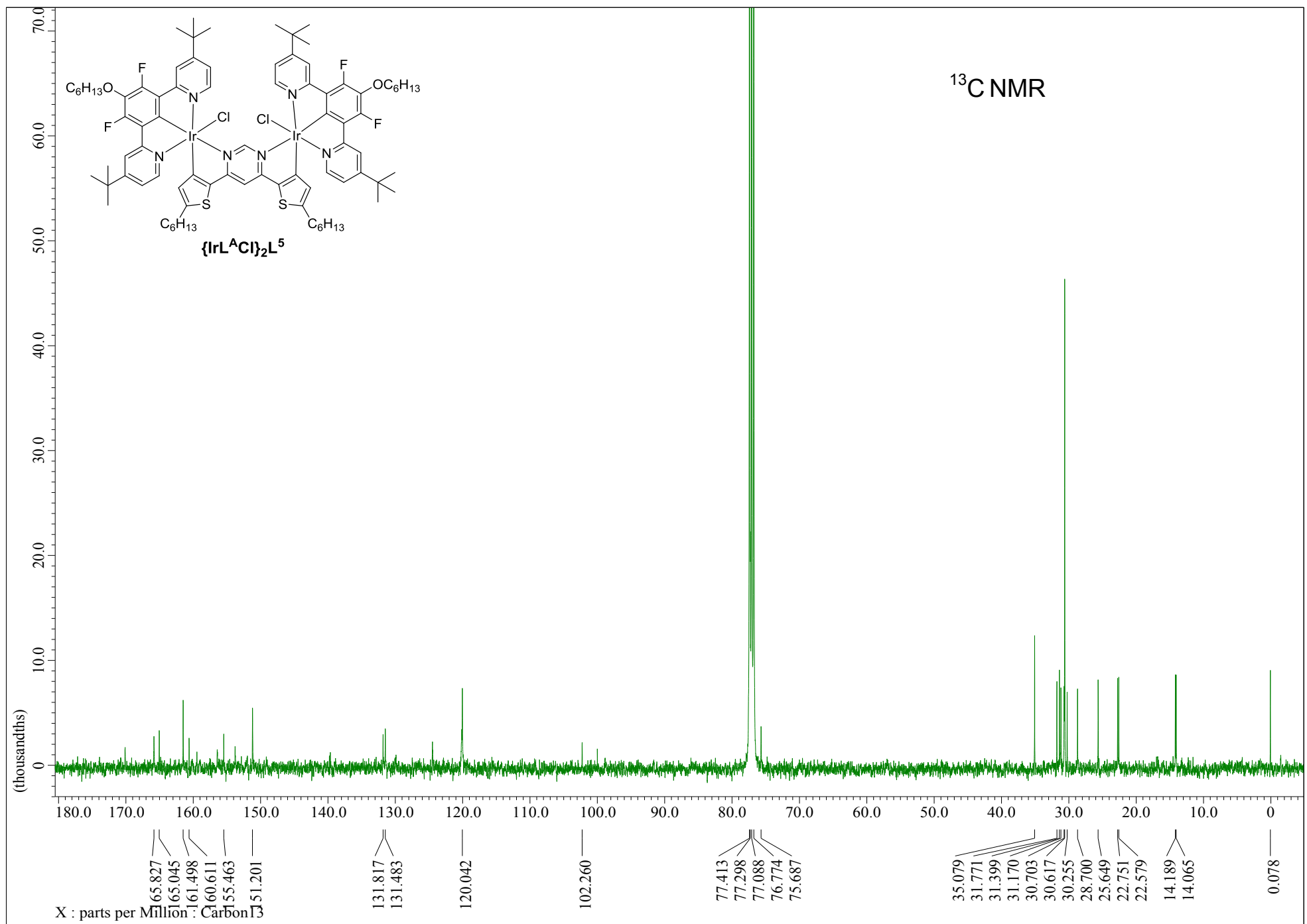


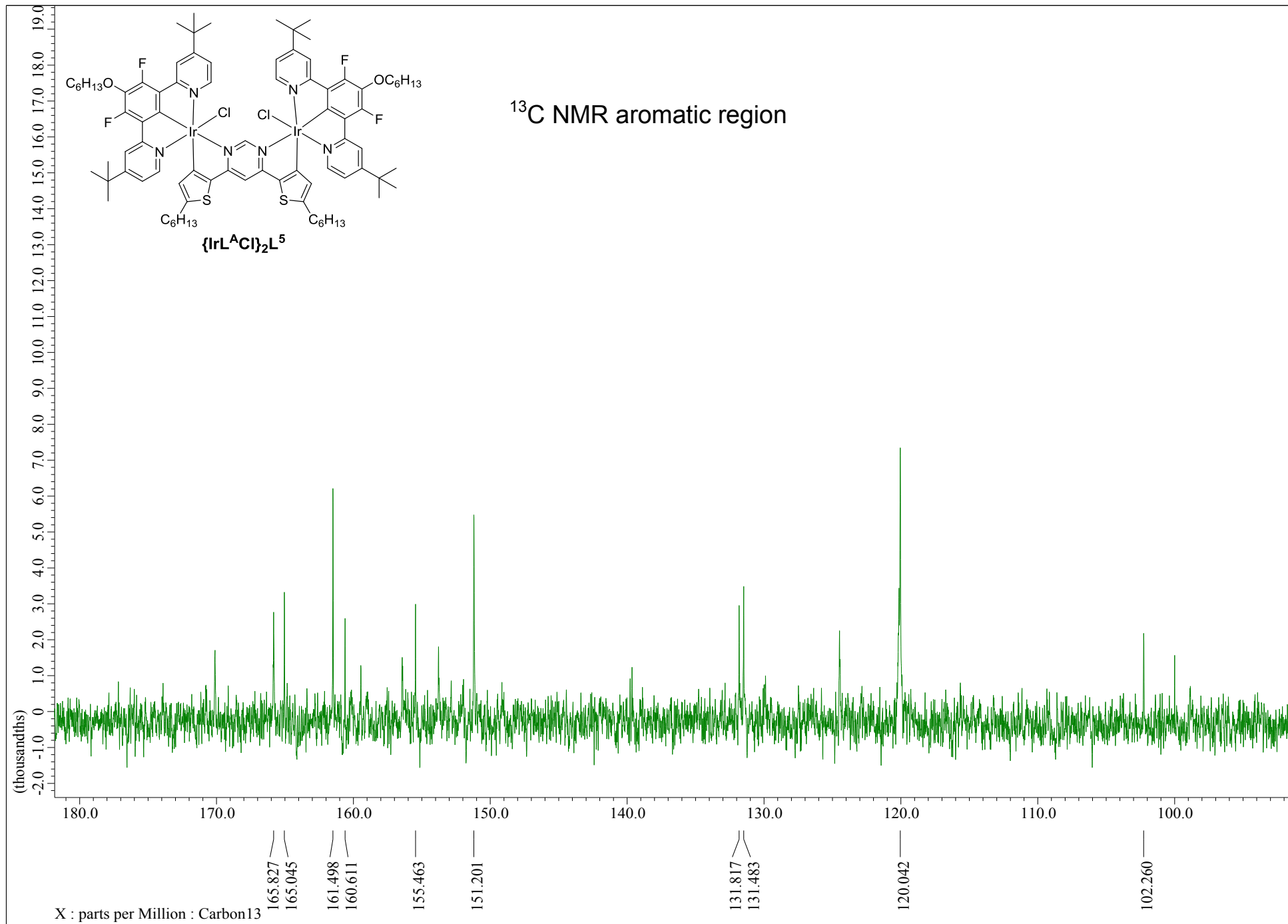


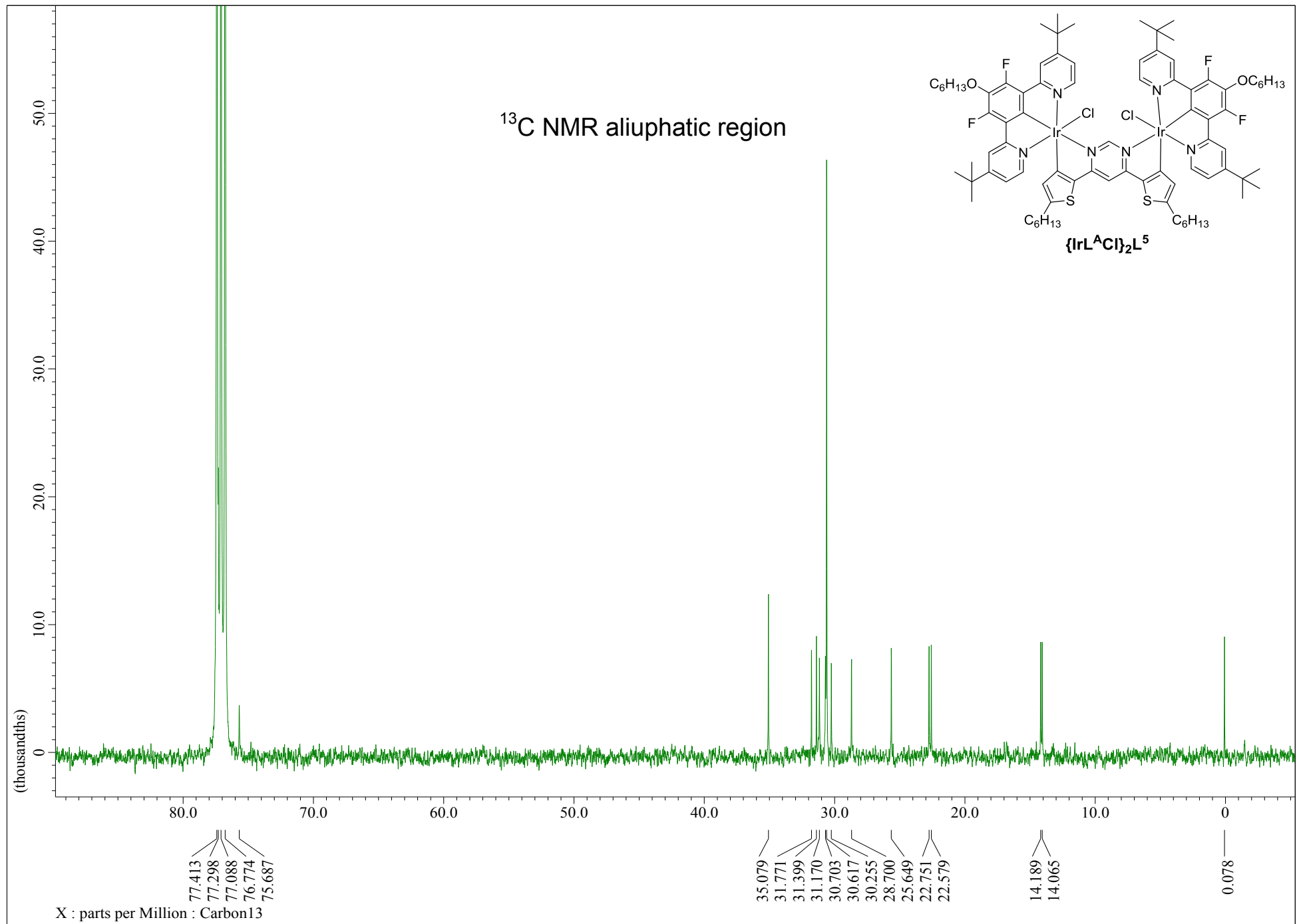


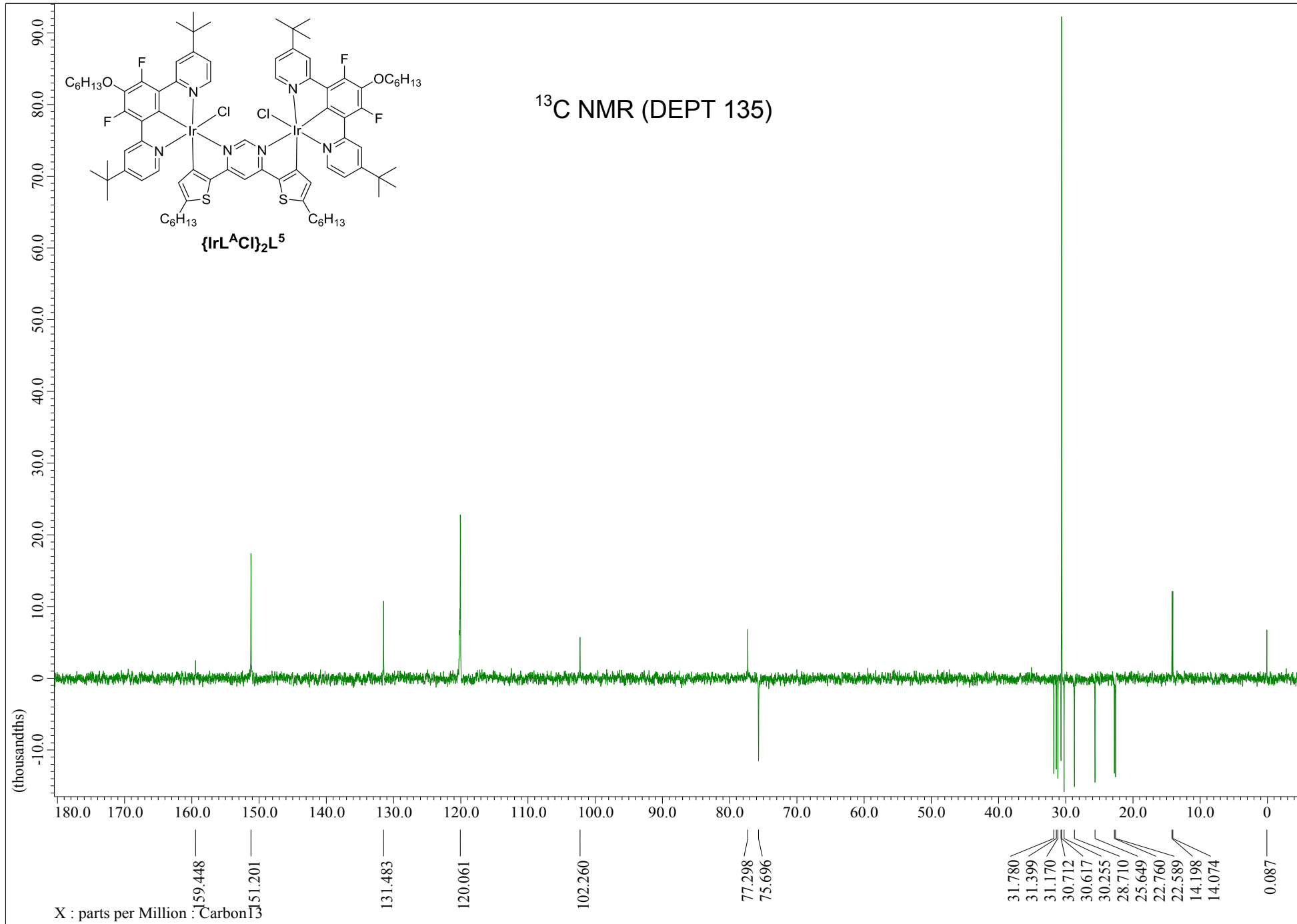






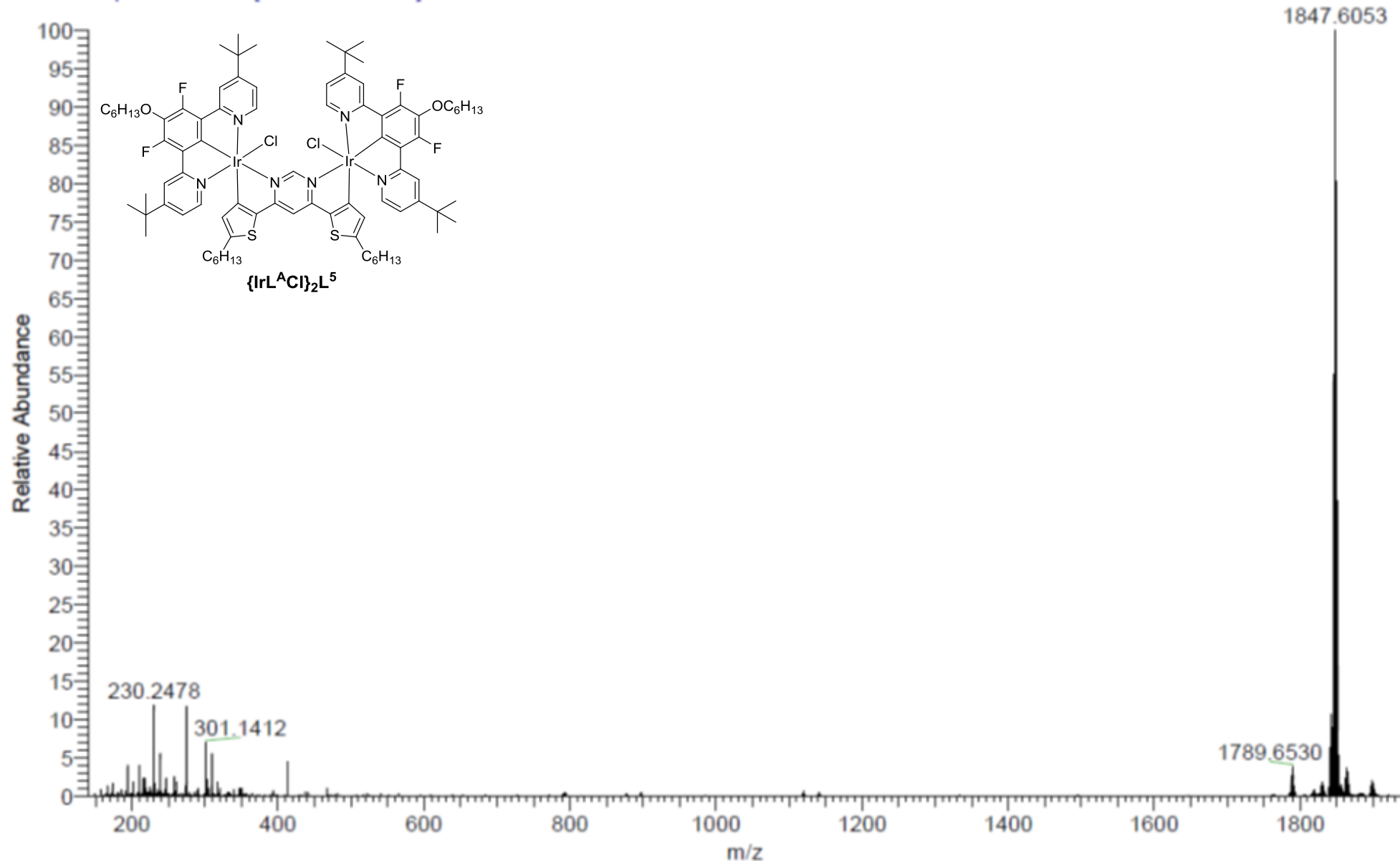






MW=1825?
(DCM)/MeCN
C84H104Cl2F4Ir2N6O2S2
NORKOZ051-OJ-HNESP #27-45 RT: 0.66-1.03 AV: 15 SM: 7G NL: 4.26E6
T: FTMS + p NSI Full ms [140.00-1935.00]

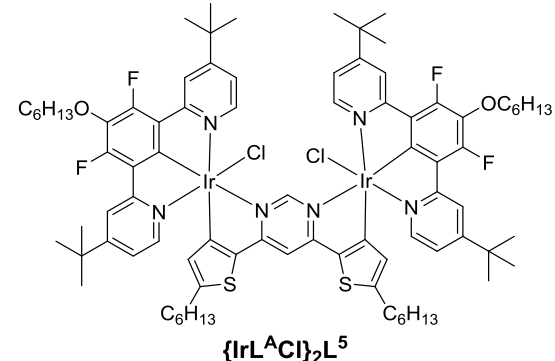
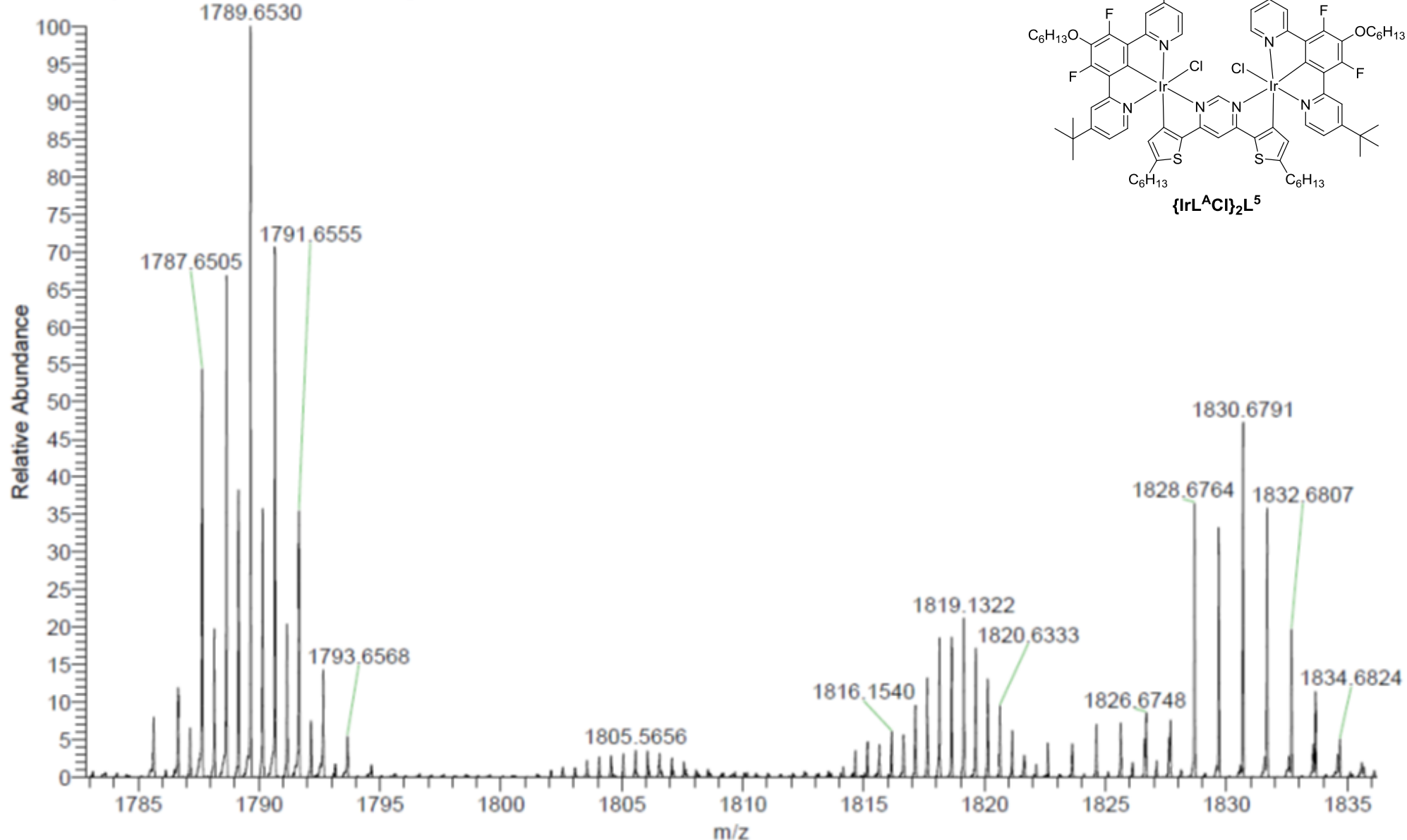
EPSRC National Facility Swansea
LTQ Orbitrap XL



MW=1825?
(DCM)/MeCN
C84H104Cl2F4Ir2N6O2S2

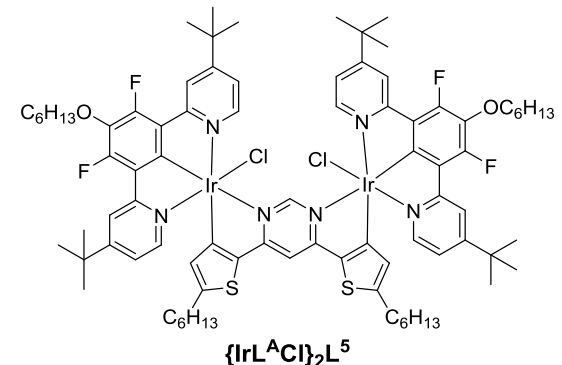
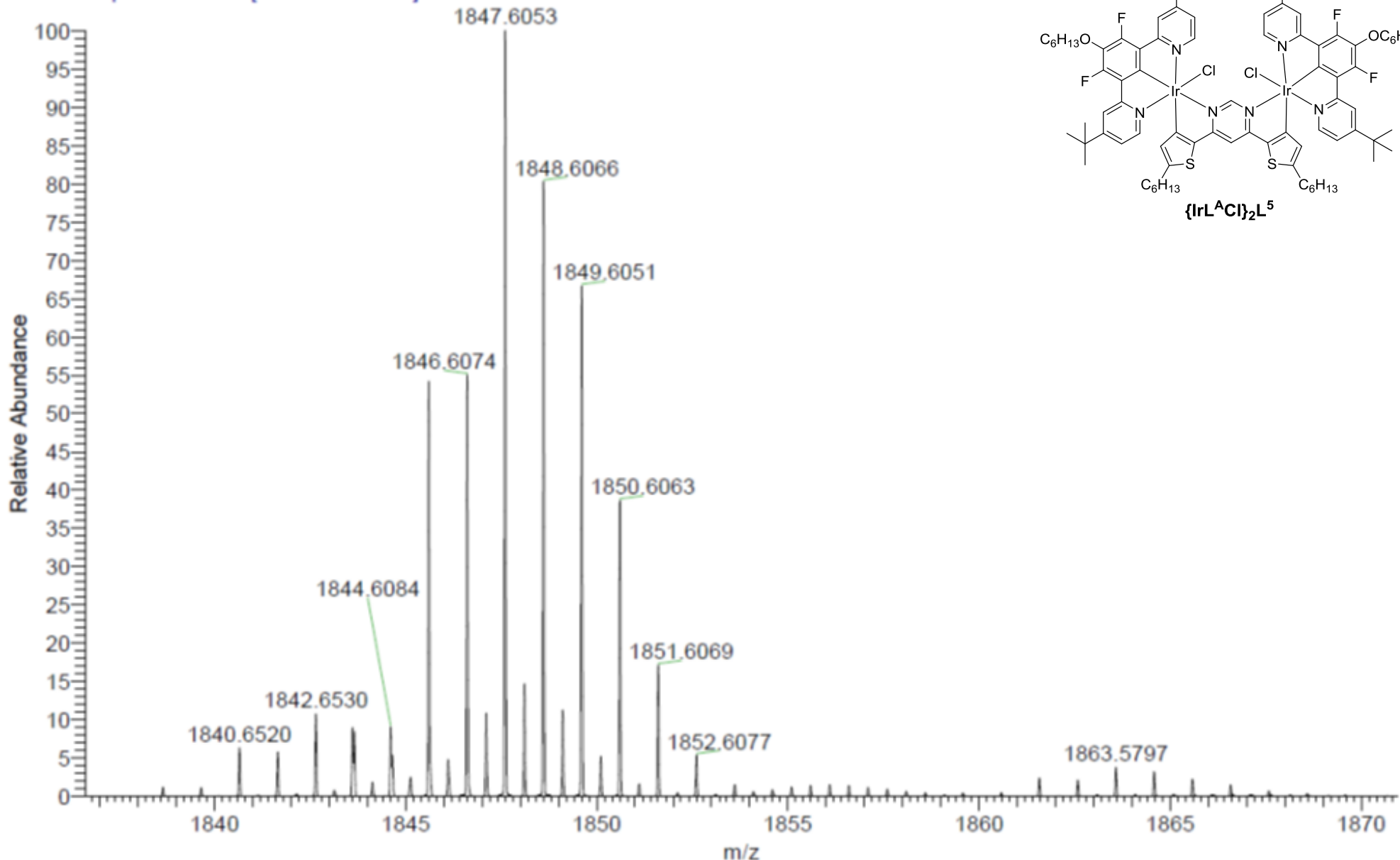
EPSRC National Facility Swansea
LTQ Orbitrap XL

NORKOZ051-OJ-HNESP #27-45 RT: 0.66-1.03 AV: 15 SM: 7G NL: 1.68E5
T: FTMS + p NSI Full ms [140.00-1935.00]



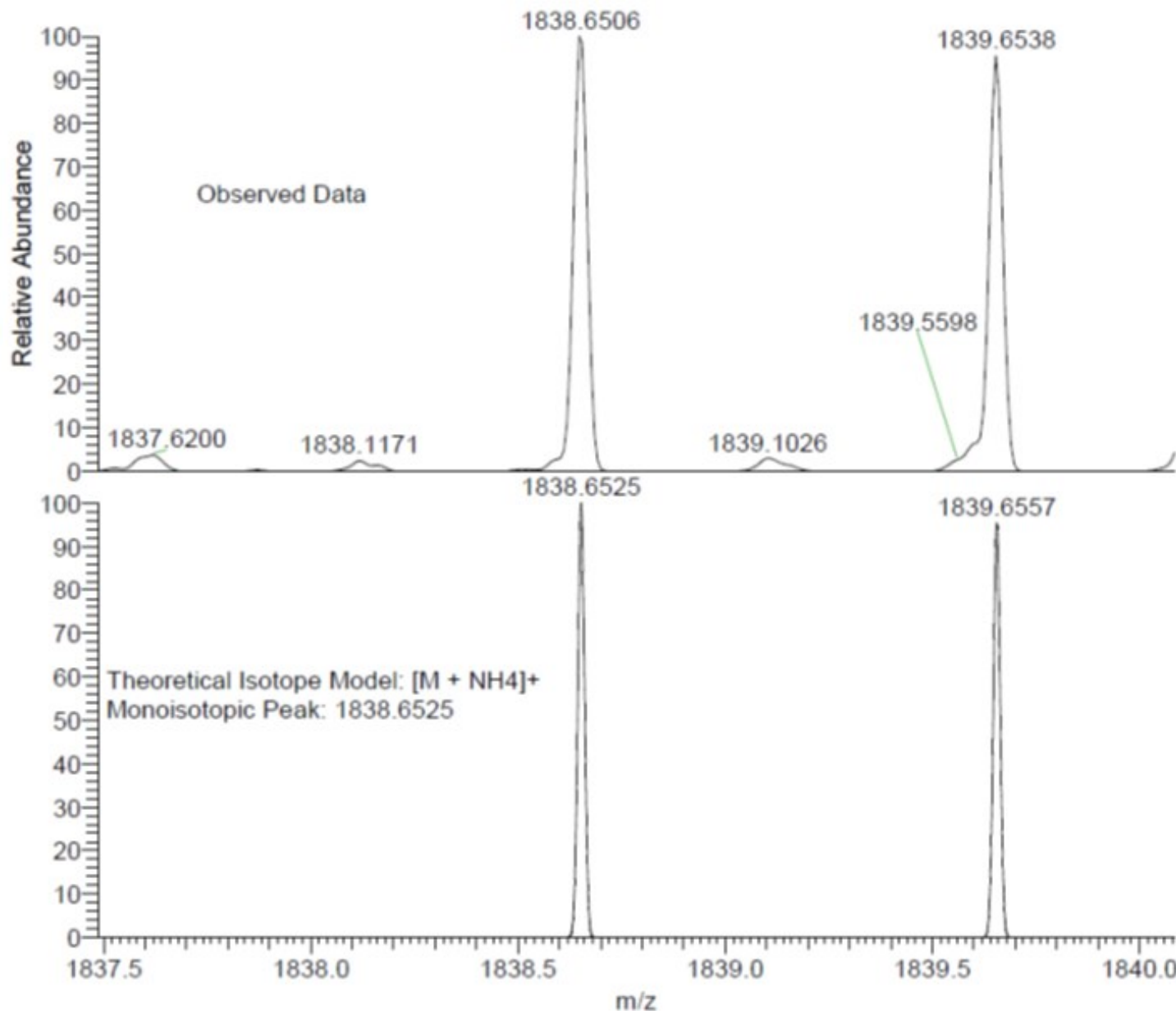
MW=1825?
(DCM)/MeCN
C84H104Cl2F4Ir2N6O2S2
NORKOZ051-OJ-HNESP #27-45 RT: 0.66-1.03 AV: 15 SM: 7G NL: 4.26E6
T: FTMS + p NSI Full ms [140.00-1935.00]

EPSRC National Facility Swansea
LTQ Orbitrap XL



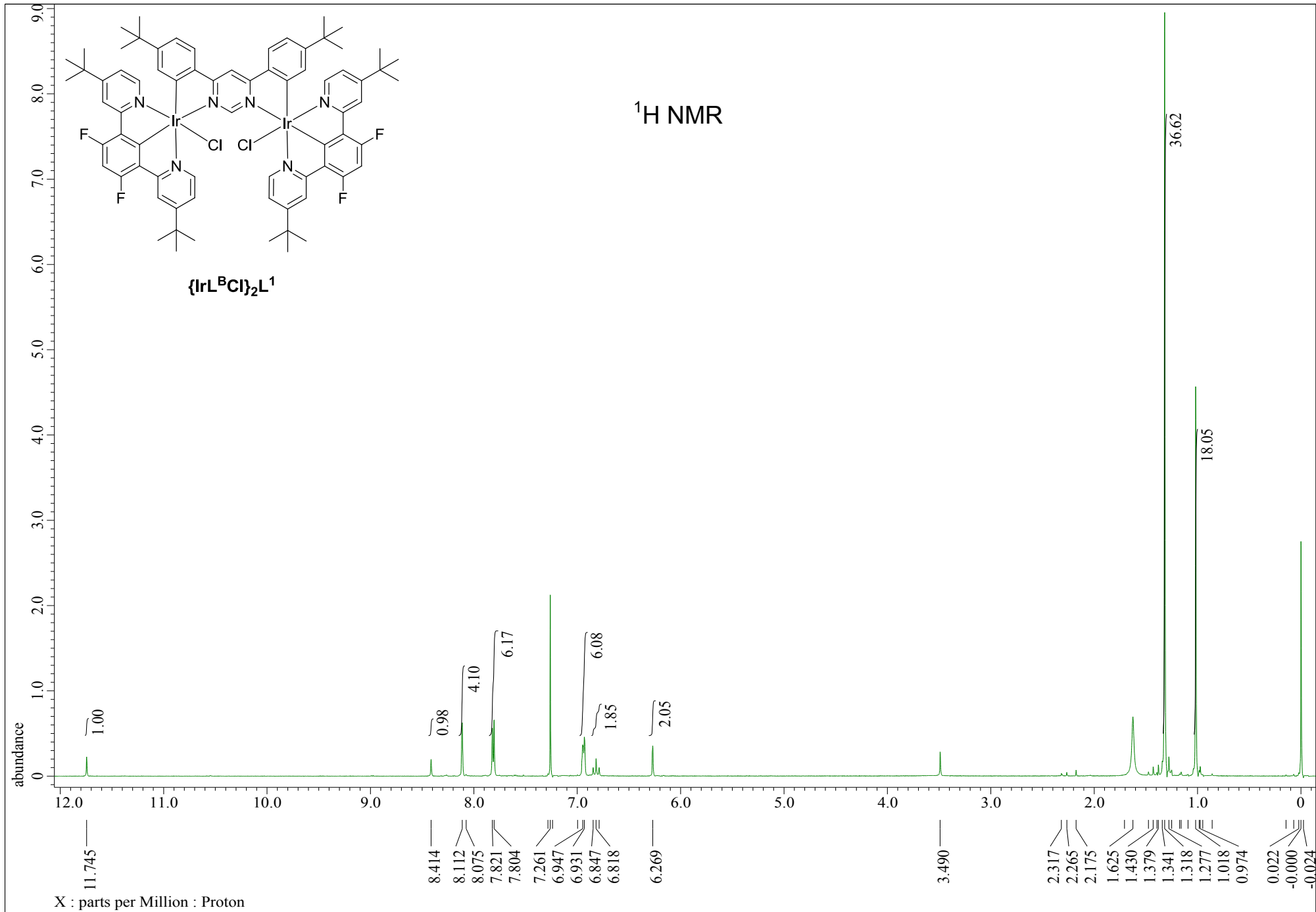
MW=1825?
(DCM)/MeCN
C84H104Cl₂F₄Ir₂N₆O₂S₂

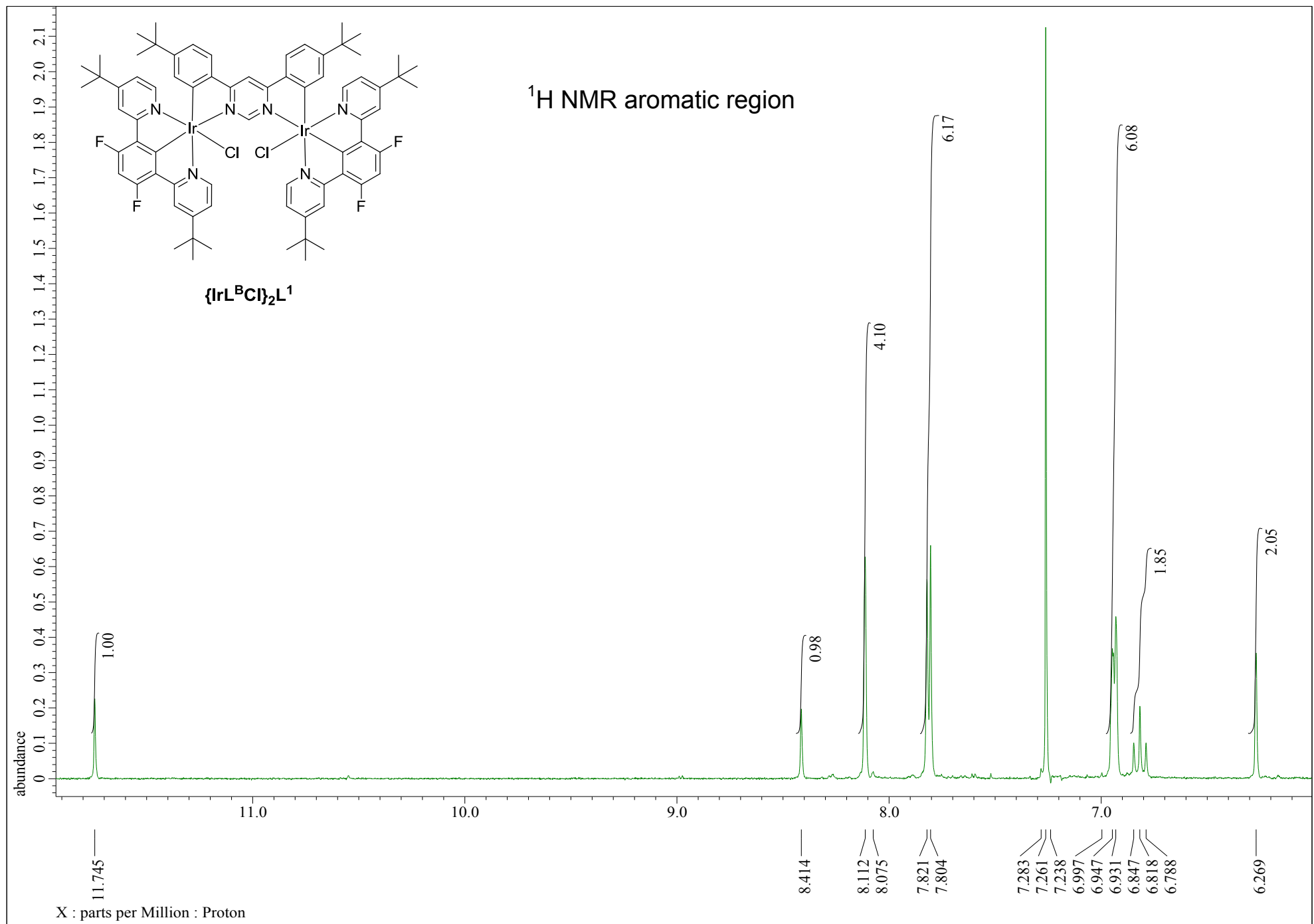
EPSRC National Facility Swansea
LTQ Orbitrap XL

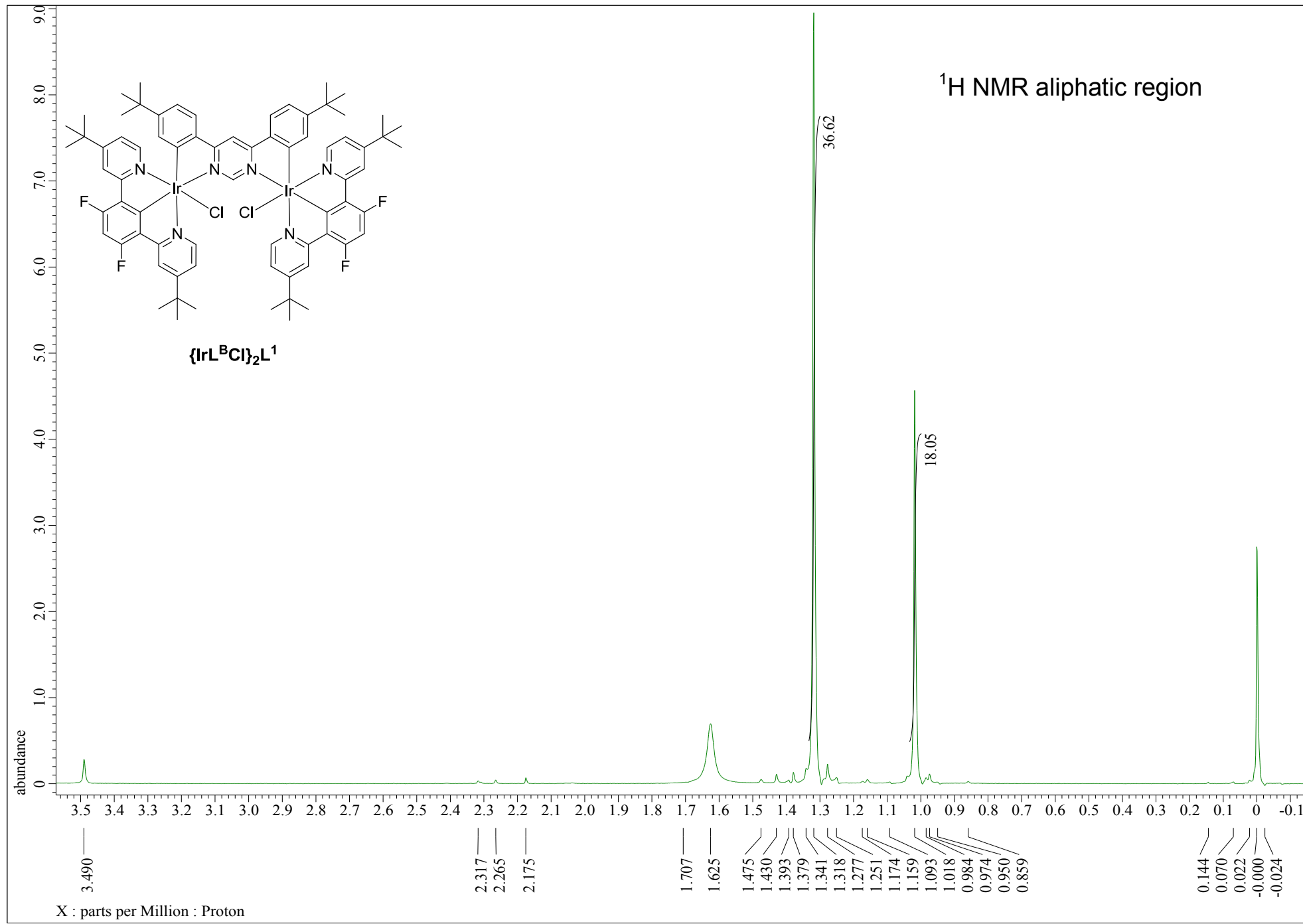


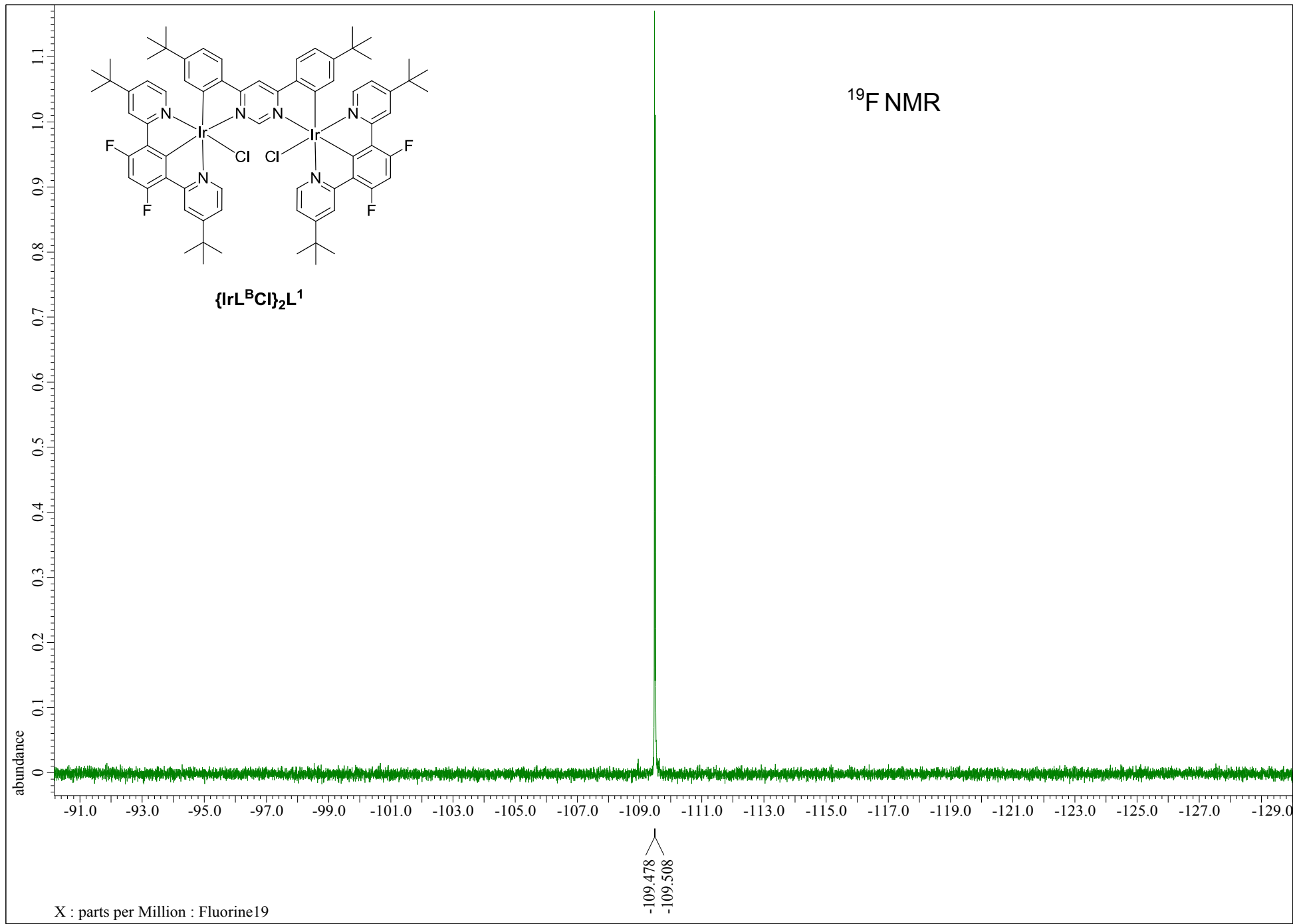
NL:
4.93E4
NORKOZ051-OJ-HNESP#27-45
RT: 0.66-1.03 AV: 15 T: FTMS + p
NSI Full ms [140.00-1935.00]

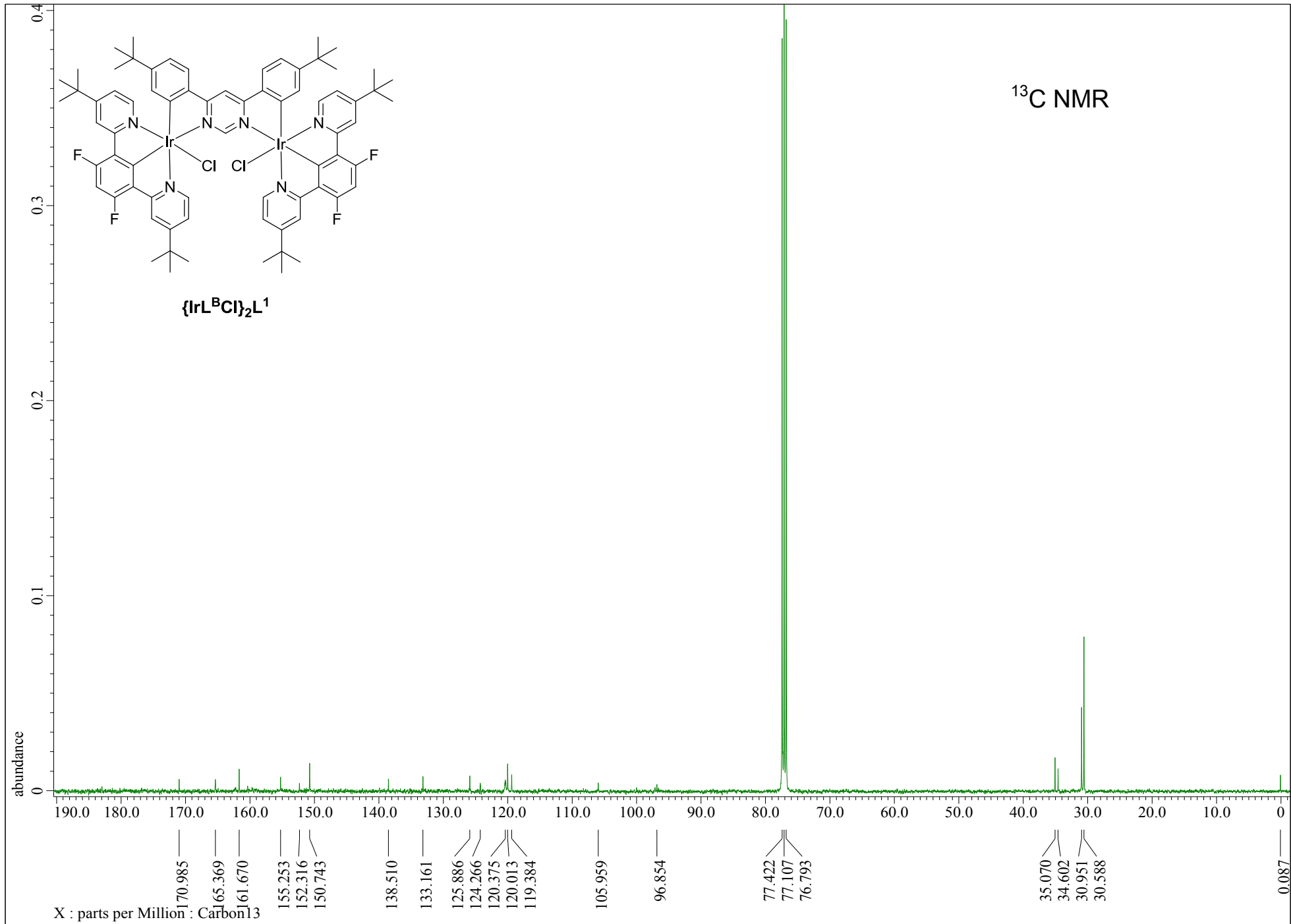
NL:
6.56E2
C₈₄H₁₀₄Cl₂F₄Ir₂N₆O₂S₂NH₄:
C₈₄H₁₀₈Cl₂F₄Ir₂N₇O₂S₂
p (gss, s /p:40) Chrg 1
R: 100000 Res .Pwr . @FWHM

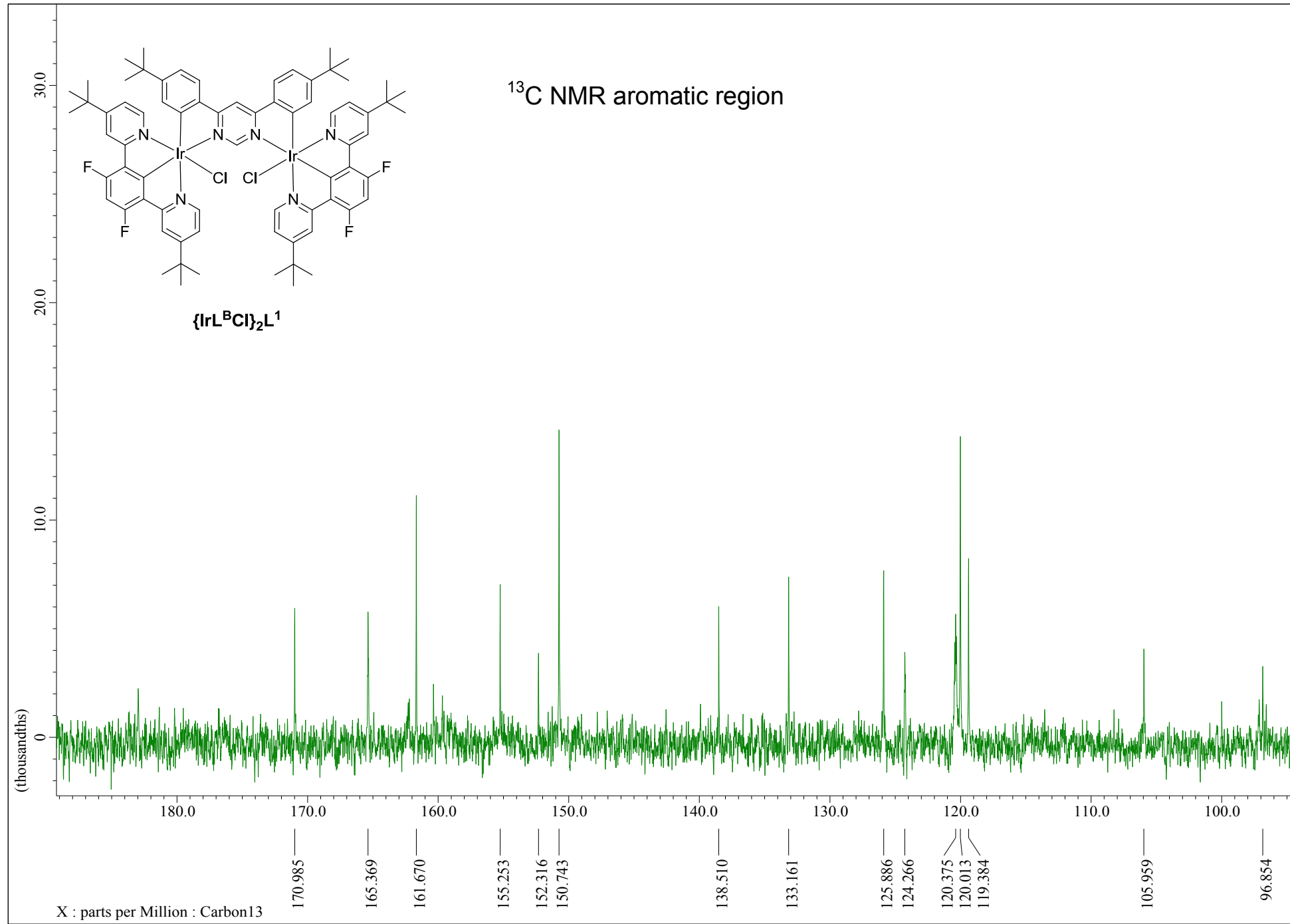


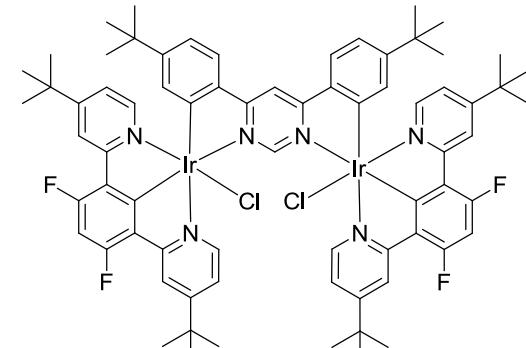
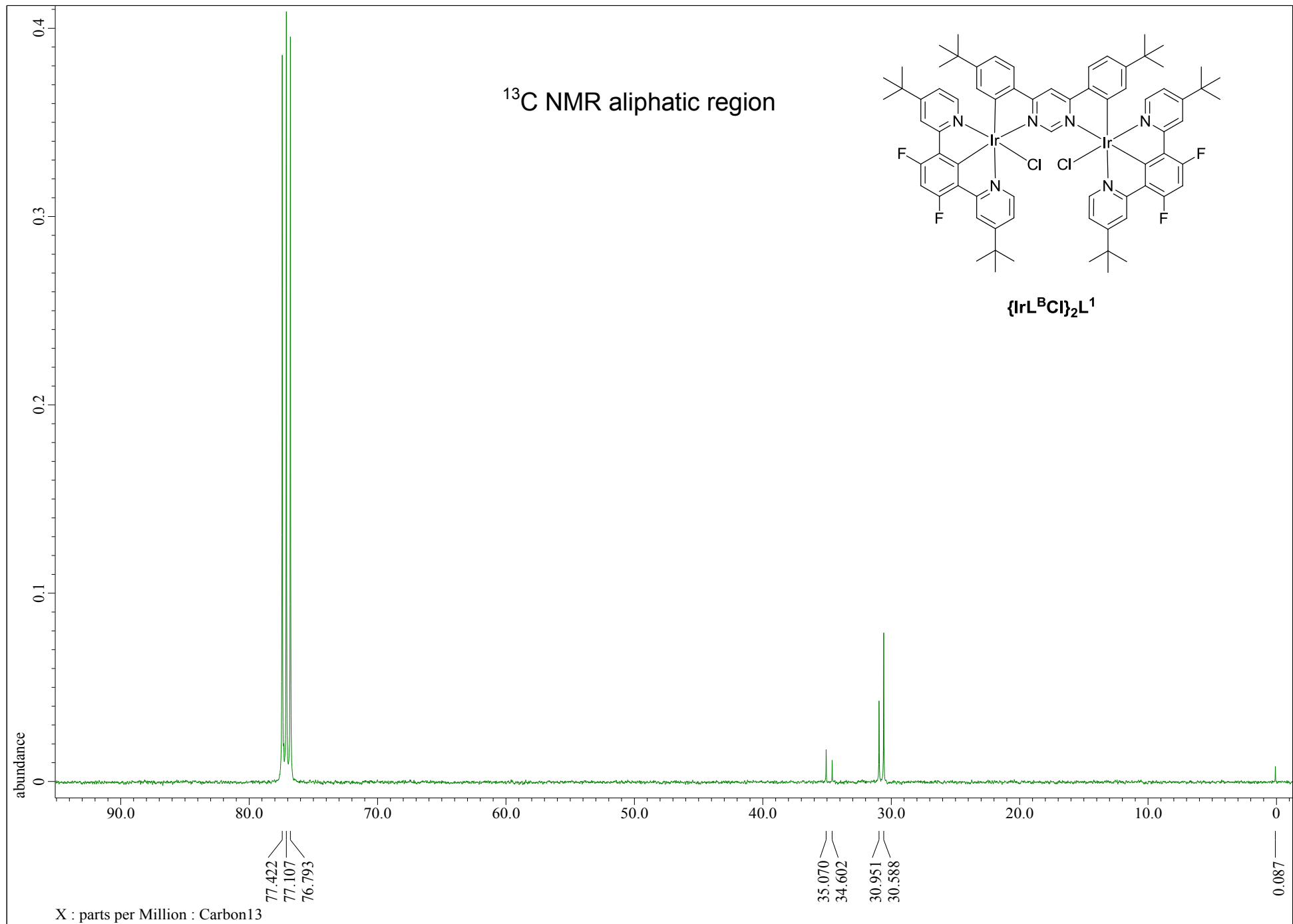




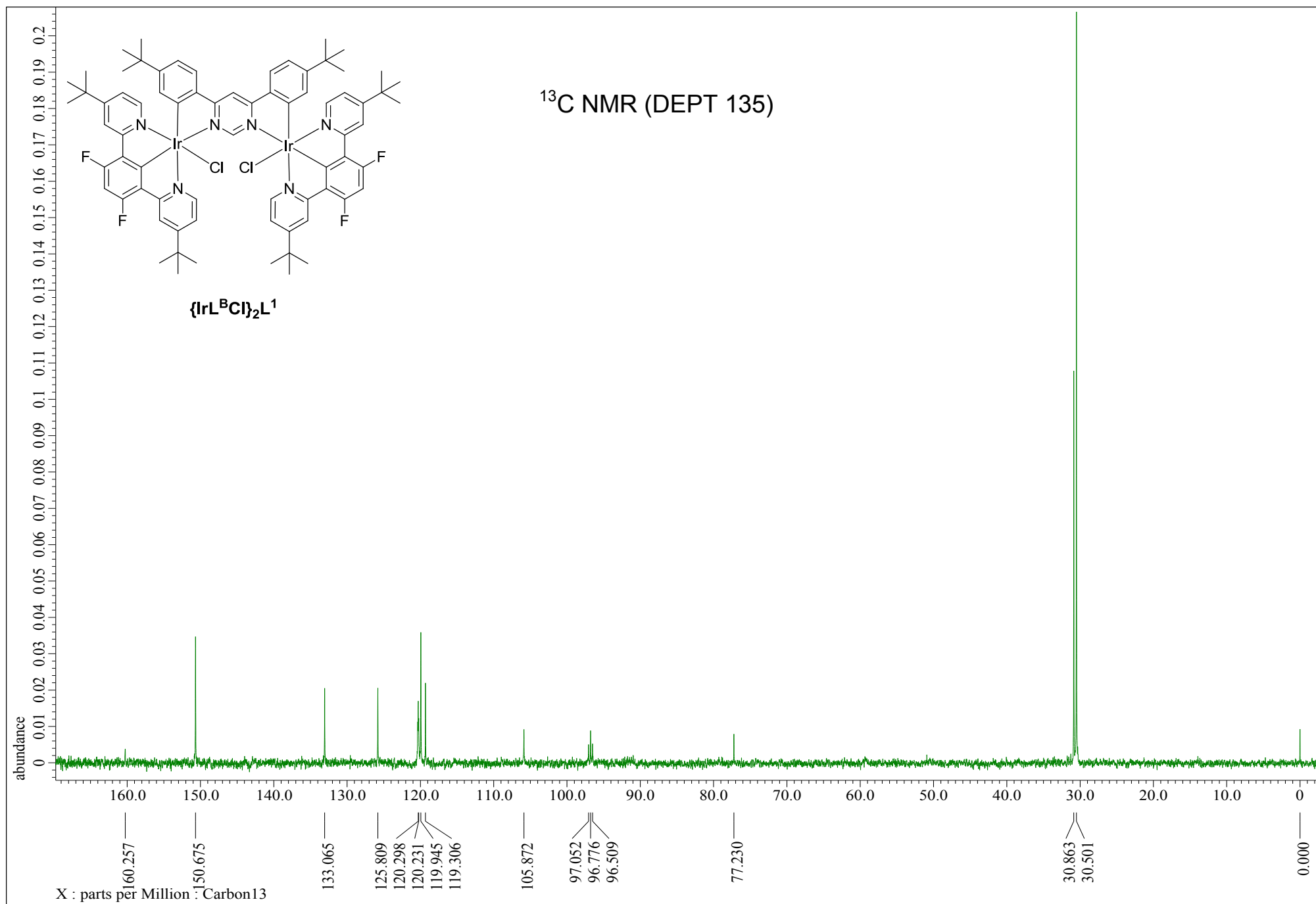








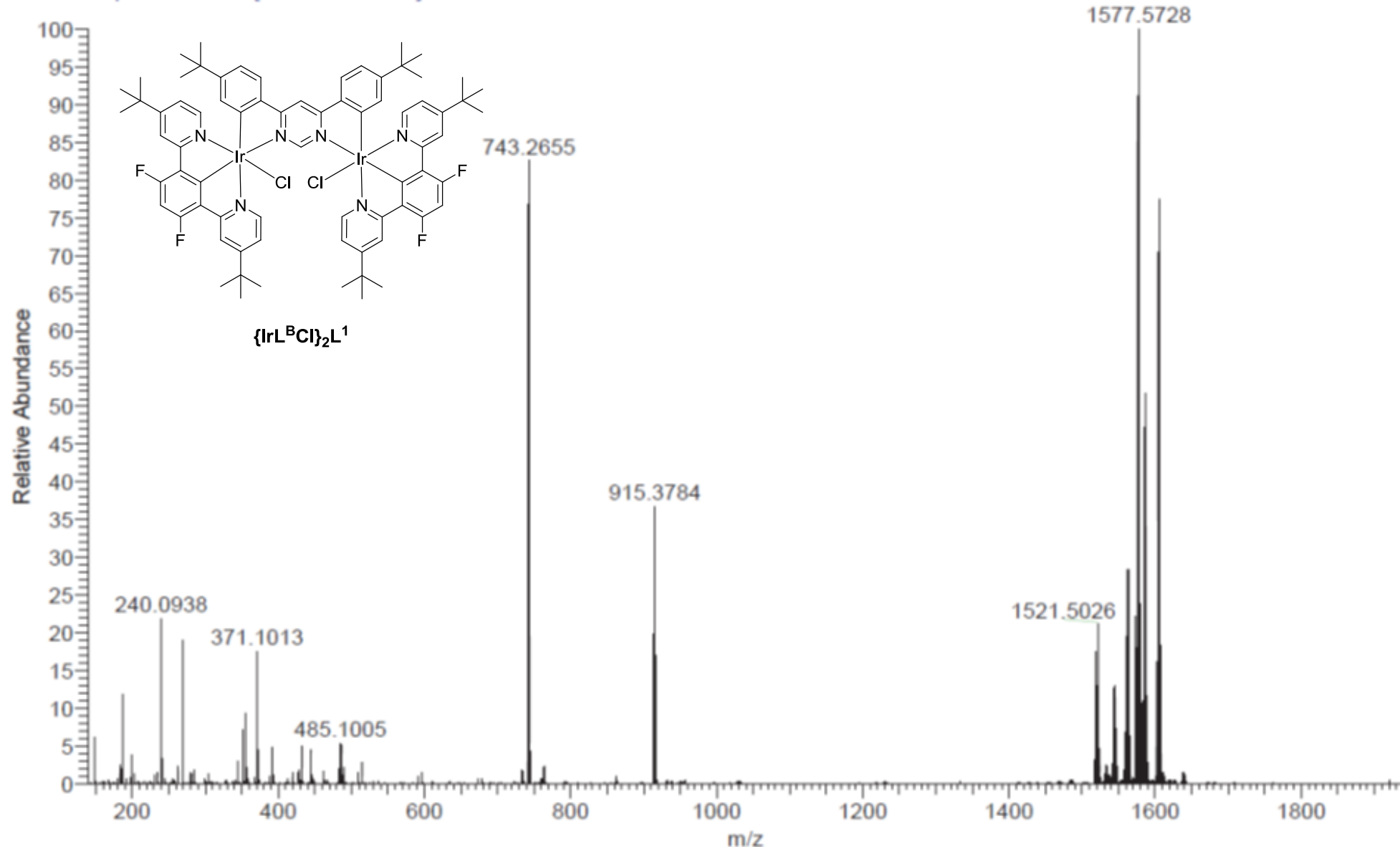
{IrL^BCl}₂L¹



MW=1556?
(DCM)/MeOH + NH₄OAc
C₇₂H₇₆Cl₂F₄Ir₂N₆

EPSRC National Facility Swansea
LTQ Orbitrap XL

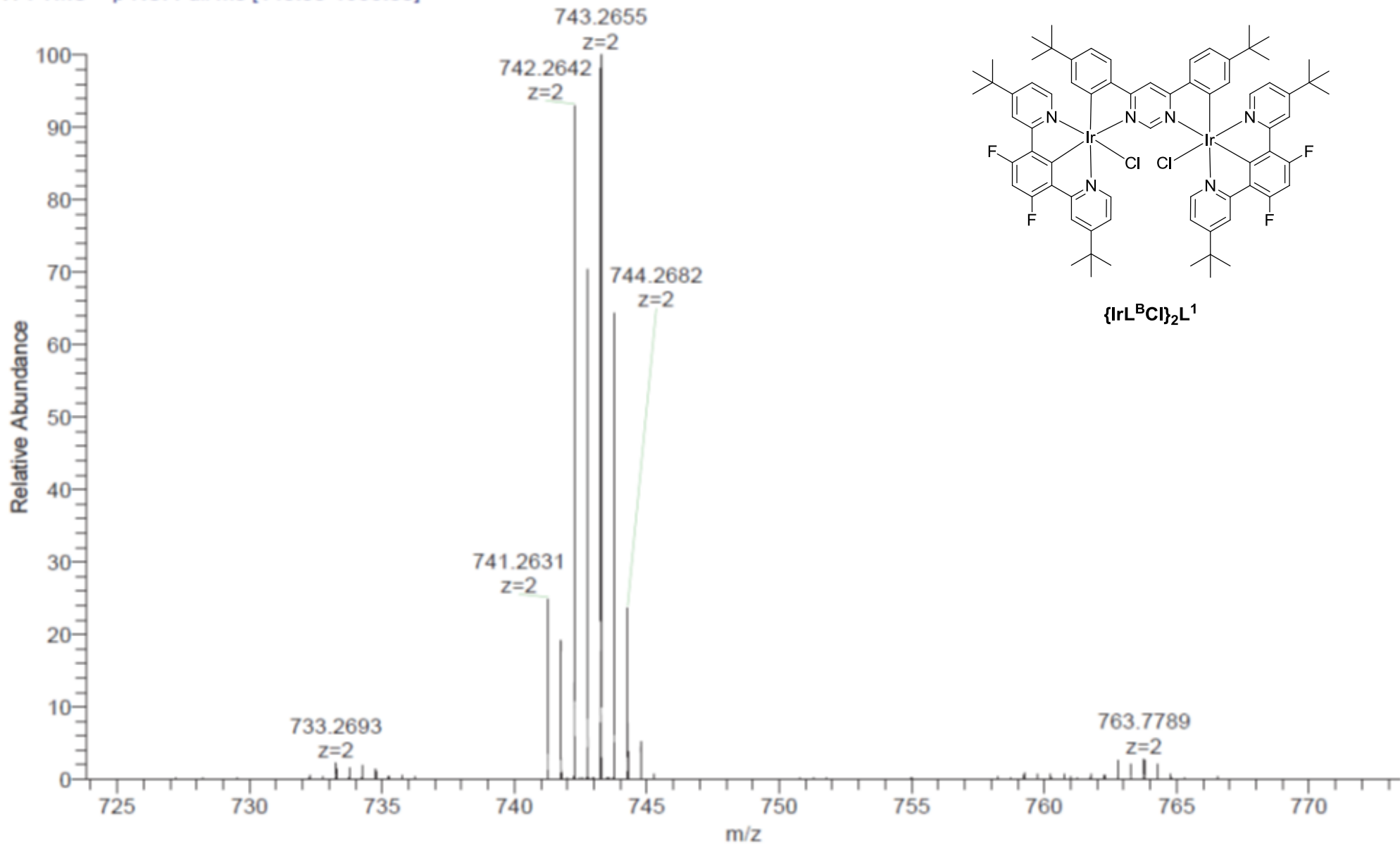
NORKOZ047-OA-HNESP #7-25 RT: 0.11-0.55 AV: 18 SM: 7G NL: 8.69E6
T: FTMS + p NSI Full ms [140.00-1935.00]

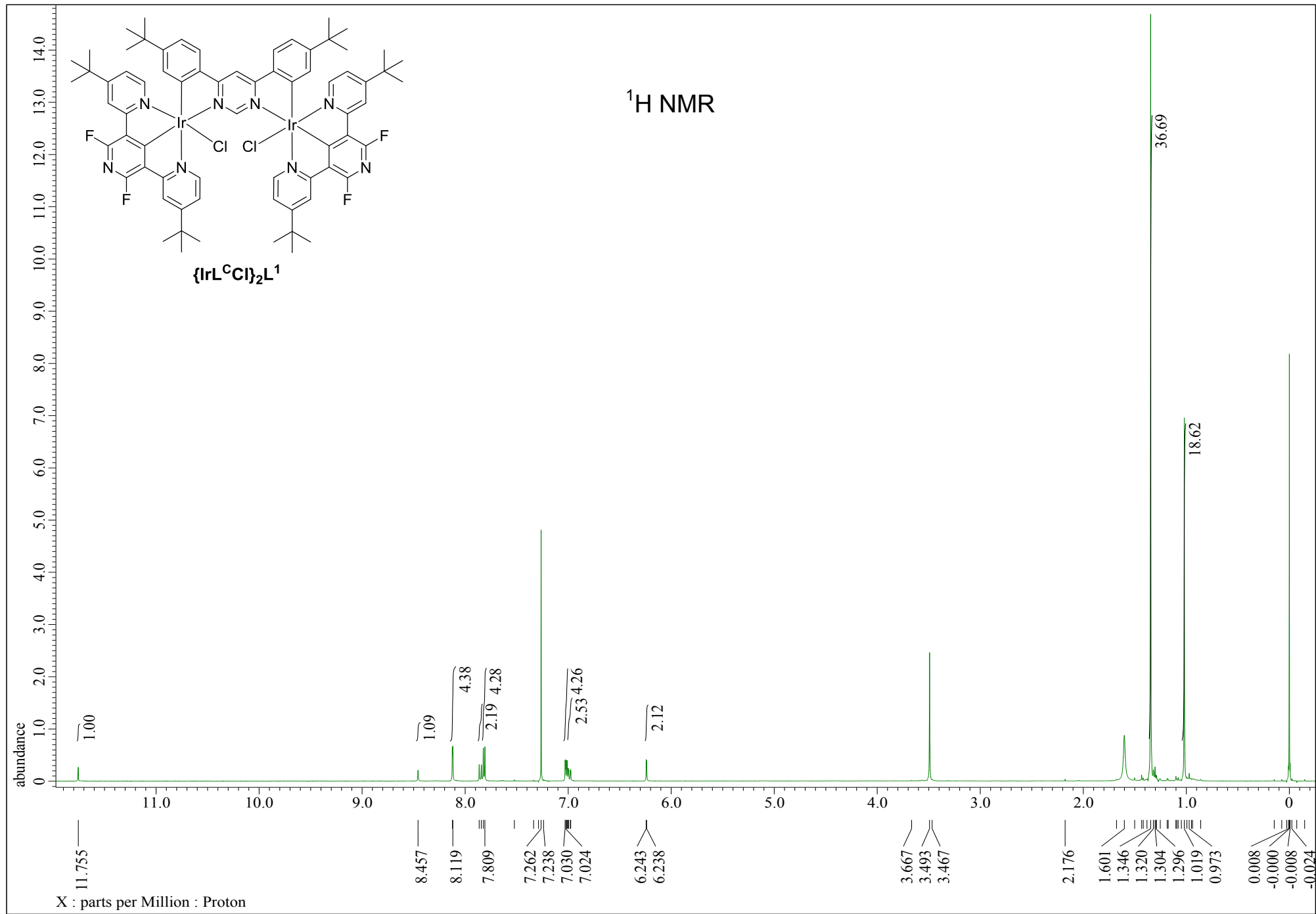


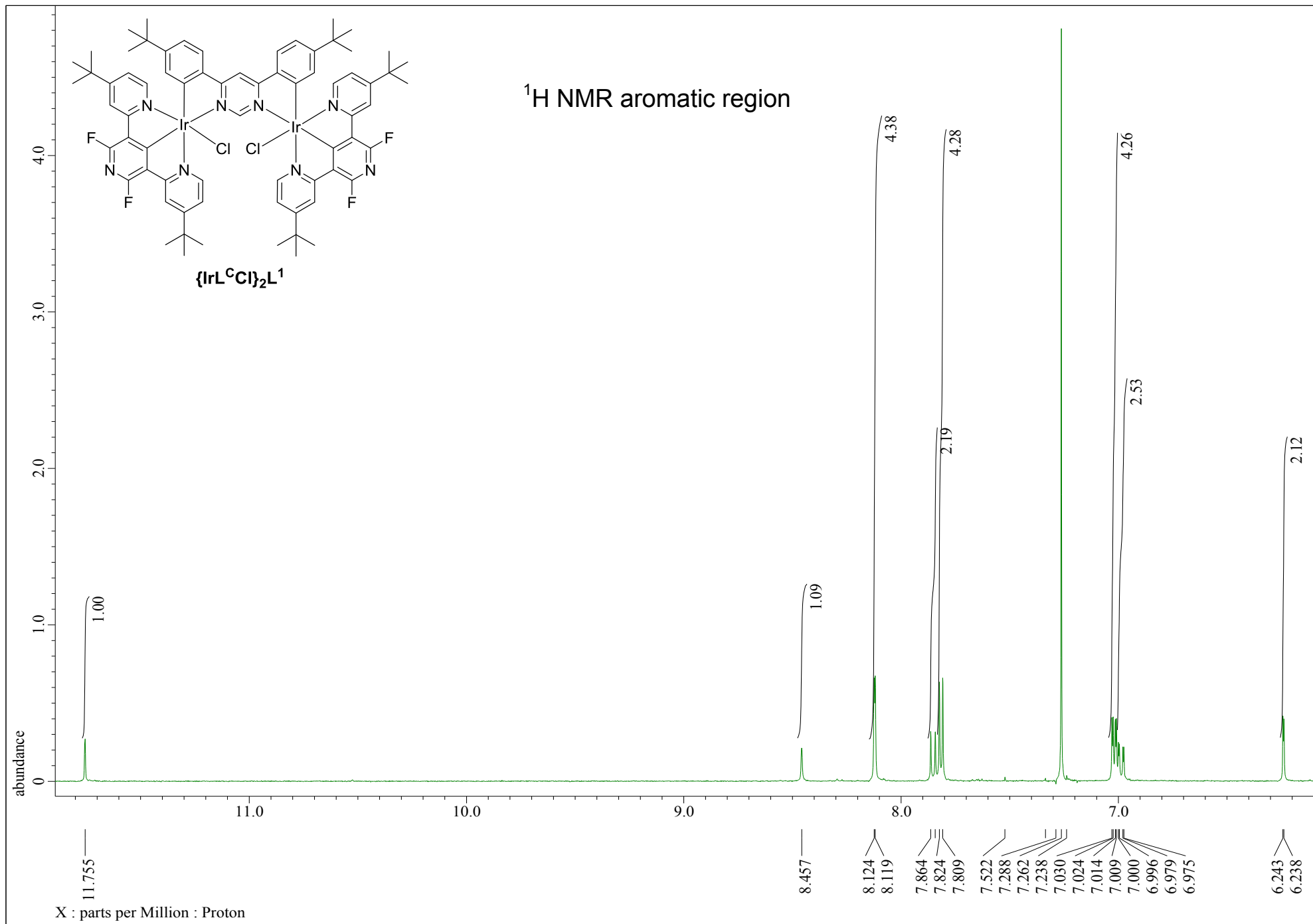
MW=1556?
(DCM)/MeOH + NH₄OAc
C72H76Cl₂F₄Ir₂N₆

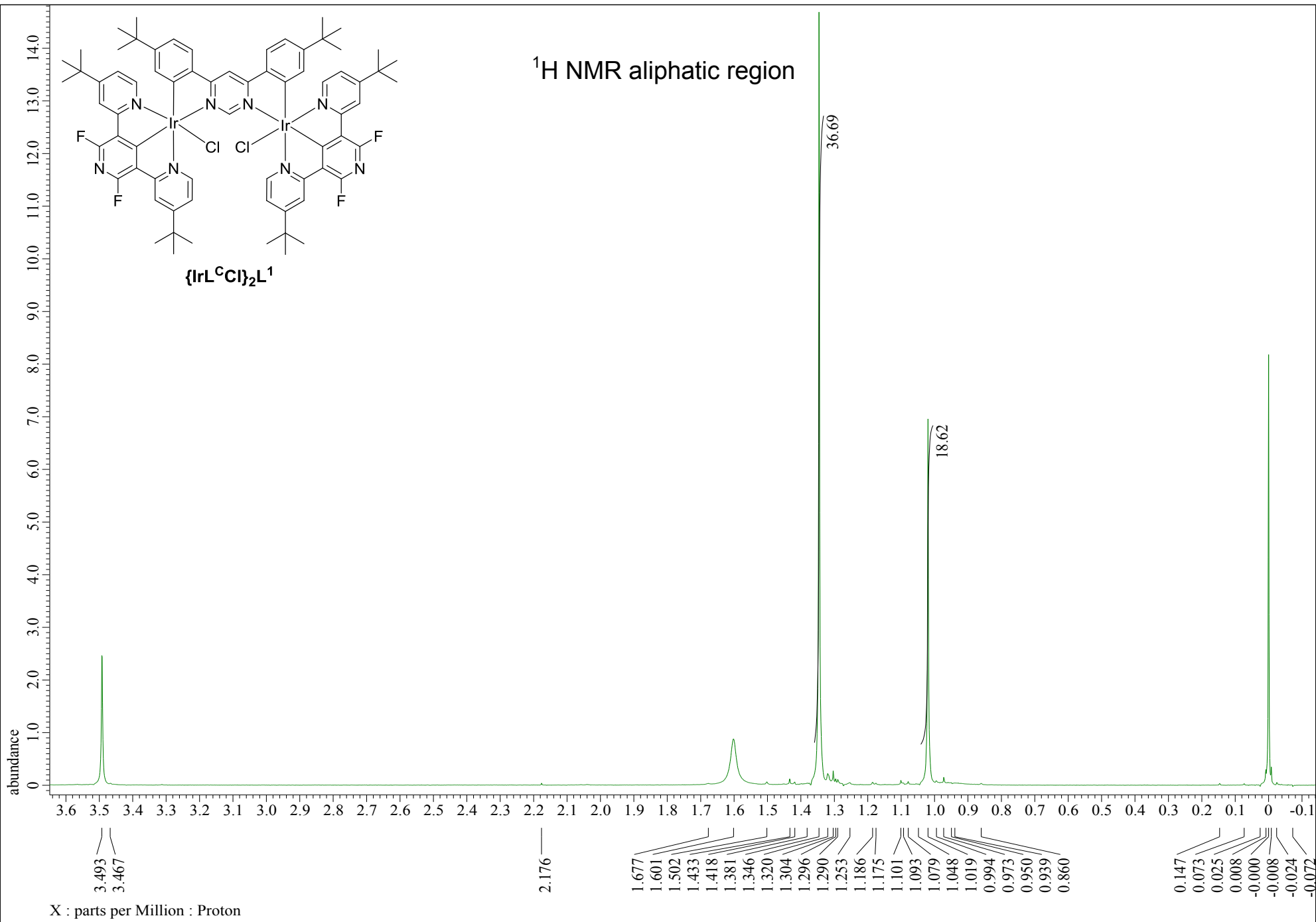
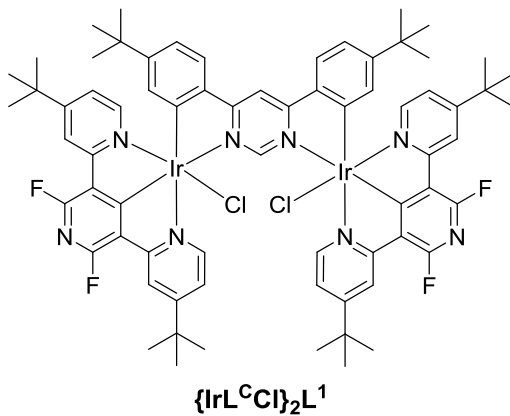
EPSRC National Facility Swansea
LTQ Orbitrap XL

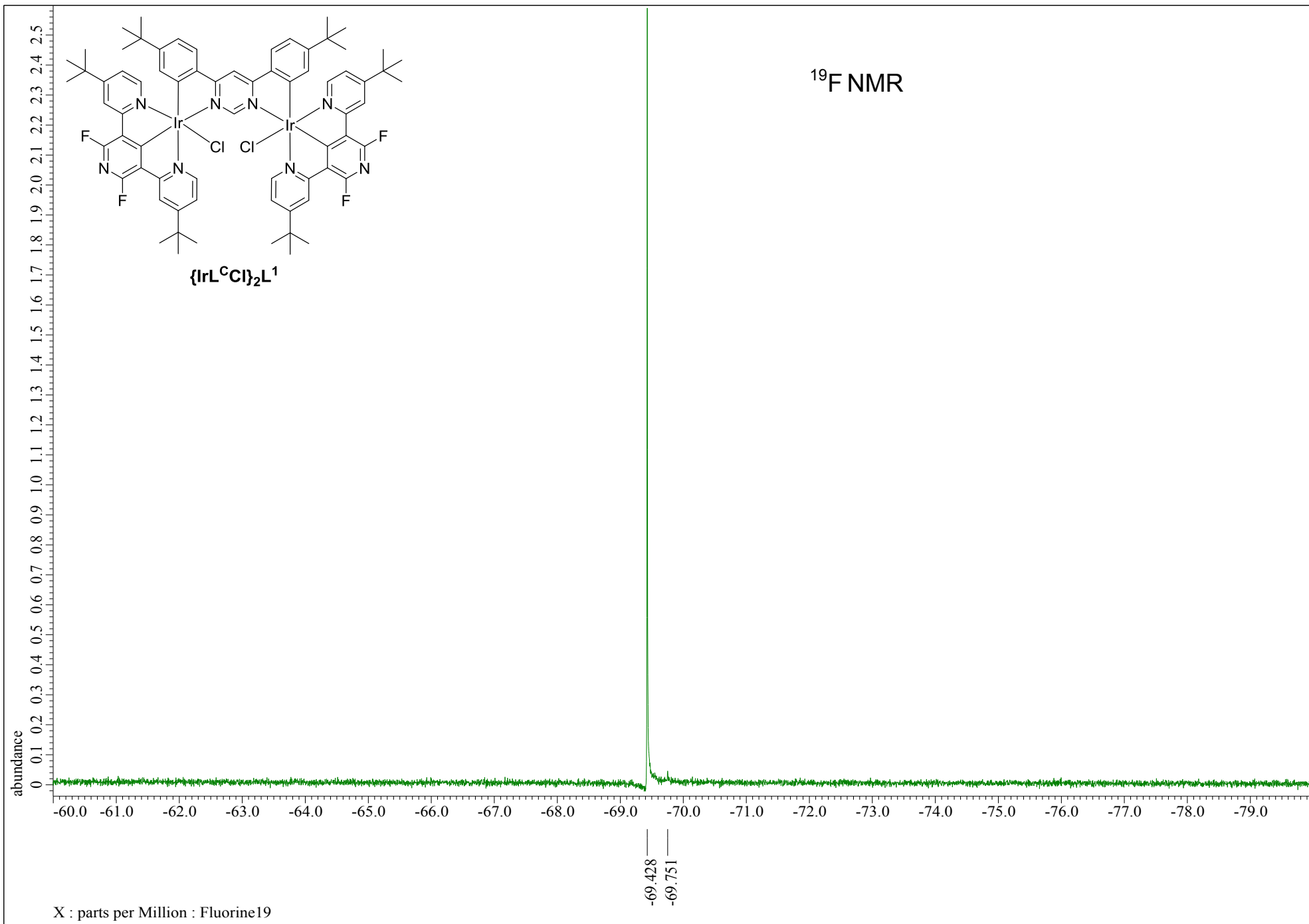
NORKOZ047-OA-HNESP #6-25 RT: 0.11-0.55 AV: 18 SM: 7G NL: 7.17E6
T: FTMS + p NSI Full ms [140.00-1935.00]

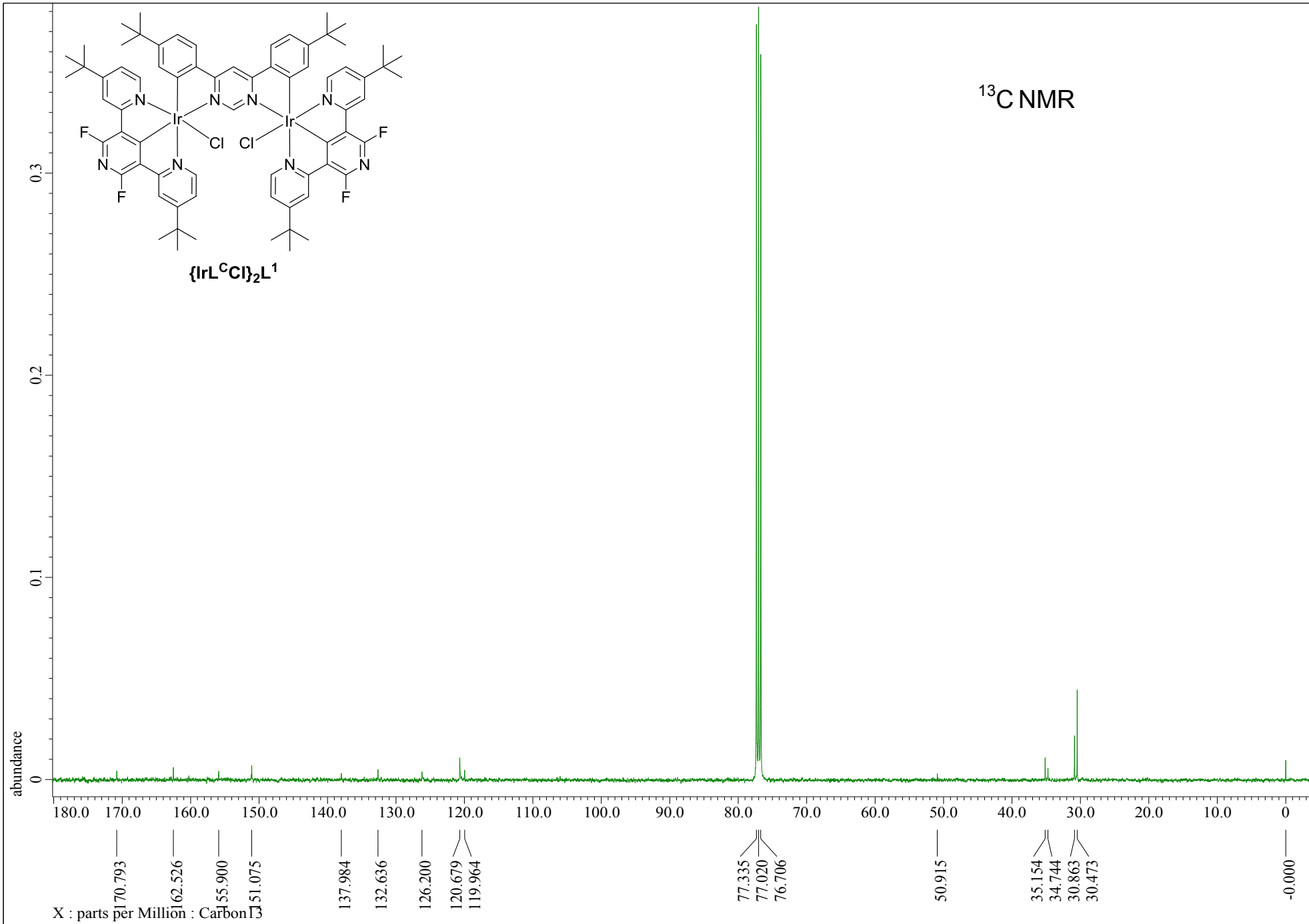


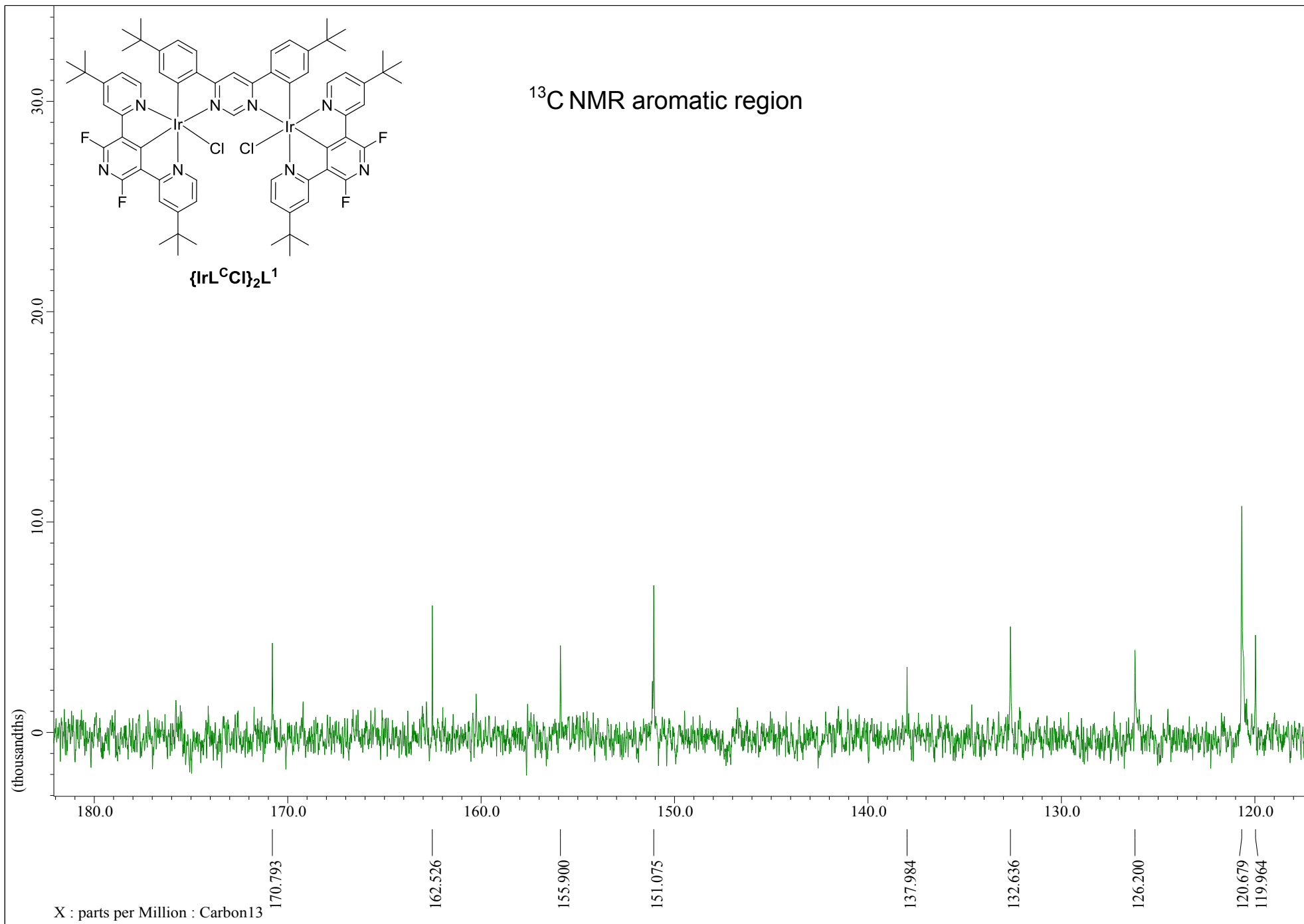


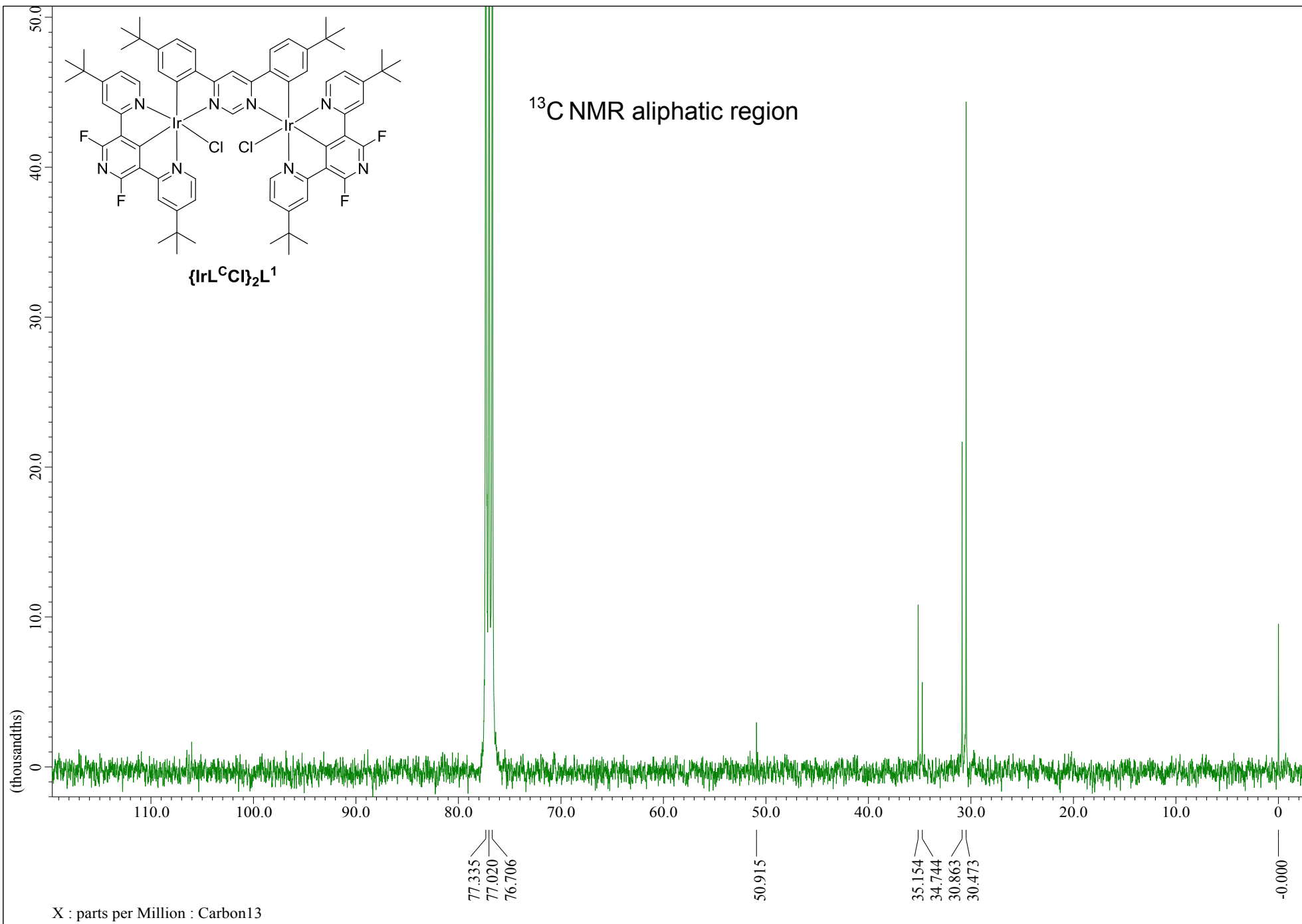


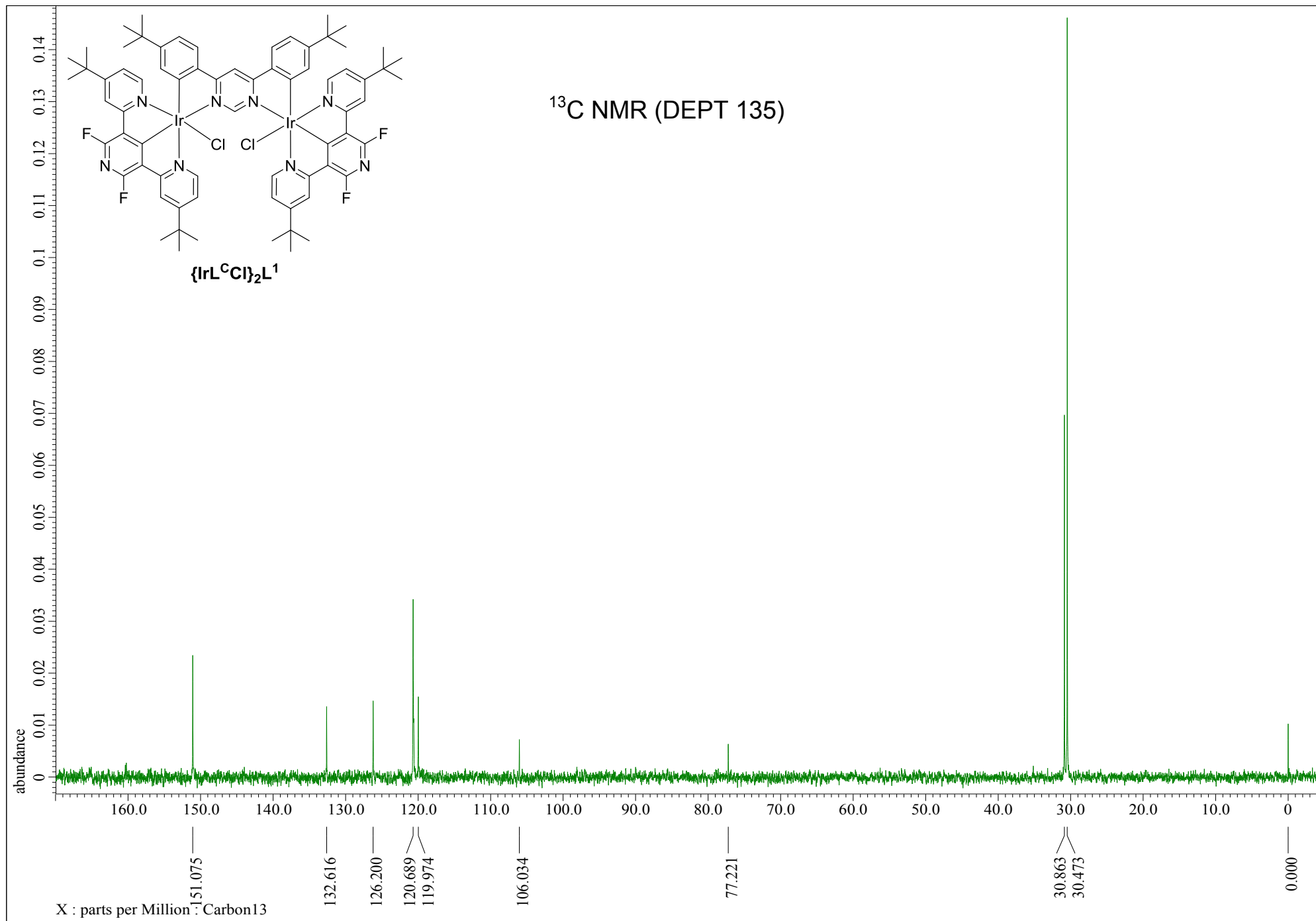








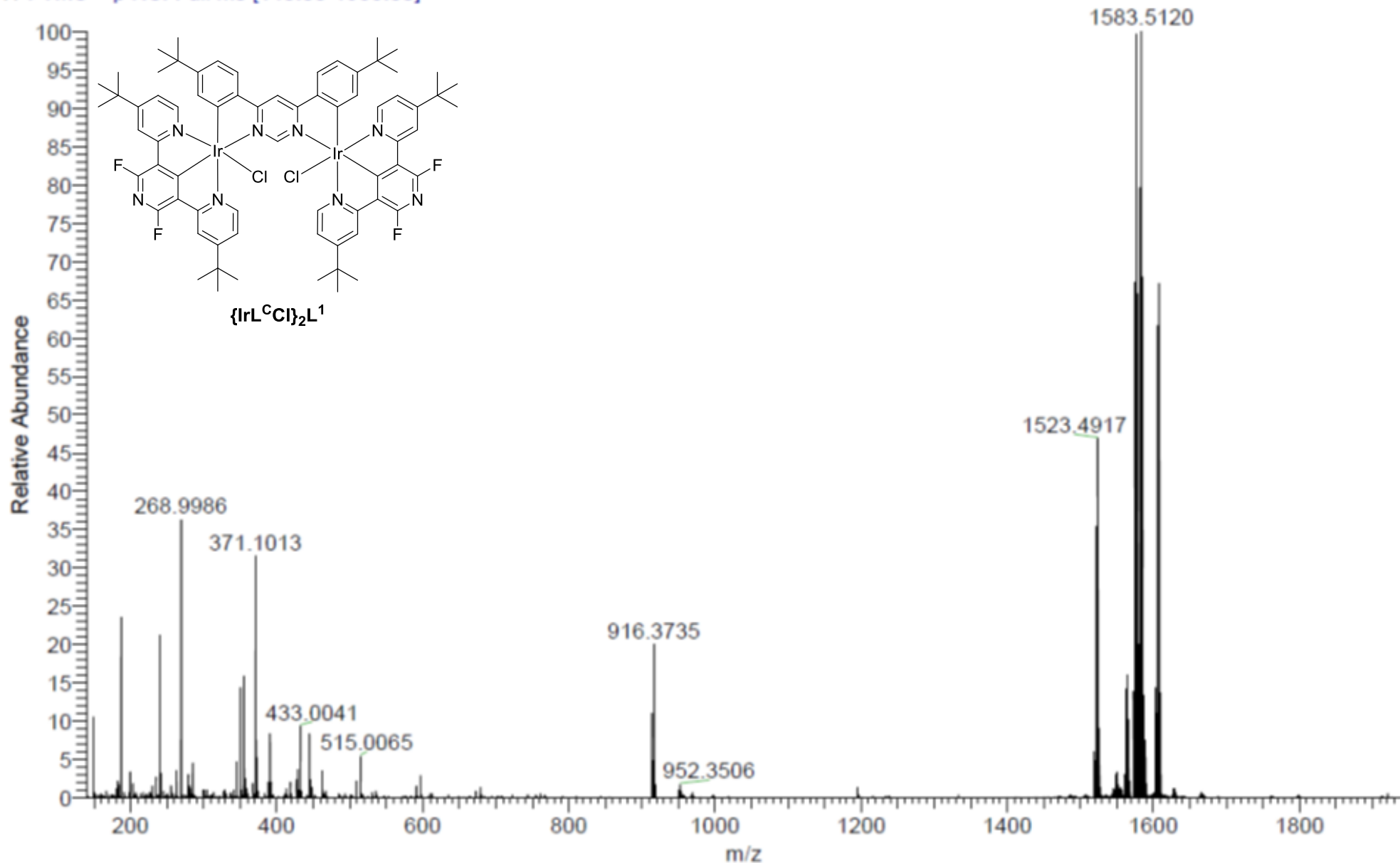
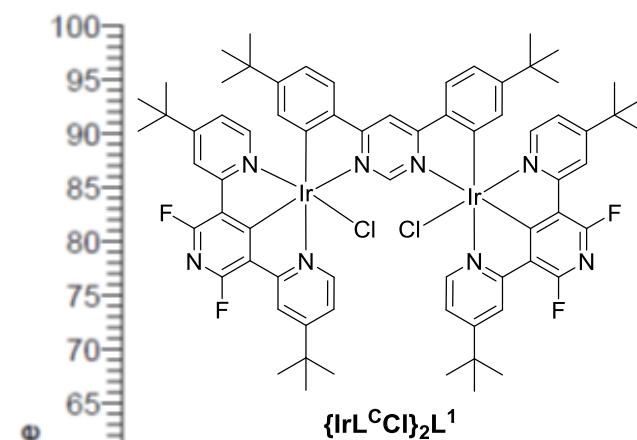




MW=1558?
(DCM)/MeOH + NH₄OAc
C70H74Cl₂F₄Ir₂N₈

EPSRC National Facility Swansea
LTQ Orbitrap XL

NORKOZ046-OA-HNESP #7-24 RT: 0.11-0.53 AV: 17 SM: 7G NL: 4.56E6
T: FTMS + p NSI Full ms [140.00-1935.00]



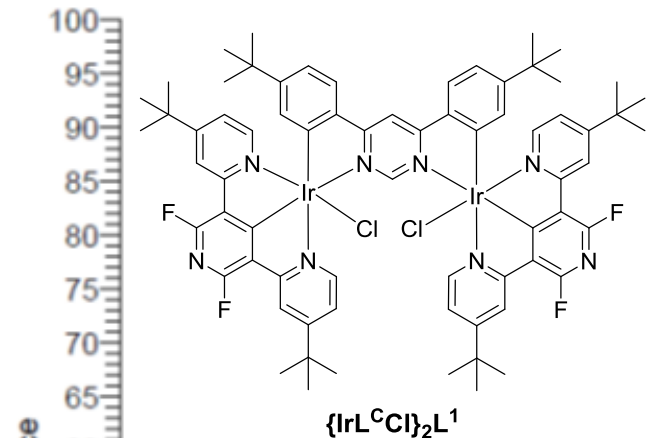
MW=1558?

(DCM)/MeOH + NH4OAc
C70H74Cl2F4Ir2N8

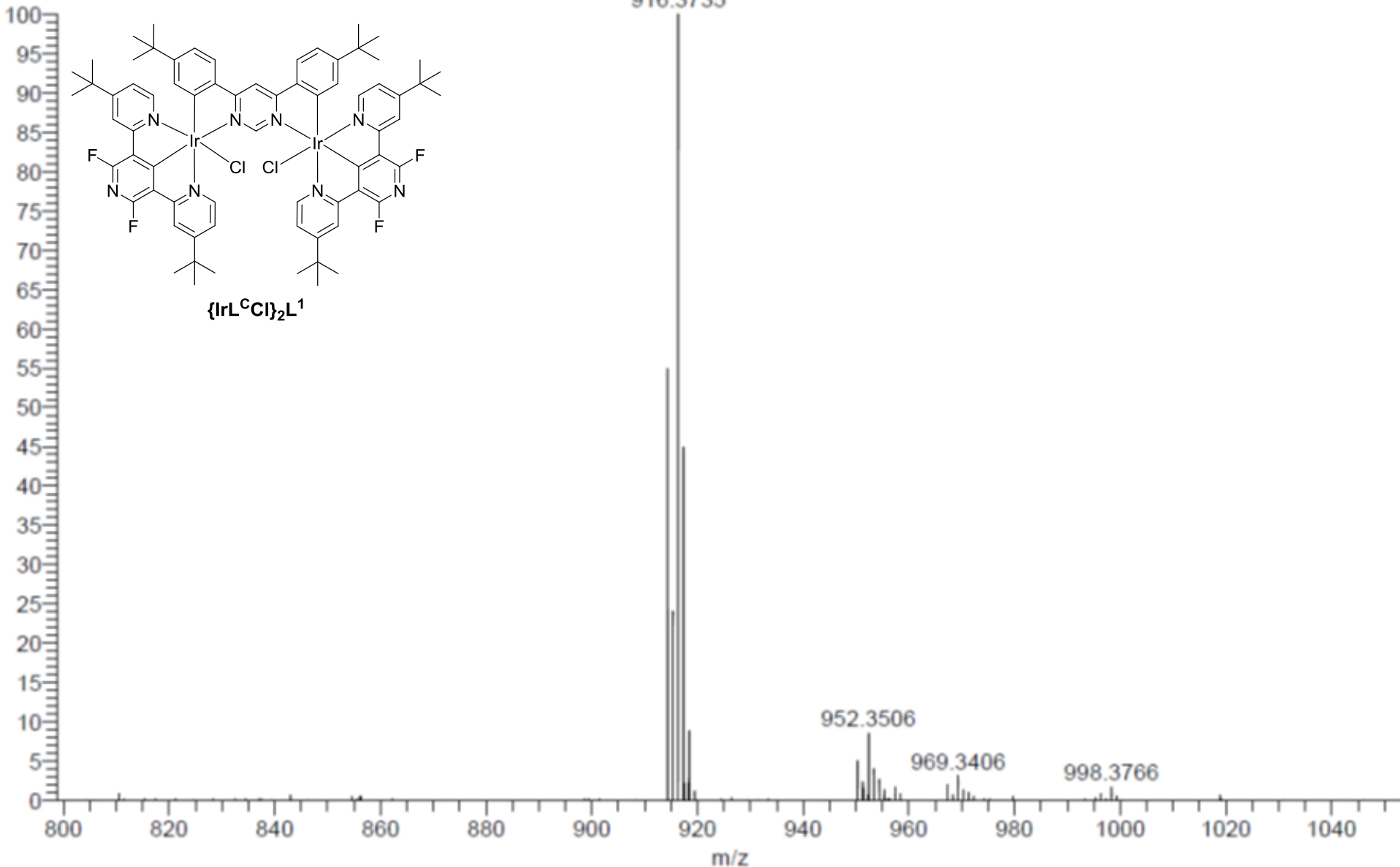
NORKOZ046-OA-HNESP #7-24 RT: 0.11-0.53 AV: 17 SM: 7G NL: 9.13E5

T: FTMS + p NSI Full ms [140.00-1935.00]

EPSRC National Facility Swansea
LTQ Orbitrap XL



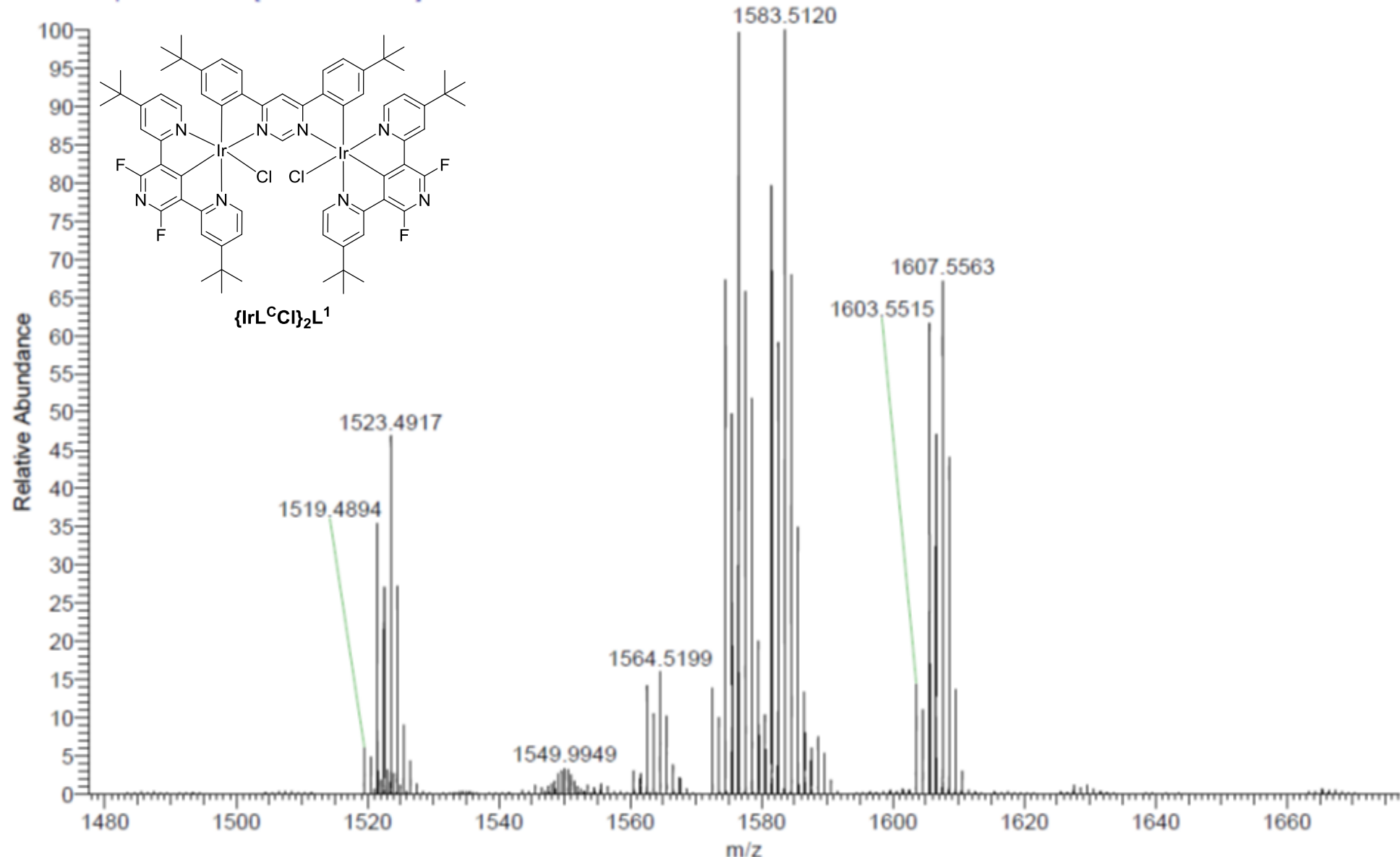
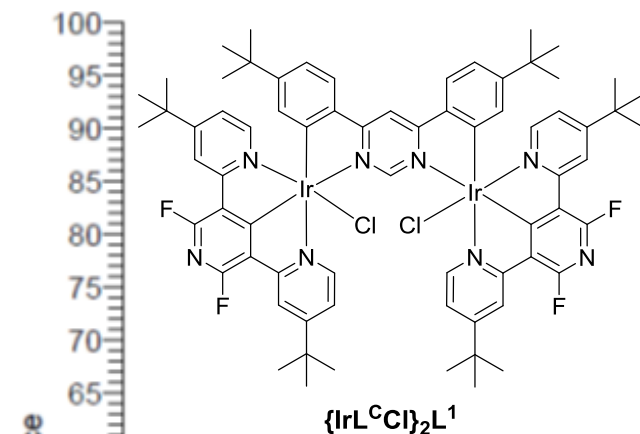
Relative Abundance

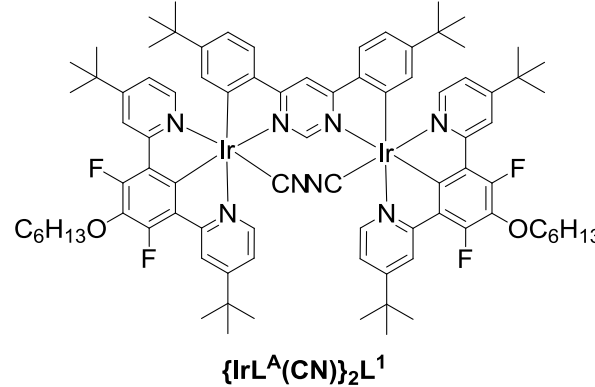


MW=1558?
(DCM)/MeOH + NH₄OAc
C₇₀H₇₄Cl₂F₄Ir₂N₈

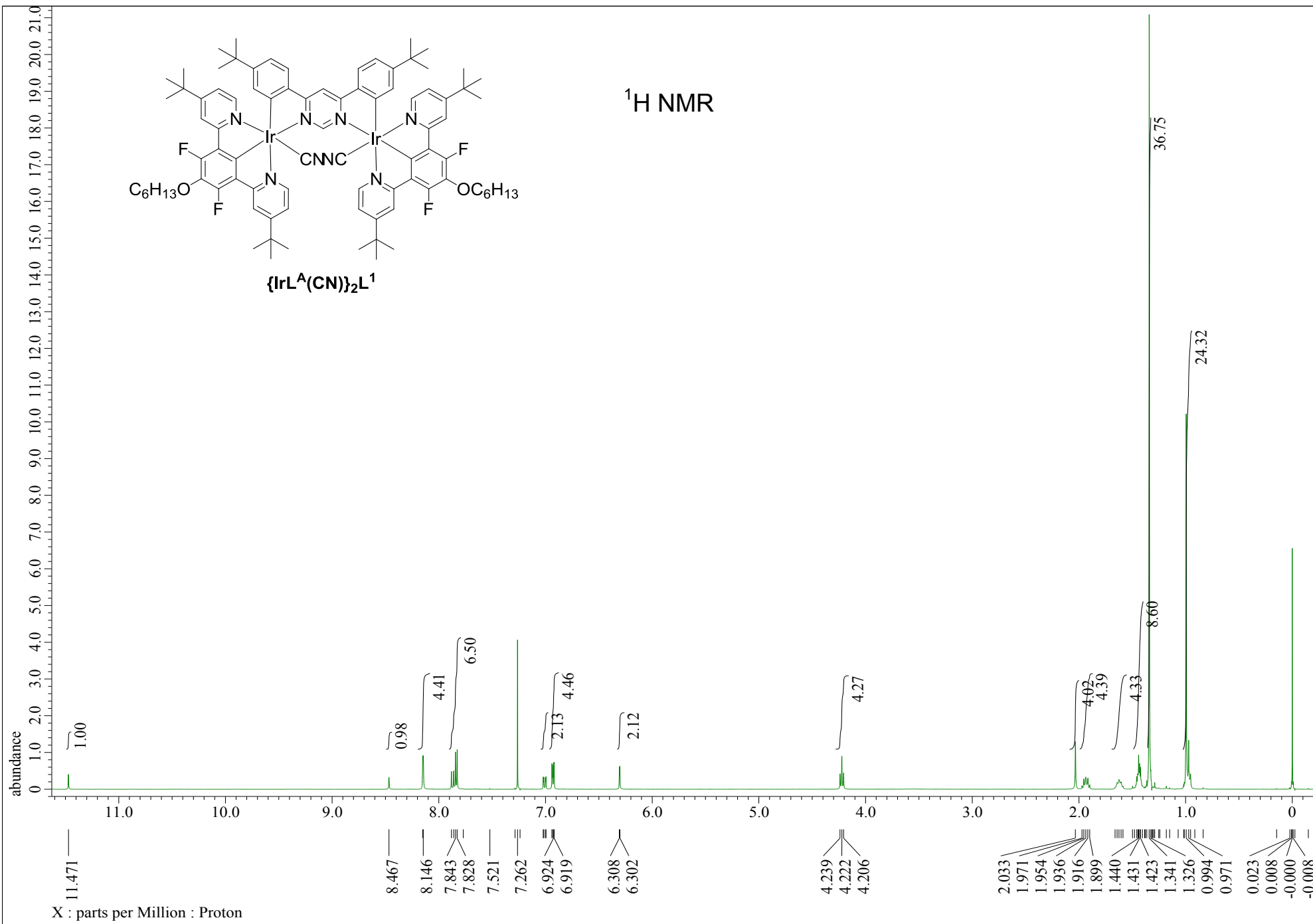
EPSRC National Facility Swansea
LTQ Orbitrap XL

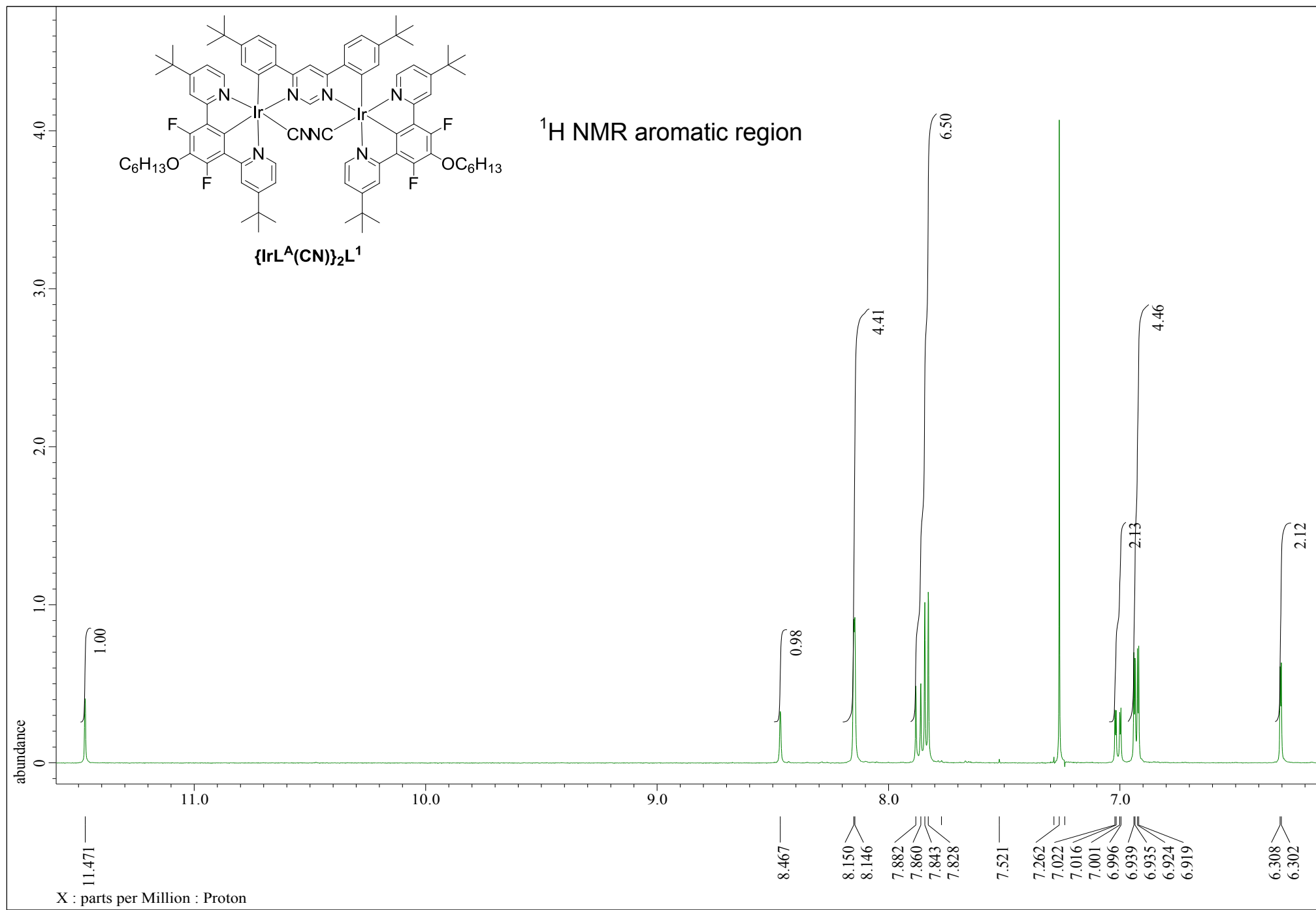
NORKOZ046-OA-HNESP #7-24 RT: 0.11-0.53 AV: 17 SM: 7G NL: 4.56E6
T: FTMS + p NSI Full ms [140.00-1935.00]

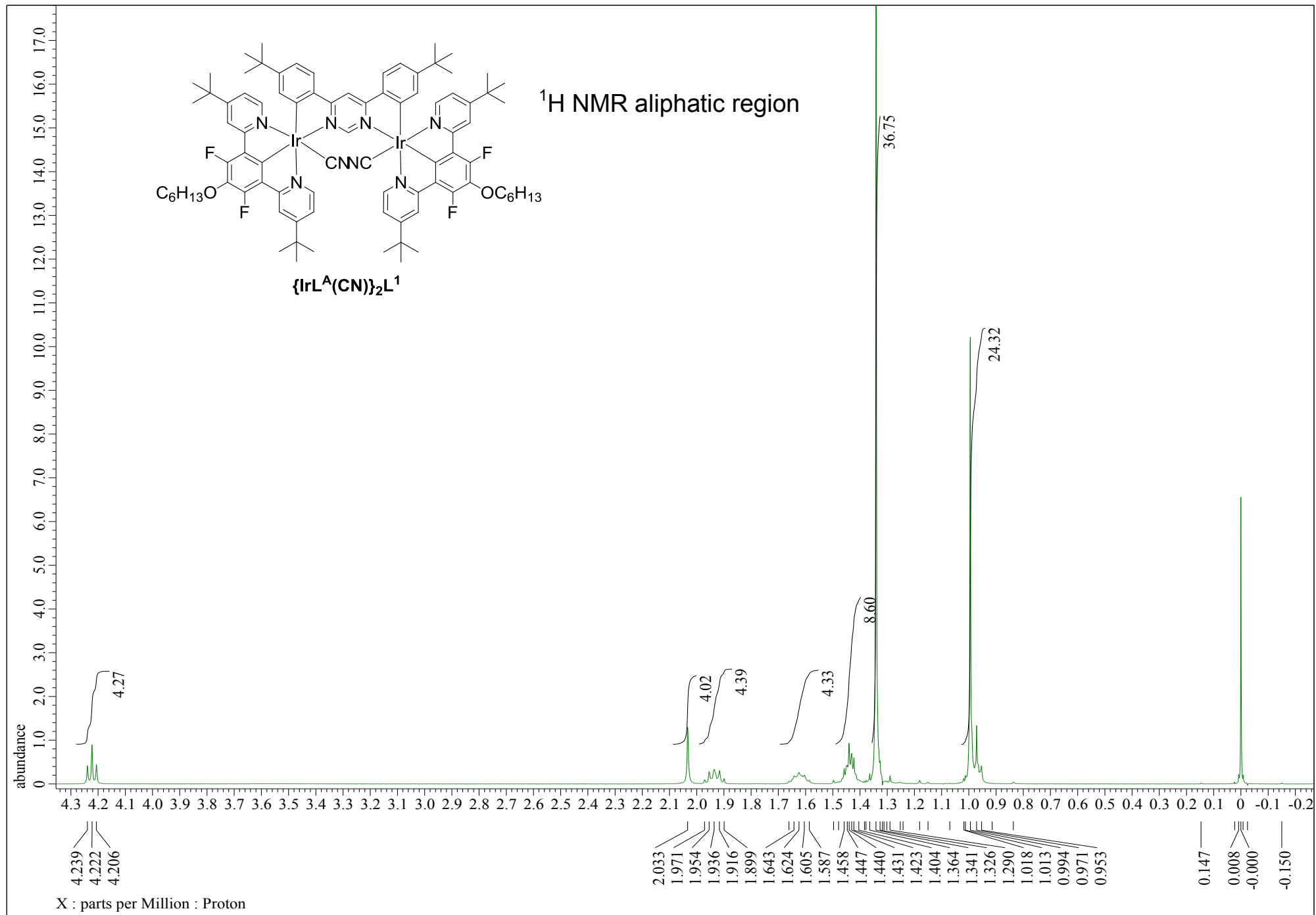


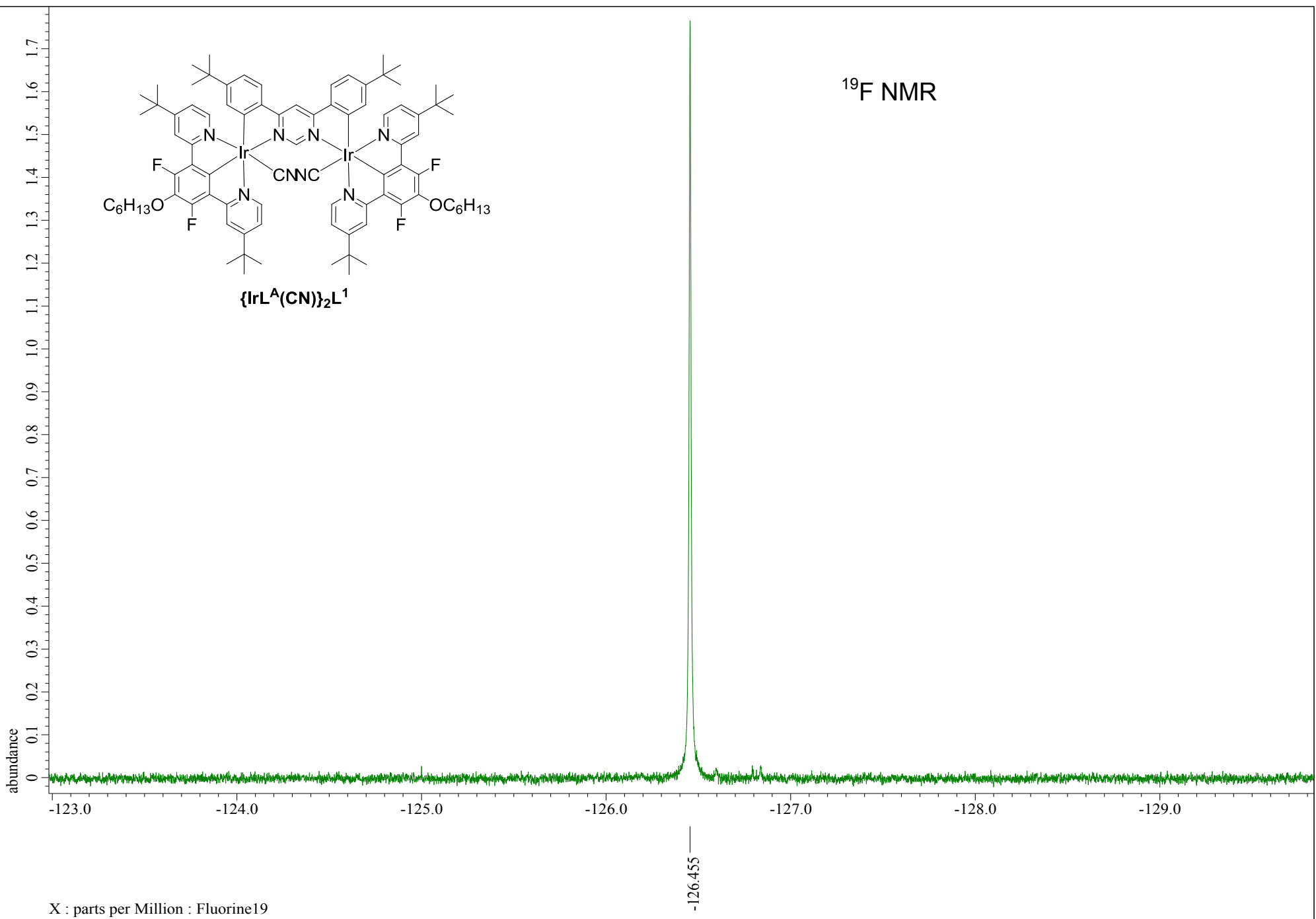


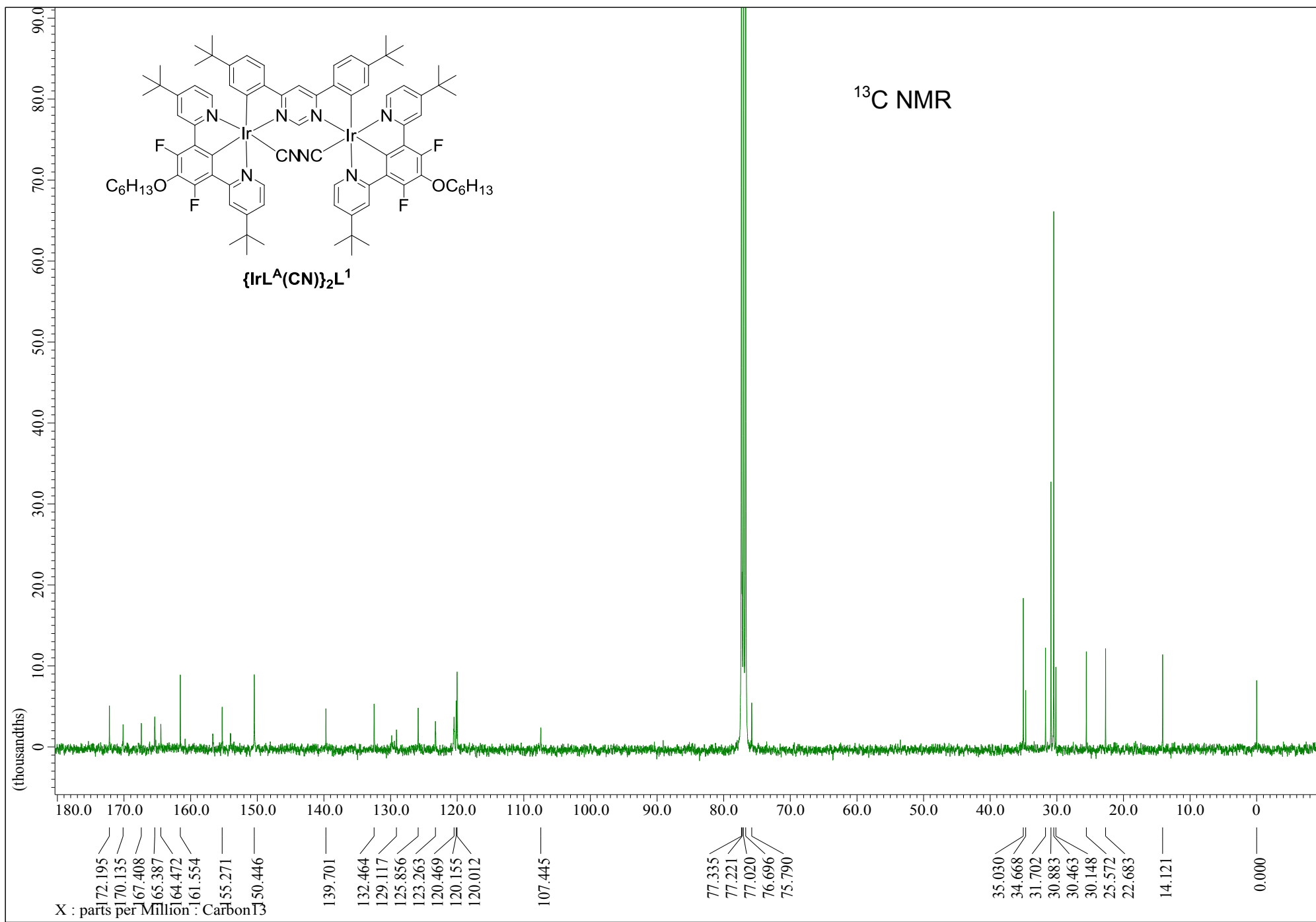
^1H NMR

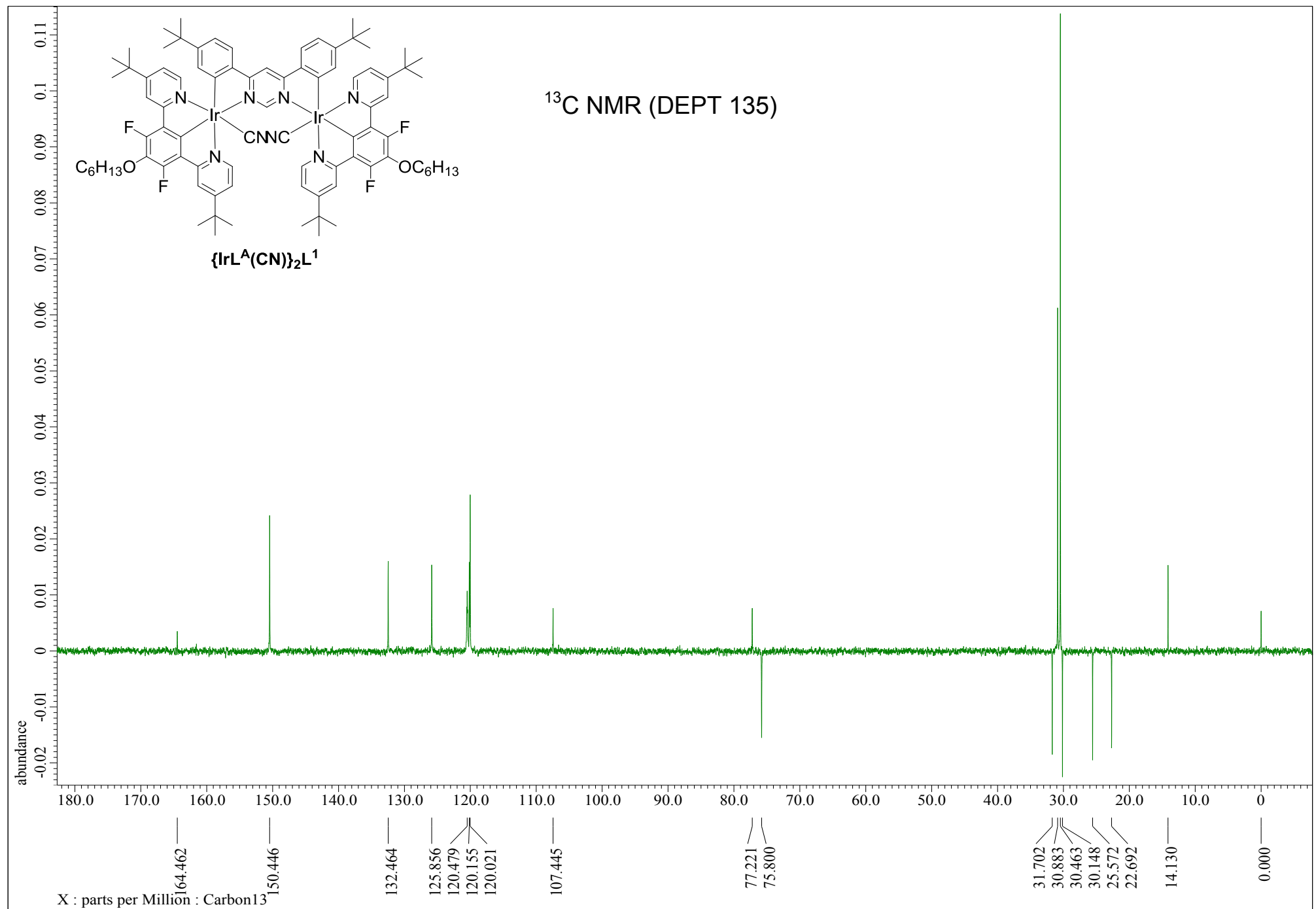








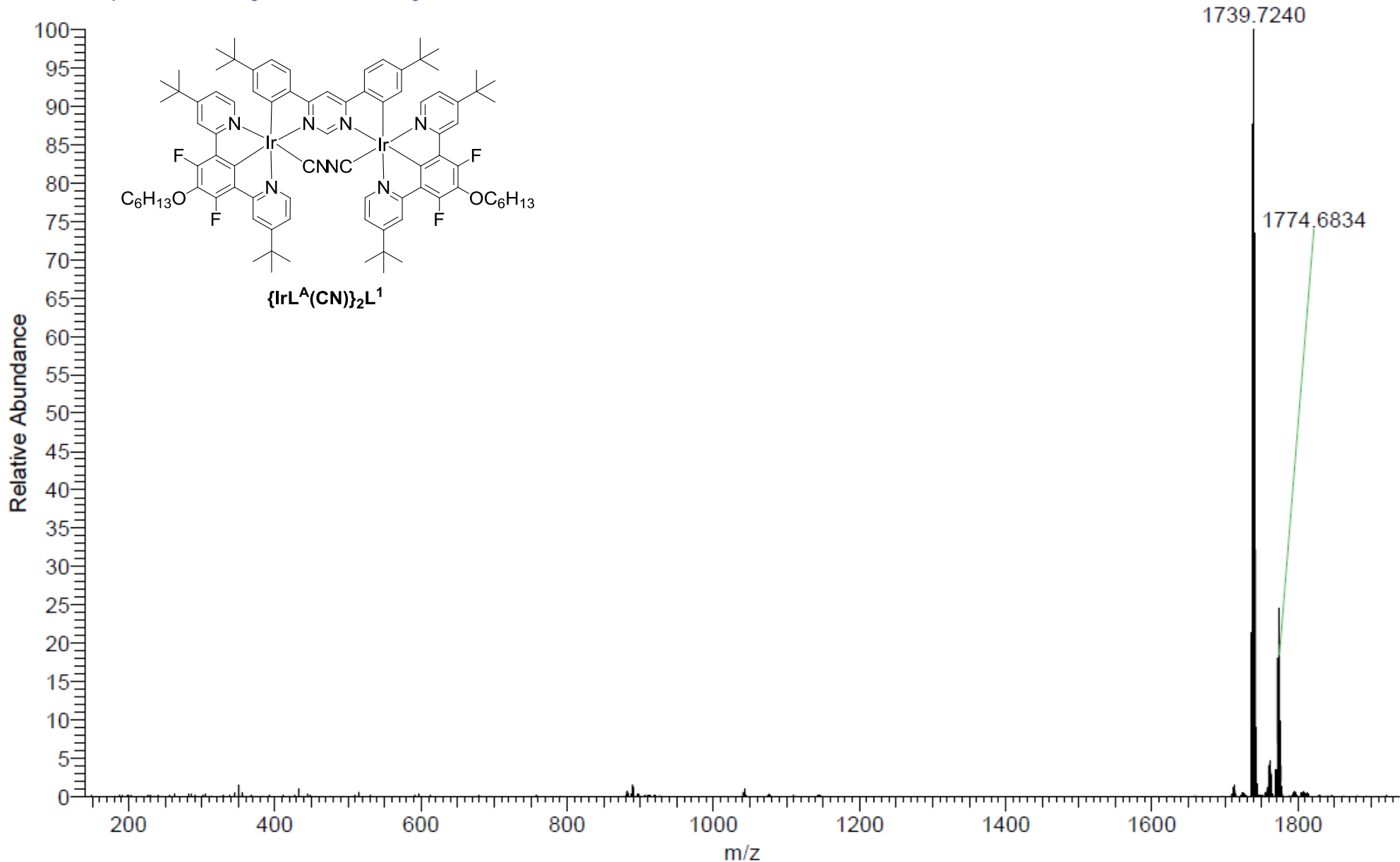




MW=1738?
(DCM)/MeOH + NH₄OAc
C₈₆H₁₀₀F₄Ir₂N₈O₂

EPSRC National Facility Swansea
LTQ Orbitrap XL

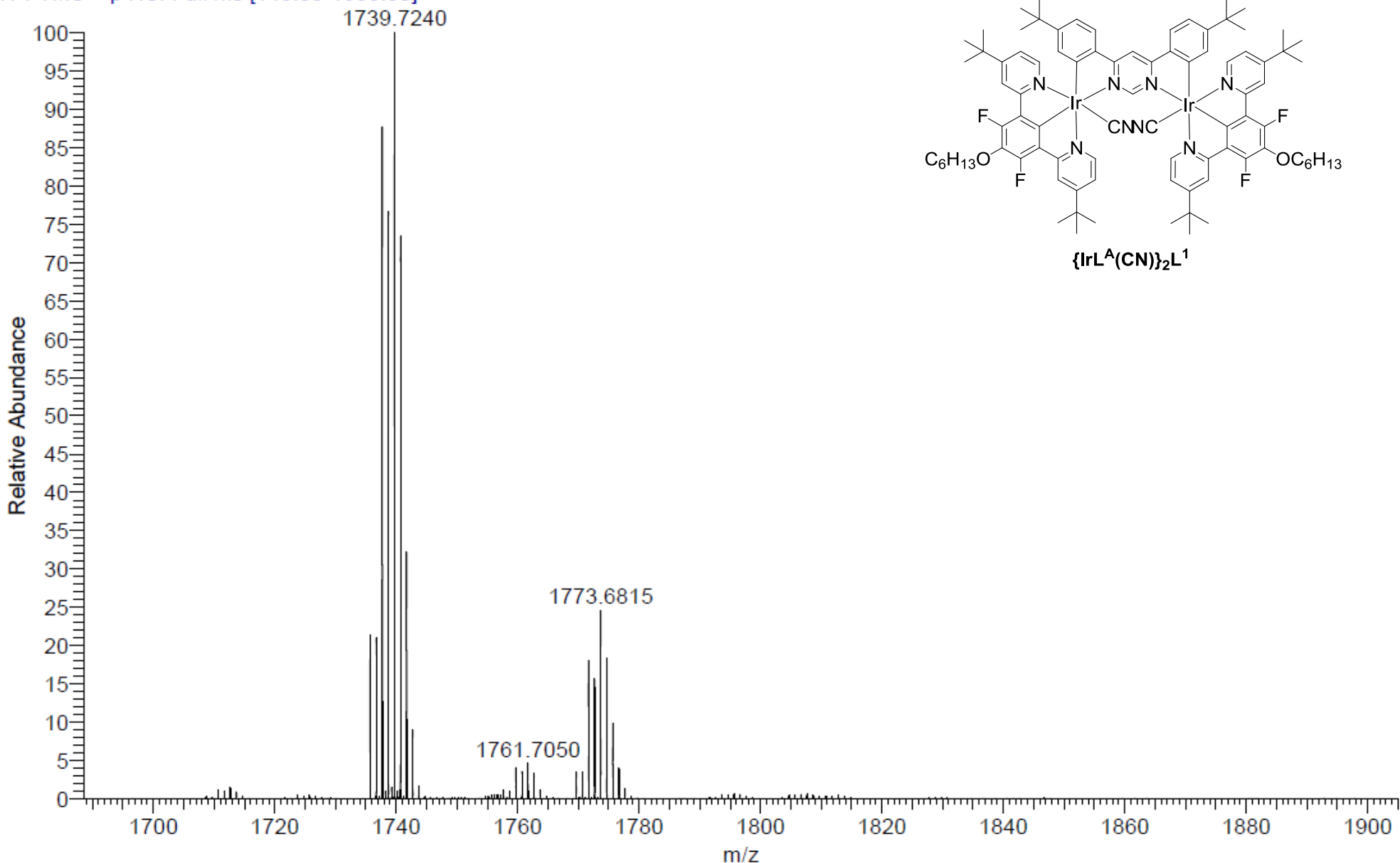
NORKOZ052-OJ-HNESP #33-46 RT: 0.72-1.04 AV: 13 SM: 7G NL: 6.39E7
T: FTMS + p NSI Full ms [140.00-1935.00]



MW=1738?
(DCM)/MeOH + NH₄OAc
C86H100F4Ir2N8O2

EPSRC National Facility Swansea
LTQ Orbitrap XL

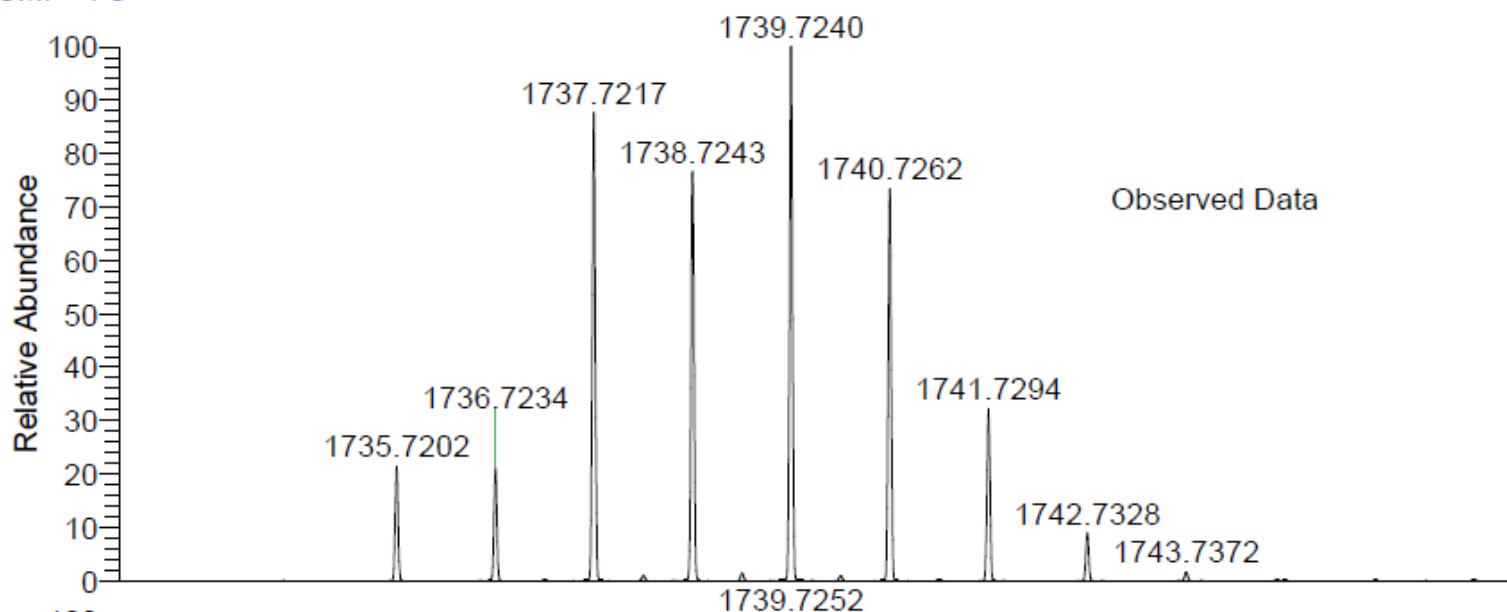
NORKOZ052-OJ-HNESP #33-46 RT: 0.72-1.04 AV: 13 SM: 7G NL: 6.39E7
T: FTMS + p NSI Full ms [140.00-1935.00]



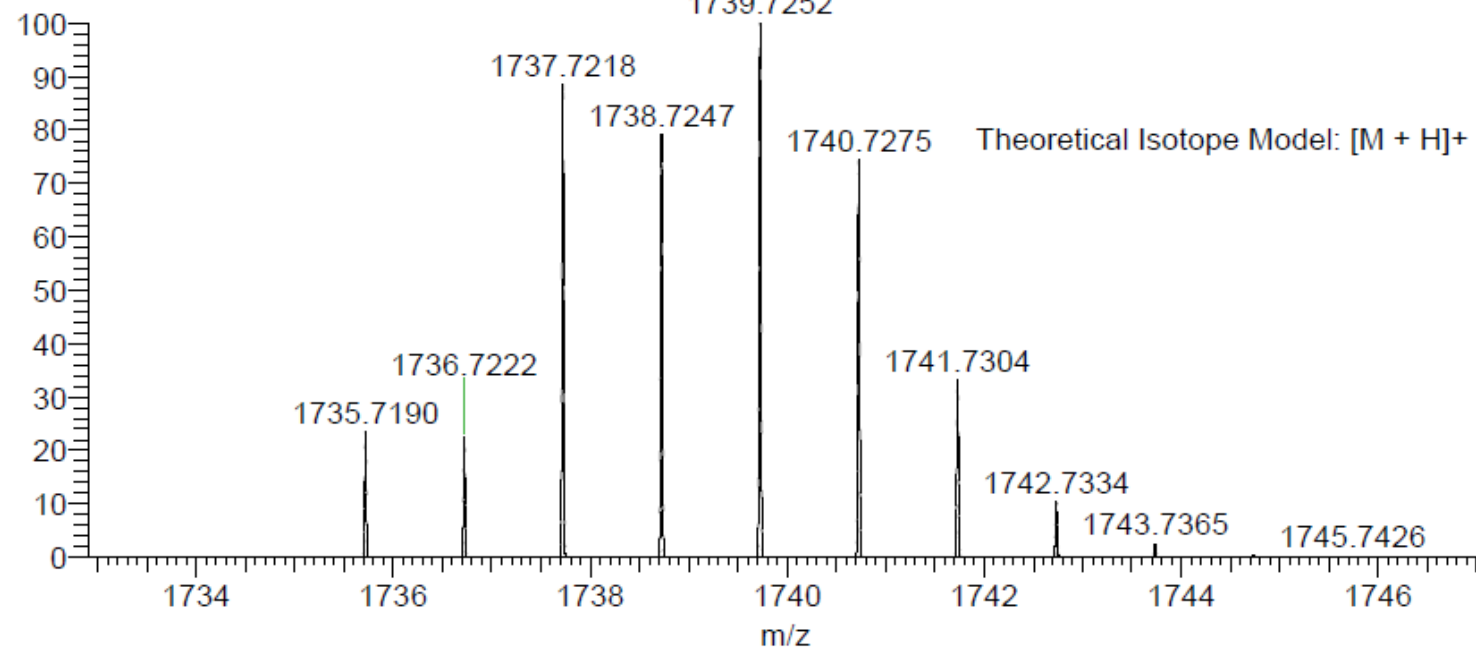
MW=1738?
(DCM)/MeOH + NH₄OAc
C₈₆H₁₀₀F₄Ir₂N₈O₂

EPSRC National Facility Swansea
LTQ Orbitrap XL

SM: 7G



NL:
6.39E7
NORKOZ052-OJ-HNESP#33-
46 RT: 0.72-1.04 AV: 13 T:
FTMS + p NSI Full ms
[140.00-1935.00]



NL:
5.26E3
C₈₆H₁₀₀F₄Ir₂N₈O₂H:
C₈₆H₁₀₁F₄Ir₂N₈O₂
p (gss, s /p:40) Chrg 1
R: 100000 Res .Pwr . @FWHM